University of Zurich[UZH]

Department of Informatics

Computational implications of the muscle synergy hypothesis

A dissertation submitted to the Faculty of Economics, Business Administration and Information Technology of the University of Zurich

for the degree of
Doctor of Science (Ph.D.)

by

Cristiano Alessandro

from Italy

Accepted on the recommendation of

Prof. Dr. Rolf Pfeifer
Prof. Dr. Etienne Burdet

2013

The Faculty of Economics, Business Administration and Information Technology of the University of Zurich herewith permits the publication of the aforementioned dissertation without expressing any opinion on the views contained therein.

Zurich, October 23, 2013

Head of the Ph.D. program in informatics: Prof. Dr. Abraham Bernstein

Acknowledgements

During the years of my PhD studies I have had the pleasure to meet many people. Scientists, friends, educators, artists, students, musicians, engineers...they all contributed to this thesis in one way or another. I would like to thank them all.

I am very grateful to Andrea d'Avella and Francesco Nori for their useful suggestions and criticisms on this work. I really appreciate the time they spent giving me supervision for the development of important aspects of this thesis. Many thanks to Prof. Etienne Burdet, who has read this thesis very carefully with genuine interest, and provided many useful and constructive comments. This manuscript has improved a lot thanks to his feedbacks, and I am sure that the future developments of this work will benefit from his suggestions as well. I would like to thank Prof. Rolf Pfeifer, who gave me the possibility to join the Artificial Intelligence Laboratory, and found the necessary funding to support my PhD. I am also grateful to Prof. Giorgio Metta and Prof. Giulio Sandini, who allowed me to spend some months at the "Robotics, Brain and Cognitive Sciences" department of the Italian Institute of Technology. Finally, my appreciation goes to Prof. Renato Pajarola for joining the Ph.D. committee.

Thanks to all the friends and colleagues at the AI Lab. I find impossible to remember all the experiences shared with Naveen Kuppuswamy. Discussion topics have ranged from research to music, from politics to literature; most importantly, we equally struggled to find our ways in our PhD studies, always trying to support each other. Hugo Gravato Marques is the only person, among my friends, who has the power to make me believe that anything "can be done, and can be ready by the end of this afternoon". We have shared the office and the experience of the EC-CEROBOT project. He has helped me with uncountable suggestions. This manuscript, as well as most of my papers, have been improved thanks to his useful comments. Juan Pablo Carbajal, with his strong ideas and personality, has helped me to understand a very noble principle: science is not only a profession, it is a value! Furthermore, we have collaborated intensively to achieve some of the results presented in this thesis. I would like to thank Mathias Weyland for his very unique philosophy of life. His creative attitude has given to our office that bit of unpredictability that is always welcome. He has helped me to solve several technicalities, and he has always been available to comment paragraphs of this thesis. I would like to thank Konstantinos Dermitzakis, Dorit Assaf and Matej Hoffman for the time we spent together inside and outside the lab, and for the very inspiring "after-lunch coffees". Max Lungarella, the human chatting machine, interviewed me before I joined the lab. His unstoppable jokes and natural optimism have often led to very efficient and funny working days. Finally, I have enjoyed collaborating with people from other labs; these include Bastien Berret, Ioannis Delis, Stefano Panzeri, and Flavio Mutti.

I would like to express all my gratitude to the entire consortium of the European project RobotDoC. Prof. Angelo Cangelosi has invested a lot of efforts trying to customize the program of this training network around the needs of each associate, and he has always found time to give us very useful advices. Special thanks to Elena Dell'Aquila, who has organized the seminars on soft-

skills and the personal coaching sessions; she gave me many friendly suggestions to get around various issues I have encountered during my PhD. Furthermore, my appreciation goes to all the RobotDoC fellows, who made each meeting very interesting and fun. This work has also been supported by the European projects ECCEROBOT and AMARSi. Besides the financial aspect, both projects have been vary motivating and have contributed to the development of this thesis.

I would like to thank all my old friends, who have guaranteed unlimited fun during my brief holiday-breaks in Catania and my weekends in Milan. Finally, the most tender thought goes to Alessandra. Thanks for understanding and supporting my goals despite the difficulties. Thanks for your love, your faith in me, and your sense of humor, that in these years has been capable to turn difficult moments into cheerful laughs. This thesis is for you!

La mia infinita gratitudine a mamma e papà non può essere espressa a parole. Tutti i miei successi non sarebbero stati possibili senza i loro insegnamenti. Mi hanno sempre dato la libertà di perseguire i miei desideri facendomi imparare dai miei errori; sono stati, e continuano ad essere, sempre pronti a darmi consigli, utili a rendere possibile l'impossibile. Grazie infinite!

Cristiano

Zurich, Switzerland
September 2013

Abstract

A long standing hypothesis in motor neuroscience suggests that the central nervous system (CNS) generates motor commands by combining a limited set of modules. This strategy would simplify motor control and learning, and it might represent one of the principles that underlie the outstanding motor skills of humans and other vertebrates. This hypothesis has recently been supported by the observation that recorded muscle activation patterns can be generated by a parsimonious set of muscle synergies (i.e. coordinated activations of groups of muscles), which appear invariant across different motor tasks. Although the analysis of muscle patterns has provided uncountable insights, a principled investigation of the hypothesized modular strategy is still lacking. The main goal of this thesis is to fill this gap, and to study the implications of such a modularity from the control point of view. To this end, we consider the problem of controlling a dynamical system by linear combinations of a limited set of control signals (i.e. motor synergies). Through this computational approach we investigate aspects of the muscle synergy hypothesis that are difficult to address by the sole analysis of recorded muscle activity. In particular we investigate which and how many synergies are required to obtain satisfactory performance, the relation between synergies and the dynamics of the musculoskeletal system, and their relation with the desired motor tasks.

The first contribution of this thesis is the formal definition of task-based synergies; i.e. generators of motor commands that guarantee the achievement of the task requirements. In order to synthesize a set of effective synergies we propose the dynamic response decomposition (DRD). This technique is tested on a planar kinematic chain for point-to-point and via-point movements; the synthesized synergies result in effective task-performance, yet greatly reducing the dimensionality of control. The DRD method shows that the shape as well as the number of synergies are strictly tailored to both the desired class of tasks and the dynamics of the system. In particular, it suggests that synergies represent solutions to prototypical task instances, and that the number of elementary control modules depends on the degree of similarity between the desired tasks. These results are supported by theoretical considerations as well as numerical simulations. Finally, we investigate the possible relation between muscle synergies and another form of modularity, the composition of motions by sequences of simpler sub-movements. Numerical simulations show that, at the control level, a sequence of synergy-based actuations leads to poorer performance than a control signal computed for the entire task without segmentation (i.e. as a single linear combination of synergies). However, segmentation might be a viable alternative to keep the number of synergies low. In summary, this thesis sheds new lights on various computational aspects of the hypothesized modular organization of the CNS, and it represents a first step towards a predictive model of muscle synergies.

Zusammenfassung

Eine prominente Hypothese der Neurowissenschaften besagt, das zentrale Nervensystem (ZNS) generiere motorische Signale durch Kombination einer beschränkten Anzahl von Modulen. Eine solche Strategie würde die motorische Steuerung sowie das Lernen vereinfachen und könnte eine der Grundlagen für die herausragenden motorischen Fertigkeiten von Menschen und anderen Wirbeltieren darstellen. Diese Hypothese wird unterstützt durch unlängst gewonnene Beobachtungen, welche zeigen, dass aufgezeichnete Muskel-Aktivierungsmuster durch eine kleine Menge von Muskel-Synergien (d.h. koordinierte Aktivierungen von Muskelgruppen) generiert werden können. Diese Synergien scheinen in Bezug auf die von den Muskeln zu lösenden Aufgabe unveränderlich zu sein. Obwohl durch die Analyse solcher Muster viele Erkenntnisse gewonnen worden sind, fehlt nach wie vor eine konzeptionelle Untersuchung dieser modularen Strategie. Das Hauptziel dieser Arbeit ist es, ebendiese Lücke zu füllen und die Implikationen dieses modularen Ansatzes aus einer Kontroll-Perspektive zu untersuchen. Um dies zu erreichen, wie ein dynamisches System und dessen Kontrolle durch lineare Kombinationen einer beschränkten Anzahl an Kontroll-Signalen, d.h. Motor-Synergien, betrachtet. Mit Hilfe dieses rechnergestützten Ansatzes werden Aspekte der Muskel-Synergie-Hypothese erforscht, welche durch die blosse Analyse aufgezeichneter motorischer Signale nur schwer zu greifen sind. Insbesondere wird untersucht, welche und wieviele Synergien für das Erreichen von zufriedenstellenden Resultate notwendig sind, was für Zusammenhänge zwischen Synergien und dem muskuloskelettalen System bestehen und wie diese wiederum mit der von den Muskeln zu lösenden Aufgabe zusammenhängen.

Der erste Beitrag dieser Arbeit ist die formale Definition von aufgabenspezifischen Synergien; d.h. das Generieren motorischer Signale, welche das Erreichen von Anforderungen für eine bestimmte Aufgabe garantieren. Um eine Reihe von effektiven Synergien zu synthetisieren, wird eine "dynamic response decomposition" (DRD) genannte Technik vorgestellt, welche an einer planaren kinematischen Kette getestet wird. Dabei werden Punkt-zu-Punkt- sowie Wegpunkt-Bewegungen untersucht, die in effektiven Synergien resultieren, welche die Dimensionalität des Kontrollproblems drastisch reduzieren. Die DRD-Technik zeigt auf, dass die Form und die Zahl der Synergien stark auf die Dynamik des Systems sowie auf die Klasse der zu lösenden Probleme zugeschnitten ist. Insbesondere legt die Technik nahe, dass Synergien Lösungen prototypischer Aufgaben sind und dass die Anzahl der elementaren Kontroll-Module vom Grad der Ähnlichkeit zwischen der zu lösenden Aufgaben abhängig ist. Die in dieser Arbeit präsentierten Resultate werden sowohl durch theoretische Überlegungen, als auch durch numerische Simulationen gestützt. Schliesslich wird ein möglicher Zusammenhang zwischen Muskel-Synergien und einer anderen Art von Modularität, der Zusammensetzung einer Reihe einfacher Bewegungen zu komplexeren Bewegungen, untersucht. Numerische Simulationen zeigen, dass letztere auf dem Kontroll-Niveau einer Bewegung resultierend aus einer einzigen linearen Kombination von Synergien unterlegen ist. Allerdings könnte eine solche Segmentierung in Unter-Bewegungen eine

praktikable Alternative sein, um die Zahl der Synergien tief zu halten. Zusammenfassend gibt diese Arbeit Aufschluss über verschiedene rechnergestützte Aspekte der modularen Organisation des ZNS und ist einer erster Schritt in die Richtung voraussagender Modelle für Muskel-Synergien.

Contents

List of Figures

List of Tables

Chapter 1

Introduction

The execution of coordinated movements has fascinated many scientists in the last centuries. Both humans and other vertebrates are able to perform a great variety of motor actions, learn new motor behaviors relatively easily, and adapt to different environmental conditions. These features result from the interplay between a very complex musculoskeletal apparatus, and an adaptable as well as efficient control system, the central nervous system (CNS). Although these phenomena have been largely studied, the fundamental mechanisms by which the CNS orchestrates the many muscles of the musculoskeletal apparatus, while coping with its complexity (e.g. large number of degrees of freedom, non-linearities, redundancy), are still not clear.

Today there is a large consensus that a modular and hierarchical organization of the movement system might be one of the principles behind the observed motor performance [Bizzi et al., 2008; d'Avella and Pai, 2010; Giszter et al., 2010; Ting and McKay, 2007]. This idea was initially introduced by Bernstein [1967] in the context of motor redundancy, and it has then evolved into different, yet related, concepts [Flash and Hochner, 2005]. The common denominator of these ideas is that motor actions emerge from the combination of a limited set of modules. This strategy would reduce the number of variables to be controlled, and therefore it might simplify motor control and learning. In this thesis we analyze one of the proposed forms of modularity, the so-called muscle synergies [d'Avella et al., 2003; Saltiel et al., 2001; Tresch et al., 1999].

One of the long-standing questions in motor neuroscience inquires which variables are controlled by the CNS (e.g. joint angles, joint torques, muscle activations). Connected to this issue, is the problem of motor redundancy, formulated in its current form by Nikolai Bernstein (1896-1966) [Bernstein, 1967]. Essentially, the number of variables that are necessary to define a motor task (e.g. reaching a point in space) is typically lower then the number of hypothetical controlled variables, therefore the same task can be performed by means of an infinite number of control strategies. At the kinematic level, the human arm (neglecting the joints of the hand) can be described as a kinematic chain with seven axes of rotation (i.e. seven degrees of freedom) [Zatsiorsky, 1997]. The task of placing the hand at a certain position, however, is defined in three coordinates (i.e. the desired position of the hand in the three dimensional space); therefore it can be fulfilled by an infinite number of joint configurations. Similar problems emerge at other levels of the motorneuron hierarchy. Since most of the joints are crossed by many muscles, the task of producing a specific joint torque has an infinite number of solutions; i.e. all the combinations of muscle forces that lead to the desired joint torque. Taking a step further, each muscle is constituted by many motor units (i.e. sets of muscle fibers and the motorneurons that innervate them); the CNS can achieve the same muscle activations by recruiting many different groups of motor units. Surprisingly enough, even though a goal can be achieved in an infinite number of ways, many studies showed very consistent and stereotypical patterns of kinematic variables and muscle activations. How does the CNS "choose" among this infinity of solutions? To give an answer to the problem

of motor redundancy, Bernstein suggested that the CNS organizes elements (i.e. joints, muscles, muscle fibers etc.) into groups called "synergies" in a task-dependent fashion. Since each synergy is hypothesized to be controlled as a single variable, the problem of motor redundancy might be ameliorated and eventually a single solutions might emerge.

In its modern connotation, muscle synergies are coordinated activations of groups of muscles[1] [d'Avella et al., 2003; Saltiel et al., 2001; Tresch et al., 1999]. Hypothetically, the central nervous system encodes a parsimonious set of synergies and combines them in a task-dependent fashion to generate appropriate motor commands. This hypothesis is typically evaluated by analyzing the spatio-temporal regularities of the electromyographic signals (EMG) recorded from a group of subjects. Decomposition-based techniques, such as principal component analysis (PCA) or non-negative matrix factorization (NMF), are used to extract the components that best reconstruct the recorded dataset. In many cases these components (i.e. synergies) appear very similar across different subjects and experimental conditions, and therefore they are regarded as indirect evidence of the hypothesized neural modularity. This methodology has been successful in explaining muscle contractions across a wide range of complex tasks (e.g. running, walking, keeping balance, reaching and other combined movements) in humans [Cappellini et al., 2006; d'Avella et al., 2008, 2006, 2011; Ivanenko et al., 2005; Torres-Oviedo and Ting, 2007, 2010], in frogs [Giszter et al., 1993; Kargo and Giszter, 2000b, 2008; Mussa-Ivaldi and Bizzi, 2000; Mussa-Ivaldi et al., 1994], cats [Ting and Macpherson, 2005; Torres-Oviedo et al., 2006], monkeys [Overduin et al., 2012, 2008], and other species [Dominici et al., 2011]. The reader is referred to [Alessandro et al., 2013b] for a detailed review of these works (see appendix A).

While many studies focus on physiological aspects of the muscle synergy hypothesis, very little research addresses the computational implications of the proposed modular controller. The production of motor commands by combining a limited set of modules might be a viable strategy to master the complexity of the musculoskeletal system; however, it limits the possible muscle activation patterns, and therefore the movements that can be executed. Thus, the CNS should encode a set of synergies that allows to suitably accommodate the behavioral needs of the organism. The characterization of such a set is a largely uncovered topic of research. Assuming the validity of the muscle synergy hypothesis, how should these synergies look like in order to allow the execution of the desired motor tasks? How many synergies are needed? How does the dynamics of the musculoskeletal system affect the synergy-set? Is there a relation between the desired tasks and these elementary control modules? Addressing these theoretical questions would certainly provide a better understanding of the muscle synergy hypothesis, and might eventually lead to a computational model to explain the experimental data. In fact, the results obtained so far are mostly descriptive in nature and do not offer such a principled investigation [Alessandro et al., 2013b]. Additionally, the approach based on the analysis of recorded EMG signals, as such, is mainly grounded at the level of motor commands. In particular, it consists in extracting the main components of the EMG dataset, and in comparing them across subjects and motor tasks. The evaluation of the muscle synergy hypothesis at the level of task is not always considered and, from our point of view, it deserves more attention. Does the set of identified muscle synergies actually lead to the task performance observed experimentally? Does it generate feasible actuations? Due to the non-linearity of the musculoskeletal system, these questions are not trivial. Negative answers would cast doubts on the proposed modular decomposition even if the EMG signals can be approximated satisfactorily.

This thesis analyzes the concept of muscle synergies from a computational point of view, and

[1] The term *synergy* has also been used in the context of another motor control hypothesis, the uncontrolled manifold hypothesis (UMH) [Latash, 2010; Latash et al., 2010]. In that context, the term refers to "a neural organization of a set of elemental variables [e.g. muscle contractions] with the purpose to ensure a certain stability properties of a performance variable produced by the whole set [e.g. desired joint configuration]" [Latash et al., 2008]. These studies are out of the scope of this thesis, however the definition of synergies we adopt is conceptually similar to the notion of M-modes, which has been introduced within the UMH.

in particular from the perspective of controlling a dynamical system. Inspired by the model of time-varying synergies [d'Avella et al., 2003], the control signals are restricted to linear combinations of a limited set of actuations (i.e. motor synergies). In order to obtain an efficient reduced-dimensional controller, the set of synergies should be chosen appropriately. Therefore, this computational approach forces us to investigate the issues discussed above, and to provide plausible explanations. First of all, the need of evaluating synergies in terms of task performance becomes clear; trivially, the goal of any controller is indeed to accomplish the desired tasks. This idea is formalized in a novel definition of synergies that is grounded at the task-level. In order to synthesize a suitable set of synergies, we propose the Dynamic Response Decomposition (DRD) method. The mathematical formulation of this method allows a variety of experimentation, and in particular it highlights important aspects of the muscle synergy hypothesis that are difficult to address by following an experimental procedure based on the analysis of EMG-signals. These aspects include the shape (i.e. waveforms) and the number of the synergies, and the dependence of these attributes on desired tasks and system dynamics.

This thesis is structured in the form of a collection of papers: the main results and achievements are summarized in the chapters, while mathematical details and technicalities are discussed in the attached papers. The manuscript is organized as follows.

Chapter 2 summarizes the main contributions of this thesis.

Chapter 3 formalizes the idea of synergy-based controllers. In this context, we detail the model of time-varying synergies (used throughout the thesis), and we interpret such a model in geometrical terms. This allows to distinguish between two perspectives on synergies. The first is grounded at the level of input-signals and is exemplified by the sole analysis of EMG-recordings (Sec. 3.2), and the second one takes into account also task performance (Sec. 3.3). We formalize the second viewpoint in the concept of task-based synergies.

Chapter 4 defines the notion of task-based synergies. Essentially, these synergies are defined as a set of actuations that, by linear combination, can generate control signals leading to the desired task performance. As such, they are evaluated based on a measure defined at the task-level, rather than at the input-level. To exemplify the proposed definition, a numerical optimization is employed to synthesize task-based synergies for a linear and a non-linear dynamical system, and to test them in relation to some desired tasks.

Chapter 5 introduces the Dynamic Response Decomposition (DRD), the formalism we developed to analyze the notion of muscle synergies. By its nature, DRD is a general method to find open-loop controllers for a dynamical system to solve desired tasks. Additionally, it is also instrumental to synthesize effective synergies in a computationally light fashion. Its performance is evaluated on a planar kinematic chain for point-to-point and via-point tasks.

Chapter 6 reports the computational insights provided by DRD on the notion of muscle synergies. DRD suggests that synergies might be solutions to prototypical tasks, and it offers a lower bound on the minimal number of synergies. Additionally, this chapter investigates the possible relation between muscle synergies and another form of modularity, the sequential concatenation of simple sub-movements, or kinematic strokes [Flash et al., 1992; Novak et al., 2003]. Via-point tasks can indeed be solved by concatenating the actuations of the constituent point-to-point movements, each obtained as a combination of synergies. Section 6.3 analyzes the advantages and the disadvantages of this approach, and for the first time it offers a proof of concept on how muscle synergies and kinematic modularity might be integrated into a unified framework. Results show

that the concatenation strategy leads to poorer performance than solving the entire task without segmentation. However, this strategy might be a viable alternative to keep the dimensionality of the controller low.

Chapter 7 discusses the results of this thesis.

Chapter 8 provides concluding remarks and proposes possible future research directions.

Appendix A, published
Alessandro, C., Delis, I., Nori, F., Panzeri, S., and Berret, B. (2013b). Muscle synergies in neuroscience and robotics: from input-space to task-space perspectives. *Frontiers in Computational Neuroscience*, 7(43).

Appendix B, published
Alessandro, C. and Nori, F. (2012). Identification of synergies by optimization of trajectory-tracking tasks. In *IEEE RAS/EMBS International Conference of Biomedical Robotics and Biomechatronics*, pages 924–930, Rome, IEEE.

Appendix C, published
Alessandro, C., Carbajal, J. P., and d'Avella, A. (2012). Synthesis and adaptation of effective motor synergies for the solution of reaching tasks. In Ziemke, T., Balkenius, C., and Hallam, J., editors, *Lecture Notes in Artificial Intelligence (LNAI)*, pages 33–43, Berlin. Springer-Verlag.

Appendix D, submitted
Alessandro, C., Carbajal, J. P., and d'Avella, A. (2013a). A computational analysis of motor synergies by dynamic response decomposition.

Appendix E reports the computational complexity of the DRD method.

Chapter 2

Thesis contributions

The main goal of this thesis is to provide a computational perspective on the hypothesis of muscle synergies. The proposed analysis is complementary to the experimental studies that have been carried out so far, which have mainly focused on physiological issues, and it might in fact guide further experimentation. In this chapter we summarize the main contributions of the thesis.

Geometrical interpretation of time-varying synergies. The main feature of a synergy-based controller is that motor signals are generated by linearly combining a limited set of primitives (i.e. synergies). In this thesis we describe each primitive in accordance with the time-varying synergy model [d'Avella et al., 2003], i.e. as a coordinated pattern of time-varying signals. While most of the previous works employ this model to explain biological data (e.g. EMG signals), this thesis offers a geometrical interpretation of it in relation to the problem of controlling a dynamical system (e.g. musculoskeletal apparatus). In a nutshell, synergies represent generators of the admissible actuations. Such actuations should approximate the desired control signals, and lead to the accomplishment of the desired task. Therefore synergies are strictly related to the task to be solved. Additionally, as tasks and corresponding actuations are related by the dynamics of the system, the latter has a direct influence on the necessary synergy-set.

Definition of task-based synergies. Considering the concept of muscle synergies from a control point of view, it becomes evident that these motor modules should lead to satisfactory task-performance. In many studies this requirement is not explicitly considered, as synergies are often evaluated only in terms of their capability to approximate the desired motor signals. In this thesis we propose a formal definition of task-based synergies; i.e. synergies that guarantee the desired performance on a series of desired tasks.

Dynamic Response Decomposition (DRD). The Dynamic Response Decomposition (DRD) is a general method to compute open-loop controllers for a dynamical system to solve desired tasks. Additionally, it provides a computationally cheap procedure for the synthesis of effective synergies. The DRD is used throughout the thesis to analyze various computational aspects of the muscle synergy hypothesis. Its software has been released as a GNU Octave package under free and open source license, and it is available online[1].

Shape and number of synergies. The set of admissible actuations, and therefore the motor tasks that can be executed, is determined by the shape and the number of synergies. Research has very

[1] http://users.elis.ugent.be/~jcarbaja/DRD/drd.html

seldom focused on a principled investigation of these attributes and on their impact on the hypothesized synergy-based controller. Thus, evaluating the validity of experimentally identified synergies becomes a real challenge. Is there a relation between synergy-set, desired tasks and system dynamics? The formulation of DRD provides a possible view on these aspects. In particular, it suggests that synergies might represent solutions to prototypical task instances. Such synergies embed essential information about the tasks to be solved and the dynamics of the system, and therefore they are successful primitives to solve similar tasks. The required number of synergies depends on the degree of similarity between the desired tasks. If the desired class of tasks is very narrow, a handful of synergies might be enough, otherwise a wider synergy-set is needed. The important implication of this result is that, from a dimensionality reduction point of view, developing different specialized sets of synergies, that can be selectively used based on the task to be solved, is more convenient than employing a single (large) set that can be used for any desired movement. Ultimately, the synergy-set is strictly tailored to the dynamics of the system as well as to the tasks to be solved. These notions are mathematically formalized within the DRD framework.

Muscle synergies and kinematic modularity. Another proposed form of modularity is the generation of complex kinematic trajectories by concatenating simpler sub-movements, or kinematic strokes. Research on muscle synergies and kinematic segmentation have evolved independently. In fact, the possible relation between these two forms of modularity is still under debate. We propose that synergies might be the low-level primitives that give rise to the kinematic strokes, and we test such an idea within the DRD framework. Our analysis suggests that the concatenation of synergy-based actuations is often less accurate than a non-segmented form of control, where the entire actuation is computed as a single combination of synergies. However, if the desired class of tasks is very diverse, the concatenation-based strategy might be a viable alternative to keep the number of synergies low.

Review on muscle synergies. Appendix A offers a comprehensive review of the research on muscle synergies that has been carried out in neuroscience and robotics.

Chapter 3

Input and task-based perspectives

This chapter analyzes the concept of muscle synergy from a geometrical and control theoretical point of view (Sec. 3.1), and interprets such a concept from two different perspectives. The first is solely grounded at the level of motor commands, and interprets muscle synergies as primitives that generate admissible control signals (Sec. 3.2). The second perspective considers muscle synergies as the elementary building blocks of an effective control architecture, and therefore it explicitly takes task-performance into account (Sec. 3.3). We are going to claim that the methodology that is typically employed in experimental neuroscience (purely based on the analysis of EMG-signals) exemplifies the first perspective, and that a task-level assessment of the hypothesized modularity of the CNS is necessary. Part of the material presented in this chapter is included in appendix A, which reviews the research on muscle synergies by emphasizing the input- or task-based perspectives of the various studies.

3.1 Time-varying synergy model

The idea of generating motor commands by combining a limited set of synergies has been formulated in a variety of models. A detailed review can be found in [Alessandro et al., 2013b], here we focus on the model that is used throughout the thesis. The *time-varying synergy model* was originally introduced by d'Avella et al. [2003], and then it has been extensively used in various experimental [d'Avella et al., 2011; Klein Breteler et al., 2007; Overduin et al., 2008] as well as computational [Chhabra and Jacobs, 2008; Mukovskiy et al., 2011; Nori and Frezza, 2005; Todorov and Ghahramani, 2003] studies. This model describes muscle activation patterns as the superposition of N_ϕ vector-valued functions of time $\boldsymbol{\phi} : \mathbb{R}^+ \to \mathbb{R}^m$ (where m is the number of muscles, and $\mathbb{R}^+$ represents the set of real numbers greater than or equal to zero):

$$\boldsymbol{u}(t) = \sum_{i=1}^{N_\phi} b_i \boldsymbol{\phi}_i(t - \tau_i). \tag{3.1}$$

Each synergy $\boldsymbol{\phi}_i(\cdot)$ represents the coordinated activation of m muscles during a given time interval, and it can be scaled in amplitude and shifted in time by means of the coefficients $b_i, \tau_i \in \mathbb{R}$; particular values of such coefficients lead to specific patterns of muscle activity.

In order to understand the implications of this model, let us consider the problem of motor coordination in terms of controlling a non-linear dynamical system representing the musculoskele-

tal apparatus. The scenario is depicted in Fig. 3.1. The "controller" has to generate the muscle activations that allow the musculoskeletal system to execute a desired motor task (blue line in the central panel). Thus muscle activations can be regarded as control signals, and are hypothetically generated according to Eq. (3.1). Depending on the task, the output variables may be joint angles, the position of the end-effector, force or impedance at the end-effector, a combination of them etc.

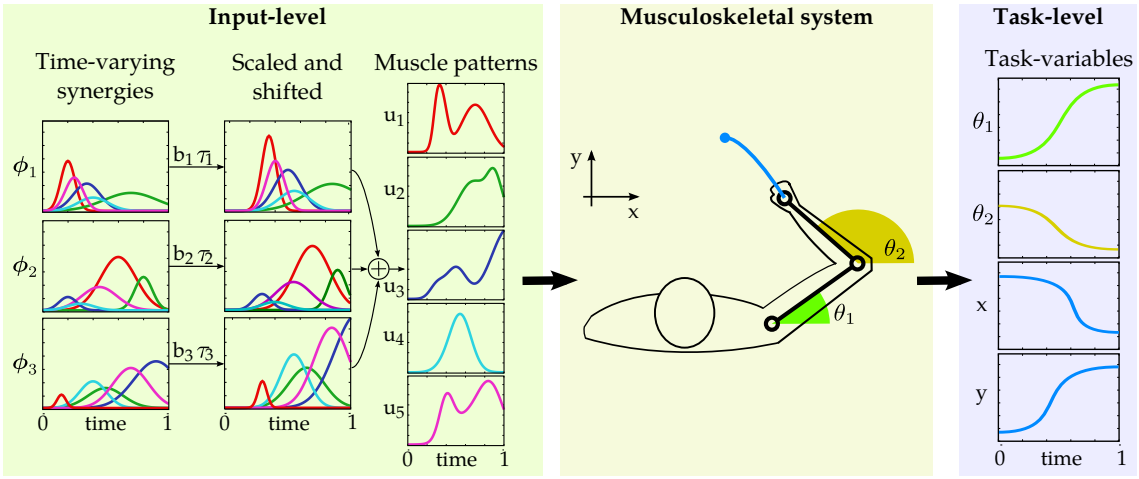

Figure 3.1: The problem of motor coordination from the control point of view. Muscle activation patterns represent the control signals to the musculoskeletal system, and are generated according to the time-varying synergy model. Synergies are time-varying recruitments of a group of muscles (5 muscles in this synthetic example) that can be scaled in amplitude and shifted in time by the coefficients a_i and τ_i. The values of these coefficients determine the generated muscle activation patterns, and therefore they should be selected appropriately to let the system execute the desired task (blue line in the central panel). In this example, the output of the system can be represented in joint-angles or in end-effector coordinates. However, depending on the desired task, other output variables may be used (e.g. end-effector force or impedance).

Classically, control signals belong to the infinite dimensional space of continuous functions. Under this assumption a number of interesting control properties (e.g. controllability and observability) can be proven. The idea behind modular control is to significantly restrict the set of admissible actuations[1] by constraining $\boldsymbol{u}(\cdot)$ to be a combination of modules. Specifically, in the model of time-varying synergy entire patterns of muscle activations are obtained by simply setting the values of the coefficients b_i and τ_i for $i = 1 \dots N_\phi$ synergies. Thus, the admissible control signals belong to a $2 \cdot N_\phi$ dimensional space.

The time-varying model bounds the admissible actuations to those that can be generated as in Eq. (3.1), and consequently it restricts the motor tasks that can be executed. In the rest of the thesis we refer to this set of actuations as the *synergy-span*. Other actuations can only be approximated by the most similar element of the this set (according to a defined measure of similarity). The shape (i.e. waveforms of $\{\boldsymbol{\phi}_i\}$) and the number of the synergies affect the synergy-span, and therefore determine the possible movements. From a **geometrical point of view**, synergies are the generators of the reduced set of admissible control signals; any desired actuation (which would theoretically lead to the desired task performance) is approximated by its projection onto the synergy-span. Since the system is non-linear, the error due to such an approximation might cause undesired task errors. Thus, the quality of a set of synergies should always be evaluated in terms of task-performance (i.e. at the task-level). A more complete characterization of muscle

[1] In this thesis the words actuations and control signals are used interchangeably.

synergies should therefore impose that such generators span a set of control signals that allow the satisfactory accomplishment of the desired tasks. In chapter 4 we propose a formal definition of this notion, i.e. a task-based definition of synergies.

In light of what has been discussed so far, in the following sections we present the main methodologies that have been employed to investigate the muscle synergy hypothesis. In experimental neuroscience synergies are often evaluated solely at the input-level (Sec. 3.2). On the other hand, computational approaches include a task-level assessment of the hypothesized modular control strategy (Sec. 3.3).

3.2 Synergies as generators of admissible control signals

In experimental neuroscience, the classical approach to evaluate the hypothesis of muscle synergies consists in searching regularities in a dataset of muscle activities. If such regularities are found, and they appear similar across motor tasks and experimental conditions, they are regarded as indirect evidence of a modular organization of the underlying neural circuitries. The model of time-varying synergies formalizes these regularities as the functions $\{\phi_i(\cdot)\}$, and the combination of modules as their delayed superpositions. The idea is then to decompose the dataset according to Eq. (3.1), and to compare the extracted components across experimental conditions.

The entire experimental procedure is depicted in Fig. 3.2 (continuous green arrows). A group of subjects is required to perform a variety of motor tasks (A); during the execution of the movements, their EMG signals are recorded (B). Finally, a linear dimensionality reduction algorithm (e.g. PCA, NMF) is employed to identify a small set of components (i.e. synergies), and to verify the extent to which their combinations can approximate the recorded dataset (C). The choice of the decomposition algorithm depends on the assumptions made on the nature of the hypothetical muscle synergies (e.g. non-negativity, orthogonality, statistical independence etc.), and on the proposed synergy model [Ting and Chvatal, 2010]. The approximation error is used to quantify the quality of the extracted synergies, and ultimately to test the validity of such a model. At this point, what remains unclear is the number of synergies that hypothetically are involved in the generation of motor commands. This issue is tackled by analyzing the trend of the approximation error as a function of the number of extracted components. The "correct" number of synergies is supposedly identified by the flattening point of this graph, i.e. the point where a drastic decrease of slope is observed. After this "elbow", the introduction of new components do not improve the quality of the reconstruction sensibly, and the residual approximation error is assumed to be due to noise in the dataset.

Let us now reinterpret this methodology in light of the considerations presented in Sec. 3.1. Essentially, the decomposition algorithm identifies the best linear approximation of the EMG dataset. Synergies are implicitly defined as the generators of the best approximating set of signals (i.e. synergy-span). A good approximation, and a high degree of similarity between the components of different datasets (recorded from different subjects or during distinct experimental conditions), lend credit to the proposed synergy model, and suggest that the motor commands might have emerged from the combination of a parsimonious set of modules. This procedure is therefore limited to the input-level (muscle activity). One might ask whether the approximations of the recorded EMG signals (i.e. combination of synergies) would actually lead to the observed task performance (Fig. 3.2, dashed green arrow). Due to the non-linearity of the musculoskeletal system, this is not guaranteed. A negative answer would imply that the proposed model is not valid.

Some of these issues have been investigated a-posteriori using realistic models of the musculoskeletal systems of different species [Berniker et al., 2009; McKay and Ting, 2012; Neptune et al., 2009]. Additionally, novel methodologies to deal with these challenges are starting to emerge in

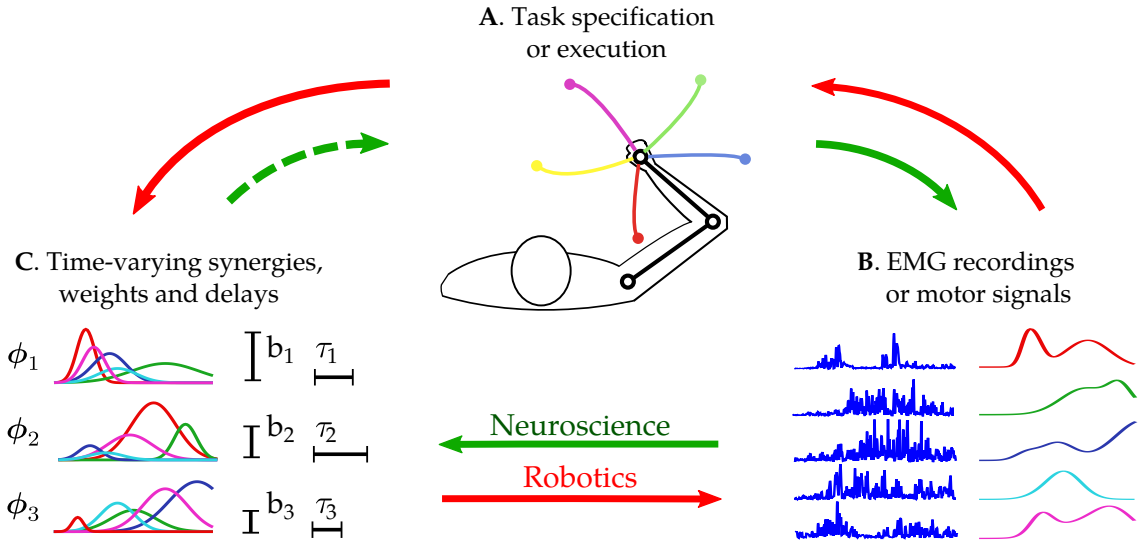

Figure 3.2: Procedures for the identification and the testing of muscle synergies. In experimental neuroscience (green arrows), initially a group of subjects perform the tasks prescribed by the experimenter (A). The EMG signals acquired during the experiments (B) are then analyzed, and a dimensionality reduction algorithm is applied to obtain the synergies (C). Very often such synergies are not evaluated at the task-level (dashed arrow), therefore there is no guarantee that they lead to the observed task performance. In robotics (red arrows), synergies are synthesized (C) based on the requirements of the desired class of tasks (A). Then they are appropriately combined to generate the motor signals (B) that solve a specific task instance. The quality of the synthesized synergies is finally tested in terms of the obtained task performance (A).

experimental neuroscience as well [Chvatal et al., 2011; Delis et al., 2013]. A shift of paradigm from an input-level to a task-level identification of muscle synergies, which seems to be already in progress, may contribute to a better understanding of the hypothetical modularity of the CNS, and of its relationship to human learning and control.

3.3 Synergies as generators of effective controllers

Building on the idea of muscle synergies, some researchers have proposed control strategies that are based on the linear combinations of a small number of predefined actuations (i.e. synergies). These studies either serve as proofs of concept for the muscle synergy hypothesis (computational motor control), or aim at developing low-dimensional methods to control artificial systems (robotics and control engineering). In both cases, their main focus is the synthesis of a small set of synergies that guarantees the accomplishment of some desired tasks.

Apart from minor variations on the theme, the general methodology of these studies can be conceptually represented as in Fig. 3.2 (continuous red arrows). The requirements of the desired tasks as well as the dynamics of the system (A) are used to guide the synthesis of a set of synergies (C). Such synergies are then appropriately combined (i.e. by means of the coefficients b_i and τ_i) based on the particular task instance to be solved. The obtained control signals (B) are then fed to the system, which executes the corresponding movement (A). If the performance of the obtained motor execution are poor in relation to the task requirements, then the set of synergies is not satisfactory. In a nutshell, synergies are interpreted as the primitives of an effective controller.

In the rest of the thesis we propose a principled investigation of the muscle synergy concept.

In particular, by following the procedure in Fig. 3.2 (continuous red arrows), we propose a formal definition of task-based synergies (chapter 4), a method for the synthesis of a set of synergies (chapter 5), and we analyze the relationship between task requirements, dynamical system and synergy set (chapter 6). In accordance with the rationale developed in this chapter, the synthesized synergies are evaluated both at the input- and at the task-level.

Chapter 4

Task-based definition of synergies

Building on the rationale presented in chapter 3, this chapter formalizes the notion of task-based synergies; i.e. generators of the actuations that guarantee the desired task-performance. This notion is tested for a linear and a non-linear dynamical system. This chapter refers to [Alessandro and Nori, 2012], appendix B.

In order to formalize the task-based definition of synergies, let us consider a set of desired tasks, defined as trajectories of the state- or output-variables of the system. As an example, these trajectories may represent sequences of positions that have to be tracked by the hand of a human subject or by the end-effector of a robot. Let us describe synergies as parametrized functions of time $\phi_i(t, p_1^i, ..., p_r^i)$. The values of the parameters $\{p_j^i\}$ determine the shapes of the synergies, and therefore they influence the actuations that can be generated by their linear combinations. Task-based synergies are identified by the optimal parameter values that minimize a measure of task performance; in [Alessandro and Nori, 2012] we use the sum of the tracking errors across the desired trajectories (training phase). The synthesized synergies are then tested for generalization (testing phase). The idea is to evaluate to which extent they can generate actuations that drive the system along a new group of trajectories (testing trajectories). It is worth reminding that synergies account for all the desired tasks, and the actuation corresponding to a specific trajectory is determined by an appropriate choice of the mixing coefficients. Therefore in the testing phase we fix the parameters $\{p_j^i\}$ to the values identified in the training phase, and we seek the synergy-weights that minimize the tracking error of the testing trajectories; the obtained error is used as a measurement of generalization.

The identification of task-based synergies was successful in both a linear and a non-linear system, and it was performed by numerical optimization. The results are shown in Fig. 4.1. The linear system is an agonist-antagonist pair of linear springs applied to a mass, where the output is the position of the mass, and the control variables are the resting lengths of the springs. The non-linear system is a pendulum, where the output is the angle of the rod with respect to the vertical axis, and the control variable is the joint torque. For both systems, each synergy ϕ_i is modeled as a polynomial of the 5^{th} order, the coefficients of which represent the parameters $\{p_j\}$. Training and testing trajectories are minimum-jerk evolutions of the output variables [Flash and Hogan, 1985]. To study the impact of the number of synergies on task-performance, we carry out the training procedure for an increasing number of synergies. For the linear system, the training error decreases drastically switching from one to two synergies, then it stabilizes to a constant value. This result is confirmed by a mathematical proof, which shows that for this system, two 5^{th} order polynomials are enough to obtain any minimum-jerk trajectory of the output variable [Alessandro and Nori, 2012]. The residual error is due to the local minimum found by the

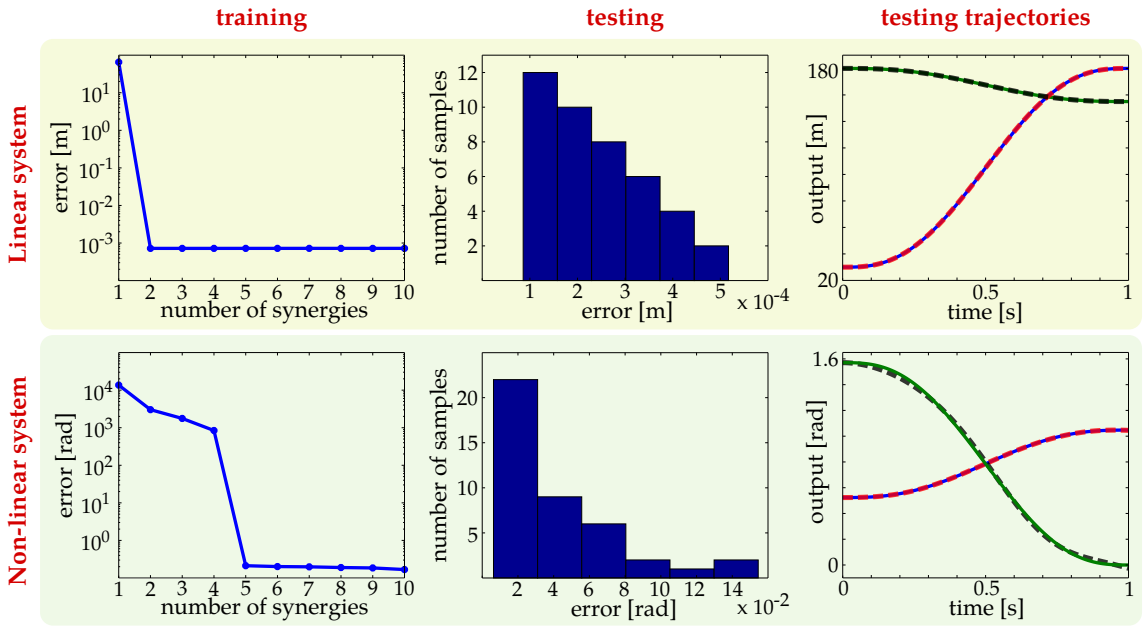

Figure 4.1: Identification and testing of task-based synergies for a linear and a non-linear dynamical system. The training procedure identifies 2 and 5 synergies for the linear and the non-linear system respectively. In both cases, the training error is comparable to the error made in tracking each of the 42 testing trajectories. The panels on the right show the desired (continuous lines) and the obtained (dashed lines) outputs for the best and the worst tracked testing trajectories.

optimization procedure. For the non-linear system, the training error decreases monotonically; however, the introduction of more than 5 synergies does not affects the performance significantly. This means that, for this system, most of the variability in the set of minimum-jerk trajectories of the output variable is captured by five control-signals described by 5^{th} order polynomials. The generalization performance is satisfactory for both systems. Training and testing errors are comparable, meaning that the synergies synthesized in the training phase (2 and 5 for the linear and the non-linear system respectively) allow the system to track the 42 testing trajectories.

In this chapter we have formalized the concept of task-based synergies and we presented some simulated examples. An issue that remains unsolved is the shapes that these synergies should have. The choice of using 5^{th} order polynomials is in fact arbitrary, and may be suboptimal. Nevertheless, the presented results allow the following non-trivial observation. The synergies optimized for the training trajectories are suitable to track many other trajectories of the same kind (i.e. minimum jerk). The relation between the class of tasks to be solved and the shape of the synergies is central to this thesis, and it will be further discussed in the next chapters.

Chapter 5

The Dynamic Response Decomposition

This chapter introduces Dynamic Response Decomposition (DRD), the control technique that we have developed to investigate the notion of muscle synergies. While the results of this analysis will be discussed in chapter 6, here we present DRD and its performance in controlling a planar kinematic chain for point-to-point and via-point tasks. This chapter refers to the papers [Alessandro et al., 2012] and [Alessandro et al., 2013a], appendices C and D respectively. The computational complexity of DRD is presented in appendix E.

5.1 Solution to task-constraints

Dynamic Response Decomposition (DRD) is a general method to find open-loop controllers for a dynamical system to solve desired tasks. The controller is defined as a linear combination of a limited set of actuations (i.e. joint-torques), termed synergies. The task is formalized by means of a set of point constraints that prescribe the desired values of the system state-variables at salient instants of time. As an example, a point-to-point reaching task constrains the desired initial ($t = 0$) and final ($t = T$) states of the dynamical system. Assuming the knowledge of the synergies $\{\boldsymbol{\phi}_i\}$, the DRD procedure can be summarized in the following steps:

1. Find a solution to the task in state variables (kinematic solution).
2. Compute the corresponding actuation $\tilde{\boldsymbol{u}}(t)$ by inverse dynamics.
3. Project $\tilde{\boldsymbol{u}}(t)$ onto the span of the synergies $\{\boldsymbol{\phi}_i\}$, obtaining the mixing coefficients $\{b_i\}$.
4. Compute the synergy-based controller $\boldsymbol{u}(t) = \sum_{i=1}^{N_\phi} b_i \boldsymbol{\phi}_i(t)$.

This procedure reflects the geometrical viewpoint discussed in Sec. 3.1: it first computes the "correct" actuation (step 2), and then it projects it onto the synergy-span (step 3-4), which is the set of admissible control signals.

The salient feature of DRD is that the kinematic solution (point 1) is obtained by linearly combining the dynamic responses (DRs) of the synergies; i.e. the time courses of the state-variables that are obtained by actuating the system with each $\boldsymbol{\phi}_i$. Mathematically, the kinematic solution is computed as $\boldsymbol{q}(t) = \sum_{i=1}^{N_\theta} a_i \boldsymbol{\theta}_i(t)$, where the vector $\boldsymbol{q}(t)$ contains the values of the system state-variables at time t, and $\{\boldsymbol{\theta}_i\}$ are the DRs. The mixing coefficients a_i are computed by imposing

the task-constraints to the linear combination of DRs (i.e. interpolation). This is done by solving the linear system of equation

$$\boldsymbol{M}\boldsymbol{a} = \boldsymbol{q_v}, \tag{5.1}$$

where the columns of the *alternant matrix* $\boldsymbol{M}$ contain the DRs evaluated at the time of the constraints, $\boldsymbol{q_v}$ is a column vector that embeds all the desired values of the system state-variables (*constraint-vector*), and $\boldsymbol{a}$ is the unknown vector of coefficients. It is possible to show that there exists a non-linear mapping between the mixing coefficients of the DRs and those of the synergies [Alessandro et al., 2012, 2013a]; its formal derivation can be found in appendix D, Eq. (D.8). The relevance of this finding will be discussed in chapter 7.

The quality of the obtained solution is assessed at different levels. The *interpolation error* evaluates the obtained kinematic solution with respect to the task constraints, the *projection error* is the distance between the actuation that solve the task $\tilde{\boldsymbol{u}}$ and $\boldsymbol{u}$, and the *forward dynamics error* measures the task performance obtained when $\boldsymbol{u}$ is used as actuation. In relation to what was discussed in chapter 3, the projection error is equivalent to the measure that is typically used in experimental neuroscience (i.e. the quality in approximating the EMG signals), and the forward dynamics error evaluates what is often neglected in those studies (i.e. the task-level error that is due to the approximation of the motor commands).

5.2 Synthesis of synergies

Until now we have assumed the knowledge of $\{\phi_i\}$, however DRD is also instrumental to synthesize an appropriate set of synergies. The procedure consists of two phases: exploration and reduction. Initially, a collection of random actuations is used to generate the DRs (exploration phase). These DRs are then employed to compute the kinematic solutions of a representative set of task instances (i.e. specific task constraints), called *proto-tasks*. The corresponding actuations are finally computed by inverse dynamics, and represent the synthesized synergies (reduction phase). As a result, such synergies are the actuations that solve the proto-tasks. In what follows, the control signals that are used during the exploration phase, and the corresponding DRs, are referred to as exploration-actuations and exploration-DRs respectively, or more generically as exploration-set or exploration-signals.

The quality of the synthesized synergies depends on the nature of the proto-tasks. In the next chapter we will discuss this point in detail; for now, let us just say that proto-tasks should belong to the class of the desired tasks (e.g. point-to-point, via-point). Intuitively, by so doing the obtained synergies will capture essential features of the system dynamics as well as of the desired tasks, and therefore they will be useful in approximating the actuations needed to perform similar movements. In order to keep the dimensionality of the controller as low as possible, synergies are added incrementally by solving the task instance characterized by the highest projection error (which thus serves as proto-task). This procedure continues until the average projection error, across the desired tasks, reaches a satisfactory threshold.

The procedure described above is applied to a simulated planar kinematic chain model of a human arm [Hollerbach and Flash, 1982]. In sections 5.4 and 5.5 we report the results obtained for point-to-point and via-point tasks. For the sake of clarity, before presenting these results, in the following section we summarize the main features and assumptions of DRD.

5.3 Features and assumptions of DRD

The main features of DRD can be summarized in the following list:

- Synergies and DRs are related by the dynamics of the system. In particular, each DR is the time course of the state-variables, that is obtained by actuating the system with one of the synergies. As a result, there are as many DRs as the number of synergies.
- The DRs are the kinematic solutions to the proto-tasks, and the synergies are the actuations leading to these kinematic solutions. Thus, there are as many synergies as the number proto-tasks.
- A kinematic solution to a desired task is obtained by linearly combining the DRs of the synergies. The corresponding actuation is then projected onto the synergy-span.
- There exists a non-linear mapping $\mathcal{F} : \mathbb{R}^{N_\theta} \rightarrow \mathbb{R}^{N_\phi}$ between the mixing coefficients of the DRs $\{a_i\}$ and those of the synergies $\{b_i\}$ (see appendices C and D for the derivation).

Let us now spend some words on the assumptions of the DRD method. In order to find a kinematic solution to a task (point 1 in Sec. 5.1), the DRs should be able to generate a state-space trajectory that fulfills the task-constraints; in other words, the linear system of equations (5.1) should have (at least) an exact solution. If this condition holds true, the projection error effectively estimates the difference between a control signal that solves the task, and its projection onto the synergy-span.

Within the procedure to synthesize synergies, the existence of an exact kinematic solution can be guaranteed by employing a large number of exploration-actuations (surely larger than the number of constraints of the proto-tasks). If the dynamical system is non-linear, very likely the resulting exploration-DRs will lead to an alternant matrix with full row-rank [Carbajal, 2012], therefore any proto-task can be solved. If the proto-tasks belong to the same class of the desired tasks, the formulation of the DRD provides a lower bound on the minimum number of synergies (and DRs) that are required to guarantee the existence of an exact kinematic solution. This point is discussed in detail in appendix D (Sec. D.3.1 and D.3.2).

Finally, to compute the actuation that leads to the kinematic solution, the inverse dynamic model of the system has to be known (point 2 in Sec. 5.1). In this thesis we provide this model a priori, however the inverse dynamics could be learned; in particular, it might be possible to identify a compact representation in the form of the mapping between the coefficients $\{a_i\}$, mixing weights of the DRs, and the coefficients $\{b_i\}$, mixing weights of the synergies. The reader is referred to Sec. 7.6 for a more detailed discussion on these topics. The biological plausibility of employing an inverse dynamical model is discussed in Sec. 7.4.

5.4 Point-to-point tasks

A point-to-point reaching task consists in reaching a final state from an initial state in a given amount of time. For a two degrees-of-freedom (dof) planar kinematic chain, a task-instance is then specified by four two-dimensional point constraints: initial and final joint angles and velocities[1]. In this section we restrict the analysis to the subclass of tasks that impose initial and final velocities equal to zero, and that are characterized by the same initial posture (i.e. a given joint-configuration). The only unspecified constraints are the joint-coordinates of the target; i.e. there are 2 free task-parameters. This allows to visualize the procedure to synthesize muscle synergies, and therefore to simplify its explanation.

Figure 5.1 shows the distribution of the projection error for an increasing number of synergies, and exemplifies the procedure that is used to incrementally add proto-tasks. Initially, two targets

[1]Note that the velocity constraints are not strictly necessary to define a point-to-point tasks. They have been added to restrict the class of desired tasks, and therefore to simplify the explanations. The same consideration holds for the other classes of tasks in the rest of the thesis.

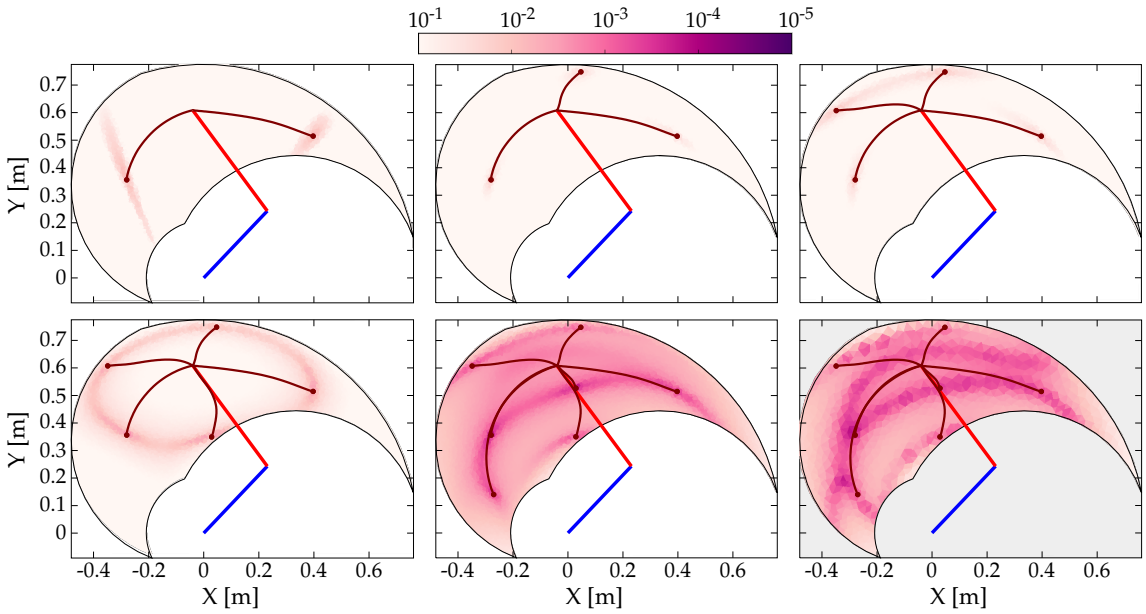

Figure 5.1: Selection of proto-tasks based on projection error for point-to-point tasks. Each panel shows the kinematic chain in its initial posture (straight segments), and the distribution of the projection error over the end-effector space (colored region). The color of each point indicates the projection error produced to reach a target in that position. The bottom right panel shows the distribution of the forward dynamics error using 7 proto-tasks (7 synergies).

are chosen randomly (top left panel); subsequent proto-tasks are then added in the regions characterized by higher projection error. As it can be seen, the introduction of new proto-tasks leads to better performance on wider regions of the end-effector space, and eventually the actuations needed to solve any point-to-point task can be reasonably approximated (projection error $< 10^{-2}$ with 7 synergies). The bottom right panel of the figure shows the forward dynamics error obtained with the 7 synergies. Comparing this panel with the bottom center one, it can be seen that the projection error reproduces the distribution of the forward dynamics error, rendering the former a good estimate of the relative forward performance across tasks. However it is important to stress that, due to the non-linearities of the dynamical system, the projection error serves only as a heuristic estimate of the actual error made when executing the task. These results show that a set of "good" synergies can drastically reduce the dimensionality of the controller, while maintaining satisfactory performance. Note that the controller has to "choose" the values of two joint-torques at each time-step, thus its dimensionality is much higher than the number of DoF of the system (in fact it is infinite dimensional if we consider actuations as continuous vector-valued functions of time). Hence, 7 synergies contribute a dimensionality reduction even if the system has 2 DoF [Alessandro et al., 2013b].

To further demonstrate that the reduction phase is not trivial, the errors resulting from the set of 7 synthesized synergies is compared to the errors corresponding to 100 random subsets of size 7 drawn from the exploration-signals (see Fig. 5.2). The testing tasks are identified by 13 desired targets distributed across the end-effector space. The 7 reduced DRs lead to an alternant matrix that can interpolate any point-to-point constraint-vector. As a result, in contrast to the case of random DRs, the obtained interpolation error is negligible for all the testing tasks ($err_I \simeq 10^{-15} \sim 0$). In terms of projection and forward dynamics error, the reduced synergies perform about 2–3 orders of magnitude better than any random subset. Additionally, they lead to high

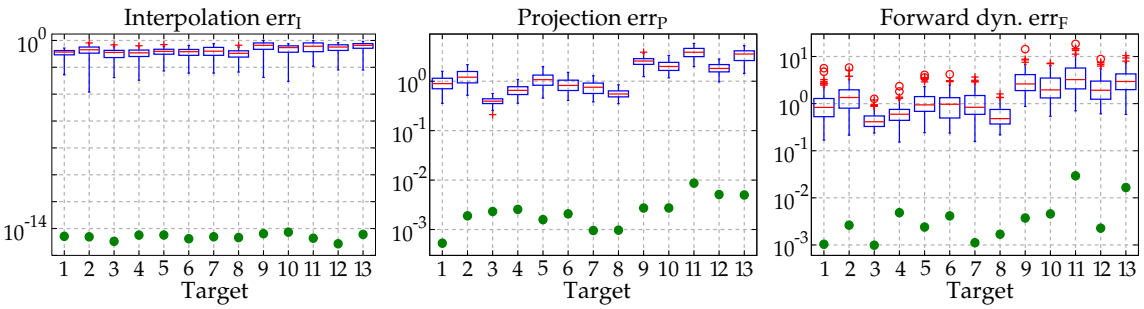

Figure 5.2: Evaluation of the reduction phase for the testing point-to-point tasks. Comparison between the synthesized synergies (filled circles) and subsets randomly selected from the exploration-actuations (box-plots; red crosses and circles are outliers).

task performance (forward dynamics errors in the range $[10^{-3}, 10^{-2}]$), yet greatly reducing the dimensionality of the controller.

5.5 Via-point reversal tasks

A via-point task consists in reaching a final state from an initial state in a given amount of time satisfying intermediate constraints called via-points. For a two-dof arm and a single via-point, each task instance is defined by the initial, the intermediate and the final desired positions and velocities (12 constraints). Here we restrict our analysis to a specific kind of via-point tasks, the reversal tasks. In this case, the desired final state coincides with the initial state. Essentially the system starts from a given configuration, reaches an intermediate target, and goes back to the initial state. The tasks considered in this section are characterized by the same initial (and final) position (i.e. a given joint-configuration), and impose initial, intermediate and final velocities equal to zero. Thus, the only free task-parameters are the joint-coordinates of the intermediate target (2 parameters). More involved tasks are discussed in chapter 6 and in appendix D.

As discussed above, proto-tasks are added incrementally. Since the position of the desired intermediate target is the only unknown, the newly added proto-task is identified by placing the via-point in the region of the operational space with the highest projection error. The introduction of additional proto-tasks (and therefore synergies) leads to lower values of the projection error; for this kind of tasks, at least 8 synergies are needed to obtain an average value $< 10^{-2}$. The similarity between the distributions of the projection and the forward dynamics error confirms that the former can be used as a qualitative estimate of the latter. Finally, the comparison between the synthesized synergies and the actuations drawn from the exploration-set shows that the reduction is a valuable procedure. Similarly to the results presented in the previous section, the synthesized synergies perform orders of magnitudes better than the exploration-actuations in terms of all the error measures. Additionally the forward dynamics errors lie in the range $[10^{-3}, 10^{-2}]$, meaning that the synthesized synergies lead to good task performance (see Sec. D.3.2).

Chapter 6

Computational insights on muscle synergies

The Dynamic Response Decomposition, beside its application for the control of dynamical systems, is instrumental to investigate aspects of the muscle synergy hypothesis that have proved to be difficult to address experimentally. In this chapter we summarize these results. Section 6.1 focuses on the shape of the synergies, Sec. 6.2 tackles the issue of the number of these elementary building-blocks, and finally Sec. 6.3 investigates another form of modularity in relation to muscle synergies, the sequential concatenation of simple sub-movements. Additional details can be found in appendix D [Alessandro et al., 2013a].

For the sake of clarity let us first introduce two concepts that we will use throughout the rest of the thesis. By *task complexity* we refer to the total number of constraints that are required to define a task. For example, for a two-dof kinematic chain, tasks with a single via-point that prescribe positions and velocities at initial, intermediate and final points have complexity equal to $6\text{x}2 = 12$ (each state variable is defined by a two-dimensional vector). In what follows we refer to task complexity with the letter C. The desired class of tasks can be further restricted by imposing certain invariant values to the state variables and their derivatives. As an example, the reversal tasks considered in this and the previous chapter impose zero velocities, and additionally fix initial and final positions to a specific point of the configuration space. Hence, although they are essentially via-point tasks, each instance is defined only by the position of the desired intermediate target. The *generality* of this class of task is therefore equal to 2 as the target is specified by two values (i.e. its joint-coordinates). In other words the generality of a class of tasks is the number of its free task-parameters.

6.1 Synergies as task solutions

The shape of the synergies determine the admissible motor commands, and therefore the tasks that can be executed. This aspect is very seldom analyzed; in fact, just a few computational studies have proposed principles that may underlie the formation of synergies (see Sec. 7.5). The dynamic response decomposition provides interesting insights on this important aspect. In particular, DRD suggests that synergies might be solutions to prototypical task instances. Specifically, in chapter 5 we stated that the proto-tasks should belong to the desired class of tasks. It is now time to support these statements with some further considerations.

The specifications of the desired class of tasks induce regularities to the corresponding control signals, and therefore restrict the desired actuations. In particular, the lower the generality of

this class, the lower the variability of the control signals. If the task is highly general, the set of required actuations will be characterized by a high degree of variability. These observations are exemplified in Fig. 6.1; as expected, the control signals corresponding to reversal tasks ($G = 2$, panel A) are on average more correlated ($\rho_s = 0.97$ and $\rho_e = 0.70$ for shoulder and elbow respectively) than the actuations corresponding to via-point reaching[1] ($G = 4$, panel B, $\rho_s = 0.67$, $\rho_e = 0.53$).

If the proto-tasks belong to the class of desired tasks, the synthesized synergies are samples of the desired actuations. As a result, they embed the characteristic features of these control signals, and therefore they can generate (by linear combination) good approximations of the other actuations belonging to the desired subset; this is particularly visible in the left panels of Fig. 6.1 (i.e. reversal movements). It is reasonable to expect that the number of required synergies is related to the generality of the desired class of tasks. Indeed if the control signals are characterized by a low degree of variability (e.g. reversal case), their essential features can be captured by an handful of samples. Otherwise, a higher number of synergies is required. These considerations are confirmed by the theoretical results presented in Sec. 6.2.

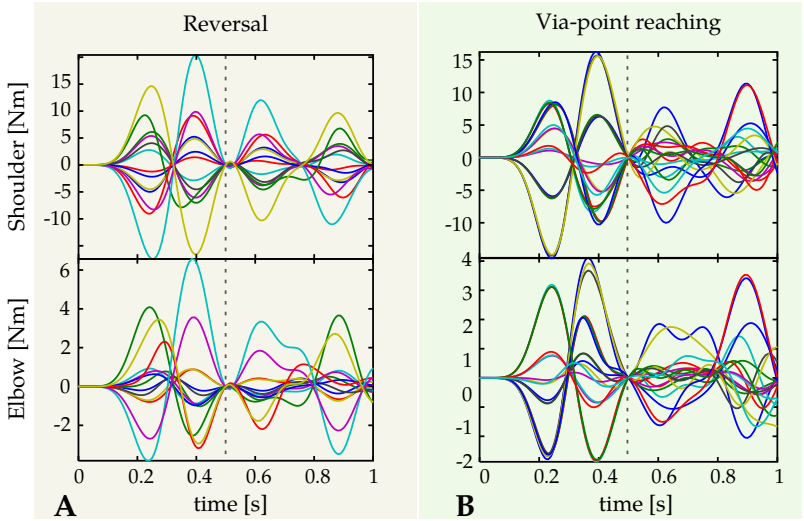

Figure 6.1: Actuations solving reversal and via-point reaching tasks. Since the latter class of tasks is more general, the corresponding control signals are less correlated than the reversal ones. This is particularly visible in the second phase of the movement (after the dashed vertical line that marks the time of the via-point). See text for the values of the correlation.

The effectiveness of the reduction phase is strictly related to the generality of the desired class of tasks. If this class is maximally generic (i.e. no task constraints impose invariant values across task instances), the control signals will not be characterized by any particular feature related to the tasks. Thus, the reduction phase becomes less useful, and the synthesized synergies will embed regularities that are solely due to the dynamics of the system. Additionally, in order to obtain good performance in all the desired tasks, a large number of synergies will be required (see Sec. 6.2). As a direct consequence, the performance of the synthesized synergies will approach the performance of generic actuations (e.g. the exploration signals). To exemplify this concept, we

[1] A via-point reaching task consists in reaching a desired state, passing through an intermediate via-point. Here we consider a class of tasks that is characterized by an invariant position of the via-point, and that imposes initial, intermediate and final velocities equal to zero. Therefore each task instance is identified by the joint-coordinates of the initial and final points (i.e. 4 free task-parameters)

synthesize synergies for three increasingly generic classes of tasks, and we use them to solve 13 reversal tasks. Figure 6.2 depicts the difference between the mean projection errors obtained by using subsets of the exploration actuations and the projection errors corresponding to the three sets of synergies. As expected, this difference diminishes for increasingly more general tasks.

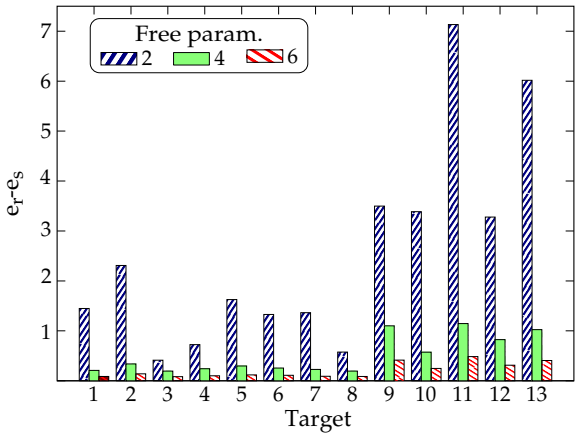

Figure 6.2: Difference between the mean projection errors obtained by using the random sets e_{ri}, and the projection errors associated to three sets of synergies e_{si} (i.e. $I_i = e_{ri} - e_{si}$ for each set i) for solving 13 reversal tasks. The three sets of synergies correspond to increasingly more general classes of tasks; i.e two, four and six free task-parameters (right diagonal blue, green, and left diagonal red bars respectively). This difference reduces for increasingly more general tasks, showing that the effectiveness of the reduction phase decreases as the actuations become less regular.

6.2 Number of synergies

How many synergies are required to implement an efficient controller? The formulation of the DRD demonstrates that this number strictly depends on the complexity of the desired class of tasks. To proceed with the explanation, let us analyze the linear system of equations that has to be solved to compute the kinematic solution (Eq. 5.1). To be able to interpolate any task constraint, the alternant matrix should have full row-rank, thus the number of columns should be greater or equal to the complexity of the task (i.e. the number of rows). Since the columns of the alternant matrix are populated by the DRs, this condition automatically poses a lower bound on the required number of synergies. Note this is only a lower bound because the alternant matrix should have C linearly independent columns, which might require more than C DRs. For a two-dof kinematic chain, general via-point tasks consist of three position and three velocity constraints (each of them is two-dimensional); thus, at least 12 DRs are required to be able to solve any task in kinematic space (see Eq. (D.5)).

The generality of the desired class of tasks has a direct influence on the minimum number of synergies. If all the tasks impose the same values to some of the state variables (i.e. low degree of generality), the corresponding elements of the constraint-vectors are invariant across task-instances. Thus, the required minimum number of linearly independent columns of the alternant matrix, and therefore the minimum number of synergies and DRs, decreases (i.e. the linear systems of equations can be solved even if the alternant matrix does not have full row-rank); see the linear systems of equations (D.12) and (D.13) as examples. In other words, similarly to what happens to the control signals (see Fig. 6.1), the constraints imposed by the class of

tasks restrict the relevant kinematic trajectories, and therefore less DRs are needed to generate them. For example, reversal tasks ($G = 2$) require 3 DRs (instead of 12, as required by maximally general tasks), while for via-point reaching ($G = 4$) this number increases to 5 [Alessandro et al., 2013a].

The lower bound discussed so far represents a necessary condition for the existence of a kinematic solution to each desired task. Such a bound is solely based on kinematic considerations. Since the dynamical system is non-linear, this number does not guarantee low values of projection and forward dynamics error. In fact, the number of synergies that is required to obtain satisfactory performance is certainly higher than the theoretical kinematic-based estimation. Figure 6.3 shows the trend of the average projection error as a function of the number of synergies for three classes of via-point tasks. Depending on the required precision, more or less synergies can be employed. In any case, as predicted from the theory, the number of required synergies increases with the generality of the desired class of tasks ($G = 2$, $G = 4$, $G = 6$ for the continuous blue, dotted red and dashed green lines respectively).

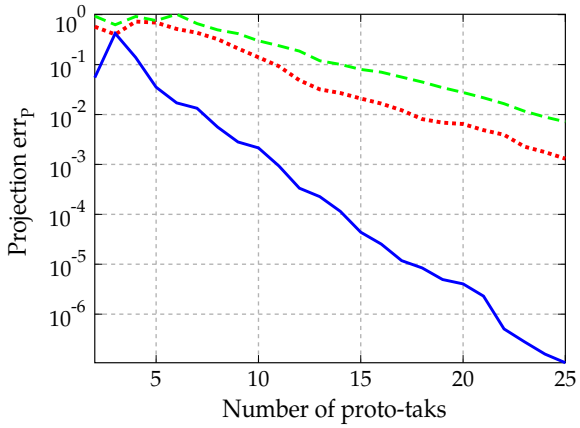

Figure 6.3: Averaged projection error as a function of the number of proto-tasks for increasingly general classes of via-point tasks. The least general tasks are reversal motions (blue continuous line), characterized by two free task-parameters (i.e. configuration of the intermediate target). An increase in generality consists in fixing only the initial posture, while intermediate target and final position represent free task-parameters (red dotted line). Finally the most general class (green dashed line) does not fix any posture (6 free task-parameters). The number of synergies that is required to achieve a given value of error increases with the generality of the class of tasks.

6.3 Muscle synergies and kinematic modularity

Reversal and via-point reaching tasks are composed of two different kinematic phases, or sub-movements: from the initial to the intermediate point, and from the intermediate to the final point. Therefore, it should be possible to generate suitable control signals by concatenating the actuations associated to the individual point-to-point tasks, each solved by means of DRD. The obtained results are consistent for both the reversal (Sec. D.3.2) and the via-point reaching tasks (Sec. D.3.3), and can be summarized as follows. The forward dynamics error of the first point-to-point task is propagated over the second sub-movement according to the dynamical properties of the system, and it might either compensate or amplify the error of the second point-to-point task. Therefore, compared to applying DRD to the entire via-point tasks, the concatenation-based

solutions are affected by an additional source of errors, which results in overall poorer forward dynamics performance. Additionally, in order to allow the kinematic compatibility between the two point-to-point trajectories, concatenation requires additional task constraints that regulate the value of the state variables at the via-point (increasing the complexity of the task). On the other hand, if the class of desired tasks is very general, solving the entire task by means of DRD may require a large number of synergies (see previous sections). In this case, the concatenation method might be a viable alternative to keep the dimensionality of the controller low. As an example, to obtain a certain level of performance on via-point reaching tasks ($G = 4$), the entire DRD solution requires 17 synergies, and the concatenation strategy needs 6 synergies for each point-to-point sub-movement. The possible implications of these results for the concept of kinematic strokes [Novak et al., 2003] are discussed in Sec. 7.3.

Chapter 7

Discussion

7.1 Summary of the results

In this thesis we have proposed an analysis of the muscle synergy hypothesis from a computational perspective; i.e. the control of a dynamical system through linear combinations of a limited set of actuations (motor synergies). While synergies are often interpreted only as the generators of the reduced input-space, here we have stressed a complementary viewpoint: synergies are the basic primitives of a modular controller, and as such they should be evaluated in terms of task-performance. We have formulated this concept in terms of the notion of task-based synergies, and we have tested it for a linear and a non-linear dynamical system.

Although a numerical optimization can be used to synthesize task-based synergies, this procedure is computationally very costly and it requires some assumptions regarding their shapes. To overcome these issues and allow a systematic investigation of synergy-based controllers, we have introduced the Dynamic Response Decomposition (DRD) method. The performance of this algorithm has been tested on a planar kinematic chain for point-to-point and via-point tasks. The DRD is a method to compute open-loop controllers that allow a dynamical system to solve desired tasks. In particular, it generates a kinematic solution to a task by combining the dynamic responses of the synergies, and it employs the inverse dynamics to compute the corresponding actuation. Such an actuation is finally projected onto the synergy-span. The reduction procedure of DRD builds a parsimonious and effective set of synergies out of an extensive set of exploration-signals by computing the actuations solving the proto-tasks. The obtained signals outperform hundreds of arbitrary choices of basic controllers taken from the exploration set. This result, that is consistent across all the error measures, suggests that synergies might represent solutions to prototypical task instances. This idea is further supported by the observation that the obtained primitives embed characteristic features of the desired control-signals, and therefore can approximate similar actuations successfully.

The number of required synergies to achieve a given task-performance depends on the generality of the desired class of tasks (i.e. number of free task-parameters); general tasks (e.g. via-point reaching) require more synergies than highly specific ones (e.g. reversal). This implies that if the proto-tasks belong to the desired class of tasks, the resulting synergy-set will be minimal. Vice-versa, if the proto-tasks are instances of a more general class, a higher number of primitives will be synthesized. Therefore, from the point of view of dimensionality reduction, it is convenient to develop a set of synergies that is specialized to a particular behavioral need. These considerations indicate that synergies are strictly tailored to the tasks to be solved. Furthermore, since they are computed by applying inverse dynamics to the kinematic solutions of the proto-tasks, they also have an explicitly dependence on the dynamics of the system.

Since via-point tasks are constituted by two distinguished kinematic phases, they could be solved by concatenating the actuations associated to the different sub-movements; such actuations are in turn generated by linearly combining appropriate point-to-point synergies. This strategy is related to the notion of kinematic primitives [Flash and Hochner, 2005], and it represents a control scheme that, for the first time, integrates this form of modularity together with muscle synergies. The obtained results show that the concatenation method accumulates the errors of the individual sub-motions, and it requires additional constraints to smoothly join the kinematic sub-movements. On the other hand, the application of DRD to the entire via-point task requires the definition of well specified proto-tasks. If these details are not available, or if the class of tasks is too general, concatenation could be a viable strategy.

The goal of this work was not to provide a model of the formation and the development of muscle synergies, nor at the current stage to claim that the reduced synergies fit human data. Rather our goal was to understand the implications of the hypothesized modular controller. Although our approach involves many assumptions and simplifications, we believe that it conceptually highlights important aspects of this form of modularity, aspects that are not always taken into account in experimental studies. Certainly, our work serves as a proof of concept for the idea of generating useful motor signals from the linear combination of a limited set of control primitives.

A simplification that is worth discussing is the usage of a kinematic chain rather than a muscle-driven skeletal model. This implies the definition of control signals (and therefore synergies) in the space of joint torques, and not in muscle activation space. In a musculoskeletal system, the non-linear relation between torques and kinematic variables is complemented by the additional non-linear dynamics that translates muscle activations into joint torques. The total mapping between muscle activations and kinematic variables is non-trivial. The chain of the two non-linear relations might either compensate each other, resulting in overall milder non-linearities, or form an even stronger one. In any case, from the conceptual point of view, the essence of the problem does not change, i.e. the possibility of controlling the output variables of a non-linear dynamical system (i.e. kinematic chain or musculoskeletal model) by means of a linear input strategy (i.e. linear combination of torques or muscle synergies). We intend to evaluate DRD in more biologically plausible systems in future developments of our work.

7.2 Relation between task-based synergies and DRD

In the previous chapters we have presented separately the definition of task-based synergies and the method to synthesize synergies in DRD. However, they are closely related to each other. The definition of task-based synergies requires a parametrization of the functions $\{\phi_i\}$. These parameters define the shapes of the synergies, and they are optimized to minimize the task-performance on a set of desired tasks. In chapter 4 we modeled each synergy as a 5^{th}-order polynomial. This was just a working assumption and, in fact this choice could be suboptimal. On the other hand, the DRD suggests that each synergies is a solution to a proto-task (see chapter 5). While this method does not impose any specific parametrization explicitly, as a matter of fact the shapes of the synergies depend on the particular proto-task instances. Thus, the constraints defining the proto-tasks can be considered as the synergy-parameters. In accordance with the definition of task-based synergies, these parameters can be optimized in order to minimize the task-performance (i.e. forward dynamics error) over a set of desired tasks. From this perspective, the synergies synthesized by means of DRD (following the above procedure) can be considered as specific cases of task-based synergies.

In practice, the numerical optimization that is required to compute task-based synergies is computationally very costly and it suffers the problem of local minima. In order to avoid these

problems and be able to perform systematic experimentation, in chapter 5 the proto-tasks were selected by means of a heuristic procedure: the newly added proto-task was chosen to be the task characterized by the highest projection error (see Sec. 5.2). Task-performance was checked a posteriori in terms of forward dynamics error. The relation between this heuristic procedure and the minimization of the forward dynamics error is non-trivial as it involves the non-linear dynamics of the system. In any case, the empirical results presented in this thesis are very encouraging: the distribution of the projection error reproduces the distribution of the forward dynamics error, and the inclusion of new synergies reduces systematically the mean projection error across tasks. A comprehensive theoretical analysis is left for future work. The development of a projection error-based procedure that produces task-based synergies would allow a deeper analysis of this concept, perhaps leading to very interesting outcomes. For example, using realistic musculoskeletal models, it could be possible to investigate the extent to which task-based synergies approximate the components extracted from experimental data (e.g. EMG-signals).

Finally, it is worth mentioning that the task-based definition of synergies is mathematically very similar to the Karhunen-Loève decomposition, or Principal Component Analysis (PCA) (see appendix B). As the Karhunen-Loève functions are the components that better approximate a random process, task-based synergies are the elementary control-signals (i.e. input to a dynamical system) leading to the best approximation of a set of desired output trajectories. In the future it will be interesting to compare task-based synergies (synthesized by means of DRD as explained above) to the principle components of the desired actuations.

7.3 DRD and muscle synergies

Due to the nonlinearity of the body dynamics, small actuation errors might lead to undesired task-performance. This justifies the need to distinguish between projection and forward dynamics error; while the former can be considered only as a heuristic measure, the latter explicitly quantifies the quality of the synergy-based controller. Many studies in experimental neuroscience analyze the validity of the muscle synergy hypothesis solely in terms of a measure that is equivalent to our projection error, i.e. the accuracy in approximating recorded EMG signals [Cheung et al., 2009a; d'Avella and Bizzi, 2005; d'Avella et al., 2003; Torres-Oviedo and Ting, 2007, 2010]. We believe that the introduction of complementary task-based measures could shed new lights on the hypothetical modularity of the CNS [Alessandro et al., 2013b; Delis et al., 2013].

In this vein, some researchers introduced the concept of functional synergies, i.e. the components of an extended dataset that includes muscle activations as well as measurements of task variables (e.g. joint angles, end-limb force) [Chvatal et al., 2011; Torres-Oviedo et al., 2006]. As a result, each component consists of two elements: a pattern of muscle contractions, and the corresponding evolution of the task variables. Such an approach is not too different from the idea behind DRD: synergies are associated to their DRs (i.e. biomechanical functionalities), which are linearly combined to obtain the kinematic solution of the task. However, the identification of functional synergies by means of non-negative matrix factorization (NMF), implies that muscle synergies and their biomechanical functionalities are scaled by the same coefficients. This contrasts with our theoretical results, which show a nonlinear relationship (the mapping $\mathcal{F}$, see Sec. 5.2) between the mixing weights of the synergies and those of the DRs (see chapter 5). Ideally, one should go beyond the use of NMF, and develop novel techniques that do not impose a linear mapping between the two sets of coefficients.

The mathematical formulation of DRD shows a clear relation between the minimum number of synergies and the difficulty of the task. To guarantee the existence of a kinematic solution, the alternant matrix should be full-row rank. In other words, the number of proto-tasks, and therefore of synergies, should at least be equal to the dimensionality of the task-constraint vector (i.e. task

complexity). If the desired class of tasks is better specified (i.e. low generality), the required number of synergies reduces. It is important to stress that these considerations represent the necessary conditions to guarantee the existence of a kinematic solution for any task that belongs to the desired class. If only specific instances of such tasks are relevant (e.g. reaching some given points of the phase space), the minimum number of synergies can be reduced even further. Having this in mind, it is not surprising that a dataset of recorded biomechanical signals can be approximated by a number of synergies that is lower than what is suggested by our framework. Such datasets are indeed recorded during specific and constrained task instances.

An important aspect of DRD is that synergies are related to the DRs through the dynamics of the system. As a result, since the DRs are feasible kinematic solutions to the proto-tasks, the obtained synergies can always be realized as actuations. The same cannot be said, in general, for synergies identified from numerical analyses of biomechanical data. Though some studies have verified the feasibility of the extracted synergies as actuations [Allen and Neptune, 2012; McGowan et al., 2010; Neptune et al., 2009], biomechanical constraints are not explicitly included in the extraction algorithms. Additionally, the employment of the system dynamics provides an automatic way to cope with smooth variations of the agent morphology. That is, both the synergies and their dynamic responses evolve together with the body. In line with Nori [2005] and Alessandro et al. [2012], these observations highlight the importance of the body in the hypothetical modularization of the CNS, an idea that is, in spirit, close to the philosophy of embodiment [Pfeifer et al., 2007].

The concatenation of point-to-point control signals to solve via-point tasks is based on the observation that movements can be composed of a sequence of kinematic strokes, or sub-movements. There is still no agreement on whether these motion chunks reflect a segmented form of control, however it has been hypothesized that they could serve as building blocks to internally represent and plan complex motions [Flash and Hochner, 2005; Giszter et al., 2010]. The relation between this form of planning modularity and muscle synergies is still under debate. Possibly, as implemented in our formulation (see Sec. 6.3 and appendix D), each kinematic stroke translates into a combination of time-varying synergies, and therefore the final movement plan corresponds to a sequence of mixing weights. This strategy is in line with the hypothesis of an intermittent controller that sequentially initiates discrete movement primitives [Fishbach et al., 2005; Karniel, 2013; Loram et al., 2010; Squeri et al., 2010]. Sub-movements might be combined in time succession, or based on the vectorial summation of overlapping preplanned trajectories [Novak et al., 2003; Pasalar et al., 2005; Roitman et al., 2004]. In this thesis we exemplify the case in which the kinematic sub-movements are sequenced in time. Interestingly enough, d'Avella et al. [2011] showed that the synergies underlying point-to-point kinematic trajectories could also account for more complex trajectories involved in reaching a jumping target, by modulation and delayed superposition. The analysis of this approach within DRD is non-trivial, and it is therefore left for future work. This development will probably involve trajectory-modification tasks rather than via-point constraints. Finally, it is important to notice that a kinematic solution to a via-point task appears to be composed of different movement-chunks even when it is obtained from a single composition of synergies. This observation supports the idea that strokes could just emerge as a result of the trajectory optimization [Dagmar and Schaal, 1999] or even be data analysis artifacts.

Lastly, we would like to speculate on a possible developmental interpretation of the method we propose to synthesize synergies. Initially, the agent explores its sensory-motor system employing a variety of actuations. Then, it attempts to solve the first tasks (proto-tasks), perhaps obtaining weak performance as the exploration phase may not have produced enough responses yet (see the box-plots in Fig. 5.2). If the agent finds an acceptable solution to a proto-task, such a solution is used to generate a new synergy (populating the set of DRs), otherwise it continues with the exploration. The failure to solve important tasks for its survival, could motivate the agent to include additional proto-tasks; Fig. 5.1 illustrates this mechanism. The development of

the synergy-set incrementally improves the overall abilities of the agent. Alternatively, existing proto-tasks could be modified. It has to be clear that we are not arguing in any way that this procedure resembles the biological mechanisms involved in the motor development of organisms; it is however interesting that our procedure allows the autonomous generation of new synergies, and the possible adaptation of existing ones to cope with changes in body dynamics. These features are in line with some recent findings [Dominici et al., 2011]. An alternative strategy for synergy development (not implemented in this thesis) might be the concatenation of movement chunks. If the agent has already developed the synergies to solve point-to-point tasks, via-point proto-tasks could be solved by the concatenation of point-to-point actuations. As shown in Fig. 5.2, the results might not be as good as when the solutions were computed ad-hoc (i.e. for the entire via-point proto-tasks). However, taking inspiration form Sosnik et al. [2004] and Rohrer et al. [2004], one could imagine that such solutions might improve with practice, eventually leading to appropriate via-point modules.

7.4 DRD, muscle synergies and internal models

One of the assumptions of the DRD method is the knowledge of the dynamical model of the system (see Sec. 5.3). This model allows to compute the actuation associated to a kinematic solution (i.e. linear combination of DRs) of a given task; such an actuation is finally projected onto the synergy-span, obtaining the weights to combine the synergies. The assumption of a dynamical inversion in the process of motor control is supported by the hypothesis of internal models [Kawato, 1999; Wolpert and Kawato, 1998].

The hypothesis of internal models postulates the existence of dedicated neural mechanisms that (i) predict the behavior associated to given motor commands (forward models), and (ii) compute the motor commands required to implement a desired motor task (inverse models). The idea that internal models are constituent parts of the motor system is supported by many behavioral [Ahmed et al., 2008; Burdet et al., 2001; Gaveau et al., 2011] as well as physiological studies [Cerminara et al., 2008; Imamizu et al., 2003; Kawato et al., 2003]. However, the relationship between internal models and muscle synergies is still under debate.

The mapping $\mathcal{F}$ between the coefficients of the DRs and those of the synergies (see Eq. (D.8)) can be interpreted as a mathematical representation of an inverse model; it indeed translates movement plans (encoded in the weights of the DRs) into motor commands (encoded in the weights of the synergies). Since this mapping depends both on the dynamics of the system and on the synergies, we speculate that muscle synergies might be involved in the neural implementation of the hypothesized internal models. This view is consistent with the recent opinion that "muscle synergies represent consistent motor modules that map intentions to actions" [Ting and McKay, 2007; Torres-Oviedo and Ting, 2010].

The existence of internal models is typically demonstrated by observing the slow adaptation of subjects to externally-imposed disturbances during the execution of a simple task (e.g. reaching) [Hirashimasend and Nozaki, 2012; Shadmehr and Mussa-Ivaldi, 1994; Tong and Flanagan, 2003]. Here we propose that such an adaptation might correspond to a gradual modification of the synergies associated to that task (and therefore of the mapping $\mathcal{F}$). This idea provides a possible explanation to the following experimental observation: the human CNS can easily switch between different tasks, but it adapts slowly to new environment-dynamics for the same movement. The former scenario might involve switching between sets of synergies previously learned. On the other hand, the adaptation to a new dynamics might imply the modification of the synergies associated to the desired task, a slower and more involved process. This hypothesis builds on one of the conclusions of this thesis, i.e. there might exist different sets of synergies associated to distinct tasks. Finally, the distinction between movement plans and motor commands renders the DRD

method a good candidate to explain the capability of humans to simultaneously adapt to various environment-dynamics associated to different plans [Hirashimasend and Nozaki, 2012], and to explain the switching between multiple solutions of the same task [Ganesh and Burdet, 2013].

7.5 Comparison with other computational studies

While many studies try to validate or falsify the hypothesis of muscle synergies, only a few researchers have focused on developing and testing control architectures based on this concept. Some of these works aim at proposing novel techniques for robot control, others intend to analyze the hypothesized modularity from a computational point of view. Our work falls into the second category; in this section we briefly compare it to similar contributions, in particular to those studies that provide a possible interpretation of muscle synergies. The reader is referred to [Alessandro et al., 2013b], appendix A, for a more comprehensive review.

Taking inspiration form the work by Mussa-Ivaldi [1997], Nori and Frezza [2005] developed a control architecture for non-linear systems based on the idea of spinal force fields [Giszter et al., 1993; Mussa-Ivaldi and Bizzi, 2000; Mussa-Ivaldi et al., 1994; Nori, 2005]. Relying on the technique of feedback linearization, the method yields a set of synergies that is able to generate a complete repertoire of movements (i.e. the system can reach any arbitrary state in an arbitrary amount of time). Thus, the authors interpreted muscle synergies as a basis of the entire set of desired control signals. Berniker et al. [2009] proposed that synergies are the input-primitives that can explain the dynamics of a reduced-order model of the agent. These primitives are found by an optimization procedure that minimizes the difference between the state-space trajectories obtained by controlling this model by linear combinations of synergies, and a representative dataset of sensory-motor data generated by perturbing the reduced dynamics with input pulses. Similarly, Todorov and Ghahramani [2003] employed an unsupervised learning procedure to identify muscle synergies from a collection of sensory-motor data, which was obtained by actuating the robot with random signals. Their work proposes that synergies are a constituent part of an inverse model of the sensory-motor system. Another interpretation suggests that synergies solely reflect the biomechanical constraints of the agent [Marques et al., 2012].

As discussed in Sec. 5.2 and 6.1, our work suggests that synergies are solutions to well-defined control problems. Similar ideas have already been proposed [Chhabra and Jacobs, 2008; Thomas and Barto, 2012; Todorov, 2009]. However, these studies do not investigate which class of problems is best suited. In this manuscript we show that these problems (i.e. proto-tasks) should belong to the same class of the desired tasks; this leads to a compact set of effective synergies. Additionally we show a clear relation between the number of synergies and two characteristics of the task: generality (i.e. number of free task-parameters), and complexity (i.e. number of constraints). Further, we propose a possible integration scheme between kinematic stroke and muscle synergies; to the best of our knowledge no other synthetic study has tested this idea.

7.6 The DRD method and its relevance to robotics

In the DRD method, once the task is solved in kinematic space, the corresponding actuation can be computed using the explicit inverse dynamical model of the system. It might appear that there is no particular advantage in projecting this solution onto the synergy set. However, the differential operator might be unknown or affected by errors; this is very often the case in robotics, where learning inverse models is still a hot topic of research [Nguyen-Tuong and Peters, 2011]. A synergy-based controller would allow to compute the appropriate actuation by evaluating the mapping $\mathcal{F}$ on the mixing coefficients of the DRs $\{a_i\}$, hence obtaining the synergy-weights $\{b_i\}$.

Since $\mathcal{F}$ is a mapping between two finite low-dimensional vector spaces, estimating this map may turn out to be easier than estimating the system dynamics. In order to estimate the map $\mathcal{F}$, the input-output data generated during the exploration phase could be used as learning data-set. The obtained relation could be instrumental to estimate a first guess of the synergy set; $\mathcal{F}$ and $\{\phi_i\}$ could then be iteratively modified until convergence. Further work is required to test these ideas.

The current formulation of the method does not include joint limits explicitly. The interpolated trajectories are valid, i.e. they do not go beyond the limits, due to the lack of intricacy of the boundaries. In higher dimensions, especially when configuration space and end-effector are not mapped one-to-one, this may not be the case anymore. Nevertheless, joint limits can be included by reformulating the interpolation as a constrained minimization problem. Another solution might be the creation of proto-tasks with a tree-topology, relating DRD to tree-based path planning algorithms [Shkolnik and Tedrake, 2011] and the concatenation of solutions.

With regard to the scalability of the DRD method, the following considerations can be made. The dimensionality of the dynamical system affects the procedure to synthesize synergies (see Sec. 5.2). For high dimensional systems, the number of parameters that have to be explored in order to identify the next proto-task (i.e. the one characterized by the highest projection error) might be large. However, if the desired class of tasks is not too general, this number can be reduced. Furthermore, instead of seeking the task with the highest projection error, one could think of defining the next proto-task as the actual task to be solved: if the current synergies do not lead to satisfactory performance, such a task could be solved by means of the exploration-set, and the obtained solution could represent the new synergy. This strategy does not involve any search, and therefore is not affected by the number of dof. It is important to note that the dimensionality of the system does not pose a problem on the actual algorithm to solve a task: this algorithm only involves solving a linear system of equation, applying inverse dynamics, and projecting the obtained actuation onto the synergy-span. Finally, the number of dof to be controlled influences the dimensionality of the task-constraint vector (i.e. complexity of the task, see chapter 6), therefore a high dimensional system requires more synergies than a lower dimensional one to achieve the same level of performance.

Despite the difficulty of the mathematical problem (i.e nonlinear differential operator), DRD seems to generate a small set of synergies that span the set of required actuations. Similar results have been reported using other nonlinear systems besides kinematic chains [Carbajal, 2012]. These are non-trivial results since the reduced synergies out-perform the subsets randomly taken from the exploration actuations (see Fig. 5.2). By gradually increasing the generality of the desired class of task, the performance difference between the synergies and the random signals reduces systematically, and the number of synergies that is required to reach a certain error threshold increases. It appears as if the reduction phase captures important features of the desired actuation space. A theoretical formulation of these empirical observations is currently under development (see Sec. 7.2).

Chapter 8

Conclusions and future work

Research on muscle synergies mainly aims at investigating the hypothesis that the CNS generates muscle activity by combining a limited set of modules. Most of experimentation focuses on physiological aspects of this concept, and is typically based on the analysis of EMG signals. This thesis examines a complementary aspect: the implications of such a hypothetical modular organization from the control point of view. To this end, we have considered the problem of controlling a dynamical system in accordance with the time-varying synergy model. This approach forces us to consider various issues that are not easy to address experimentally, and to provide possible explanations.

The first, yet fundamental, implication of a synergy-based controller is that the admissible motor signals are restricted to those that can be generated by combinations of synergies (i.e. synergy-span). This consequently limits the motor tasks that can be executed. The shape and the number of synergies determine synergy-span, therefore such attributes should be chosen to accommodate the desired actuations (i.e. the actuations that solve the desired tasks). The quality of the synergy-set should always be evaluated in relation to task-performance. Indeed, due to the non-linearity of the dynamical system (e.g. musculoskeletal apparatus), an apparently low control error could cause an unsatisfactory accomplishment of the desired task. This concept is formalized in the definition of task-based synergies.

The proposed Dynamic Response Decomposition method is able to generate effective synergies, greatly reducing the dimensionality of the problem, while keeping a good performance level. Its formulation shows a clear relation between synergies and desired tasks. In particular, it suggests that synergies are solutions to prototypical task instances; in other words, they may be samples of the desired set of actuations. Such synergies embed essential features of these actuations, and therefore they can generate (by linear combination) good approximations of similar control-signals. It is important to note that tasks and corresponding actuations are related by the dynamics of the system, which hence has a direct influence on the synergy-set. Furthermore the formulation of DRD offers a lower bound on the minimum number of required synergies; this number increases with the generality of the desired class of tasks. This implies that, from the standpoint of dimensionality reduction, developing different specialized sets of synergies, that are selectively used based on the desired movement, is more convenient than employing a single (large) synergy-set for any task.

In relation to the notion of kinematic strokes, synergies might represent the low-level primitives that are combined to implement the single sub-movements. Simple point-to-point synergies can be used to generate solutions to via-point tasks by concatenating the actuations associated to the individual movement phases. However, the usage of specific via-point synergies reduces the possible sources of errors, and in many cases it leads to better task performance.

The future developments of this research point towards different directions. It will be inter-

esting to validate the predictions of the DRD (e.g. number and shape of the synergies) on real biological data. Since these predictions are highly dependent on the dynamical system used, a first step will be the evaluation of our method on realistic musculoskeletal models. This approach will guide further experimentation to improve DRD, paving the way towards a predictive model of muscle synergies.

From the theoretical point of view, we are currently studying the mathematical properties of the synthesized synergies. These synergies will be compared to the main components of the desired actuation-set as identified by various decomposition methods (e.g. PCA, ICA, NMF). We will then check if there is any connection between these methods and the formulation of DRD. Very related to this issue is the relation between DRD and the definition of task-based synergies. The optimization of the proto-tasks to minimize task-level error might indeed lead to a set of synergies that approximates optimally the desired actuation-set.

Finally, the DRD will be further extended. The inclusion of joint-limits in the formulation will facilitate its application to dynamical systems in which the joint-boundaries are highly intricate. Furthermore, we will tackle the challenge of learning the low-dimensional mapping between the mixing weights of the DRs and those of the synergies. An automatic identification of this relation would allow to apply DRD to robots in which the inverse dynamical model is unknown. This mapping is a compact expression of the inverse dynamics of the system, therefore a clever strategy for its automatic learning would represent an important contribution to the field of machine learning for robotics, where learning inverse models is currently a hot topic of research.

Remarks

I am happy to provide the code to reproduce all the results presented in this thesis. The software of the DRD is available as a GNU Octave package under free and open source license. The reader is encouraged to download[1], test, report bugs and submit improvements to the algorithm.

Part of this work was awarded 2^{nd} prize in the best poster competition at the *Ninth Computational Motor Control Workshop*, Ben-Gurion University, Beer-Sheva, Israel. May, 2013.
Alessandro, C., Carbajal, J.P., d'Avella, A., Nori, F. (2013). Computational implications of the muscle synergy hypothesis.

In addition to the work presented in this thesis, during the period of my PhD I have contributed to other research projects. The following papers summarize the obtained results:

Wittmeier, S., Alessandro, C., Bascarevic, N., Dalamagkidis, K., Diamond, A., Jäntsch, M., Jovanovic, K., Knight, R., Marques, H. G., Milosavljevic, P., Svetozarevic, P., Potkonjak, V., Pfeifer, R., Knoll, A., and Holland, O. (2012). Towards anthropomimetic robotics. *Artificial Life*. 19(1):171-193.

Mutti, F., Alessandro, C., Angioletti, M., Bianchi, A., Gini, G. (2012). Learning and evaluation of a vergence control system inspired by Hering's law. *The Fourth IEEE RAS/EMBS International Conference on Biomedical Robotics and Biomechatronics*. Roma, Italy. June 24-27, 2012. pag. 931-936.

Kuppuswamy, N., Alessandro, C. (2011) Impact of body parameters on dynamic movement primitives for robot control. *The European Future Technologies Conference and Exhibition, FET 2011*. Budapest, Hungary.

[1] http://users.elis.ugent.be/~jcarbaja/DRD/drd.html

Marques, G. H., Jäntsch, M., Wittmeier, S., Alessandro, C., Lungarella, M., Knight, R., Holland, O. (2010). ECCE1: the first of a series of anthropomimetic musculoskeletal upper torsos. *IEEE International Conference on Humanoid Robotics, Humanoid 2010*. Nashville, USA.

Bibliography

Ahmed, A. A., Wolpert, D. M., and Flanagan, J. R. (2008). Flexible representations of dynamics are used in object manipulation. *Current Biology*, 18(10):763–768.

Alessandro, C., Carbajal, J. P., and d'Avella, A. (2012). Synthesis and Adaptation of Effective Motor Synergies for the Solution of Reaching Tasks. In Ziemke, T., Balkenius, C., and Hallam, J., editors, *Lecture Notes in Artificial Intelligence (LNAI)*, pages 33–43, Berlin. Springer-Verlag.

Alessandro, C., Carbajal, J. P., and d'Avella, A. (2013a). A computational analysis of motor synergies by dynamic response decomposition. *(submitted)*.

Alessandro, C., Delis, I., Nori, F., Panzeri, S., and Berret, B. (2013b). Muscle synergies in neuroscience and robotics: from input-space to task-space perspectives. *Frontiers in Computational Neuroscience*, 7(43).

Alessandro, C. and Nori, F. (2012). Identification of Synergies by Optimization of Trajectory Tracking Tasks. In *IEEE RAS/EMBS International Conference on Biomedical Robotics and Biomechatronics*, pages 924–930, Rome. IEEE.

Allen, J. L. and Neptune, R. R. (2012). Three-dimensional modular control of human walking. *Journal of Biomechanics*, 45(12):2157–2163.

Bell, A. J. and Sejnowski, T. J. (1995). An information-maximization approach to blind separation and blind deconvolution. *Neural Computation*, 7:1129–1159.

Berniker, M. (2005). *Linearity, motor primitives and low-dimensionality in the spinal organization of motor control*. PhD thesis, Massachusetts Institute of Technology.

Berniker, M., Jarc, A., Bizzi, E., and Tresch, M. C. (2009). Simplified and effective motor control based on muscle synergies to exploit musculoskeletal dynamics. *Proceedings of the National Academy of Sciences of the United States of America*, 106(18):7601–7606.

Bernstein, N. A. (1967). *The Co-ordination and Regulation of Movements*. Pergamon.

Bicchi, A., Gabiccini, M., and Santello, M. (2011). Modelling natural and artificial hands with synergies. *Philosophical Transactions of the Royal Society of London. Series B: Biological Sciences*, 366(1581):3153–61.

Bizzi, E., Cheung, V. C. K., d'Avella, A., and Saltiel, P. F. (2008). Combining modules for movement. *Brain Research Reviews*, 57:125–133.

Bizzi, E., Hogan, N., Mussa-Ivaldi, F. A., and Giszter, S. (1992). Does the nervous system use equilibrium-point control to guide single and multiple joint movements? *Behavioral and Brain Sciences*, 15(4):603–613.

Brochier, T., Spinks, R. L., Umilta, M. A., and Lemon, R. N. (2004). Patterns of muscle activity underlying object-specific grasp by the macaque monkey. *Journal of Neurophysiology*, 92(3):1770–1782.

Broer, H. and Takens, F. (2011). *Dynamical Systems and Chaos*. Springer, New York Dordrecht Heidelberg London.

Brown, C. Y. and Asada, H. H. (2007). Inter-finger coordination and postural synergies in robot hands via mechanical implementation of principal components analysis. In *IEEE/RSJ International Conference on Intelligent Robots and Systems*, pages 2877–2882, San Diego, California, USA. IEEE.

Buciu, I. and Pitas, I. (2004). A new sparse image representation algorithm applied to facial expression recognition. In *Machine Learning for Signal Processing. Proceedings of the 14th IEEE Signal Processing Society Workshop*, pages 539–548, Sao Luis, Brazil. IEEE.

Burdet, E., Osu, R., Franklin, D. W., Milner, T. E., and Kawato, M. (2001). The central nervous system stabilizes unstable dynamics by learning optimal impedance. *Nature*, 414(6862):446–449.

Cappellini, G., Ivanenko, Y. P., Dominici, N., Poppele, R. E., and Lacquaniti, F. (2010). Migration of motor pool activity in the spinal cord reflects body mechanics in human locomotionj. *Journal of Neurophysiology*, 104(6):3064–3073.

Cappellini, G., Ivanenko, Y. P., Poppele, R. E., and Lacquaniti, F. (2006). Motor patterns in human walking and running. *Journal of Neurophysiology*, 95(6):3426–3437.

Carbajal, J. P. (2012). *Harnessing Nonlinearities: Generating Behavior from Natural Dynamics*. Phd, University of Zürich.

Cerminara, N. L., Apps, R., and Marple-Horvat, D. E. (2008). An internal model of a moving visual target in the lateral cerebellum. *Journal of Physiology*, 587(2):429–442.

Cheung, V. C. K., d'Avella, A., and Bizzi, E. (2009a). Adjustments of motor pattern for load compensation via modulated activations of muscle synergies during natural behaviors. *Journal of Neurophysiology*, 101(3):1235–1257.

Cheung, V. C. K., d'Avella, A., Tresch, M. C., and Bizzi, E. (2005). Central and Sensory Contributions to the Activation and Organization of Muscle Synergies during Natural Motor Behaviors. *The Journal of Neuroscience*, 25(27):6419–6434.

Cheung, V. C. K., Piron, L., Agostini, M., Silvoni, S., Turolla, A., and Bizzi, E. (2009b). Stability of muscle synergies for voluntary actions after cortical stroke in humans. *Proceedings of the National Academy of Sciences of the United States of America*, 106(46):19563–8.

Cheung, V. C. K., Turolla, A., Agostini, M., Silvoni, S., Bennis, C., Kasi, P., Paganoni, S., Bonato, P., and Bizzi, E. (2012). Muscle synergy patterns as physiological markers of motor cortical damage. *Proceedings of the National Academy of Sciences of the United States of America*, 109(36):14652–14656.

Chhabra, M. and Jacobs, R. A. (2006). Properties of Synergies Arising from a Theory of Optimal Motor Behavior. *Neural Computation*, 18(10):2320–2342.

Chhabra, M. and Jacobs, R. A. (2008). Learning to Combine Motor Primitives Via Greedy Additive Regression. *The Journal of Machine Learning Research*, 9(6):1535–1558.

Chiovetto, E., Berret, B., Delis, I., Panzeri, S., and Pozzo, T. (2013). Investigating reduction of dimensionality during single-joint elbow movements: a case study on muscle synergies. *Frontiers in Computational Neuroscience*, 7:11.

Chvatal, S. A., Torres-Oviedo, G., Safavynia, S. A., and Ting, L. H. (2011). Common muscle synergies for control of center of mass and force in nonstepping and stepping postural behaviors. *Journal of Neurophysiology*, 106(2):999–1015.

Ciocarlie, M. T. and Allen, P. K. (2009). Hand Posture Subspaces for Dexterous Robotic Grasping. *The International Journal of Robotics Research*, 28(7):851–867.

Clark, D. J., Ting, L. H., Zajac, F. E., Neptune, R. R., and Kautz, S. a. (2010). Merging of healthy motor modules predicts reduced locomotor performance and muscle coordination complexity post-stroke. *Journal of Neurophysiology*, 103(2):844–57.

da Silva, M., Durand, F., and Popović, J. (2009). Linear Bellman combination for control of character animation. *ACM Transactions on Graphics*, 28(3):1.

Dagmar, S. and Schaal, S. (1999). Segmentation of endpoint trajectories does not imply segmented control. *Experimental Brain Research*, 124:118–136.

Darlington, R. B. (1968). Multiple regression in psychological research and practice. *Psychological Bulletin*, 69(3):161–182.

d'Avella, A. and Bizzi, E. (2005). Shared and specific muscle synergies in natural motor behaviors. *Proceedings of the National Academy of Sciences*, 102(8):3076–3081.

d'Avella, A., Fernandez, L., Portone, A., and Lacquaniti, F. (2008). Modulation of phasic and tonic muscle synergies with reaching direction and speed. *Journal of Neurophysiology*, 100(3):1433–54.

d'Avella, A. and Pai, D. K. (2010). Modularity for sensorimotor control: evidence and a new prediction. *Journal of Motor Behavior*, 42(6):361–369.

d'Avella, A., Portone, A., Fernandez, L., and Lacquaniti, F. (2006). Control of fast-reaching movements by muscle synergy combinations. *The Journal of Neuroscience*, 26(30):7791–7810.

d'Avella, A., Portone, A., and Lacquaniti, F. (2011). Superposition and modulation of muscle synergies for reaching in response to a change in target location. *Journal of Neurophysiology*, 106(6):2796–2812.

d'Avella, A., Saltiel, P., and Bizzi, E. (2003). Combinations of muscle synergies in the construction of a natural motor behavior. *Nature Neuroscience*, 6:300–308.

d'Avella, A. and Tresch, M. C. (2002). Modularity in the motor system: decomposition of muscle patterns as combinations of time-varying synergies. In Dietterich, T., Becker, S., and Ghahramani, Z., editors, *Advances in neural information processing systems*, volume 14, pages 141–148. MIT press, Massachusetts.

de Rugy, A., Loeb, G. E., and Carroll, T. J. (2012). Muscle coordination is habitual rather than optimal. *The Journal of Neuroscience*, 32(21):7384–7391.

Delis, I., Berret, B., Pozzo, T., and Panzeri, S. (2013). Quantitative evaluation of muscle synergy models: a single-trial task decoding approach. *Frontiers in Computational Neuroscience*, 7:8.

Delis, I., Chiovetto, E., and Berret, B. (2010). On the origins of modularity in motor control. *The Journal of Neuroscience*, 30(22):7451–7452.

Deshpande, A. D., Xu, Z., Weghe, M. J. V., Brown, B. H., Ko, J., Chang, L. Y., Wilkinson, D. D., Bidic, S. M., and Matsuoka, Y. (2013). Mechanisms of the anatomically correct testbed hand. *IEEE/ASME Transactions on Mechatronics*, 18(1):238–250.

Dominici, N., Ivanenko, Y. P., Cappellini, G., D'Avella, A., Mondì, V., Cicchese, M., Fabiano, A., Silei, T., Di Paolo, A., Giannini, C., Poppele, R. E., and Lacquaniti, F. (2011). Locomotor primitives in newborn babies and their development. *Science*, 334(6058):997–9.

Drew, T., Kalaska, J., and Krouchev, N. (2008). Muscle synergies during locomotion in the cat: a model for motor cortex control. *The Journal of Physiology*, 586:1239–1245.

Fautrelle, L., Ballay, Y., and Bonnetblanc, F. (2010). Muscular synergies during motor corrections: investigation of the latencies of muscle activities. *Behavioural Brain Research*, 214(2):428–36.

Fishbach, A., Roy, S. A., Bastianen, C., Miller, L. E., and Houk, J. C. (2005). Kinematic properties of on-line error corrections in the monkey. *Experimental Brain Research*, 164(4):42–457.

Fishbach, A., Roy, S. A., Bastianen, C., Miller, L. E., and Houk, J. C. (2007). Deciding when and how to correct a movement: discrete submovements as a decision making process. *Experimental Brain Research*, 177(1):45–63.

Flash, T. and Henis, E. (1991). Arm trajectory modifications during reaching towards visual targets. *Journal of Cognitive Neuroscience*, 3(3):220–230.

Flash, T., Henis, E., Inzelbergb, R., and Korczynb, A. (1992). Timing and sequencing of human arm trajectories: normal and abnormal motor behaviour. *Human Movement Science*, 11(1-2):83–100.

Flash, T. and Hochner, B. (2005). Motor primitives in vertebrates and invertebrates. *Current Opinion in Neurobiology*, 15(6):660–666.

Flash, T. and Hogan, N. (1985). The coordination of arm movements: an experimentally confirmed mathematical model. *The Journal of Neuroscience*, 5:1688–1703.

Gabiccini, M., Bicchi, a., Prattichizzo, D., and Malvezzi, M. (2011). On the role of hand synergies in the optimal choice of grasping forces. *Autonomous Robots*, 31(2-3):235–252.

Ganesh, G. and Burdet, E. (2013). Motor planning explains human behaviour in tasks with multiple solutions. *Robotics and Autonomous Systems*, 61(4):362 – 368.

Gaveau, J., Paizis, C., Berret, B., Pozzo, T., and Papaxanthis, C. (2011). Sensorimotor adaptation of point-to-point arm movements after spaceflight: the role of internal representation of gravity force in trajectory planning. *Journal of Neurophysiology*, 16(2):620–629.

Giese, M., Mukovskiy, A., and Park, A. (2009). Real-time synthesis of body movements based on learned primitives. In Cremers, D., Rosenhahn, B., and Yuille, A., editors, *Statistical and Geometrical Approaches to Visual Motion Analysis*, pages 107–127. Springer Verlag, Berlin Heidelberg.

Giszter, S. F., Hart, C. B., and Silfies, S. P. (2010). Spinal cord modularity: evolution, development, and optimization and the possible relevance to low back pain in man. *Experimental Brain Research*, 200(3-4):283–306.

Giszter, S. F. and Kargo, W. J. (2000). Conserved temporal dynamics and vector superposition of primitives in frog wiping reflexes during spontaneous extensor deletions. *Neurocomputing*, 32-33:775–783.

Giszter, S. F., Mussa-Ivaldi, F. A., and Bizzi, E. (1993). Convergent force fields organized in the frog's spinal cord. *Journal of Neuroscience*, 13(2):467–491.

Gizzi, L., Nielsen, J.-F., Felici, F., Ivanenko, Y. P., and Farina, D. (2011). Impulses of activation but not motor modules are preserved in the locomotion of subacute stroke patients. *Journal of Neurophysiology*, 106(1):202–210.

Golledge, H. D., Panzeri, S., Zheng, F., Pola, G., Scannell, J. W., Giannikopoulos, D. V., Mason, R. J., Tovée, M. J., and Young, M. P. (2003). Correlations, feature-binding and population coding in primary visual cortex. *Neuroreport*, 14(7):1045–1050.

Golub, G. H. and van Van Loan, C. F. (1996). *Matrix Computations*. Johns Hopkins University Press; 3rd edition.

Harris, C. and Wolpert, D. (1998). Signal-dependent noise determines motor planning. *Nature*, 394(6695):780–784.

Hart, C. B. and Giszter, S. F. (2004). Modular premotor drives and unit bursts as primitives for frog motor behaviors. *The Journal of Neuroscience*, 24(22):5269–82.

Hart, C. B. and Giszter, S. F. (2010). A neural basis for motor primitives in the spinal cord. *The Journal of Neuroscience*, 30(4):1322–1336.

Hauser, H., Neumann, G., Ijspeert, A. J., and Maass, W. (2011). Biologically inspired kinematic synergies enable linear balance control of a humanoid robot. *Biological Cybernetics*, 104(4-5):235–49.

Henis, E. A. and Flash, T. (1995). Mechanisms underlying the generation of averaged modified trajectories. *Biological Cybernetics*, 72(5):407–419.

Hirashimasend, M. and Nozaki, D. (2012). Distinct motor plans form and retrieve distinct motor memories for physically identical movements. *Current Biology*, 22(5):432–436.

Hoffmann, M., Marques, H., Arieta, A., Sumioka, H., Lungarella, M., and Pfeifer, R. (2010). Body schema in robotics: A review. *Autonomous Mental Development, IEEE Transactions on*, 2(4):304 –324.

Hogan, N. J. (1984). Adaptive control of mechanical impedance by coactivation of antagonist muscles. *IEEE Transactions on Automatic Control*, 29(8):681–690.

Holdefer, R. N. and Miller, L. E. (2002). Primary motor cortical neurons encode functional muscle synergies. *Experimental Brain Research*, 146(2):233–43–.

Hollerbach, J. M. and Flash, T. (1982). Dynamic interactions between limb segments during planar arm movement. *Biological Cybernetics*, 44(1):67–77.

Hug, F., Turpin, N. a., Couturier, A., and Dorel, S. (2011). Consistency of muscle synergies during pedaling across different mechanical constraints. *Journal of Neurophysiology*, 106(1):91–103.

Ijspeert, A. J., Nakanishi, J., Hoffmann, H., Pastor, P., and Schaal, S. (2013). Dynamical movement primitives: learning attractor models for motor behaviors. *Neural Computation*, 25(25):328–373.

Imamizu, H., Kuroda, T., Miyauchi, S., Yoshioka, T., and Kawato, M. (2003). Modular organization of internal models of tools in the human cerebellum. *Proceedings of the National Academy of Sciences*, 100(9):5461–5466.

Ivanenko, Y. P., Cappellini, G., Dominici, N., Poppele, R. E., and Lacquaniti, F. (2005). Coordination of locomotion with voluntary movements in humans. *The Journal of Neuroscience*, 25(31):7238–7253.

Ivanenko, Y. P., Cappellini, G., Poppele, R. E., and Lacquaniti, F. (2008). Spatiotemporal organization of alpha-motoneuron activity in the human spinal cord during different gaits and gait transitions. *The European Journal of Neuroscience*, 27(12):3351–68.

Ivanenko, Y. P., Grasso, R., Zago, M., Molinari, M., Scivoletto, G., Castellano, V., Macellari, V., and Lacquaniti, F. (2003). Temporal components of the motor patterns expressed by the human spinal cord reflect foot kinematics. *Journal of Neurophysiology*, 90(5):3555–65.

Ivanenko, Y. P., Poppele, R. E., and Lacquaniti, F. (2004). Five basic muscle activation patterns account for muscle activity during human locomotion. *The Journal of Physiology*, 556(Pt 1):267–82.

Ivanenko, Y. P., Poppele, R. E., and Lacquaniti, F. (2006a). Motor control programs and walking. *The Neuroscientist*, 12(4):339–48.

Ivanenko, Y. P., Poppele, R. E., and Lacquaniti, F. (2006b). Spinal cord maps of spatiotemporal alpha-motoneuron activation in humans walking at different speeds. *Journal of Neurophysiology*, 95(2):602–618.

Kargo, W. J. and Giszter, S. F. (2000a). Afferent roles in hindlimb wipe-reflex trajectories: free-limb kinematics and motor patterns. *Journal of Neurophysiology*, 83(3):1480–1501.

Kargo, W. J. and Giszter, S. F. (2000b). Rapid correction of aimed movements by summation of force-field primitives. *The Journal of Neuroscience*, 20(1):409–426.

Kargo, W. J. and Giszter, S. F. (2008). Individual premotor drive pulses, not time-varying synergies, are the units of adjustment for limb trajectories constructed in spinal cord. *The Journal of N euroscience*, 28(10):2409–2425.

Kargo, W. J. and Nitz, D. A. (2003). Early skill learning is expressed through selection and tuning of cortically represented muscle synergies. *The Journal of Neuroscience*, 23(35):11255–11269.

Kargo, W. J., Ramakrishnan, A., Hart, C. B., Rome, L. C., and Giszter, S. F. (2010). A simple experimentally based model using proprioceptive regulation of motor primitives captures adjusted trajectory formation in spinal frogs. *Journal of Neurophysiology*, 103(1):573–90.

Karniel, A. (2013). The minimum transition hypothesis for intermittent hierarchical motor control. *Frontiers in Computational Neuroscience*, 7(12).

Kawato, M. (1999). Internal models for control and trajectory planning. *Current Opinion in Neurobiology*, 9:718–727.

Kawato, M., Kuroda, T., Imamizu, H., Nakano, E., Miyauchi, S., and Yoshioka, T. (2003). Internal forward models in the cerebellum: fmri study on grip force and load force coupling. In C. Prablanc, D. Pelisson, Y. R., editor, *Neural Control of Space Coding and Action Production*, volume 142 of *Progress in Brain Research*, pages 171 – 188. Elsevier.

Kelso, J. A. S. (1982). *Human Motor Behaviour: An Introduction*. Psychology Press.

Khansari-Zadeh, S. M. and Billard, A. (2011). Learning stable non-linear dynamical systems with gaussian mixture models. *IEEE Transaction on Robotics*, 27(5):943–957.

Klein Breteler, M. D., Simura, K. J., and Flanders, M. (2007). Timing of muscle activation in a hand movement sequence. *Cerebral Cortex*, 17(4):803–815.

Krishnamoorthy, V., Goodman, S., Zatsiorsky, V., and Latash, M. L. (2003a). Muscle synergies during shifts of the center of pressure by standing persons: identification of muscle modes. *Biological Cybernetics*, 89(2):152–161.

Krishnamoorthy, V., Latash, M. L., Scholz, J. P., and Zatsiorsky, V. M. (2003b). Muscle synergies during shifts of the center of pressure by standing persons. *Experimental Brain Research*, 152(3):281–292.

Krouchev, N., Kalaska, J. F., and Drew, T. (2006). Sequential activation of muscle synergies during locomotion in the intact cat as revealed by cluster analysis and direct decomposition. *Journal of Neurophysiology*, 96(4):1991–2010.

Kutch, J. J., Kuo, A. D., Bloch, A. M., and Rymer, W. Z. (2008). Endpoint force fluctuations reveal flexible rather than synergistic patterns of muscle cooperation. *Journal of Neurophysiology*, 100(5):2455–71.

Kutch, J. J. and Valero-Cuevas, F. J. (2012). Challenges and new approaches to proving the existence of muscle synergies of neural origin. *PLoS Computational Biology*, 8(5):e1002434.

Lacquaniti, F., Ivanenko, Y. P., and Zago, M. (2012a). Development of human locomotion. *Current Opinion in Neurobiology*, 22(5):822–828.

Lacquaniti, F., Ivanenko, Y. P., and Zago, M. (2012b). Patterned control of human locomotion. *The Journal of Physiology*, 590(Pt 10):2189–2199.

Latash, M. L. (2010). Motor synergies and the equilibrium-point hypothesis. *Motor Control*, 14(3):294–322.

Latash, M. L., Gorniak, S., and Zatsiorsky, V. M. (2008). Hierarchies of synergies in human movements. *Kinesiology (Zagreb)*, 40(1):29–38.

Latash, M. L., Levin, M. F., Scholz, J. P., and Schöner, G. (2010). Motor control theories and their applications. *Medicina (Kaunas)*, 46(6):382–392.

Lee, D. D. and Seung, S. H. (1999). Learning the parts of objects by non-negative matrix factorization. *Nature*, 401:788–791.

Loeb, E., Giszter, S. F., Saltiel, P. F., Bizzi, E., and Mussa-Ivaldi, F. A. (2000). Output units of motor behavior: an experimental and modeling study. *Journal of Cognitive Neuroscience*, 12(1):78–97.

Loram, I. D., Gollee, H., Lakie, M., and Gawthrop, P. J. (2010). Human control of an inverted pendulum: Is continuous control necessary? is intermittent control effective? is intermittent control physiological? *The Journal of Physiology*, 589:307–324.

Malhotra, M., Rombokas, E., Theodorou, E., Todorov, E., and Matsuoka, Y. (2012). Reduced dimensionality control for the ACT hand. In *IEEE International Conference on Robotics and Automation (ICRA)*, pages 5117–5122, St. Paul, Minnesota, USA. IEEE.

Mardia, K. V., Kent, J. T., and Bibby, J. M. (1980). *Multivariate Analysis*. Academic Press, San Diego, California, USA.

Marques, H., Schaffner, P., and Kuppuswamy, N. (2012). Unsupervised Learning of a Reduced Dimensional Controller for a Tendon Driven Robot Platform. In Ziemke, T., Balkenius, C., and Hallam, J., editors, *Lecture Notes in Artificial Intelligence (LNAI)*, pages 351–360, Berlin. Springer-Verlag.

Matarić, M. J., Williamson, M., Demiris, J., and Mohan, A. (1998a). Behavior-based primitives for articulated control. In *Proceedings of the fifth international conference on simulation of adaptive behavior on From animals to animats 5*, pages 165–170, Cambridge, MA, USA. MIT Press.

Matarić, M. J., Zordan, V. B., and Mason, Z. (1998b). Movement control methods for complex, dynamically simulated agents: Adonis dances the macarena. In *Proceedings of the second international conference on Autonomous agents*, AGENTS '98, pages 317–324, New York, NY, USA. ACM.

Matarić, M. J., Zordan, V. B., and Williamson, M. M. (1999). Making complex articulated agents dance. *Autonomous Agents and Multi-Agent Systems*, 2(1):23–43.

McGowan, C. P., Neptune, R. R., Clark, D. J., and Kautz, S. A. (2010). Modular control of human walking: Adaptations to altered mechanical demands. *Journal of Biomechanics*, 43(3):412–419.

McKay, J. L. and Ting, L. H. (2008). Functional muscle synergies constrain force production during postural tasks. *Journal of Biomechanics*, 41(2):299–306.

McKay, J. L. and Ting, L. H. (2012). Optimization of Muscle Activity for Task-Level Goals Predicts Complex Changes in Limb Forces across Biomechanical Contexts. *PLoS Computational Biology*, 8(4):e1002465.

Meyer, D. E., Abrams, R. A., Kornblum, S., Wright, C. E., and Smith, J. E. K. (1988). Optimality in human motor performance: ideal control of rapid aimed movements. *Psychological Review*, 95:340–370.

Mezger, J., Ilg, W., and Giese, M. (2005). Trajectory synthesis by hierarchical spatio-temporal correspondence: Comparison of different methods. In *Proceedings of the 2nd symposium on Applied perception in graphics and visualization (APGV)*, pages 25–32, New York, USA. ACM.

Monaco, V., Ghionzoli, A., and Micera, S. (2010). Age-related modifications of muscle synergies and spinal cord activity during locomotion. *Journal of Neurophysiology*, 104(4):2092–2102.

Morasso, P. and Mussa-Ivaldi, F. A. (1982). Trajectory formation and handwriting: a computational model. *Biological Cybernetics*, 45(2):131–142.

Muceli, S., Boye, A. T. l., D'Avella, A., and Farina, D. (2010). Identifying representative synergy matrices for describing muscular activation patterns during multidirectional reaching in the horizontal plane. *Journal of Neurophysiology*, 103(3):1532–1542.

Mukovskiy, A., Slotine, J., and Giese, M. (2011). Analysis and design of the dynamical stability of collective behavior in crowds. In *International Conference on Computer Graphics, Visualization and Computer Vision 2011(WSCG)*, pages 69–76, Pilsen, Czech Republic.

Mussa-Ivaldi, F. A. (1997). Nonlinear force fields: a distributed system of control primitives for representing and learning movements. In *IEEE International Symposium on Computational Intelligence in Robotics and Automation*, pages 84–90, Albuquerque, New Mexico, USA. IEEE.

Mussa-Ivaldi, F. A. and Bizzi, E. (2000). Motor learning through the combination of primitives. *Philosophical Transactions of the Royal Society of London - Series B: Biological Sciences*, 355(1404):1755–1769.

Mussa-Ivaldi, F. A. and Giszter, S. F. (1992). Vector field approximation: a computational paradigm for motor control and learning. *Biological Cybernetics*, 67(6):491–500.

Mussa-Ivaldi, F. A., Giszter, S. F., and Bizzi, E. (1994). Linear combinations of primitives in vertebrate motor control. *Proceedings of the National Academy of Sciences of the United States of America (PNAS)*, 19(16):7534–7538.

Nazarpour, K., Barnard, A., and Jackson, A. (2012). Flexible cortical control of task-specific muscle synergies. *The Journal of Neuroscience*, 32(36):12349–12360.

Neptune, R. R., Clark, D. J., and Kautz, S. A. (2009). Modular control of human walking: a simulation study. *Journal of Biomechanics*, 42(9):1282–1287.

Nguyen-Tuong, D. and Peters, J. (2011). Model learning for robot control: a survey. *Cognitive Processing*, 12(4):319–340.

Nori, F. (2005). *Symbolic Control with Biologically Inspired Motion Primitives*. PhD thesis, Università degli Studi di Padova.

Nori, F. and Frezza, R. (2005). A control theory approach to the analysis and synthesis of the experimentally observed motion primitives. *Biological Cybernetics*, 93(5):323–342.

Nori, F., Metta, G., and Sandini, G. (2008). Exploiting motor modules in modular contexts in humanoid robotics. In Schuster, A., editor, *Robust Intelligent Systems*, pages 209–229. Springer London.

Novak, K., Miller, L., and Houk, J. (2003). Features of motor performance that drive adaptation in rapid hand movements. *Experimental Brain Research*, 148(3):388–400.

Overduin, S. A., d'Avella, A., Carmena, J. M., and Bizzi, E. (2012). Microstimulation activates a handful of muscle synergies. *Neuron*, 76:1071–1077.

Overduin, S. A., d'Avella, A., Roh, J., and Bizzi, E. (2008). Modulation of muscle synergy recruitment in primate grasping. *The Journal of Neuroscience*, 28(4):880 – 892.

Park, A.-n., Mukovskiy, A., Omlor, L., and Giese, M. A. (2008a). Self organized character animation based on learned synergies from full-body motion capture data. In *International Conference on Cognitive Systems (CogSys)*, Karlsruhe, Germany.

Park, A.-n., Mukovskiy, A., Omlor, L., and Giese, M. A. (2008b). Synthesis of Character Behaviour by Dynamic Interaction of Synergies Learned from Motion Capture Data. In *International Conference of in Central Europe on Computer Graphics,Visulazation and Computer Vision (WSCG)*, pages 9–16, Pilsen, Czech Republic.

Pasalar, S., Roitman, A. V., and Ebner, T. J. (2005). Effects of speeds and force fields on submovements during circular manual tracking in humans. *Experimental Brain Research*, 163(2):214–225.

Perreault, E. J., Chen, K., Trumbower, R. D., and Lewis, G. (2008). Interactions with compliant loads alter stretch reflex gains but not intermuscular coordination. *Journal of Neurophysiology*, 99(5):2101–2113.

Pfeifer, R., Lungarella, M., and Iida, F. (2007). Self-organization, embodiment, and biologically inspired robotics. *Science*, 318(5853):1088–1093.

Philips, S., Berisha, V., and Spanias, A. (2009). Energy-constrained discriminant analysis. In *IEEE International Conference on Acoustics, Speech and Signal Processing (ICASSP)*, Taipei, Taiwan.

Pollick, F. E., Maoz, U., Handzelc, A. A., Giblind, P. J., Sapiroe, G., and Flashc, T. (2009). Three-dimensional arm movements at constant equi-affine speed. *Cortex*, 45(3):325–339.

Quiroga, R. Q. and Panzeri, S. (2009). Extracting information by neuronal populations:information theory and decoding approaches. *Nature Reviews Neuroscience*, 10:173–185.

Ranganathan, R. and Krishnan, C. (2012). Extracting synergies in gait: using emg variability to evaluate control strategies. *Journal of Neurophysiology*, 108(5):1537–1544.

Roh, J., Cheung, V. C. K., and Bizzi, E. (2011). Modules in the brain stem and spinal cord underlying motor behaviors. *Journal of Neurophysiology*, 106(3):1363–78.

Roh, J., Rymer, W. Z., and Beer, R. F. (2012). Robustness of muscle synergies underlying three dimensional force generation at the hand in healthy humans. *Journal of Neurophysiology*, 107(8):2123–2142.

Roh, J., Rymer, W. Z., Perreault, E. J., Yoo, S. B., and Beer, R. F. (2013). Alterations in upper limb muscle synergy structure in chronic stroke survivors. *Journal of Neurophysiology*, 109(3):768–781.

Rohrer, B., Fasoli, S., Krebs, H. I., Volpe, B., Frontera, W. R., Stein, J., and Hogan, N. (2004). Submovements grow larger, fewer, and more blended during stroke recovery. *Motor Control*, 8(4):472–483.

Roitman, A. V., Massaquoi, S. G., Takahashi, K., and Ebner, T. J. (2004). Kinematic analysis of manual tracking in monkeys: characterization of movement intermittencies during a circular tracking task. *Journal of Neurophysiology*, 91(2):901–911.

Rombokas, E., Malhotra, M., and Matsuoka, Y. (2011). Task-specific demonstration and practiced synergies for writing with the ACT hand. In *IEEE International Conference on Robotics and Automation (ICRA)*, pages 5363–5368, Shanghai, China. IEEE.

Safavynia, S. A. and Ting, L. H. (2012). Task-level feedback can explain temporal recruitment of spatially fixed muscle synergies throughout postural perturbations. *Journal of Neurophysiology*, 107(1):159–177.

Saltiel, P., Wyler-Duda, K., D'Avella, A., Tresch, M. C., and Bizzi, E. (2001). Muscle synergies encoded within the spinal cord: evidence from focal intraspinal NMDA iontophoresis in the frog. *Journal of Neurophysiology*, 85(2):605–619.

Santello, M., Flanders, M., and Soechting, J. F. (1998). Postural hand synergies for tool use. *The Journal of Neuroscience*, 18(23):10105–15.

Schaal, S., Peters, J., Nakanishi, J., and Ijspeert, A. (2005). Learning movement primitives. In Dario, P. and Chatila, R., editors, *Robotics Research*, volume 15 of *Tracts in Adv. Rob.*, pages 561–572. Springer.

Schneidman, E., Bialek, W., and II, M. J. B. (2003). Synergy, redundancy, and independence in population codes. *The Journal of Neuroscience*, 23(37):11539–11553.

Shadmehr, R. and Mussa-Ivaldi, F. A. (1994). Adaptive representation of dynamics during learning of a motor task. *The Journal of Neuroscience*, 14(5):3208–3224.

Shkolnik, A. and Tedrake, R. (2011). Sample-based planning with volumes in configuration space. *arXiv:1109.3145v1*.

Soechting, J. and Terzuolo, C. (1987). Organization of arm movements in three-dimensional space. wrist motion is piecewise planar. *Neuroscience*, 23:53–61.

Sosnik, R., Hauptmann, B., Karni, A., and Flash, T. (2004). When practice leads to co-articulation: the evolution of geometrically defined movement primitives. *Experimental Brain Research*, 154(4):422–438.

Squeri, V., Masia, L., Casadio, M., Morasso, P., and Vergaro, E. (2010). Force-field compensation in a manual tracking task. *PLoS ONE*, 5(6):e11189.

Stark, H. and Woods, J. W. (1986). *Probability, Random Processes, and Estimation Theory for Engineers*. Prentice-Hall Inc.

Stein, P. S. G. (2008). Motor pattern deletions and modular organization of turtle spinal cord. *Brain Research Reviews*, 57(1):118–124.

Thomas, P. and Barto, A. (2012). Motor primitive discovery. In *International Conference on Development and Learning - EpiRob (ICDL)*, San Diego, California, USA.

Ting, L. H. and Chvatal, S. A. (2010). Decomposing muscle activity in motor tasks: methods and interpretation. In Danion, F. and Latash, M. L., editors, *Motor Control: Theories, Experiments, and Applications*, chapter 5, pages 102–138. Oxford University Press, New York, USA.

Ting, L. H. and Macpherson, J. M. (2005). A limited set of muscle synergies for force control during a postural task. *Journal of Neurophysiology*, 93(1):609–613.

Ting, L. H. and McKay, J. L. (2007). Neuromechanics of muscle synergies for posture and movement. *Current Opinion in Neurobiology*, 17(6):622–8.

Todorov, E. (2009). Compositionality of optimal control laws. In Koller, D., Bengio, Y., Bottou, L., and Culotta, A., editors, *Advances in Neural Information Processing Systems, 2009a*, volume 3, pages 1856–1864. Nips Foundation (http://books.nips.cc).

Todorov, E. and Ghahramani, Z. (2003). Unsupervised learning of sensory-motor primitives. In *Proceedings of the 25th International Conference of the IEEE Engineering in Medicine and Biology Society*, pages 1750–1753. IEEE.

Todorov, E., Li, W., and Pan, X. (2005). From task parameters to motor synergies: A hierarchical framework for approximately-optimal control of redundant manipulators. *Journal of Robotic Systems*, 22(11):691–710.

Tong, C. and Flanagan, J. R. (2003). Task-specific internal models for kinematic transformations. *Journal of Neurophysiology*, 90(2):578–585.

Torres-Oviedo, G., Macpherson, J. M., and Ting, L. H. (2006). Muscle synergy organization is robust across a variety of postural perturbations. *Journal of Neurophysiology*, 96(3):1530–1546.

Torres-Oviedo, G. and Ting, L. H. (2007). Muscle synergies characterizing human postural responses. *Journal of Neurophysiology*, 98(4):2144–2156.

Torres-Oviedo, G. and Ting, L. H. (2010). Subject-specific muscle synergies in human balance control are consistent across different biomechanical contexts. *Journal of Neurophysiology*, 103(6):3084–3098.

Tresch, M. and Jarc, A. (2009). The case for and against muscle synergies. *Current Opinion in Neurobiology*, 19(6):601–607.

Tresch, M. C., Cheung, V. C., and d'Avella, A. (2006). Matrix factorization algorithms for the identification of muscle synergies: evaluation on simulated and experimental data sets. *Journal of Neurophysiology*, 95(4):2199–2212.

Tresch, M. C., Saltiel, P., and Bizzi, E. (1999). The construction of movement by the spinal cord. *Nature Neuroscience*, 2(2):162–167.

Tresch, M. C., Saltiel, P., D'Avella, A., and Bizzi, E. (2002). Coordination and localization in spinal motor systems. *Brain Research Reviews*, 40(1-3):66–79.

Valero-Cuevas, F. J., Venkadesan, M., and Todorov, E. (2009). Structured Variability of Muscle Activations Supports the Minimal Intervention Principle of Motor Control. *Journal of Neurophysiology*, 102(1):59–68.

Waltz, R. A., Morales, J. L., Nocedal, L., and Orban, D. (2006). An interior algorithm for nonlinear optimization that combines line search and trust region steps. *Mathematical Programming*, 107(3):391–408.

Weiss, E. J. and Flanders, M. (2004). Muscular and postural synergies of the human hand. *Journal of Neurophysiology*, 92(1):523–535.

Welch, T. D. J. and Ting, L. H. (2007). A feedback model reproduces muscle activity during human postural responses to support surface translations. *Journal of Neurophysiology*, 99(2):1032–1038.

Wolpert, D. and Kawato, M. (1998). Multiple paired forward and inverse models for motor control. *Neural Networks*, 11:1317–1329.

Yakovenko, S., Krouchev, N., and Drew, T. (2010). Sequential activation of motor cortical neurons contributes to intralimb coordination during reaching in the cat by modulating muscle synergies. *Journal of Neurophysiology*, 105(1):388–409.

Yu, J., Tian, Q., Rui, T., and Huang, T. S. (2007). Integrating discriminant and descriptive information for dimension reduction and classification. *IEEE Transactions on Circuits and Systems for Video Technology*, 17(3):372–377.

Zatsiorsky, V. (1997). *Kinematics of Human Motion*. Human Kinetics.

Zhang, A., Malhotra, M., and Matsuoka, Y. (2011). Musical piano performance by the ACT Hand. In *IEEE International Conference on Robotics and Automation (ICRA)*, pages 3536–3541, Shanghai, China. IEEE.

Appendix A

Muscle synergies in neuroscience and robotics: from input-space to task-space perspectives

Reprinted from:

Alessandro, C., Delis, I., Nori, F., Panzeri, S., and Berret, B. (2013). Muscle synergies in neuroscience and robotics: from input-space to task-space perspectives. *Frontiers in Computational Neuroscience*, 7(43).

Abstract

In this paper we review the works related to muscle synergies that have been carried-out in neuroscience and control engineering. In particular, we refer to the hypothesis that the central nervous system (CNS) generates desired muscle contractions by combining a small number of predefined modules, called muscle synergies. We provide an overview of the methods that have been employed to test the validity of this scheme, and we show how the concept of muscle synergy has been generalized for the control of artificial agents. The comparison between these two lines of research, in particular their different goals and approaches, is instrumental to explain the computational implications of the hypothesized modular organization. Moreover, it clarifies the importance of assessing the functional role of muscle synergies: although these basic modules are defined at the level of muscle activations (input-space), they should result in the effective accomplishment of the desired task. This requirement is not always explicitly considered in experimental neuroscience, as muscle synergies are often estimated solely by analyzing recorded muscle activities. We suggest that synergy extraction methods should explicitly take into account task execution variables, thus moving from a perspective purely based on input-space to one grounded on task-space as well.

A.1 Introduction

One of the fundamental questions in motor control concerns the mechanisms that underlie muscle contractions during the execution of movements. The complexity of the musculoskeletal apparatus as well as its dynamical properties allow biological systems to perform a wide variety of motor tasks Bizzi et al. [1992]; on the other hand, such a complexity has to be mastered by efficient strategies implemented in the CNS. How does the CNS "choose" among the infinity of solutions of a given motor task (i.e. Bernstein problem) [Bernstein, 1967]? How are motor intentions translated into muscle activations? How can biological systems learn and plan movements so rapidly? A prominent hypothesis suggests that motor circuitries are organized in a modular fashion, so that muscle activations can be realized by flexibly combining such modules. Modularity has been observed in various forms such as kinematic strokes, spinal force fields and muscle synergies [Flash and Hochner, 2005]; this paper provides an overview of the findings related to the so-called muscle synergies, as well as the application of such a concept in robotics and character animations.

Muscle synergies are defined as coordinated activations of a group of muscles[1]. It has been suggested that the CNS encodes a set of synergies, and it combines them in a task-dependent fashion in order to generate the muscle contractions that lead to the desired movement (muscle synergy hypothesis). Evidence for this organization relies on the spatio-temporal regularities observed in the EMG (Electromyography) activities of several species [Bizzi et al., 2008; Tresch et al., 2002]. Since in many cases these regularities appear to be very similar across subjects and motor tasks (i.e. robustness of muscle synergies), scientists have proposed that they might reflect a modular organization of the underlying neural circuitries. Assuming that muscle activations represent the control input to the musculoskeletal system, in this context muscle synergies are implicitly defined as input-space generators (i.e. components that are able to generate the necessary input signals).

From a computational point of view, a modular organization based on muscle synergies is very attractive. The activations of many muscles is hypothetically implemented by modulating the contributions of a small set of predefined muscle synergies. Such a dimensionality reduction may simplify motor control and learning, and it may contribute to the adaptability observed in biological systems [Mussa-Ivaldi and Bizzi, 2000]. This observation has recently motivated roboticists and control engineers to develop control strategies that are based on the same concept: combination of a small number of predefined actuations. In addition to the possible dimensionality reduction, the modularity of such scheme has the advantage that improved performance may be achieved incrementally by introducing additional synergies to the controller. The price to be paid is the restriction of the possible actuations to those that can be obtained by combining the synergies (i.e. synergies span set). This also implies a reduction of the possible movements that the controlled system can perform.

In the two fields of neuroscience and control engineering, research on muscle synergies is characterized by radically different goals and approaches (see Fig. A.1). In the context of controlling artificial systems, the main goal is the synthesis of a small set of synergies that instantiates an effective control strategy. The obtained controller, as such, is mainly evaluated in

[1]The term *synergy* has also been used in the context of another motor control hypothesis, the uncontrolled manifold hypothesis (UMH) [Latash, 2010; Latash et al., 2010]. In that context, the term refers to "a neural organization of a set of elemental variables [e.g. muscle contractions] with the purpose to ensure a certain stability properties of a performance variable produced by the whole set [e.g. desired joint configuration]" [Latash et al., 2008]. These studies are out of the scope of this paper, however we will discuss the concept of M-modes, that has been introduced in the UMH but it is very similar to the definition of synergies we adopt in this manuscript.

relation to task-accomplishment, and in particular it should be able to generate a set of feasible actuations that allows the agent to perform a wide variety of tasks. In neuroscience, on the other hand, the main goal is to validate or falsify the hypothesis of muscle synergy. The typical approach consists in analyzing a dataset of recorded muscle activities, and in verifying if such a dataset is compatible with the proposed modular decomposition; the hypothetical synergies are inferred by applying a decomposition algorithm to the dataset of EMG signals. Unlike in control engineering, the major focus of this line of research resides at the motor level (i.e. the input-space of muscle activations); the evaluation of the hypothesized modular organization at the level of task is not always considered and, from our point of view, it deserves more attention. Does the set of identified muscle synergies actually lead to the task performance observed experimentally? Does it generate feasible actuations? These issues have been investigated a-posteriori using realistic models of the musculoskeletal systems of different species [Berniker et al., 2009; McKay and Ting, 2012; Neptune et al., 2009]. Additionally, novel methodologies to deal with these challenges are starting to emerge in experimental neuroscience as well [Chvatal et al., 2011; Delis et al., 2013]. We believe that a shift of paradigm from an input-space to a task-space identification of muscle synergies, which seems to be already in progress, may contribute to a better understanding of the hypothetical modularity of the CNS, and of its relationship to human learning and control. In particular in this review we argue that task-space constraints could be directly integrated in the decomposition algorithm used to extract the synergies.

This paper reviews the studies that investigate the hypothesis of muscle synergies, as well as the methods to control artificial systems that have been developed taking inspiration from this hypothesis. The organization of the paper follows the rationale developed so far. Initially, in Sec. A.2, we provide a mathematical formulation of the concept of muscle synergies, we detail different synergy models (proposed as the mechanisms to generate muscle contractions), and we analyze their computational implications. In Sec. A.3 we discuss the works that evaluate the hypothesis of muscle synergies solely in the space of input-signals, and the ones that seek more direct neural evidence. Then, in Sec. A.4, we present the studies that evaluate synergies also at the task-level; this section includes robotics, characters animation, as well as neuroscience. Finally, in Sec. A.5 we offer further discussions and concluding remarks.

A.2 Models of muscle synergy

The concept of muscle synergy has been formalized in a variety of mathematical models. We will present these models in the context of controlling a generic dynamical system. This formulation is sufficiently generic to represent both the control of the musculoskeletal system and the control of an artificial agent. Furthermore, it is useful to explain the computational implications of the various synergy models, and to clarify the difference between input-space and task-space evaluation of a set of synergies.

The generic dynamical system we employ can be represented as follows:

$$\dot{\mathbf{x}}(t) = f(\mathbf{x}(t), t) + g(\mathbf{x}(t), t)\mathbf{u}(t), \tag{A.1}$$

where t represents time, $\mathbf{x}(t) \in \mathbb{R}^n$ is the system state variable at time t (e.g. angular positions and velocities of the joints), and $\mathbf{u}(t) \in \mathbb{R}^m$ is the system input at time t (e.g. muscle activations or joint torques). Within this framework, the variable to be controlled is denoted as $\mathbf{y}(t) \in \mathbb{R}^p$, and it is a generic function of the system state: $\mathbf{y}(t) = h(\mathbf{x}(t))$. The task is defined in terms of a set of constraints applied on the time evolution of this variable. Typical examples of tasks include reaching ($\mathbf{y}(t_f) = \mathbf{y}_d$ where t_f is the desired reaching time), and tracking ($\mathbf{y}(t) = \mathbf{y}_d(t)\ \forall t$, where

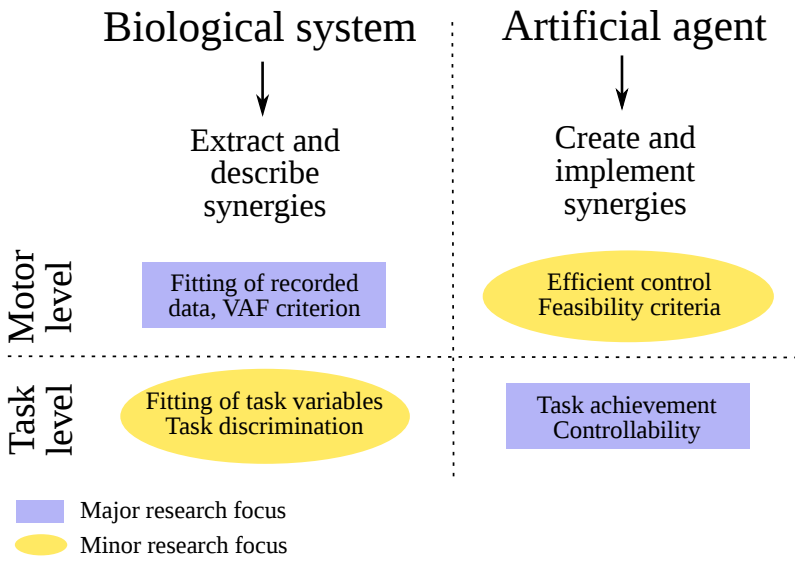

Figure A.1: Comparative scheme between research on muscle synergies in neuroscience and control engineering.

$\mathbf{y}_d(\cdot)$ is the desired trajectory to be tracked). We refer to the task-space, as the space where the task $\mathbf{y}_d$ is defined; similarly, the input-space is the space of the input signals $\mathbf{u}(\cdot)$. The relation between these two spaces is given by the dynamics of the system. It is now clear that a given control input should always be evaluated in relation to the error between the corresponding evolution of the controlled variable and the desired task; in other words, it should always be evaluated in task space.

Classically, control inputs $\mathbf{u}(\cdot)$ belong to the infinite dimensional space of continuous functions. Under this assumption a number of interesting control properties (e.g. controllability and observability) can be proven. The idea behind modular control, is to significantly restrict the control input space by constraining $\mathbf{u}(\cdot)$ to be a combination of modules, or muscle synergies. The various muscle synergy models can be distinguished based on the mathematical formalization of this combination, and they are described in the following (see Fig. A.2 for a schematic representation). An empirical comparison of these models is proposed by Chiovetto et al. [2013].

Temporal and synchronous synergies In these models, the control input is defined as a linear combination of k vectors $\mathbf{w} \in \mathbb{R}^m$, with 1-dimensional time-varying coefficients $a(t) : \mathbb{R}^+ \to \mathbb{R}$ (Fig. A.2A):

$$\mathbf{u}(t) = \sum_{j=1}^{k} a_j(t)\mathbf{w}_j. \tag{A.2}$$

Each vector $\mathbf{w}_j$ specifies a balance between the input variables (e.g. balance between muscle activations), and its coefficient $a_j(t)$ determines its temporal evolution. In the *temporal synergy model*, the coefficients $\{a_j(t)\}$ serve as the task-independent predefined modules, and the vectors $\{\mathbf{w}_j\}$ represent the new (task-dependent) control input. As a result, this model reduces the control space to $k \cdot m$ dimensions; i.e. the k m-dimensional vectors $\mathbf{w}_j$ have to be appropriately specified to fulfill the desired task $\mathbf{y}_d$. Synergies are thus interpreted as the temporal patterns that are recruited selectively by different muscles. In literature, temporal synergies are also referred to as temporally fixed muscle synergies. An important special case, the *premotor drive model*, is obtained

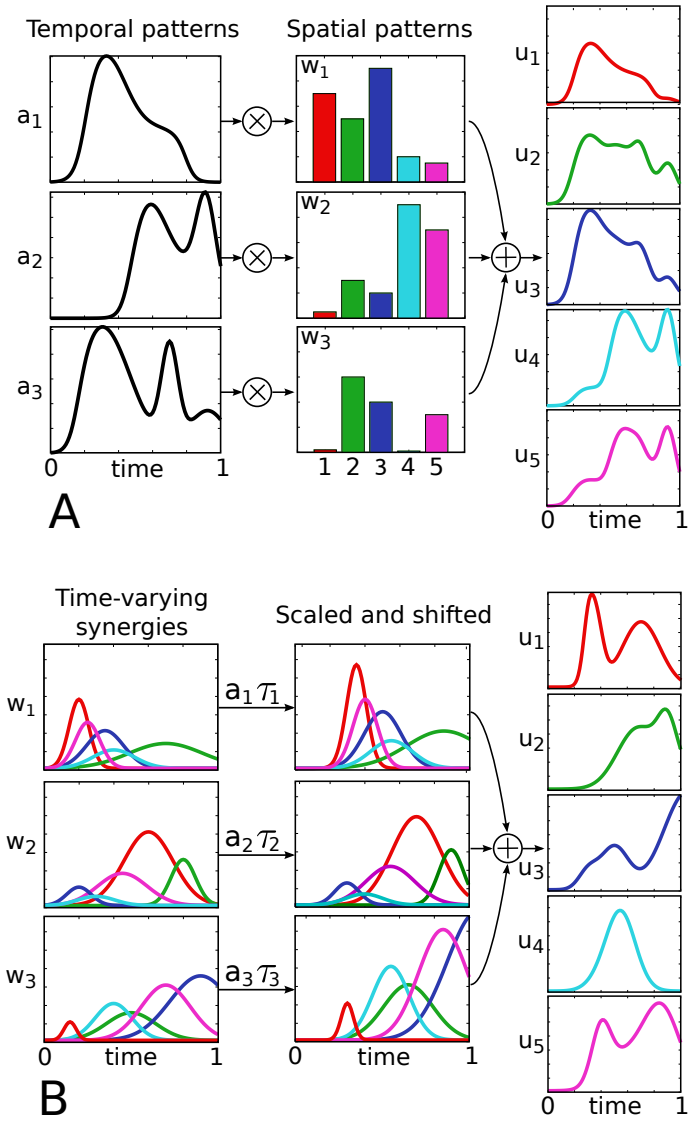

Figure A.2: Different models of muscle synergies. The temporal and the synchronous models explain motor signals as linear combinations of muscle balance vectors (spatial patterns), with 1-dimensional time-varying coefficients (A). In the temporal model, these coefficients serve as task-independent predefined modules, and the spatial patterns as the new (task-dependent) control input. In the synchronous model, on the other hand, the control input is represented by the temporal patterns, while the spatial patterns act as predefined modules. Finally, time-varying synergies are spatio-temporal predefined motor patterns, which can be scaled in amplitude and shifted in time by the new input coefficients.

by defining the temporal coefficients as $a_j(t) = A_j\phi(t-\tau_j)$. In this case, the time course of the vectors $\mathbf{w}_j$ are determined by a common function $\phi(t)$, called premotor drive or burst pulse, that can be modulated in amplitude and shifted in time. In contrast, the *synchronous synergy model* defines the task-independent synergies as the vectors $\mathbf{w}_j$. The the new control input $\{a_j(t)\}$ belongs to the infinite dimensional space of the one-dimensional real functions. Therefore this model, unlike the previous one, provides a dimensionality reduction only if the number of synergies is lower then the number of input variables, i.e. $k < m$. Synchronous synergies are co-varying group of muscles, and are also called time-invariant synergies, spatially fixed muscle synergies, or muscle modes.

Time-varying synergies This model defines the control input as the superposition of k task-independent vector-valued functions $\mathbf{w}(t) : \mathbb{R}^+ \to \mathbb{R}^m$ (Fig. A.2B):

$$\mathbf{u}(t) = \sum_{j=1}^{k} a_j \mathbf{w}_j(t - \tau_j). \tag{A.3}$$

Each synergy $\mathbf{w}_j$ can be scaled in amplitude and shifted in time by means of the coefficients $a_j, \tau_j \in \mathbb{R}$. These coefficients represent the new control input, and have to be chosen in order to accomplish the task $\mathbf{y}_d$. As a result, the new input space is reduced to a $2 \cdot k$ dimensional space. Neuroscientifically, these synergies are genuine spatiotemporal muscle patterns which do not make any explicit spatial and temporal separation. As such, according to this model, muscles within the same time-varying synergy do not necessarily co-vary.

A.3 Synergies as input-space generators

As discussed above, muscle synergies can be considered as input-space generators. Whether or not these generators are implemented in the CNS, and how they are eventually coordinated through the sensorimotor loops, is a main stream of research in motor neuroscience. To tackle this question, scientists have employed two main approaches. One of them is solely based on the analysis of EMG signals, therefore it can only provide indirect evidence of a modular neural organization. The other approach aims at locating the areas of the CNS where muscle synergies might be implemented, therefore providing a direct evidence. These methodologies as well as the obtained results are discussed in the following.

A.3.1 Indirect EMG-based evidence

The classical approach to evaluate the hypothesis of muscle synergies consists in searching spatio-temporal regularities (i.e. synergies) in a dataset of muscle activities (Fig. A.3, continuous green arrows). Such a dataset is obtained by recording the EMG signals from a group of subjects/animals that are performing some prescribed motor tasks. As such, this methodology is mainly based on considerations grounded at the input level. The possibility to discriminate the various task instances from motor signals represents the only (a-posteriori) task-related verification of the identified synergies (see Fig. A.1).

Linear dimensionality reduction algorithms are employed to identify a small set of components (i.e. synergies) that approximate the EMG dataset according to the chosen synergy model (see Sec. A.2). The number of synergies to be extracted has to be specified a-priori by the experimenter, as it constitutes an input parameter of the decomposition algorithm. The choice

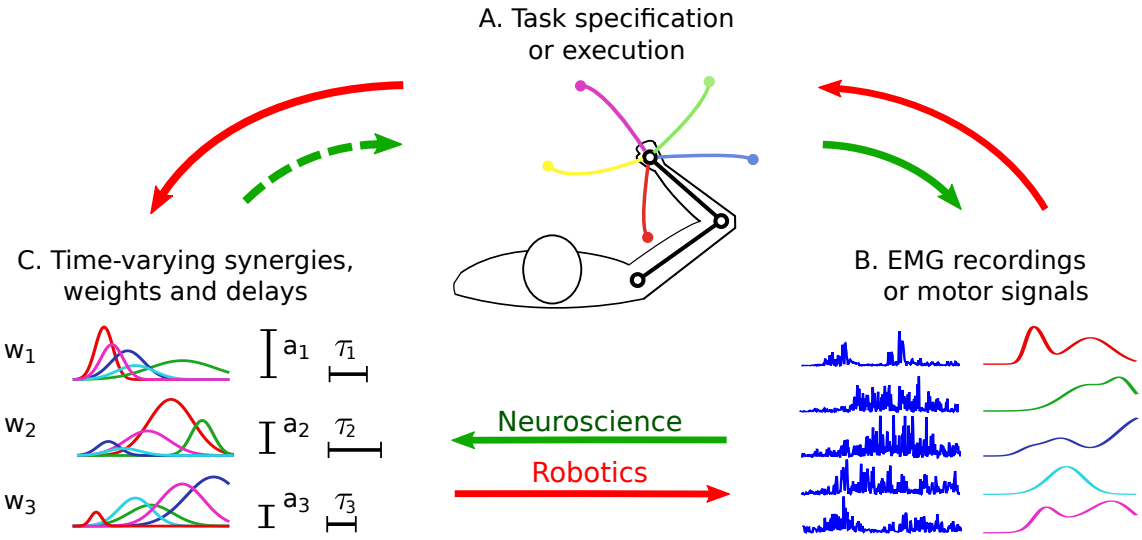

Figure A.3: Procedures for the identification and the testing of muscle synergies. In experimental neuroscience (green arrows), initially a group of subjects perform the tasks prescribed by the experimenter (A). The EMG signals acquired during the experiments (B) are then analyzed, and a dimensionality reduction algorithm is applied to obtain the synergies (C). Very often such synergies are not evaluated at the task-level (dashed arrow), therefore there is no guarantee that they lead to the observed task performance. In robotics (red arrows), synergies are synthesized (C) based on the requirements of the desired class of tasks (A). Then they are appropriately combined to generate the motor signals (B) to solve a specific task instance. The quality of the synthesized synergies is finally tested in terms of the obtained task performance (A). Without loss of generality, the figure presents the time-varying synergy model; however, the previous description holds for all the models.

of the decomposition algorithm to be used depends on the assumptions made on the nature of the hypothetical muscle synergies (e.g. non-negativity, orthogonality, statistical independence etc.) [Ting and Chvatal, 2010]. Principal component analysis (PCA) [Mardia et al., 1980] looks for orthogonal synergies that account for as much of the variability in the data as possible. Similarly, Factor analysis (FA) [Darlington, 1968] seeks the smallest set of synergies that can account for the common variance (correlation) of a set of muscles. Independent Component Analysis (ICA) [Bell and Sejnowski, 1995] maximizes the statistical independence of the extracted components, thus it assumes that synergies represents independent information sources. Non-negative matrix factorization (NMF) [Lee and Seung, 1999] enforces the extracted synergies and their activation coefficients to be non-negative; this constraint reflects the non-negativity of neural and muscle activations ("pull-only" behavior). Additionally, NMF does not assume that the generators are statistically independent, thus it is more compatible with the observation that activations of multiple synergies are correlated [Saltiel et al., 2001]. Finally, the extraction of time-varying synergies is performed by an NMF-based algorithm developed ad-hoc that allows the components to be shifted in time [d'Avella and Tresch, 2002].

To assess the quality of the extracted synergies, the so-called VAF (Variance Accounted For) metric is typically used (see Fig. A.1). VAF quantifies the percentage of variability in the EMG dataset that is accounted for by the extracted synergies. High values of VAF indicate good reconstruction of the recorded EMGs, which lends credit to the extracted synergy set; low VAF values cast doubt on the extracted synergies, indicating that they do not explain a large part of the EMG variance. This metric is also used for determining the dimensionality of the synergy space. The criteria used for this purpose rely on the assumption that most of the EMG

variability is attributable to task-dependent muscle activations, whereas a small portion is due to several sources of noise. Under this assumption, the number of synergies is defined either by the point where the VAF-graph (i.e the curve that describes the trend of the VAF as function of the number of synergies, which increases monotonically) reaches a threshold level (e.g. 90%) [Torres-Oviedo et al., 2006], or by its flattening point, i.e. the point where a drastic decrease of slope is observed. Such an "elbow" is in fact interpreted as the point that separates "structured" and noise-dependent variability, and therefore it can be used to define the minimum number of synergies that capture the task-related features [d'Avella et al., 2006; Tresch et al., 2006]. Besides the VAF metric, other metrics (e.g. log-likelihood [Tresch et al., 2006]) have been proposed to evaluate the effectiveness of extracted synergies (still in input space); a thorough discussion of these metrics is beyond the scope of the present review. As depicted in Fig. A.1, this indirect methodology is mainly restricted to the analysis of input-level data. A complementary metric based on single-trial task-decoding techniques has been proposed by Delis et al. [2013].

A significant amount of experiments has been conducted in frogs, cats, primates as well as humans in order to test the validity of the above-mentioned synergy models, and by extension, of the muscle synergy hypothesis itself. A pioneering study showed that a small set of synchronous muscle synergies could generate a large number of reflexive motor patterns produced by cutaneous stimulations of the frog hindlimb [Tresch et al., 1999]. This study also demonstrated that microstimulations of the spinal cord produced very similar muscle synergies to the ones generated by the freely moving animal. Qualitatively similar synergies were also found by intraspinal microstimulation [Saltiel et al., 2001]. The above analysis was then extended in order to identify spatiotemporal patterns of muscle activities (i.e., time-varying muscle synergies) [d'Avella et al., 2003]. A few time-varying synergies were shown to underlie the muscle patterns required to let the frog kick in different directions, and their recruitment was directly related to movement kinematics. These findings were further generalized to a wide variety of frog natural motor behaviors such as jumping, swimming, and walking; evidence for both synchronous and time-varying synergies was reported [d'Avella and Bizzi, 2005]. Additionally, this study revealed that some synergies are shared across motor behaviors, while others are behavior specific.

The synergy models described in Sec. A.2 do not include sensory feedback, however the original experiments on animals involved sensory-triggered reflexive movements. In fact, only a few studies have systematically investigated the influence of sensory feedback in the muscle synergy organization. Cheung et al. [2005] analyzed the EMG signals collected from the bullfrog during locomotor behaviors before and after having interrupted its sensory pathways (i.e. deafferentation). Their findings support the existence of centrally organized synchronous muscle synergies that are modulated by sensory inflow. Further support was provided by showing that an appropriate modulation of the synergy activations could explain immediate motor adjustments, and that these synergies were robust across different dynamic conditions [Cheung et al., 2009a]. A discussion on the role of sensory feedback is provided in Sec. A.5.

A number of studies have examined the generalization of the above results to other species. In primates, Overduin et al. [2008] found that three time-varying synergies described a large repertoire of grasping tasks. Shape and size of the grasped objects were shown to modulate the recruitment strength as well as the timing of each synergy. In this way, this study validated that time-varying synergies account for salient task differences, and their activations can be tuned to adapt to novel behavioral contexts. Along the same lines, Brochier et al. [2004] provided further support for such a robust and distinctive synergistic organization of primates' muscle patterns during grasping. Analysis of single-trial EMG signals demonstrated that the time-varying activation of three synchronous synergies was reproducible across repetitions of the same

grasping task and allowed unequivocal identification of the object grasped in each single trial. In cats, Ting's group showed that muscle synergies could be mapped onto the control of task-level variables; such experiments will be detailed in Sec. A.4.2.

The framework of muscle synergies has been successful also in characterizing the spatio-temporal organization of muscle contractions during human reaching tasks. Muscle patterns observed during movements in different directions [d'Avella et al., 2006] and speed [d'Avella et al., 2008] were accurately reconstructed by appropriate linear combinations of synergies, which appeared very similar across subjects. The synergies that were extracted from muscle activities during unloaded reaching (i.e. subjects did not hold any load in their hands) accounted for the EMG signals obtained during loaded conditions. The recruitment of the individual synergies, as well as their onset time, were consistently modulated with movement direction, and did not change substantially with movement speed. This observation was further confirmed by Muceli et al. [2010]; in this study a small set of specialized synchronous synergies was able to explain a large set of multijoint movements in various directions. Finally, visually guided online corrections during center-out reaching were tested recently. The synergistic strategy was shown to be robust and more effective in explaining the corrective muscle patterns than the individual muscle activities [d'Avella et al., 2011]. Furthermore, it was shown that to correct ongoing reaching movements, the CNS may either modulate existing synergies [d'Avella et al., 2011], or reprogram new ones [Fautrelle et al., 2010].

Roh et al. [2012] showed that an appropriate set of synergies could reconstruct the average patterns of muscle activation observed during isometric forces production in humans. The EMG signals were obtained for different force magnitude, directions and initial postures. The extracted synergies were very similar across conditions, and they were able to explain the corresponding datasets. Each synergy seemed to underlie a specific force direction, while its activation coefficient appeared correlated to the force magnitude. In another series of experiments, a small set of synchronous synergies was able to explain static hand postures and discriminate the shapes of grasped objects [Weiss and Flanders, 2004]. Moreover, a few time-varying synergies succeeded in revealing the spatiotemporal patterns of muscle activity during hand shape transitions, as in fingerspelling [Klein Breteler et al., 2007].

A relevant series of experiments showed that muscle activations involved in human postural control can be explained in terms of combinations of muscle synergies. A set of synchronous muscle synergies was able to explain muscle activations involved in postural stabilization; the EMG variation observed among trials and perturbation directions was accounted for by appropriate modulations of the synergies activation coefficients [Torres-Oviedo and Ting, 2007]. In order to verify that the extracted synergies did not depend only on the specific biomechanical context, in a new experiment a set of subjects were asked to react to support perturbation from different postural configurations [Torres-Oviedo and Ting, 2010]. The extracted synergies were very similar across the different conditions; however, in some cases task-specific muscle synergies needed to be added to the original synergy set to obtain a satisfactory EMG reconstruction. As the various postures lead to different patterns of sensory inflow, these results rule out the possibility that the observed synergies are only determined by specific patterns of sensory stimulations. On the contrary, they support the hypothesis that different muscle postural responses are generated by task-related modulations of the synergy activation levels. Such a hypothesis found evidence in the experiments performed by Safavynia and Ting [2012], where the temporal recruitment of the identified synchronous muscle synergies were explained by a mathematical model that explicitly takes into account the kinematic of the subject's center-of-mass (CoM). The authors then concluded that synchronous muscle synergies are recruited according to an estimate of

task-related variables. The same model was previously used to fit the activations of each muscle independently during the same postural perturbation tasks [Welch and Ting, 2007]. Related to postural control, Krishnamoorthy and colleagues analyzed the muscle activations that underlie shifts of the centers of pressure (COP) of standing subjects [Krishnamoorthy et al., 2003a,b]. In this experiment three "muscle modes", extracted by means of PCA, explained most of the variability of the integrated EMG signals. Such components are equivalent to synchronous muscle synergies as defined in Sec. A.2, and they are characterized by the authors as the independent elemental variables that are controlled synergistically (in the sense of the UMH) by the CNS to stabilize the COP. Specifically, the model assumes that the location of the COP is modified by linear combinations of the M-modes, and their mixing coefficients represent the independent variables controlled by the CNS. Perreault et al. [2008] examined the organization of reflexes involved in postural stabilization in both stiff and compliant environments; although reflexive responses are modulated by the direction of perturbation, they showed that the synchronous muscle synergies appear very similar across conditions.

Another scenario that provides evidence to the hypothesis of muscle synergies is human locomotion [Ivanenko et al., 2006a; Lacquaniti et al., 2012b]. Ivanenko et al. [2004] showed that five temporal synergies could reconstruct the muscle activity involved in locomotion tasks. These patterns are robust across walking speeds and gravitational loads, and they relate to foot kinematics [Ivanenko et al., 2003]. Additionally, the same temporal synergies (accompanied by additional ones) were observed during the coordination of locomotion with additional voluntary movements [Ivanenko et al., 2005]. Similar results have been reported in other locomotor behaviors such as running [Cappellini et al., 2006] and pedaling [Hug et al., 2011].

Finally, some experiments have investigated how the hypothetical synergy organization of the CNS evolves during onthogenetic development [Lacquaniti et al., 2012a]. Dominici et al. [2011] observed that the two temporal synergies identified in stepping neonates are retained through development, and they are augmented by two new patterns first revealed in toddlers. The final set of synergies was observed in several animal species, consistent with the hypothesis that, despite substantial phylogenetic distances and morphological differences, locomotion is built starting from common temporal synergies. This conclusion was also supported by the comparison of temporal synergies extracted from young and elderly people, which revealed no significant effect of aging on synergy compositionality and activation [Monaco et al., 2010].

A.3.2 Direct neural evidence

The studies presented so far support the existence of synergistic muscle activations during the sensorimotor control of movements. However, these methods are indirect, in the sense that the presence of synergistic structures within the CNS can only be inferred. What remains to be tested is whether the uncovered muscle organization is neurally implemented in the CNS and, if so, in which areas. Alternatively, one could argue that the extracted synergies represent a phenomenological output of the motor coordination required for movement execution. For instance, recently Kutch and Valero-Cuevas [2012] designed carefully thought experiments and simulations to show that muscle synergies can be observed even if the nervous system does not control muscles in groups. The authors demonstrated that muscle synergies, as detected via dimensionality reduction methods (see Sec. A.3.1), may originate from biomechanical couplings and/or from constraints of the task. Similar conclusions were already reached by Valero-Cuevas et al. [2009], who showed that the observed within-trial variability of EMG data underlying the production of fingertip forces, was incompatible with the (unique) associated muscle synergy that would have been extracted. Although these findings do not directly falsify the muscle synergy hypothesis,

they cast at least some doubts about the sole neural origin of modularity.

This underlies the need for a more critical assessment of the validity of the muscle synergy hypothesis. In this direction, a number of recent studies sought evidence for a neural implementation of muscle synergies, and examined which regions of the CNS may express synergies and their activations. This question has been addressed by attempting to relate neural activity with simultaneously recorded muscle activity during performance of different motor tasks. Using such an approach, Holdefer and Miller [2002] provided direct support for the existence of neural substrates of muscle synergies in monkey's primary motor cortex. In particular, they studied the activity of neurons and muscles during the execution of a variety of reaching and pointing movements, and they found that the discharge of individual neurons represents the activation of functional groups of muscles. In addition, Hart and Giszter [2010] showed that some interneurons of the frog spinal cord were better correlated with temporal synergies than with individual muscles. Therefore, they suggested that these neural populations constitute a neural basis for synergistic muscle activations [Delis et al., 2010]. Another study demonstrated that the sequential activation of populations of neurons in the cat's motor cortex initiates and sequentially modifies the activity of a small number of functionally distinct groups of synergistic muscles [Yakovenko et al., 2010]. Similarly, Overduin et al. [2012] showed that microstimulations of specific regions of the motor cortex of two rhesus macaques corresponded to well-defined spatial patterns of muscle activations. These synchronous synergies were very similar to those extracted from the same animals during natural reaching and grasping behaviors. Extending this research line in the context of motor learning, Kargo and Nitz [2003] showed that early skill learning is expressed through selection and tuning of primary motor cortex firing rates, which specify temporal patterns of synergistic muscle contractions in the frog's limb. Finally, Roh et al. [2011] analyzed the muscle patterns of the frog before and after transection at different levels of the neuraxis: brain stem, medulla and spinal cord respectively. They found that medulla and spinal cord are sufficient for the expression of most (but not all) muscle synergies, which are likely activated by descending commands from supraspinal areas. Similarly, Hart and Giszter [2004] examined the compositionality of temporal synergies in decerebrated and spinalized frogs. Their results indicated that in both cases temporal synergies consisted of pulsed or burst-like activations of groups of muscles. They also showed that brainstem frogs had more focused muscle groups and showed richer behaviors than spinalized equivalents.

In humans, the main approach to locate hypothetical muscle synergies has been to analyze brain-damaged patients. Comparing the synergies extracted from healthy and brain-damaged subjects could provide hints about the neural centers involved in the synergistic control of muscles. In this vein, examining motor tasks involving arm and hand movements, Cheung et al. [2009b] showed that the synchronous synergies extracted from the arm affected by a stroke were strikingly similar to the ones extracted from the unaffected arm, concluding that muscle synergies were located in regions of the CNS that were not damaged. In a second study involving subjects with more severe motor impairment [Cheung et al., 2012], they found that synchronous synergies may be modified according to three distinct patterns — including preservation, merging, and fractionation of muscle synergies — reflecting the multiple neural responses that occur after cortical damage. These patterns varied as a function of both the severity of functional impairment and the temporal distance from stroke onset. Similarly, Roh et al. [2013] found systematic alterations of the upper limb synergies involved in isometric force production in stroke patients with severe motor impairment. However, these alterations did not involve merging or fractionation of normal synergies. Clark et al. [2010] investigated the modular organization of locomotion in stroke patients. They found a coordination pattern consisting of fewer synchronous synergies than for the healthy subjects. These synergies resulted from merging of the synergies observed

in healthy subjects, suggesting reduced independence of neural control signals. In contrast, Gizzi et al. [2011] demonstrated that the temporal waveforms of the synergy activation signals, but not the synchronous synergies, were preserved after stroke.

Finally, a different but worth-mentioning approach has been the attempt to map the activity of leg muscles onto the alpha-motoneuron pools along the rostrocaudal axis of the spinal cord during human locomotion [Ivanenko et al., 2008, 2006b]. Using this procedure, the authors could infer the temporal and spatial spinal motor output for all the muscles of the legs during a variety of human walking conditions, and relate them to the control of task-relevant variables such as center of mass displacements. Overall, their findings support the existence of some spinal circuitry that implement temporal synergies. The strength of this approach resides in the explicit use of anatomical and clinical charts that document the innervation of the lower limb muscles from the lumbosacral enlargement [Cappellini et al., 2010].

A.4 Synergies from the perspective of the task-space

A.4.1 From input-space to task-space: general rationale

The methodology presented in Sec. A.3.1 undeniably led to many crucial insights, however it does not guarantee that the extracted synergies account for the observed task performance. VAF-like metrics only measure the capability of the synergies to reconstruct/fit the dataset of recorded "input-signals" (i.e. EMG data). Moreover, in some studies, such signals are averaged across movement repetitions. In this case, the VAF constitutes an average indicator, and it does not quantify the capability of the synergies to reconstruct each individual trial [Ranganathan and Krishnan, 2012]. Since the musculoskeletal apparatus is a non-linear system, these approximations of the recorded muscle activities may not lead to the observed task performance ([Broer and Takens, 2011], paragraph 1.1), a condition that would harm the validity of the hypothesized modular control structure. On a similar note, the extracted synergies might generate unfeasible joint torques. Finally, even if the dataset of muscle activity is very well approximated, additional muscles that are not recorded during the experiment might have a crucial role in the generation of the movement. These issues emerge because the dynamics of the musculoskeletal system (i.e. its input-output relation) is not directly taken into account in the synergy decomposition algorithms.

In this section we review those works that attempt to relate muscle synergies to performance variables defined in task-space. Initially, we present the concepts of functional synergies and spinal force fields. The former constitutes a valid strategy to include the task variables into the classical EMG-based analysis; the latter provides task-based evidence for neurally implemented muscle synergies. Then, we discuss some studies that, in the context of biomechanics, employ plausible musculoskeletal models to test the movements obtained from experimentally extracted muscle synergies. Finally, we shift our attention to robotics and characters animation. In these fields, the main challenge is the synthesis of a small set of synergies that reduces the dimensionality of control and, at the same time, spans a subspace of actuations that allows the agent to perform a wide variety of tasks (Fig. A.3, red arrows). Ideally, the synthesized synergies should preserve controllability and reachability of the system. Loosely speaking, this means that any desired system state can be reached by an appropriate control input (i.e. combination of synergies) in a finite amount of time. At the motor level, it is important that the synergies generate feasible actuations; additional properties, such as the generation of optimal control signals, may also be desirable (see Fig. A.1).

A.4.2 Functional muscle synergies and spinal force fields

In most of the works presented so far, the functional role of muscle synergies is estimated a-posteriori by analyzing the dependence of the recruitment coefficients (i.e. gain and/or onset time) on the task conditions (e.g. reaching direction, force magnitude and direction, perturbation direction). Typically, each muscle synergy is assumed to underlie the task-level functionality observed in conjunction with the higher values of its activation coefficient. As an example, the analysis of directional tuning curves illustrated that some of the synergies were directly related to reaching in specific directions [d'Avella et al., 2008]. A different approach is taken by a pool of studies which define the concept of functional synergies; i.e. components, typically extracted by means of NMF, of a dataset containing both EMG signals and measurements of defined task-related variables. As a result, each component consists of two elements: a balance of muscle contractions (i.e. synchronous muscle synergy), and the evolution of the task-related variables induced by such a muscle synergy (task-related vector). In our view, the concept of functional synergies provides a way to tackle the drawbacks of input-based extraction algorithms: if a set of functional muscle synergies extracted from a training-set is able to reconstruct both the EMG and, more importantly, the task-related signals observed in another set of data (testing set), then it is more likely that combinations of such muscle synergies will generate the appropriate control signals to perform the task successfully.

Functional muscle synergies were analyzed in the context of postural tasks in experiments with humans [Chvatal et al., 2011] and cats [Ting and Macpherson, 2005; Torres-Oviedo et al., 2006]. The task-related variables were defined as the forces measured under the feet of the subject, which reacted to unexpected motions of the support surface. The experiments showed that each subject exhibited the same functional synergies for both stepping and non-stepping responses to perturbations [Chvatal et al., 2011], suggesting that a common pool of muscle synergies, with specific biomechanical functionalities, can be used by the CNS to drive the motion of the CoM independently of the subject's behavioral response. The functional synergies extracted from the non-stepping data were able to reconstruct the EMG signals, the CoM acceleration and the direction (not the magnitude) of the forces recorded during stepping responses; however, an additional stepping-specific muscle synergy was needed to increase the quality of EMG reconstruction. Generality and robustness of functional synergies were also analyzed in postural experiments with cats [Torres-Oviedo et al., 2006]. In this study, a group of cats experienced both translations and rotations of the support surface. Functional muscle synergies were extracted from a dataset containing EMG signals and ground forces observed for different postural configurations (i.e. distances between the anterior and the posterior legs). The functional synergies extracted during surface translations for the most natural posture were able to reconstruct the data observed in all the other conditions (i.e. different postural configurations and surface rotations). Moreover, functional synergies appeared very similar across subjects. These results suggested that each muscle synergy implements a specific biomechanical functionality [Ting and Macpherson, 2005], which is general across tasks and robust across subjects.

The methodology proposed by Ting and colleagues is undoubtedly a valuable attempt to identify muscle synergies that are directly related to task execution, however it presents some limitations. First, NMF extracts non-negative components and coefficients; while this constraint is well justified at the muscle activation level (see Sec. A.3.1), task variables may exhibit negative values. Second and more important, in addition to a linear superposition also at the task-level, this decomposition procedure assumes that both EMG signals and task-variables are generated with the same mixing coefficients. Although it is possible to obtain a good fit of a given dataset, due to the non-linearity of the musculoskeletal system, this assumption does not hold in general.

A radically different approach to investigate the modularity of motor circuitries consists in analyzing the so called spinal force fields. This method is grounded on the seminal discovery that electrical stimulations of individual regions of the frog's spinal cord produce peculiar isometric endpoint forces that depend on the posture of the limb; the direction of the force vectors within each of these fields is invariant over time, while their magnitudes are characterized by a specific time evolution. Additionally, each of these force fields features a specific point of convergence. Structures with these characteristics can be generated by groups of coactive and linearly covarying muscles [Giszter et al., 1993; Mussa-Ivaldi et al., 1994]. In particular, only a small subset of all the possible muscle combinations leads to robust and convergent force fields [Loeb et al., 2000]. Therefore, the observation of such characteristics in an experimentally measured force field can be regarded as an indirect evidence for spinally implemented temporal muscle synergies (see Sec. A.2). Kargo and Giszter [2000b] showed that rapid corrections of movements in wiping frogs can be explained as linear combinations of spinal force fields. Additional evidence was obtained by examining the force fields generated by frogs [Giszter and Kargo, 2000] and turtles [Stein, 2008] that exhibited deletion of motor patterns. Another method to investigate the nature of spinal circuits is the analysis of feedback mechanisms in relation to force fields. Different external excitations of the frog's muscle spindles during wiping reflexes led to structurally invariant force fields across time. Furthermore, the bursts of muscle activity underlying the wiping behavior and the balance of activations across muscles were not altered by the spindle feedback. Instead, feedback regulated the amplitude and the timing of each single burst. Since these variables did not covary across the pulses, the authors concluded that individual premotor drive pulses and not time-varying synergies are the units of spinal activity [Kargo and Giszter, 2008]. Such hypothetical neural organization is compatible with the synergy scheme proposed by Drew et al. [2008] and Krouchev et al. [2006] for locomotive behaviors. These schemes allow a sequential activation of coordinated groups of muscles, a mechanism that can be implemented in the premotor drive model by modulating the onset time of the bursts. Spinal force fields are effectively task-level representations of hypothetical neural modules, however this methodology does not provide any estimate of what the corresponding muscle synergies may look like. Moreover, the relation between linear combinations of muscle synergies and linear combinations of force fields is far from being trivial.

A.4.3 Neuromechanical modeling

Although many studies in experimental motor control provide support to the hypothesis of muscle synergies, it is hard to test whether the proposed control model can effectively lead to the task performance observed experimentally and generalize to other tasks. This issue can be tackled computationally by employing biologically plausible models of the musculoskeletal apparatus.

A pool of studies investigate if a modular organization like the synchronous synergy model can explain a complex task like human walking [Allen and Neptune, 2012; McGowan et al., 2010; Neptune et al., 2009]. A set of synergies are identified from a dataset of recorded EMG signals by means of NMF. Such "modules" are then used to generate the muscle control inputs to a musculoskeletal model of the human legs. Using these synergies as a first guess, a numerical procedure optimizes the relative level of muscle activation within each module and the time course of the weighting coefficients; the objective is to minimize the difference between the results of the forward simulation and the values of the task variables measured experimentally. The walking kinematic and the ground reaction forces are well reproduced by 5 modules, if the motion is constrained in 2D [Neptune et al., 2009], and 6 modules for 3D walking [Allen and Neptune, 2012]. Additional simulations reveal that the muscle groups identified during normal walking

are able to emulate walking tasks with very different mechanical demands (i.e. change in mass and weight of the models) [McGowan et al., 2010]. These results agree with the theoretical considerations formulated by Nori et al. [2008]. Finally, this research shows that each module is associated to a specific biomechanical functionality (e.g. body support, forward propulsion, leg swing and balancing).

Related results are presented by McKay and Ting [2008, 2012]. The goal of these studies is to predict the patterns of muscle activities and the ground reaction forces observed experimentally in unrestrained balance tasks with cats [Torres-Oviedo et al., 2006]. Muscle contractions for an anatomically-realistic musculoskeletal model of the cat are computed; the used optimization procedure constrains task-related variables (i.e. center of mass) to the experimental results. Although many different cost functions are tested, the best predictions are achieved by minimizing control effort (i.e. total squared muscle activation). Predictions improve if muscle contractions are constrained to linear combinations of the experimentally derived synergies [Torres-Oviedo et al., 2006]; however the overall control effort increases, and the range of admissible ground forces reduces substantially. Furthermore, these studies validate the assumption made by Torres-Oviedo et al. [2006] that the ground reaction forces associated to each synergy rotate as a function of the limb axis. These results suggest that muscle synergies are feasible physiological mechanisms for the implementation of near-optimal or "good-enough" motor behaviors [de Rugy et al., 2012].

Kargo et al. [2010] employed a biomechanical model of the frog hindlimb to test whether the model of premotor drive could account for the wiping behavior observed experimentally [Kargo and Giszter, 2008]. The parameters of the premotor drive model (i.e. muscle groups, pulse time course, and amplitude and phasing of the single synergies) are initially identified to reproduce experimental isometric forces and free limb movement kinematics. As expected, starting from different limb postures the derived feedforward control fail in driving the simulated limb toward the target. However, as showed by Kargo and Giszter [2008], appropriate feedback modulations of the amplitude and the phase shift of the drive burst, and the adjustment of muscle balance based on the initial configuration of the limb, are enough to generate successful muscle activations. Furthermore, the limb trajectories obtained with and without feedback are very similar to those observed in intact and deafferented [Kargo and Giszter, 2000a] frogs respectively. These results support the model of premotor drives, in which feedback mechanisms preserve the duration of the pulses.

Berniker [2005] analyzed mathematically the control scheme of muscle synergies and proposed a principle for its formation [Berniker et al., 2009]. A linear reduced-dimensional dynamical model that preserves (to the best extent possible) the natural dynamic of the original system is initially computed. Synergies are defined as the minimal set of input vectors that influence the output of the reduced-order model [Berniker, 2005], and that minimally restrict the commands (and the resulting responses) useful to solve the desired tasks [Berniker et al., 2009]. Practically, this set is found by optimizing the synergy matrix over a representative dataset of desired sensory-motor signals. This method was able to synthesize a set of synergies for the model of the frog hindlimb that were very similar to the ones observed experimentally [Cheung et al., 2005]. Furthermore, the synergy-based controller produced muscle activations and kinematic trajectories that were comparable with the ones obtained with the best-case controller (that can activate each muscle independently).

A.4.4 Robotics and character animation

In the context of robotics and characters animation, the concept of muscle synergies is appealing as it provides a strategy to reduce the number of variables to be controlled (synchronous synergy model), or more generically, the dimensionality of the control signals (time-varying synergy model). Animated characters are embedded in physical environments (i.e. dominated by physics laws) thus the associated control problem is totally equivalent to the control of a musculoskeletal model or of a humanoid robot. In this section we present the works that have been carried out in these fields of research.

The work proposed by Mussa-Ivaldi [1997] is one of the first attempts to develop a controller based on the modularity observed in biological systems [Mussa-Ivaldi and Giszter, 1992]. The idea is that the motion of a kinematic chain can be determined by a force field applied to its end effector. Inspired by the experiments performed by Giszter et al. [1993], such a force-field results from the linear combination of basic fields, each characterized by a single equilibrium point in operational space. Results show that, for a simulated planar kinematic chain, an appropriate choice of the basis-field coefficients can produce a wide variety of end-effector trajectories. Similarly, Matarić et al. [1999] used force fields to drive joint torque controllers on a rigid-body animated character [Matarić et al., 1998a,b].

Although the concept of spinal-force field is very similar, Mussa-Ivaldi's work does not directly use the notion of synergy as defined in Sec. A.2. A step forward is taken by Nori and Frezza, who propose a mathematical formulation for a set of actuations (i.e. synergies) that comply with the hypothetical properties of spinal-force fields [Mussa-Ivaldi and Bizzi, 2000]. The mathematical description of the synergies is derived from the closed-form solution of an optimal control problem. Additionally, a feedback controller assures that the system follows the desired trajectory towards the synergy equilibrium position. It is proved that the proposed formulation guarantees system controllability[2]. The synthesized synergies are successfully tested on a simulated two-degrees-of-freedom (dof) planar kinematic chain [Nori, 2005; Nori and Frezza, 2005].

The idea that each synergy solves a well-defined control problem (e.g. to lead the system to a specific equilibrium position [Nori and Frezza, 2005]), appears in several other studies [Alessandro and Nori, 2012; Chhabra and Jacobs, 2008; Todorov, 2009]. Chhabra and Jacobs [2008] propose a method called Greedy Additive Regression (GAR). A library of task-specific actuations (synergies) are kept in memory. When a new task has to be performed, a suitable actuation is initially searched in the linear span of these synergies. If the lowest task-error is above a certain threshold, the task will be solved via traditional methods (e.g. feedback error learning), and the obtained actuation will be added to the library. If the library already contains the maximum number of synergies allowed, the least used one will be removed. The obtained results suggest that the synergies synthesized via GAR outperform primitives based on PCA if the dynamical system is non-linear (planar kinematic chain), and there is no statistical difference for linear systems. However, no theoretical explanation is provided.

In the same vein, Todorov [2009] proved that, for a certain class of stochastic optimal control problems, an appropriate change of variable in the Bellman equation allows to obtain the optimal control policy as a linear combination of some primitives. These primitives are, in turns, solutions to other optimal control problems. Such a method has recently been tested in the context of

[2] In control theory, a system is said to be controllable if an external input can move the system from any initial state to any final state in a finite time interval.

character animation [da Silva et al., 2009]. It is important to clarify that this theory provides a theoretical grounding to the compositionality of optimal control laws, but like GAR it does not provide a method to compute such primitives. In fact, although new efficient methods have been proposed recently, solving an optimal control problem remains quite computationally intense, and it might be unfeasible for systems with a large number of dof.

Another mathematical framework, that has recently been developed in the context of character animations, is based on the optimal anechoic mixture decomposition model, mathematically equivalent to the time-varying synergy decomposition. Specifically, complex kinematic animations are obtained by mixing primitive source signals that are learned from motion captured data [Giese et al., 2009; Mezger et al., 2005; Park et al., 2008a,b]. Within this framework a number of interesting results have been achieved, including a mathematical proof of stability properties for groups of characters that interact in various ways [Mukovskiy et al., 2011].

The procedure presented by Alessandro et al. [2012] is grounded on a method to solve generalized reaching tasks called Dynamic Response Decomposition (DRD). In this context, a task is defined as a list of constraints on the values of the state variables at given points of time. Initially, a state-space solution is computed by interpolating these constraints by means of a set of dynamic responses (i.e. evolutions of the state variables); then, inverse dynamics is used to obtain the corresponding actuations. Based on this technique, the following two-phase procedure allows to synthesize a set of synergies. An extensive collection of generic actuations are used to generate the system dynamic responses (exploration phase); in a second stage (reduction phase), they are used to interpolate a small set of tasks. The corresponding actuations proved to be effective synergies for additional reaching tasks on a simulated planar kinematic chain. Like GAR, this procedure generates synergies in the form of feedforward controllers, and it allows to modify incrementally the library of synergies. However, DRD provides a computationally fast method to solve the task. This technique has proved its efficacy empirically, but a solid theoretical grounding is still lacking.

Most of the methods presented so far require an accurate analytical model of the system dynamics. Such a model is not always available, and for certain robots, it might be difficult to identify. Todorov and Ghahramani [2003] propose a method to synthesize synergies by means of unsupervised learning. Their work emphasizes the role of muscle synergies in an hypothetical hierarchical control scheme similar to the one proposed by Safavynia and Ting [2012]: receptive fields translate sensory signals to internal variables, and muscle synergies translate high-level control signals applied to these variables to actual muscle contractions. From this perspective, receptive fields along with motor primitives must form an inverse model of the sensory-motor system. This mapping is learned by fitting a probabilistic model to a dataset of sensory-motor signals generated by actuating the robot with random pulses. The use of the learned synergies as low-level controllers substantially reduces the time needed to learn a desired policy, however their capability to generalize to additional control laws is not explicitly tested.

Alessandro and Nori [2012] define synergies as parametrized functions of time that serve as feedforward controllers. The identification procedure consists in finding the values of the parameters such that appropriate linear combinations of the resulting synergies drive the dynamical system over a set of desired trajectories (training set). The synergies identified are then tested for generalization; the idea is to evaluate to which extent they can generate actuations that drive the system along a new group of trajectories (testing set). This procedure has been evaluated successfully in simulation and does not require the analytical form of the system dynamics. However, it is computationally very intense as it involves heavy optimizations. In essence, this work proposes a new formal definition of the concept of muscle synergies: elementary controls

that are evaluated in terms of task-performance (i.e. tracking error), rather then in terms of approximation of the input space.

Thomas and Barto [2012] formulate the problem of primitive (i.e. synergy) discovery within the framework of reinforcement learning. In this case, the problem that the agent has to solve is a Markov Decision Process (MDP), and each primitive is a parametrized feedback control policy. The idea is to identify the optimal parameters that maximize the expected reward for a given task, when the control is restricted to linear combinations of the learned primitives. This method is tested on a simulated planar kinematic chain actuated with artificial muscles. Primitives are identified on reaching tasks, and they are successfully tested in a scenario that involves reaching and avoiding obstacles. This work clearly shows the advantage of a synergy-based framework in terms of learning speed of novel control policies. This method is in essence similar to the one proposed by Alessandro et al. [2012], however it identifies complete feedback control policies rather then single feedforward synergies.

The time-varying synergy model greatly reduces the dimensionality of the problems by encoding actuations with synergy-coefficients, however at the same time it introduces a complication. As the new input variables are piecewise constant, it is difficult (although possible) to implement feedback loops. The synchronous model ameliorates this problem and, to some extent, it allows adapting traditional control strategies to the new reduced-dimensional control input.

Some researchers employ the synchronous synergy model to control the tendon-driven robotic ACT hand [Deshpande et al., 2013] in a reduced dimensional space [Malhotra et al., 2012; Rombokas et al., 2011; Zhang et al., 2011]. Similarly to Todorov and Ghahramani [2003], dimensionality reduction is applied both in the sensory space and in the actuation space. The "observation synergies" transform sensory readings (tendon lengths) into a lower dimensional variable; the "control synergies" translates synergy-coefficients (as defined in Sec. A.2) to motor signals. Model adaptive control and PIDs are applied to the reduced dimensional input, and allow the robotic hand to perform tasks like writing [Malhotra et al., 2012; Rombokas et al., 2011] and playing piano [Zhang et al., 2011]. The synergy matrices (observation and control) are computed by applying PCA and NMF to a dataset of tendon-lengths obtained as a result of defined hand motions. It is noteworthy that the more similar this motions are to the ones required to solve the task, the better the quality of the obtained synergy-based controller. This is clearly not surprising, but it highlights the importance of task-related variables in the formation of muscle synergies [Todorov et al., 2005].

Marques et al. [2012] identify synchronous synergies by means of an unsupervised Hebbian-like algorithm that captures the correlations between motor signals and sensory readings. Each synergy thus summarizes the levels of correlation between each motor and one of the sensors. The time modulation of each synergy to solve a given task is then obtained by means of a supervised learning procedure that aims at reducing the task error. Unlike many other works in robotics, the exploratory strategy proposed to generate the dataset of sensory-motor data does not exploit any prior information about the desired motor tasks, therefore muscle synergies are implicitly interpreted as patterns of motor coordinations that solely reflect the biomechanical constraints of the robot. This method has been tested on a single-joint tendon driven robot.

In the context of robotic hands, many researchers adopted the idea of postural-synergies, or eigengrasps. This concept derived by the observation that the variability of finger postures during human grasps can be explained by a few principal components [Santello et al., 1998], i.e.

eigengrasps. Similarly, constraining the finger-joints positions of a robotic hand in such a way that the useful grasping postures can be obtained by superposing a small number of components, would result in a substantial simplification of the grasping problem. Ciocarlie and Allen [2009] derived a theoretical formulation of the problem of stable grasping in the low dimensional space of the postural-synergies; such a formulation is further improved by Gabiccini et al. [2011] for complain grasps. These studies are further analyzed and discussed by Bicchi et al. [2011], who presented them from the point of view of modeling the process of grasping and active touch. Finally, Brown and Asada [2007] proposed a direct mechanical implementation of the eigengrasps. In all these works, the quantitative details of the postural-synergies are taken from human experiments and adapted to the robot mechanical structure; the problem of finding a set of synergies that is optimized for a given robotic hand is left as future research.

Reduced dimensionality based on postural synergies is also explored by Hauser et al. [2011] for the task of balancing a humanoid robot. The authors propose a mathematical formulation, as well as a method to construct kinematic synergies (i.e. predefined balance between joint positions) that are directly linked to task variables (e.g. for balance control, the center of pressure). Additionally, the synergies are constructed in such a way that the mapping from synergy coefficients to task variables is linear (similar to the work proposed by Nori and Frezza [2005] but in kinematic space). This allows to use a simple Proportional-Integral-Derivative controller (PID) on the synergy coefficients to control the center of pressure of the robot, as long as the movements are slow enough to neglect dynamic disturbances. The proposed method is demonstrated both in simulation and in a real humanoid.

As a final note, it is important to say that the concept of modularity has been employed in robot control in many other ways. In most of these works modules are defined as kinematic-based controllers that are combined sequentially to obtain complex joint trajectories [Ijspeert et al., 2013; Khansari-Zadeh and Billard, 2011]. In this regard, these works are more related to the concept of kinematic stroke than to muscle synergies [Pollick et al., 2009]. These works are out of the scope of this paper, as we focus on controllers that, in accordance with the models of muscle synergies, are based on (parallel) superpositions of primitives in input space.

A.5 Conclusions and perspectives

The hypothesis of muscle synergies, that proposes a modular organization of the neural circuitry involved in muscle coordination, has been proved very difficult to validate or falsify [Tresch and Jarc, 2009]. As discussed in Sec. A.3, a substantial body of evidence in favor of this hypothesis comes from the observation that the main components of EMG recordings are robust across behaviors, biomechanical contexts, and individuals. In addition, the successful control of artificial agents confirm the computational feasibility of the hypothesized synergy-based controller (Sec. A.4). However, there also exist experiments that, for the case of the human hand, seem to disprove the hypothesis of muscle synergies [Kutch et al., 2008; Valero-Cuevas et al., 2009]. As a matter of fact, there is no real consensus yet on whether muscle synergies effectively represent a modular organization of the CNS, or they merely result from the methodology employed during the experiments.

The works that are based on the control of artificial agents (e.g. musculoskeletal models, robots, animated characters) clarify the importance of evaluating synergies in task-space. In this context, the idea is to synthesize a set of synergies that guarantees the accomplishment of the desired tasks (Fig. A.3, red arrows). On the contrary, the main focus of experimental motor

control has been to identify the synergies that better reconstruct the recorded EMG dataset (Fig. A.3, continuous green arrows), and to understand their neural substrate. This approach implicitly assumes that a well reconstructed input signal leads to the observed task performance. Given the non-linear dynamics of the musculoskeletal system, this assumption might not hold. For this reason, in our view the hypothesis of muscle synergies should be tested by validating an input-output model (i.e. from muscle activations to task-variables), rather than fitting a model of the input data alone (Fig. A.3, dashed green arrow). In fact, we could speculate that muscle synergies encode a form of body schema [Hoffmann et al., 2010] that allows translating intentions to motor plans (i.e. the inverse dynamic model of the musculoskeletal system) [Torres-Oviedo and Ting, 2010].

The concept of functional synergies represents a first attempt to relate muscle synergies to task variables. However, as discussed in Sec. A.4.2, EMG and task-level components are assumed to be activated by the same coefficients. This assumption cannot hold in general because the musculoskeletal system is non-linear; rather, input-space and task-space coefficients should be related by a non-linear mapping (as described by Alessandro et al. [2012]). To address this issue, one should go beyond the use of NMF, and develop novel techniques that do not impose a linear mapping between the two sets of coefficients. Additionally one could try to reconstruct the task-variables with more general non-linear methods instead of imposing a linear combination also at the task level. In the same spirit of the procedure used so far, such a technique should optimize the reconstruction error of the EMG signals, and constrain a good fit of the task-variables. In any case, the generality of the extracted functional synergies should be tested. To the best of our knowledge, the model of functional synergies was never used as a predictive framework. It would be extremely interesting to evaluate the extent to which functional synergies identified during the execution of a certain set of tasks, are able to predict the muscle activations observed during the execution of another task that involve the same task variables. If such prediction was unsuccessful, the experimenter could conclude that the identified muscle synergies do not really encode the hypothesized biomechanical functionalities, or that the same functionalities might be encoded by different synergies. In general, the model of muscle synergies has very seldom been used to make predictions.

An alternative strategy to verify the relationship between muscle synergies and task execution (Fig. A.3, dashed green arrow), is to evaluate if they can account for task-related variations of single movement executions [Delis et al., 2013]. In practice, one might assess the capability of these synergies to decode each repetition of different motor tasks. In other words, one should be able to classify the motor tasks from the activation coefficients of the extracted synergies. If the decoding capability is satisfactory, one might conclude that the synergies not only constitute a low dimensional, but also a functional representation of the motor commands. This idea might be used to develop novel extraction algorithms that include task decoding objectives directly in the optimization procedure. The identified synergies would then maximize not only the reconstruction of the original motor patterns, but also the capability of disambiguating task-relevant trial-to-trial variations. Unlike the dimensionality reduction methods used so far, this approach would rely on supervised learning techniques to exploit information about the task. Possible alternatives to standard extraction algorithms include energy constrained discriminant analysis [Philips et al., 2009], the discriminant NMF [Buciu and Pitas, 2004], and the hybrid discriminant analysis [Yu et al., 2007].

The use of single-trial analysis, like the decoding strategy proposed above, may be useful for addressing some open problems that are relevant to this review. First, the development of such techniques may be useful to identify muscle activation components of relatively low

amplitude that reflect unique information about the task [Quiroga and Panzeri, 2009]; such components would be completely lost if an average across several trials is performed prior to the analysis. Second, such single-trial analysis techniques may be used to investigate the existence of trial-to-trial correlations across synergy activations, and to evaluate their functional role in controlling and performing task-related movement [Golledge et al., 2003; Schneidman et al., 2003]. Finally, approaches based on single-trial analysis of neural activity could also be instrumental in clarifying the existence of a neural basis for the muscle synergies [Hart and Giszter, 2004, 2010; Nazarpour et al., 2012; Ranganathan and Krishnan, 2012]. For example, they could in principle be applied to decode the task from single-trial neural population patterns that regulate the activation of synergies, and also to determine which patterns encode task differences, and which carry additional or independent information to that carried by other patterns [Delis et al., 2010].

Finally, an important aspect that is worth discussing is the role of feedback loops. In the case of synchronous synergies, the time course of the mixing coefficients can be adjusted on-line by means of appropriate feedback controllers; this is the reason of the popularity of such a model in the context of robotics. On the contrary, the models of temporal and time-varying synergies, in which the actuation time course are directly embedded in the synergies themselves, naturally represent feedforward controllers. As a result, the evolution of the task-variables intimately depends on the initial condition of the dynamical system. Alternatively, these synergies might be defined as functions of both time and state-variables; such an approach would characterize temporal and time-varying synergies as generators of complete control policies [Nori and Frezza, 2005; Thomas and Barto, 2012; Todorov, 2009].

In conclusion, we believe that the evidence reviewed here provides support for the existence of muscle synergies. However many issues are still unresolved. A deeper investigation of the relationship between synergies and task variables might help to address some of the open questions. In general, a closer coordination between experimental and computational research might lead to a more objective assessment of the muscle synergy hypothesis in task-space, and a better understanding of the modularity of the CNS.

Acknowledgment

This research was supported by the EU project RobotDoC under 235065 from the 7th Framework Programme (Marie Curie Action ITN) and the EU project AMARSi (ICT-248311).

Bibliography

Alessandro, C., Carbajal, J. P., and d'Avella, A. (2012). Synthesis and Adaptation of Effective Motor Synergies for the Solution of Reaching Tasks. In Ziemke, T., Balkenius, C., and Hallam, J., editors, *Lecture Notes in Artificial Intelligence (LNAI)*, pages 33–43, Berlin. Springer-Verlag.

Alessandro, C. and Nori, F. (2012). Identification of Synergies by Optimization of Trajectory Tracking Tasks. In *IEEE RAS/EMBS International Conference on Biomedical Robotics and Biomechatronics*, pages 924–930, Rome. IEEE.

Allen, J. L. and Neptune, R. R. (2012). Three-dimensional modular control of human walking. *Journal of Biomechanics*, 45(12):2157–2163.

Bell, A. J. and Sejnowski, T. J. (1995). An information-maximization approach to blind separation and blind deconvolution. *Neural Computation*, 7:1129–1159.

Berniker, M. (2005). *Linearity, motor primitives and low-dimensionality in the spinal organization of motor control*. PhD thesis, Massachusetts Institute of Technology.

Berniker, M., Jarc, A., Bizzi, E., and Tresch, M. C. (2009). Simplified and effective motor control based on muscle synergies to exploit musculoskeletal dynamics. *Proceedings of the National Academy of Sciences of the United States of America*, 106(18):7601–7606.

Bernstein, N. A. (1967). *The Co-ordination and Regulation of Movements*. Pergamon.

Bicchi, A., Gabiccini, M., and Santello, M. (2011). Modelling natural and artificial hands with synergies. *Philosophical Transactions of the Royal Society of London. Series B: Biological Sciences*, 366(1581):3153–61.

Bizzi, E., Cheung, V. C. K., d'Avella, A., and Saltiel, P. F. (2008). Combining modules for movement. *Brain Research Reviews*, 57:125–133.

Bizzi, E., Hogan, N., Mussa-Ivaldi, F. A., and Giszter, S. (1992). Does the nervous system use equilibrium-point control to guide single and multiple joint movements? *Behavioral and Brain Sciences*, 15(4):603–613.

Brochier, T., Spinks, R. L., Umilta, M. A., and Lemon, R. N. (2004). Patterns of muscle activity underlying object-specific grasp by the macaque monkey. *Journal of Neurophysiology*, 92(3):1770–1782.

Broer, H. and Takens, F. (2011). *Dynamical Systems and Chaos*. Springer, New York Dordrecht Heidelberg London.

Brown, C. Y. and Asada, H. H. (2007). Inter-finger coordination and postural synergies in robot hands via mechanical implementation of principal components analysis. In *IEEE/RSJ International Conference on Intelligent Robots and Systems*, pages 2877–2882, San Diego, California, USA. IEEE.

Buciu, I. and Pitas, I. (2004). A new sparse image representation algorithm applied to facial expression recognition. In *Machine Learning for Signal Processing. Proceedings of the 14th IEEE Signal Processing Society Workshop*, pages 539–548, Sao Luis, Brazil. IEEE.

Cappellini, G., Ivanenko, Y. P., Dominici, N., Poppele, R. E., and Lacquaniti, F. (2010). Migration of motor pool activity in the spinal cord reflects body mechanics in human locomotionj. *Journal of Neurophysiology*, 104(6):3064–3073.

Cappellini, G., Ivanenko, Y. P., Poppele, R. E., and Lacquaniti, F. (2006). Motor patterns in human walking and running. *Journal of Neurophysiology*, 95(6):3426–3437.

Cheung, V. C. K., d'Avella, A., and Bizzi, E. (2009a). Adjustments of motor pattern for load compensation via modulated activations of muscle synergies during natural behaviors. *Journal of Neurophysiology*, 101(3):1235–1257.

Cheung, V. C. K., d'Avella, A., Tresch, M. C., and Bizzi, E. (2005). Central and Sensory Contributions to the Activation and Organization of Muscle Synergies during Natural Motor Behaviors. *The Journal of Neuroscience*, 25(27):6419–6434.

Cheung, V. C. K., Piron, L., Agostini, M., Silvoni, S., Turolla, A., and Bizzi, E. (2009b). Stability of muscle synergies for voluntary actions after cortical stroke in humans. *Proceedings of the National Academy of Sciences of the United States of America*, 106(46):19563–8.

Cheung, V. C. K., Turolla, A., Agostini, M., Silvoni, S., Bennis, C., Kasi, P., Paganoni, S., Bonato, P., and Bizzi, E. (2012). Muscle synergy patterns as physiological markers of motor cortical damage. *Proceedings of the National Academy of Sciences of the United States of America*, 109(36):14652–14656.

Chhabra, M. and Jacobs, R. A. (2008). Learning to Combine Motor Primitives Via Greedy Additive Regression. *The Journal of Machine Learning Research*, 9(6):1535–1558.

Chiovetto, E., Berret, B., Delis, I., Panzeri, S., and Pozzo, T. (2013). Investigating reduction of dimensionality during single-joint elbow movements: a case study on muscle synergies. *Frontiers in Computational Neuroscience*, 7:11.

Chvatal, S. A., Torres-Oviedo, G., Safavynia, S. A., and Ting, L. H. (2011). Common muscle synergies for control of center of mass and force in nonstepping and stepping postural behaviors. *Journal of Neurophysiology*, 106(2):999–1015.

Ciocarlie, M. T. and Allen, P. K. (2009). Hand Posture Subspaces for Dexterous Robotic Grasping. *The International Journal of Robotics Research*, 28(7):851–867.

Clark, D. J., Ting, L. H., Zajac, F. E., Neptune, R. R., and Kautz, S. a. (2010). Merging of healthy motor modules predicts reduced locomotor performance and muscle coordination complexity post-stroke. *Journal of Neurophysiology*, 103(2):844–57.

da Silva, M., Durand, F., and Popović, J. (2009). Linear Bellman combination for control of character animation. *ACM Transactions on Graphics*, 28(3):1.

Darlington, R. B. (1968). Multiple regression in psychological research and practice. *Psychological Bulletin*, 69(3):161–182.

d'Avella, A. and Bizzi, E. (2005). Shared and specific muscle synergies in natural motor behaviors. *Proceedings of the National Academy of Sciences*, 102(8):3076–3081.

d'Avella, A., Fernandez, L., Portone, A., and Lacquaniti, F. (2008). Modulation of phasic and tonic muscle synergies with reaching direction and speed. *Journal of Neurophysiology*, 100(3):1433–54.

d'Avella, A., Portone, A., Fernandez, L., and Lacquaniti, F. (2006). Control of fast-reaching movements by muscle synergy combinations. *The Journal of Neuroscience*, 26(30):7791–7810.

d'Avella, A., Portone, A., and Lacquaniti, F. (2011). Superposition and modulation of muscle synergies for reaching in response to a change in target location. *Journal of Neurophysiology*, 106(6):2796–2812.

d'Avella, A., Saltiel, P., and Bizzi, E. (2003). Combinations of muscle synergies in the construction of a natural motor behavior. *Nature Neuroscience*, 6:300–308.

d'Avella, A. and Tresch, M. C. (2002). Modularity in the motor system: decomposition of muscle patterns as combinations of time-varying synergies. In Dietterich, T., Becker, S., and Ghahramani, Z., editors, *Advances in neural information processing systems*, volume 14, pages 141–148. MIT press, Massachusetts.

de Rugy, A., Loeb, G. E., and Carroll, T. J. (2012). Muscle coordination is habitual rather than optimal. *The Journal of Neuroscience*, 32(21):7384–7391.

Delis, I., Berret, B., Pozzo, T., and Panzeri, S. (2013). Quantitative evaluation of muscle synergy models: a single-trial task decoding approach. *Frontiers in Computational Neuroscience*, 7:8.

Delis, I., Chiovetto, E., and Berret, B. (2010). On the origins of modularity in motor control. *The Journal of Neuroscience*, 30(22):7451–7452.

Deshpande, A. D., Xu, Z., Weghe, M. J. V., Brown, B. H., Ko, J., Chang, L. Y., Wilkinson, D. D., Bidic, S. M., and Matsuoka, Y. (2013). Mechanisms of the anatomically correct testbed hand. *IEEE/ASME Transactions on Mechatronics*, 18(1):238–250.

Dominici, N., Ivanenko, Y. P., Cappellini, G., D'Avella, A., Mondì, V., Cicchese, M., Fabiano, A., Silei, T., Di Paolo, A., Giannini, C., Poppele, R. E., and Lacquaniti, F. (2011). Locomotor primitives in newborn babies and their development. *Science*, 334(6058):997–9.

Drew, T., Kalaska, J., and Krouchev, N. (2008). Muscle synergies during locomotion in the cat: a model for motor cortex control. *The Journal of Physiology*, 586:1239–1245.

Fautrelle, L., Ballay, Y., and Bonnetblanc, F. (2010). Muscular synergies during motor corrections: investigation of the latencies of muscle activities. *Behavioural Brain Research*, 214(2):428–36.

Flash, T. and Hochner, B. (2005). Motor primitives in vertebrates and invertebrates. *Current Opinion in Neurobiology*, 15(6):660–666.

Gabiccini, M., Bicchi, a., Prattichizzo, D., and Malvezzi, M. (2011). On the role of hand synergies in the optimal choice of grasping forces. *Autonomous Robots*, 31(2-3):235–252.

Giese, M., Mukovskiy, A., and Park, A. (2009). Real-time synthesis of body movements based on learned primitives. In Cremers, D., Rosenhahn, B., and Yuille, A., editors, *Statistical and Geometrical Approaches to Visual Motion Analysis*, pages 107–127. Springer Verlag, Berlin Heidelberg.

Giszter, S. F. and Kargo, W. J. (2000). Conserved temporal dynamics and vector superposition of primitives in frog wiping reflexes during spontaneous extensor deletions. *Neurocomputing*, 32-33:775–783.

Giszter, S. F., Mussa-Ivaldi, F. A., and Bizzi, E. (1993). Convergent force fields organized in the frog's spinal cord. *Journal of Neuroscience*, 13(2):467–491.

Gizzi, L., Nielsen, J.-F., Felici, F., Ivanenko, Y. P., and Farina, D. (2011). Impulses of activation but not motor modules are preserved in the locomotion of subacute stroke patients. *Journal of Neurophysiology*, 106(1):202–210.

Golledge, H. D., Panzeri, S., Zheng, F., Pola, G., Scannell, J. W., Giannikopoulos, D. V., Mason, R. J., Tovée, M. J., and Young, M. P. (2003). Correlations, feature-binding and population coding in primary visual cortex. *Neuroreport*, 14(7):1045–1050.

Hart, C. B. and Giszter, S. F. (2004). Modular premotor drives and unit bursts as primitives for frog motor behaviors. *The Journal of Neuroscience*, 24(22):5269–82.

Hart, C. B. and Giszter, S. F. (2010). A neural basis for motor primitives in the spinal cord. *The Journal of Neuroscience*, 30(4):1322–1336.

Hauser, H., Neumann, G., Ijspeert, A. J., and Maass, W. (2011). Biologically inspired kinematic synergies enable linear balance control of a humanoid robot. *Biological Cybernetics*, 104(4-5):235–49.

Hoffmann, M., Marques, H., Arieta, A., Sumioka, H., Lungarella, M., and Pfeifer, R. (2010). Body schema in robotics: A review. *Autonomous Mental Development, IEEE Transactions on*, 2(4):304–324.

Holdefer, R. N. and Miller, L. E. (2002). Primary motor cortical neurons encode functional muscle synergies. *Experimental Brain Research*, 146(2):233–43–.

Hug, F., Turpin, N. a., Couturier, A., and Dorel, S. (2011). Consistency of muscle synergies during pedaling across different mechanical constraints. *Journal of Neurophysiology*, 106(1):91–103.

Ijspeert, A. J., Nakanishi, J., Hoffmann, H., Pastor, P., and Schaal, S. (2013). Dynamical movement primitives: learning attractor models for motor behaviors. *Neural Computation*, 25(25):328–373.

Ivanenko, Y. P., Cappellini, G., Dominici, N., Poppele, R. E., and Lacquaniti, F. (2005). Coordination of locomotion with voluntary movements in humans. *The Journal of Neuroscience*, 25(31):7238–7253.

Ivanenko, Y. P., Cappellini, G., Poppele, R. E., and Lacquaniti, F. (2008). Spatiotemporal organization of alpha-motoneuron activity in the human spinal cord during different gaits and gait transitions. *The European Journal of Neuroscience*, 27(12):3351–68.

Ivanenko, Y. P., Grasso, R., Zago, M., Molinari, M., Scivoletto, G., Castellano, V., Macellari, V., and Lacquaniti, F. (2003). Temporal components of the motor patterns expressed by the human spinal cord reflect foot kinematics. *Journal of Neurophysiology*, 90(5):3555–65.

Ivanenko, Y. P., Poppele, R. E., and Lacquaniti, F. (2004). Five basic muscle activation patterns account for muscle activity during human locomotion. *The Journal of Physiology*, 556(Pt 1):267–82.

Ivanenko, Y. P., Poppele, R. E., and Lacquaniti, F. (2006a). Motor control programs and walking. *The Neuroscientist*, 12(4):339–48.

Ivanenko, Y. P., Poppele, R. E., and Lacquaniti, F. (2006b). Spinal cord maps of spatiotemporal alpha-motoneuron activation in humans walking at different speeds. *Journal of Neurophysiology*, 95(2):602–618.

Kargo, W. J. and Giszter, S. F. (2000a). Afferent roles in hindlimb wipe-reflex trajectories: free-limb kinematics and motor patterns. *Journal of Neurophysiology*, 83(3):1480–1501.

Kargo, W. J. and Giszter, S. F. (2000b). Rapid correction of aimed movements by summation of force-field primitives. *The Journal of Neuroscience*, 20(1):409–426.

Kargo, W. J. and Giszter, S. F. (2008). Individual premotor drive pulses, not time-varying synergies, are the units of adjustment for limb trajectories constructed in spinal cord. *The Journal of N euroscience*, 28(10):2409–2425.

Kargo, W. J. and Nitz, D. A. (2003). Early skill learning is expressed through selection and tuning of cortically represented muscle synergies. *The Journal of Neuroscience*, 23(35):11255–11269.

Kargo, W. J., Ramakrishnan, A., Hart, C. B., Rome, L. C., and Giszter, S. F. (2010). A simple experimentally based model using proprioceptive regulation of motor primitives captures adjusted trajectory formation in spinal frogs. *Journal of Neurophysiology*, 103(1):573–90.

Khansari-Zadeh, S. M. and Billard, A. (2011). Learning stable non-linear dynamical systems with gaussian mixture models. *IEEE Transaction on Robotics*, 27(5):943–957.

Klein Breteler, M. D., Simura, K. J., and Flanders, M. (2007). Timing of muscle activation in a hand movement sequence. *Cerebral Cortex*, 17(4):803–815.

Krishnamoorthy, V., Goodman, S., Zatsiorsky, V., and Latash, M. L. (2003a). Muscle synergies during shifts of the center of pressure by standing persons: identification of muscle modes. *Biological Cybernetics*, 89(2):152–161.

Krishnamoorthy, V., Latash, M. L., Scholz, J. P., and Zatsiorsky, V. M. (2003b). Muscle synergies during shifts of the center of pressure by standing persons. *Experimental Brain Research*, 152(3):281–292.

Krouchev, N., Kalaska, J. F., and Drew, T. (2006). Sequential activation of muscle synergies during locomotion in the intact cat as revealed by cluster analysis and direct decomposition. *Journal of Neurophysiology*, 96(4):1991–2010.

Kutch, J. J., Kuo, A. D., Bloch, A. M., and Rymer, W. Z. (2008). Endpoint force fluctuations reveal flexible rather than synergistic patterns of muscle cooperation. *Journal of Neurophysiology*, 100(5):2455–71.

Kutch, J. J. and Valero-Cuevas, F. J. (2012). Challenges and new approaches to proving the existence of muscle synergies of neural origin. *PLoS Computational Biology*, 8(5):e1002434.

Lacquaniti, F., Ivanenko, Y. P., and Zago, M. (2012a). Development of human locomotion. *Current Opinion in Neurobiology*, 22(5):822–828.

Lacquaniti, F., Ivanenko, Y. P., and Zago, M. (2012b). Patterned control of human locomotion. *The Journal of Physiology*, 590(Pt 10):2189–2199.

Latash, M. L. (2010). Motor synergies and the equilibrium-point hypothesis. *Motor Control*, 14(3):294–322.

Latash, M. L., Gorniak, S., and Zatsiorsky, V. M. (2008). Hierarchies of synergies in human movements. *Kinesiology (Zagreb)*, 40(1):29–38.

Latash, M. L., Levin, M. F., Scholz, J. P., and Schöner, G. (2010). Motor control theories and their applications. *Medicina (Kaunas)*, 46(6):382–392.

Lee, D. D. and Seung, S. H. (1999). Learning the parts of objects by non-negative matrix factorization. *Nature*, 401:788–791.

Loeb, E., Giszter, S. F., Saltiel, P. F., Bizzi, E., and Mussa-Ivaldi, F. A. (2000). Output units of motor behavior: an experimental and modeling study. *Journal of Cognitive Neuroscience*, 12(1):78–97.

Malhotra, M., Rombokas, E., Theodorou, E., Todorov, E., and Matsuoka, Y. (2012). Reduced dimensionality control for the ACT hand. In *IEEE International Conference on Robotics and Automation (ICRA)*, pages 5117–5122, St. Paul, Minnesota, USA. IEEE.

Mardia, K. V., Kent, J. T., and Bibby, J. M. (1980). *Multivariate Analysis*. Academic Press, San Diego, California, USA.

Marques, H., Schaffner, P., and Kuppuswamy, N. (2012). Unsupervised Learning of a Reduced Dimensional Controller for a Tendon Driven Robot Platform. In Ziemke, T., Balkenius, C., and Hallam, J., editors, *Lecture Notes in Artificial Intelligence (LNAI)*, pages 351–360, Berlin. Springer-Verlag.

Matarić, M. J., Williamson, M., Demiris, J., and Mohan, A. (1998a). Behavior-based primitives for articulated control. In *Proceedings of the fifth international conference on simulation of adaptive behavior on From animals to animats 5*, pages 165–170, Cambridge, MA, USA. MIT Press.

Matarić, M. J., Zordan, V. B., and Mason, Z. (1998b). Movement control methods for complex, dynamically simulated agents: Adonis dances the macarena. In *Proceedings of the second international conference on Autonomous agents*, AGENTS '98, pages 317–324, New York, NY, USA. ACM.

Matarić, M. J., Zordan, V. B., and Williamson, M. M. (1999). Making complex articulated agents dance. *Autonomous Agents and Multi-Agent Systems*, 2(1):23–43.

McGowan, C. P., Neptune, R. R., Clark, D. J., and Kautz, S. A. (2010). Modular control of human walking: Adaptations to altered mechanical demands. *Journal of Biomechanics*, 43(3):412–419.

McKay, J. L. and Ting, L. H. (2008). Functional muscle synergies constrain force production during postural tasks. *Journal of Biomechanics*, 41(2):299–306.

McKay, J. L. and Ting, L. H. (2012). Optimization of Muscle Activity for Task-Level Goals Predicts Complex Changes in Limb Forces across Biomechanical Contexts. *PLoS Computational Biology*, 8(4):e1002465.

Mezger, J., Ilg, W., and Giese, M. (2005). Trajectory synthesis by hierarchical spatio-temporal correspondence: Comparison of different methods. In *Proceedings of the 2nd symposium on Applied perception in graphics and visualization (APGV)*, pages 25–32, New York, USA. ACM.

Monaco, V., Ghionzoli, A., and Micera, S. (2010). Age-related modifications of muscle synergies and spinal cord activity during locomotion. *Journal of Neurophysiology*, 104(4):2092–2102.

Muceli, S., Boye, A. T. l., D'Avella, A., and Farina, D. (2010). Identifying representative synergy matrices for describing muscular activation patterns during multidirectional reaching in the horizontal plane. *Journal of Neurophysiology*, 103(3):1532–1542.

Mukovskiy, A., Slotine, J., and Giese, M. (2011). Analysis and design of the dynamical stability of collective behavior in crowds. In *International Conference on Computer Graphics, Visualization and Computer Vision 2011(WSCG)*, pages 69–76, Pilsen, Czech Republic.

Mussa-Ivaldi, F. A. (1997). Nonlinear force fields: a distributed system of control primitives for representing and learning movements. In *IEEE International Symposium on Computational Intelligence in Robotics and Automation*, pages 84–90, Albuquerque, New Mexico, USA. IEEE.

Mussa-Ivaldi, F. A. and Bizzi, E. (2000). Motor learning through the combination of primitives. *Philosophical Transactions of the Royal Society of London - Series B: Biological Sciences*, 355(1404):1755–1769.

Mussa-Ivaldi, F. A. and Giszter, S. F. (1992). Vector field approximation: a computational paradigm for motor control and learning. *Biological Cybernetics*, 67(6):491–500.

Mussa-Ivaldi, F. A., Giszter, S. F., and Bizzi, E. (1994). Linear combinations of primitives in vertebrate motor control. *Proceedings of the National Academy of Sciences of the United States of America (PNAS)*, 19(16):7534–7538.

Nazarpour, K., Barnard, A., and Jackson, A. (2012). Flexible cortical control of task-specific muscle synergies. *The Journal of Neuroscience*, 32(36):12349–12360.

Neptune, R. R., Clark, D. J., and Kautz, S. A. (2009). Modular control of human walking: a simulation study. *Journal of Biomechanics*, 42(9):1282–1287.

Nori, F. (2005). *Symbolic Control with Biologically Inspired Motion Primitives*. PhD thesis, Università degli Studi di Padova.

Nori, F. and Frezza, R. (2005). A control theory approach to the analysis and synthesis of the experimentally observed motion primitives. *Biological Cybernetics*, 93(5):323–342.

Nori, F., Metta, G., and Sandini, G. (2008). Exploiting motor modules in modular contexts in humanoid robotics. In Schuster, A., editor, *Robust Intelligent Systems*, pages 209–229. Springer London.

Overduin, S. A., d'Avella, A., Carmena, J. M., and Bizzi, E. (2012). Microstimulation activates a handful of muscle synergies. *Neuron*, 76:1071–1077.

Overduin, S. A., d'Avella, A., Roh, J., and Bizzi, E. (2008). Modulation of muscle synergy recruitment in primate grasping. *The Journal of Neuroscience*, 28(4):880 – 892.

Park, A.-n., Mukovskiy, A., Omlor, L., and Giese, M. A. (2008a). Self organized character animation based on learned synergies from full-body motion capture data. In *International Conference on Cognitive Systems (CogSys)*, Karlsruhe, Germany.

Park, A.-n., Mukovskiy, A., Omlor, L., and Giese, M. A. (2008b). Synthesis of Character Behaviour by Dynamic Interaction of Synergies Learned from Motion Capture Data. In *International Conference of in Central Europe on Computer Graphics,Visulazation and Computer Vision (WSCG)*, pages 9–16, Pilsen, Czech Republic.

Perreault, E. J., Chen, K., Trumbower, R. D., and Lewis, G. (2008). Interactions with compliant loads alter stretch reflex gains but not intermuscular coordination. *Journal of Neurophysiology*, 99(5):2101–2113.

Philips, S., Berisha, V., and Spanias, A. (2009). Energy-constrained discriminant analysis. In *IEEE International Conference on Acoustics, Speech and Signal Processing (ICASSP)*, Taipei, Taiwan.

Pollick, F. E., Maoz, U., Handzelc, A. A., Giblind, P. J., Sapiroe, G., and Flashc, T. (2009). Three-dimensional arm movements at constant equi-affine speed. *Cortex*, 45(3):325–339.

Quiroga, R. Q. and Panzeri, S. (2009). Extracting information by neuronal populations:information theory and decoding approaches. *Nature Reviews Neuroscience*, 10:173–185.

Ranganathan, R. and Krishnan, C. (2012). Extracting synergies in gait: using emg variability to evaluate control strategies. *Journal of Neurophysiology*, 108(5):1537–1544.

Roh, J., Cheung, V. C. K., and Bizzi, E. (2011). Modules in the brain stem and spinal cord underlying motor behaviors. *Journal of Neurophysiology*, 106(3):1363–78.

Roh, J., Rymer, W. Z., and Beer, R. F. (2012). Robustness of muscle synergies underlying three dimensional force generation at the hand in healthy humans. *Journal of Neurophysiology*, 107(8):2123–2142.

Roh, J., Rymer, W. Z., Perreault, E. J., Yoo, S. B., and Beer, R. F. (2013). Alterations in upper limb muscle synergy structure in chronic stroke survivors. *Journal of Neurophysiology*, 109(3):768–781.

Rombokas, E., Malhotra, M., and Matsuoka, Y. (2011). Task-specific demonstration and practiced synergies for writing with the ACT hand. In *IEEE International Conference on Robotics and Automation (ICRA)*, pages 5363–5368, Shanghai, China. IEEE.

Safavynia, S. A. and Ting, L. H. (2012). Task-level feedback can explain temporal recruitment of spatially fixed muscle synergies throughout postural perturbations. *Journal of Neurophysiology*, 107(1):159–177.

Saltiel, P., Wyler-Duda, K., D'Avella, A., Tresch, M. C., and Bizzi, E. (2001). Muscle synergies encoded within the spinal cord: evidence from focal intraspinal NMDA iontophoresis in the frog. *Journal of Neurophysiology*, 85(2):605–619.

Santello, M., Flanders, M., and Soechting, J. F. (1998). Postural hand synergies for tool use. *The Journal of Neuroscience*, 18(23):10105–15.

Schneidman, E., Bialek, W., and II, M. J. B. (2003). Synergy, redundancy, and independence in population codes. *The Journal of Neuroscience*, 23(37):11539–11553.

Stein, P. S. G. (2008). Motor pattern deletions and modular organization of turtle spinal cord. *Brain Research Reviews*, 57(1):118–124.

Thomas, P. and Barto, A. (2012). Motor primitive discovery. In *International Conference on Development and Learning - EpiRob (ICDL)*, San Diego, California, USA.

Ting, L. H. and Chvatal, S. A. (2010). Decomposing muscle activity in motor tasks: methods and interpretation. In Danion, F. and Latash, M. L., editors, *Motor Control: Theories, Experiments, and Applications*, chapter 5, pages 102–138. Oxford University Press, New York, USA.

Ting, L. H. and Macpherson, J. M. (2005). A limited set of muscle synergies for force control during a postural task. *Journal of Neurophysiology*, 93(1):609–613.

Todorov, E. (2009). Compositionality of optimal control laws. In Koller, D., Bengio, Y., Bottou, L., and Culotta, A., editors, *Advances in Neural Information Processing Systems, 2009a*, volume 3, pages 1856–1864. Nips Foundation (http://books.nips.cc).

Todorov, E. and Ghahramani, Z. (2003). Unsupervised learning of sensory-motor primitives. In *Proceedings of the 25th International Conference of the IEEE Engineering in Medicine and Biology Society*, pages 1750–1753. IEEE.

Todorov, E., Li, W., and Pan, X. (2005). From task parameters to motor synergies: A hierarchical framework for approximately-optimal control of redundant manipulators. *Journal of Robotic Systems*, 22(11):691–710.

Torres-Oviedo, G., Macpherson, J. M., and Ting, L. H. (2006). Muscle synergy organization is robust across a variety of postural perturbations. *Journal of Neurophysiology*, 96(3):1530–1546.

Torres-Oviedo, G. and Ting, L. H. (2007). Muscle synergies characterizing human postural responses. *Journal of Neurophysiology*, 98(4):2144–2156.

Torres-Oviedo, G. and Ting, L. H. (2010). Subject-specific muscle synergies in human balance control are consistent across different biomechanical contexts. *Journal of Neurophysiology*, 103(6):3084–3098.

Tresch, M. and Jarc, A. (2009). The case for and against muscle synergies. *Current Opinion in Neurobiology*, 19(6):601–607.

Tresch, M. C., Cheung, V. C., and d'Avella, A. (2006). Matrix factorization algorithms for the identification of muscle synergies: evaluation on simulated and experimental data sets. *Journal of Neurophysiology*, 95(4):2199–2212.

Tresch, M. C., Saltiel, P., and Bizzi, E. (1999). The construction of movement by the spinal cord. *Nature Neuroscience*, 2(2):162–167.

Tresch, M. C., Saltiel, P., D'Avella, A., and Bizzi, E. (2002). Coordination and localization in spinal motor systems. *Brain Research Reviews*, 40(1-3):66–79.

Valero-Cuevas, F. J., Venkadesan, M., and Todorov, E. (2009). Structured Variability of Muscle Activations Supports the Minimal Intervention Principle of Motor Control. *Journal of Neurophysiology*, 102(1):59–68.

Weiss, E. J. and Flanders, M. (2004). Muscular and postural synergies of the human hand. *Journal of Neurophysiology*, 92(1):523–535.

Welch, T. D. J. and Ting, L. H. (2007). A feedback model reproduces muscle activity during human postural responses to support surface translations. *Journal of Neurophysiology*, 99(2):1032–1038.

Yakovenko, S., Krouchev, N., and Drew, T. (2010). Sequential activation of motor cortical neurons contributes to intralimb coordination during reaching in the cat by modulating muscle synergies. *Journal of Neurophysiology*, 105(1):388–409.

Yu, J., Tian, Q., Rui, T., and Huang, T. S. (2007). Integrating discriminant and descriptive information for dimension reduction and classification. *IEEE Transactions on Circuits and Systems for Video Technology*, 17(3):372–377.

Zhang, A., Malhotra, M., and Matsuoka, Y. (2011). Musical piano performance by the ACT Hand. In *IEEE International Conference on Robotics and Automation (ICRA)*, pages 3536–3541, Shanghai, China. IEEE.

Appendix B

Identification of synergies by optimization of trajectory-tracking tasks

Alessandro, C. and Nori, F. (2012). Identification of synergies by optimization of trajectory-tracking tasks. In *IEEE RAS/EMBS International Conference of Biomedical Robotics and Biomechatronics*, pages 924–930, Rome, IEEE.

Abstract

According to the model of muscle synergies, the central nervous system (CNS) is organized in a modular structure, such that any muscle activation can be produced as a linear superposition of predefined time-varying profiles (i.e. synergies). This organization might contribute to simplify the control of the musculoskeletal apparatus. Taking inspiration from these findings, we propose a method to identify the synergies that can be used to control a given dynamical system for the task of tracking a set of trajectories. Further, we show how the same approach can be applied to assess the impact of the number of synergies on the performance of the control method. From the theoretical point of view, we provide a novel interpretation of synergies inspired by the Karhunen-Loève decomposition; furthermore, our method suggests that the quality of a set of synergies should be measured in task space rather then in input space.

B.1 Introduction

One of the current trends in human motor control is the idea that the CNS generates muscle activations by combining a finite number of muscle synergies, i.e. activations of muscles with specific time-varying profiles [d'Avella et al., 2003]. There is evidence that weighted linear combinations of these elementary controls can account for a variety of tasks [d'Avella and Bizzi, 2005; d'Avella et al., 2006].

From the computational point of view, the concept of muscle synergies is very attractive [Chhabra and Jacobs, 2006]. Admissible controls are restricted to the vector space spanned by a finite number of elementary inputs. As a result, the control of an inherently non-linear system like the human musculoskeletal apparatus is tackled by employing a linear approach. Furthermore, learning a task reduces to finding the right combination of muscle synergies (i.e. weights for their linear combination) instead of finding a time sequence of input to each muscle.

This work is a first step towards a control scheme that takes inspiration from the idea of muscle synergies. We propose a method to identify the synergies that can optimally drive a given mechanical system along a set trajectories. From the theoretical point of view, this work contributes a novel interpretation of muscle synergies that is inspired by the Karhunen-Loève decomposition [Stark and Woods, 1986], and that capitalizes in assessing the quality of these control actions in task space (in terms of tracking error) rather then in inputs space (as it is typically done in neuroscience [d'Avella et al., 2006, 2003]).

This paper is organized as follows. Sec. B.2 describes some related work. Sec. B.3 presents the mathematical details of the method proposed for the identification of muscle synergies. Sec. B.4 shows how the method can be used to study the performance of the controller as a function of the number of synergies. Sec. B.5 details the experiments performed and Sec. B.6 shows the results. Finally Sec. B.7 derives the conclusions, presents a short discussion and states future research directions.

B.2 Related work

In neuroscience, muscle synergies are typically identified by applying a decomposition method (e.g. PCA , ICA, non-negative matrix factorization) to a dataset of EMG data extracted from a group of subjects while they are performing a given set of actions. The goal is to find the generators of the vector space that best approximate the dataset of EMG signals. The number of synergies to be extracted is not known in advance and it is typically an input parameter to the decomposition algorithm.

In robotics and control engineering, some effort has been made to develop control strategies inspired by the concept of muscle synergies. Besides the technological aspects, these studies also provide computational approaches to interpret, model and test the idea of muscle synergies. In [Nori, 2005] the authors derive analytically an optimal set of primitives for the system previously feedback-linearized; this method applies if the system is feedback linearizable and its dynamical model is known in analytical form. Other researchers approximate the dynamics of the system with a lower order linear dynamical model, and obtain a set of primitives by algebraic considerations on its matrices [Berniker, 2005]. Another approach consists of applying a learning procedure to a training set of sensory-motor data generated by actuating the robot with random pulses [Berniker et al., 2009; Todorov and Ghahramani, 2003]. Although it bypasses the limitations of the analytical formulation, this method does not explain the physical meaning of the extracted synergies.

B.3 Identification of synergies

The interpretation of muscle synergies presented in this paper, as well as the method we propose for their identification, generalizes the Karhunen-Loève decomposition [Stark and Woods, 1986] to the input-output relation of a dynamical system. To make this clear, in this section we first give a general definition of synergies (Sec. B.3.1), and then, after a brief discussion on this decomposition (Sec. B.3.2), we detail the method proposed to compute optimal synergies for control (Sec. B.3.3).

B.3.1 Definition of synergies

In their most general connotation, synergies constitute a finite set of control actions (i.e. input to the system to be controlled) that, by linear combinations, lead to a specific set of output trajectories.

Let us consider a dynamical system

$$\begin{aligned} \dot{\boldsymbol{x}} &= f(\boldsymbol{x}) + g(\boldsymbol{x})\boldsymbol{u} \\ \boldsymbol{y} &= h(\boldsymbol{x}) \end{aligned} \tag{B.1}$$

where $\boldsymbol{u} \in \mathbb{R}^m$ is the input vector and $\boldsymbol{y}$ is the output.

In accordance with the definition [d'Avella et al., 2003], we model each synergy as a function of time, $\boldsymbol{\phi}_i(t)$. Any valid input sequence $\boldsymbol{u}(t)$ is assumed to be generated as a linear combination of these functions

$$\boldsymbol{u}(t) = \sum_{i=1}^{k} c_i \boldsymbol{\phi}_i(t) \qquad \boldsymbol{\phi}_i : \mathbb{R}^+ \to \mathbb{R}^m \tag{B.2}$$

where $c_i \in \mathbb{R}$. Given a set of k synergies $\{\boldsymbol{\phi}_i(t)\}_{i=1\dots k}$, defined to be task-independent, the weights $\{c_i\}_{i=1\dots k}$ encode a specific input sequence and therefore, depending on the initial conditions of the system, the corresponding output trajectory.

The synergies $\{\boldsymbol{\phi}_i(t)\}_{i=1\dots k}$ are the generators of the vector space of the admissible control actions. Therefore, the number and the shape of these elementary inputs have to be chosen appropriately to maximize the range of control that can be obtained.

B.3.2 Karhunen-Loève decomposition

Let's consider a stochastic process $\{X_t\}_{t\in[a,b]}$ with null expected value (i.e. $E[X_t] = 0, \forall t \in [a,b]$). It can be proven that X_t can be represented by means of another stochastic process $\hat{X}_t$ that is defined as the infinite linear combination of deterministic orthonormal functions $\{\phi_1(t), \phi_2(t), \dots\}$ in $L^2([a,b])$:

$$X_t \sim \hat{X}_t \qquad \text{with} \qquad \hat{X}_t = \sum_{i=1}^{\infty} c_i \phi_i(t) \tag{B.3}$$

where the stochastic coefficients are chosen so as to minimize a suitable distance between X_t and $\hat{X}_t$:

$$\mathbf{c}(\phi_1, \phi_2 \dots) = \underset{c_1, c_2, \dots}{\operatorname{argmin}} \; d(X_t, \hat{X}_t) \tag{B.4}$$

Truncating the linear combination to k components, $\hat{X}_t$ becomes an approximation of X_t, therefore also the minimum distance d depends on $\{\phi_1, \dots, \phi_k\}$:

$$d^*(\phi_1, \dots, \phi_k) = \min_{c_1, \dots, c_k} d(X_t, \hat{X}_t). \tag{B.5}$$

Thus, it makes sense to compute the functions $\{\phi_1, \ldots, \phi_k\}$ that results in the minimum error:

$$[\phi_1^*, \ldots, \phi_k^*] = \underset{\phi_1,\ldots,\phi_k}{\operatorname{argmin}} \; d^*(\phi_1, \ldots, \phi_k). \tag{B.6}$$

It can be shown that the best basis $\{\phi_i(t)\}_{i=1\ldots k}$ (in the sense of the mean-squared error between X_t and $\hat{X}_t$) is the Karhunen-Loève decomposition, which corresponds to the well known principal component analysis (PCA) when the stochastic process $\{X_t\}_{t\in[a,b]}$ is replaced by the discrete and finite time process $\{X_n\}_{n=1\ldots N}$ [Stark and Woods, 1986].

B.3.3 Identification and testing of synergies

Let us specify the shape of each synergy by means of a set of parameters[1], $\boldsymbol{\phi}_i(t, a_0^i, ..., a_r^i)$. Further, let us call $\hat{\boldsymbol{y}}(\boldsymbol{x}_0, \boldsymbol{u}(t))$ the output trajectory of the system, obtained from the initial condition $\boldsymbol{x}_0$ and the input sequence $\boldsymbol{u}(t)$.

If $\{\boldsymbol{y}_1(t), ..., \boldsymbol{y}_n(t)\}$ is a set desired output trajectories (used as training set), identifying the appropriate synergies translates into finding the parameters $\{a_0^i, ..., a_r^i\}_{i=1..k}$ such that linear combinations of the corresponding $\boldsymbol{\phi}_i(t)$ lead to the best approximation of the desired set. Thus, we can define the quality measure of the set of synergies as follows:

$$d(\boldsymbol{y}, \hat{\boldsymbol{y}}) = \sum_{j=1}^{n} \left\| \hat{\boldsymbol{y}} \left(\boldsymbol{x}_0^j, \sum_i c_i^j \boldsymbol{\phi}_i(t) \right) - \boldsymbol{y}_j(t) \right\| \tag{B.7}$$

where $\|\cdot\|$ is an appropriately chosen norm of a function. The expression within norm represents the error between the output of the system and the j-th desired trajectories (i.e. tracking error). It is worth noting that while the weights c_i depend on the trajectories to be approximated (i.e. they are task-dependent), the set of synergies accounts for the entire desired set. Further, we assume that $\boldsymbol{y}_i(0) = h(\boldsymbol{x}_0^i)$.

The identification of the parameters (learning phase) can be performed by executing the following minimization:

$$[\boldsymbol{\phi}_1, \ldots, \boldsymbol{\phi}_k, \boldsymbol{c}] = \underset{\substack{a_0^1,\ldots,a_r^k \\ c_1^1,\ldots,c_k^n}}{\operatorname{argmin}} \; d(\boldsymbol{y}, \hat{\boldsymbol{y}}) \tag{B.8}$$

where, in the left hand side, we enclosed all the synergy-combinators in the vector $\boldsymbol{c}$, and we substituted the synergy-coefficients with the corresponding $\boldsymbol{\phi}_i$.

It now becomes easy to notice the similarity between Eq. (B.5)-(B.6) and Eq. (B.8). More precisely, X_t is equivalent to the set of desired trajectories, and $\hat{X}_t$ is equivalent to the output that can be obtained from linear superposition of elementary controls. In other words, as the Karhunen-Loève functions are the components that better approximate the random process X_t, we interpret muscle synergies as the elementary controls that better drive the system (B.1) along the set of trajectories $\boldsymbol{y}_i$ (in the sense of the norm between $\boldsymbol{y}$ and $\hat{\boldsymbol{y}}$).

The synergies identified in the training phase should then be tested for generalization (testing phase). The idea is to evaluate to which extent they can generate input that drive the system along a new group of trajectories (testing set). An optimization similar to Eq. (B.8) is used to identify the synergy-combinators c_i^j that minimize the error in tracking each of the testing trajectories; the parameters a are kept constant to the values identified in the training phase. The obtained errors are used as a measure of the generality of the set of synergies.

The method to perform the optimization as well as the norm used to compute the errors can be chosen by the designer.

[1] For clarity reason in the rest of the manuscript the dependency on the parameters is omitted.

B.4 Minimum number of synergies

The number of synergies defines the dimensionality of the new input space, therefore a small number of these elementary controls is a desired feature of the controller. The optimization method (B.8) can also be used to investigate the minimum number of synergies required to obtain a certain tracking accuracy. By performing the same minimization (i.e. on the same dynamical system and the same desired trajectories) for different number of synergies, it is indeed possible to derive the trend of the error as a function of the number of these elementary controls. In fact, while for some linear systems this question can be addressed by mathematical proof (see appendix), it could be problematic to do so for non-linear systems.

One of the challenges in employing any local optimization-based method is the issue of the local minima; the minimization algorithm could discover a local minima of the objective function instead of a global one. From a practical point of view, sub-optimal solutions might still lead to acceptable tracking performance (see Sec. B.6). However, if the goal is to compare the performance obtained with different number of synergies, local solutions are undesirable. Sure enough, if the algorithm outputs sub-optimal solutions, the trend of the error as a function of the number of synergies could be an artifact. For example, assuming that the error should not become larger increasing the number of synergies, the local minimum obtained with n+1 synergies might be higher than the one obtained with n synergies, while the global minima follows the expected trend.

Elaborating on these consideration we have developed an algorithm that, although does not solve the problem of the local minima (i.e. the solution computed can be sub-optimal), seems to compute the qualitatively correct trend of the error. The main intuition is that by starting the minimization with n+1 synergies from the solution obtained in the previous step (i.e. with n synergies) the error should not increase. Indeed, since the additional parameters add approximation power to the algorithm and the previous solution already lies on a minimum, either the gradient of the objective function stays zero or the previous solution can move towards a smaller objective function value (leading to a decrement of the error). To avoid that, due to a flat gradient (e.g. saddle point), the values of the parameters to be optimized do not change, 15 optimizations are performed in parallel starting from different initial conditions around the previous solution. The initial conditions are extracted from a multivariate Gaussian random distribution centered in the previous solution and having a standard deviation equal to 0.005 on each dimension (diagonal covariance matrix). The parameters leading to the lowest objective function value are considered the solution of this iteration and are used as initial conditions for the next one. Although it does not prevent the minimization to compute sub-optimal solutions, this approach seems to generate the qualitatively correct trend of error (see Sec. B.6.1). Algorithm 1 describes this procedure in pseudo-code.

B.5 Experimental methods

B.5.1 Dynamical systems

The method proposed in Sec. B.3.3 is evaluated in simulation of both a linear and a non-linear dynamical system. Although the systems are quite simple, they capture some interesting features that are worth studying since they are present both in the human musculoskeletal apparatus and in different types of robots; i.e. redundancy, compliance and trigonometric non-linearities.

Linear system The linear system resembles an agonist-antagonist pair of compliant actuators applied on a mass m; since the forces produced by the linear springs always lie on the same direc-

Algorithm 1 ERRORTREND(f, k, ns, σ)

Require: The objective function f
The maximum number of synergies k
The number of starting points ns
The standard deviation σ.
Ensure: The tracking errors err.

```
initConds ← RAND(ns)
allSolutions ← MINIMISEALL(f, initConds)
err[1] ← MIN(allSolutions)
for i = 2 → k do
    initConds ← RANDGAUSS(err[i − 1], σ, ns)
    allSolutions ← MINIMISEALL(f, initConds)
    err[i] ← MIN(allSolutions)
    i ← i + 1
end for
```

tion, the mass can only move in one dimension. This system (see Fig. B.1) can be described by the following mathematical model:

$$\ddot{x} = \frac{1}{m}\left(-k_1(x - x_1) - k_2(x_2 - x) - c\dot{x}\right) \tag{B.9}$$

where k_1 and k_2 are the spring constants and c is the coefficient of a dissipative force. The output of the system is chosen to be the position x of the mass, while the elongation of the springs represent the inputs x_1 and x_2. The system is linear, compliant and redundant (i.e. the number of inputs exceeds the number of the output variables).

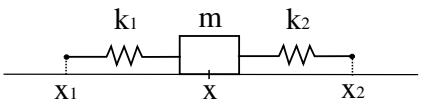

Figure B.1: Agonist-antagonist linear system.

Non-linear system The non-linear system is the well-known pendulum, that can be trivially described by the following dynamical model

$$\ddot{\vartheta} = -\frac{g}{r}\sin(\vartheta) + \frac{\tau}{r} \tag{B.10}$$

where g is the gravitational acceleration and r the length of the rod. The output of the system, ϑ, is the angle between the rod and the vertical axis, and the input τ is the torque applied on the revolute joint. This system has been chosen because it is characterized by the same non-linearities as each kinematic chain, such as most robotic manipulators; i.e. trigonometric non-linearities. Moreover, because of its simplicity, it is a good starting point to investigate the effectiveness of controlling a non-linear plant by linear combinations of elementary inputs.

B.5.2 Desired trajectories

The tasks that the controlled systems have to accomplish consist in tracking a set of desired trajectories. Each of these is defined as the smoothest trajectory to reach a final position from an initial position in a given amount of time. As described in [Hogan, 1984], smoothness can be quantified by the third derivative of the trajectory itself (i.e. jerk). There is evidence that minimum-jerk trajectories can be used to model the hand-motion of a human subject who is instructed to bring his hand from an starting to an ending position in a certain amount of time [Flash and Hogan, 1985]. Assuming the movement to start and end with zero velocity and acceleration, at time t_0 and t_f respectively, the following expression describes the minimum-jerk trajectory of the coordinate x from x_0 to x_f:

$$x(t) = x_0 + (x_0 - x_f)(15\rho^4 - 6\rho^5 - 10\rho^3) \tag{B.11}$$

were $\rho = \frac{t}{t_f - t_0}$.

For each experiment, both training and testing set consist of minimum-jerk trajectories characterized by 1 s of duration ($t_0 = 0$ and $t_f = 1$) and 100 time samples. Initial and final positions are specified in Sec. B.6. Mathematically, the set of desired outputs is restricted to the subspace of L^2 of the minimum-jerk trajectories.

B.5.3 Synergy model

Both for the linear and the non-linear systems, each synergy consists of as many parametrized functions as the number of input variables (i.e. two for the agonist-antagonist pair and one for the pendulum). For the purposes of this paper these functions are defined as 5-th order polynomials:

$$\phi(t) = a_0 + a_1 t + a_2 t^2 + a_3 t^3 + a_4 t^4 + a_5 t^5 \tag{B.12}$$

therefore, if m is the number of input variables, for each synergy $6m$ parameters need to be identified. The reason of this choice is that for the linear dynamical system (B.9), 5-th order polynomials can span the whole output space of minimum-jerk trajectories (see the appendix for the mathematical proof). This choice does not affect the generality of the method described in Sec. B.3.3.

The optimization described in Sec. B.3.3, Eq. (B.8), is performed numerically in Matlab® (R2011a, Mathworks, Inc.) using the fmincon solver and the interior-point algorithm [Waltz et al., 2006].

In Eq. (B.7), the error between the desired trajectories and the output of the system is computed using Euclidean norm.

B.6 Results

B.6.1 Agonist-antagonist linear pair

The results presented in this section are obtained with the following parameters of the dynamical model: $m = 1$ Kg, $k_1 = k_2 = 1$ N/m, and $c = 1.5$ Ns/m. The three training minimum-jerk trajectories are defined by the initial positions 60, 120 and 180 m, and the final position 50 m. Forty-two testing trajectories are defined as follows. The interval $[30; 180]$ m is discretized in 7 equally (and maximally) spaced points; any pair of different points corresponds to the initial and final position of a testing minimum-jerk trajectory.

Fig. B.2A depicts the trend of the error in tracking the desired training trajectories; the input to the system consists of appropriate linear combinations of the extracted synergies. This plot is computed using Algorithm 1. It can be noted that there is a drastic decrement of the error

	a_0	a_1	a_2	a_3	a_4	a_5
ϕ_{11}	15.48	21.36	75.02	-195.10	88.47	-5.95
ϕ_{12}	19.08	21.82	68.95	-193.58	84.27	-1.76
ϕ_{21}	0.49	0.62	2.04	-5.46	2.43	-6.17
ϕ_{22}	0.48	0.60	2.00	-5.47	2.43	-6.15

Table B.1: Optimal synergies identified for the agonist-antagonist linear system. The coefficient ϕ_{ij} indicates the j-th element of the synergy i.

switching from one to two synergies; the use of any additional synergy does not seem to play a role in minimizing the tracking performance. This result is confirmed by mathematical proof (see appendix).

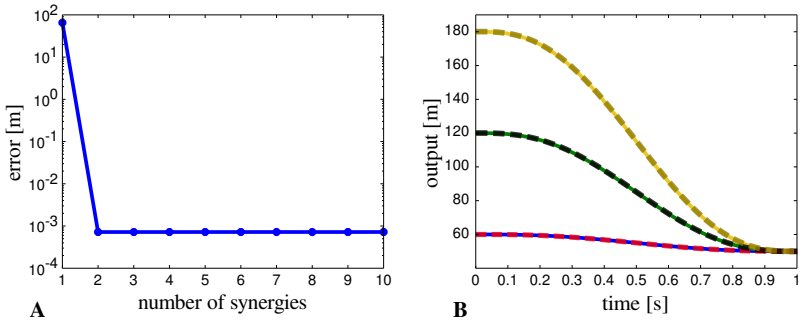

Figure B.2: Performance of the synergies identified for the agonist-antagonist linear system. Trend of the error as a function of the number of synergies (A), and performance of tracking the training trajectories (continuous lines, B).

While Fig. B.2A describes qualitatively the expected theoretical results (i.e. two synergies are enough to obtain the best possible tracking performance), quantitatively the minimization generates a sub-optimal solution; the lowest tracking error is equal to 10^{-7} while an exact mathematical solution should be characterized by an error equal to 0 (i.e. 10^{-16} considering the precision of the machine used and the numerical minimization error).

Practically, the obtained sub-optimal solution leads to satisfactory tracking performance (error = 10^{-3} m). Table B.1 reports the optimal coefficients of the two synergies as obtained by optimization (B.8). The similarity between the coefficients of ϕ_{i1} and ϕ_{i2} is due to the inherent symmetry of the mechanical system (see Fig. B.1). Fig. B.2B depicts the three training trajectories (continuous lines) and the corresponding outputs of the system (dashed lines).

The results obtained in the test of generalization confirm that two synergies span the entire output space of minimum-jerk trajectories (see appendix). The tracking errors for the 42 testing trajectories are distributed in the order of magnitude of 10^{-4} m (see Fig. B.3A). Fig. B.3B shows the tracking performance for the best tracked (x_0=180, x_f=155 m) and the worst tracked ($x_0 = 30$, $x_f = 180$ m) testing trajectories.

B.6.2 Pendulum

To obtain the results presented in this section, the parameters of the dynamical model are: $r = 0.1$ m and $g = 9.81$ m/s^2. The three training trajectories are characterized by the initial positions $\pi/4$, $\pi/3$ and $-\pi/6$ rad, and the final position $-\pi/3$ rad. Forty-two testing trajectories are defined as

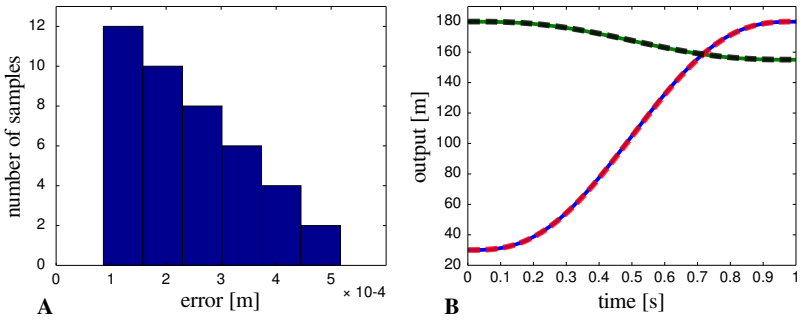

Figure B.3: Distribution of the tracking errors for the testing trajectories (A). Real (dashed lines) and desired (continuous lines) output for the best and the worst tracked testing trajectories (B).

	a_0	a_1	a_2	a_3	a_4	a_5
ϕ_1	4.83	4.45	2.09	4.86	2.61	-1.57
ϕ_2	-0.38	-0.32	0.35	-0.03	-0.07	-0.39
ϕ_3	-0.30	0.70	-0.28	-0.23	-0.02	0
ϕ_4	-0.06	-0.03	-0.22	-0.18	-0.05	-0.06
ϕ_5	-0.10	-0.16	0.27	0	-0.06	0.02

Table B.2: Optimal synergy coefficients identified for the non-linear system (pendulum).

follows. The interval $\left[0; \frac{\pi}{2}\right]$ rad is discretized in 7 equally (and maximally) spaced points; any couple of different points corresponds to the initial and final positions of a testing minimum-jerk trajectory. The interval $\left[\frac{\pi}{2}, \pi\right]$ is not considered because it would lead to the same coefficient c_i (apart from a minus sign), and therefore practically to the same control actions.

Fig. B.4A shows the evolution of the tracking error as a function of the number of synergies. After having reached the value of 10^{-1} rad (i.e. 10^{-3} rad in average for each sample) with 5 synergies, the introduction of new elementary controls does not significantly affects the error.

Table B.2 summarizes the coefficients of the 5 synergies identified by the algorithm on the training-set. Their performance in tracking the training-set can be seen in Fig. B.4B. The output of the system (dashed lines) is generally close to the corresponding desired behavior (continuous lines) for all the trajectories.

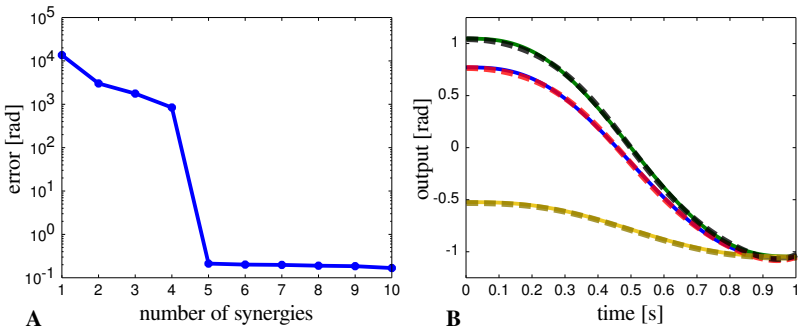

Figure B.4: Performance of the synergies identified for the non linear system (pendulum). Trend of the error as a function of the number of synergies (A), and performance of tracking the training trajectories (continuous lines, B).

Unlike the linear case (see Sec. B.6.1), for this non-linear system there is no mathematical evidence of the minimum number of synergies required to span the whole output space of minimum-jerk trajectories. However, the results of the generalization tests provide evidence that 5 synergies can lead to good performance in tracking trajectories that do not belong to the training set. The distribution of the error shows that the most of the testing trajectories can be tracked with an error of 10^{-2} rad in order of magnitude (see Fig. B.5A). Fig. B.5B shows the tracking performance for the best tracked (x_0=0.52, x_f=1.04 rad) and the worst tracked ($x_0 = 1.57$, $x_f = 0$ rad) testing trajectories.

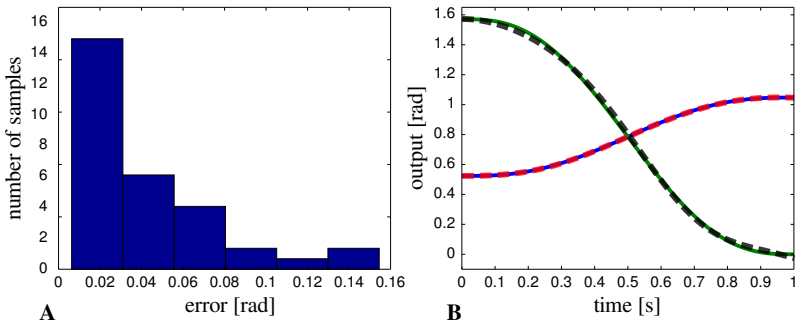

Figure B.5: Distribution of the tracking errors for the testing trajectories (A). Real (dashed lines) and desired (continuous lines) output for the best and the worst tracked testing trajectories (B).

B.7 Conclusions and future work

B.7.1 Conclusions

This paper proposes a method to identify a set of basis functions, referred as synergies, that can be used to control a given dynamical system. Any admissible input to the system is expressed as a linear combination of these elementary controls, defined as parametrized functions of time. The method proposed consists of optimizing the set of parameters that define each synergy with the goal of minimizing the error between the output of the system, controlled by appropriate linear superposition of the synergies, and a set of desired training trajectories.

The method to identify the synergies has been evaluated in simulation for a linear and a non-linear system. The performance in tacking the desired trajectories is satisfactory. Moreover, the results obtained in the test of generalization show that the synergies identified lead to good tracking performance on minimum-jerk trajectories not used for the training. The algorithm proposed to derive the trend of the tracking error as a function of the number of synergies seems to produce results compatible with the theory and it has been used to establish the number of synergies to be employed for each of the experiments.

B.7.2 Discussion

The idea underlying the model of muscle synergies is to approximate the (non-linear) vector space of muscle activations (i.e. input space) with a linear vector space defined by the synergies (that serve as generators). The quality of the identified synergies is typically measured in

the input space as the error in approximating a dataset of EMG data [d'Avella and Bizzi, 2005; d'Avella et al., 2006, 2003]. In this paper we took a different approach by proposing a (PCA-like) interpretation of synergies that minimizes approximation-errors directly in the task space (e.g. errors in tracking a given set of trajectories). This difference is quite relevant as there exist mechanical systems (e.g. unstable systems) that produce very different output-trajectories in response to very small differences in the input space. Furthermore, there is evidence that, in humans, control actions are formulated in task space [Kelso, 1982].

The similarity between our method and the Karhunen-Loève decomposition can be summarized as follows. As the latter finds the functions that best approximate a stochastic process, the method we propose seeks the synergies that produce the best approximation of a set of desired output trajectories. Clearly, the scopes of the two methods are different: the former operates on stochastic processes, the latter operates on the input-output relationship of dynamical systems. Although in this paper we have only considered deterministic systems, the human musculoskeletal apparatus is inherently noisy [Harris and Wolpert, 1998]. Form this point of view, our interpretation of muscle synergies becomes even more related to the Karhunen-Loève decomposition, as the output trajectories of a noisy dynamical system can be considered stochastic processes.

The main advantage of employing a synergy-like controller is the dimensionality reduction it follows. According to the *time-varying* synergy model [d'Avella et al., 2003] employed in this work, an input sequence that potentially belongs to an infinite dimensional space (e.g. the space of continuous vector valued functions), is obtained by superimposing linearly a finite number of time-varying synergies. As opposed to a time-variant sequence of input to each actuator, the new input to the system is the finite set of time-invariant synergy-combinators. Noteworthy, even if there might be a larger number of synergies then actuators (as in the case of the pendulum – see Sec. B.6), the dimensionality is anyway reduced due to the shift from time-variant to time-invariant input signals. The same would not hold if we employed the so called *synchronous-synergy* model [Cheung et al., 2005]; i.e. muscle synergies are constant coefficients and the synergy-combinators are time-variant input signals. In that model, to obtain a dimensionality reduction the number of synergies needs to be lower then the number of actuators. Additionally, it is worth reminding that the same set of synergies generates a wide repertoire of motions (i.e. minimum-jerk trajectories). Especially in the case of non-linear dynamics, this consideration justifies the number of required synergies, that might appear high if compared to the dimensionality of the state space (see Sec. B.6.2). The identification procedure basically requires to solve the control problem for the training trajectories; however, once the appropriate synergies are identified, learning a new motion reduces to finding only the synergy-combinators, simplifying substantially the subsequent learning problems.

Similarly to the work presented in Sec. B.2, this paper proposes a method to synthesize synergies for control. In line with the analytical procedures [Berniker, 2005; Nori, 2005], our method gives a clear mathematical interpretation of muscle synergies; however, it does not require the dynamical model of the system in analytical form. Moreover, unlike [Berniker, 2005; Berniker et al., 2009], our synergies are optimized to perform trajectory tracking, rather then reaching tasks.

B.7.3 Future Work

A natural continuation of this work consists in evaluating the performance of the synergies identification algorithm in more complex biologically-inspired systems.

The method proposed here will be tested, and eventually improved, in order to track generic trajectories belonging to L^2. This will most probably require to model the synergies with universal function approximators; indeed it is not obvious to compute, for a given dynamical system and a given set of desired trajectories, the synergy-shapes that guarantee good tracking performance.

Finally, we will make an effort to introduce feedback in the control paradigm and to examine

its impact in the set of synergies previously identified [Cheung et al., 2005].

Appendix

Proposition 1. *For the dynamical system* (B.9)*, two input synergies consisting of 5-th order polynomials span the whole output space of minimum-jerk trajectories* (B.11)*.*

Proof. Let us compute the first and the second derivative of (B.11)

$$\dot{x} = (x_0 - x_f)(60\rho^3 - 30\rho^4 - 30\rho^2) \tag{B.13}$$

$$\ddot{x} = (x_0 - x_f)(180\rho^2 - 120\rho^3 - 60\rho) \tag{B.14}$$

and define a new variable $s = x_0 - x_f$. Substituting (B.11), (B.13) and (B.14) in (B.9), and expressing the input variables x_1 and x_2 by polynomials of 5-th order, we obtain[2]

$$\begin{aligned} s(180\rho^2 - 120\rho^3 - 60\rho) = \\ - 2\left[x_0 + s(15\rho^4 - 6\rho^5 - 10\rho^3)\right] + \\ + s(45\rho^4 + 45\rho^2 - 90\rho^3) + \\ + a_0 + a_1 t + a_2 t^2 + a_3 t^3 + a_4 t^4 + a_5 t^5 + \\ + b_0 + a_1 t + b_2 t^2 + b_3 t^3 + b_4 t^4 + b_5 t^5 \end{aligned} \tag{B.15}$$

To achieve an analytical solution, the coefficients of the unknown polynomials have to account for the corresponding terms of the equation. In particular, the polynomial obtained by the sum of the unknown polynomials has to be

$$-12s\rho^5 - 15s\rho^4 - 50s\rho^3 + 135s\rho^2 - 60s\rho + 2x_0 \tag{B.16}$$

Expression (B.16) can be rewritten as

$$\begin{bmatrix} s & x_0 \end{bmatrix} \begin{bmatrix} -12\rho^5 - 15\rho^4 - 50\rho^3 + 135\rho^2 - 60\rho \\ 2 \end{bmatrix}$$

where the vector $[s, x_0]$ is the only term that depends on the desired trajectory. Thus, the problem of finding a set of synergies that span the whole output space of the minimum-jerk trajectories translates into finding a basis of the space $\mathbb{R}^2$. Having dimension 2, all the basis of the space $\mathbb{R}^2$ consist of two linearly independent vectors. □

Acknowledgement

This research was supported by the EU project RobotDoC under 235065 from the 7th Framework Programme (Marie Curie Action ITN) and the EU project ITALK (ICT-214668).

[2]Without loss of generality here we considered $m = 1$, $k_1 = k_2 = 1$ and $c = 1.5$.

Bibliography

Berniker, M. (2005). *Linearity, motor primitives and low-dimensionality in the spinal organization of motor control*. PhD thesis, Massachusetts Institute of Technology.

Berniker, M., Jarc, A., Bizzi, E., and Tresch, M. C. (2009). Simplified and effective motor control based on muscle synergies to exploit musculoskeletal dynamics. *Proceedings of the National Academy of Sciences of the United States of America*, 106(18):7601–7606.

Cheung, V. C. K., d'Avella, A., Tresch, M. C., and Bizzi, E. (2005). Central and Sensory Contributions to the Activation and Organization of Muscle Synergies during Natural Motor Behaviors. *The Journal of Neuroscience*, 25(27):6419–6434.

Chhabra, M. and Jacobs, R. A. (2006). Properties of Synergies Arising from a Theory of Optimal Motor Behavior. *Neural Computation*, 18(10):2320–2342.

d'Avella, A. and Bizzi, E. (2005). Shared and specific muscle synergies in natural motor behaviors. *Proceedings of the National Academy of Sciences*, 102(8):3076–3081.

d'Avella, A., Portone, A., Fernandez, L., and Lacquaniti, F. (2006). Control of fast-reaching movements by muscle synergy combinations. *The Journal of Neuroscience*, 26(30):7791–7810.

d'Avella, A., Saltiel, P., and Bizzi, E. (2003). Combinations of muscle synergies in the construction of a natural motor behavior. *Nature Neuroscience*, 6:300–308.

Flash, T. and Hogan, N. (1985). The coordination of arm movements: an experimentally confirmed mathematical model. *The Journal of Neuroscience*, 5:1688–1703.

Harris, C. and Wolpert, D. (1998). Signal-dependent noise determines motor planning. *Nature*, 394(6695):780–784.

Hogan, N. J. (1984). Adaptive control of mechanical impedance by coactivation of antagonist muscles. *IEEE Transactions on Automatic Control*, 29(8):681–690.

Kelso, J. A. S. (1982). *Human Motor Behaviour: An Introduction*. Psychology Press.

Nori, F. (2005). *Symbolic Control with Biologically Inspired Motion Primitives*. PhD thesis, Università degli Studi di Padova.

Stark, H. and Woods, J. W. (1986). *Probability, Random Processes, and Estimation Theory for Engineers*. Prentice-Hall Inc.

Todorov, E. and Ghahramani, Z. (2003). Unsupervised learning of sensory-motor primitives. In *Proceedings of the 25th International Conference of the IEEE Engineering in Medicine and Biology Society*, pages 1750–1753. IEEE.

Waltz, R. A., Morales, J. L., Nocedal, L., and Orban, D. (2006). An interior algorithm for nonlinear optimization that combines line search and trust region steps. *Mathematical Programming*, 107(3):391–408.

Appendix C

Synthesis and adaptation of effective motor synergies for the solution of reaching tasks

Alessandro, C., Carbajal, J. P., and d'Avella, A. (2012). Synthesis and adaptation of effective motor synergies for the solution of reaching tasks. In Ziemke, T., Balkenius, C., and Hallam, J., editors, *Lecture Notes in Artificial Intelligence (LNAI)*, pages 33–43, Berlin. Springer-Verlag.

Abstract

Taking inspiration from the hypothesis of muscle synergies, we propose a method to generate open loop controllers for an agent solving point-to-point reaching tasks. The controller output is defined as a linear combination of a small set of predefined actuations, termed synergies. The method can be interpreted from a developmental perspective, since it allows the agent to autonomously synthesize and adapt an effective set of synergies to new behavioral needs. This scheme greatly reduces the dimensionality of the control problem, while keeping a good performance level. The framework is evaluated in a planar kinematic chain, and the quality of the solutions is quantified in several scenarios.

C.1 Introduction

Humans are able to perform a wide variety of tasks with great flexibility; learning new motions is relatively easy, and adapting to new situations (e.g. change in the environment or body growth) is usually dealt with no particular effort. The strategies adopted by the central nervous system (CNS) to master the complexity of the musculoskeletal apparatus and provide such performance are still not clear. However, it has been speculated that an underlying modular organization of the CNS may simplify the control and provide the observed adaptability. There is evidence that the muscle activity necessary to perform various tasks (e.g. running, walking, keeping balance, reaching and other combined movements) may emerge from the combination of predefined muscle patterns, the so-called *muscle synergies* [d'Avella et al., 2003]. This organization seems to explain muscle activity across a wide range of combined movements [Cappellini et al., 2006; d'Avella et al., 2008; Ivanenko et al., 2005].

The scheme of muscle synergies is inherently flexible and adaptable. Different actions are encoded by specific combinations of a small number of predefined synergies; this reduces the computational effort and the time required to learn new useful behaviors. The learning scheme can be regarded as developmental since information previously acquired (i.e. synergies) can be reused to generate new behaviors [Dominici et al., 2011]. Finally, improved performance can be easily achieved by introducing additional synergies. Thus, the hypothetical scheme of muscle synergies would contribute to the autonomy and the flexibility observed in biological systems, and it could inspire new methods to endow artificial agents with such desirable features.

In this paper we propose a method to control a dynamical system (i.e. the agent) in point-to-point reaching tasks by linear combinations of a small set of predefined actuations (i.e. synergies). Our method initially solves the task in state variables by interpolation; then, it identifies the combination of synergies (i.e. actuation) that generate the closest kinematic trajectory to the computed interpolant. Additionally, we propose a strategy to synthesize a small set of synergies that is tailored to the task and the agent. The overall method can be interpreted in a developmental fashion; i.e. it allows the agent to autonomously synthesize and update its own synergies to increase the performance of new reaching tasks.

Other researchers in robotics and control engineering have recently proposed architectures inspired by the concept of muscle synergies. In [Nori, 2005] the authors derive an analytical form of a set of primitives that can drive a feedback linearized system (known analytically) to any point of its configuration space. In [Alessandro et al., 2012] the authors present a numerical method to identify synergies that optimally drive the system over a set of desired trajectories. This method does not require an analytical description of the system, and it has the advantage of assessing the quality of the synergies in task space. However, it is computationally expensive as it involves heavy optimizations. In [Todorov and Ghahramani, 2003] muscle synergies are identified by applying an unsupervised learning procedure to a collection of sensory-motor data obtained by actuating a robot with random signals. In [Schaal et al., 2005] the architecture of the dynamic movement primitives (DMP) is proposed as a novel tool to formalize control policies in terms of predefined differential equations. Linear combinations of Gaussian functions are used as inputs to modify the attractor landscapes of these equations, and to obtain the desired control policy.

In contrast to these works, our method to synthesize synergies does not rely on feedback linearization, nor on repeated integrations of the dynamical system. The method is grounded on the input-output relation of the dynamical system (as in [Todorov and Ghahramani, 2003]), and it provides a computationally fast method to obtain the synergy combinators to solve a given task. Furthermore, our method is inherently adaptable as it allows the on-line modification of the set of synergies to accommodate to new reaching tasks.

C.2 Definitions and Methods

In this section we introduce the mathematical details of the method we propose. After some definitions, we present the core element of our method: a general procedure to compute actuations that solve point-to-point reaching tasks (see Sec. C.2.1). Subsequently, in Section C.2.2, we propose a framework for the synthesis and the development of a set of synergies.

Let us consider a differential equation modeling a physical system $\mathcal{D}(\boldsymbol{q}(t)) = \boldsymbol{u}(t)$, where $\boldsymbol{q}(t)$ represents the time-evolution of its configuration variables (their derivatives with respect to time are $\dot{\boldsymbol{q}}(t)$), and $\boldsymbol{u}(t)$ is the actuation applied. Inspired by the hypothesis of muscle synergies[1] [d'Avella et al., 2003], we formulate the actuation as a linear combination of predefined motor co-activation patterns:

$$\boldsymbol{u}(t) = \sum_{i=1}^{N_\phi} \boldsymbol{\phi}_i(t) b_i := \boldsymbol{\Phi}(t)\boldsymbol{b}, \tag{C.1}$$

where the functions $\boldsymbol{\phi}_i(t) \in \boldsymbol{\Phi}$ are called *motor synergies*. The notation $\boldsymbol{\Phi}(t)$ describes a formal matrix where each column is a different synergy. If we consider a time discretization, $\boldsymbol{\Phi}(t)$ becomes a $N\dim(\boldsymbol{q})$-by-N_ϕ matrix, where N is the number of time steps, $\dim(\boldsymbol{q})$ the dimension of the configuration space and N_ϕ the number of synergies.

We define *dynamic responses* (DR) of the set of synergies as the responses $\boldsymbol{\theta}_i(t) \in \boldsymbol{\Theta}$ of the system to each synergy (i.e. forward dynamics):

$$\mathcal{D}(\boldsymbol{\theta}_i(t)) = \boldsymbol{\phi}_i(t) \qquad i = 1...N_\phi. \tag{C.2}$$

with initial conditions chosen arbitrarily.

C.2.1 Solution to point-to-point reaching tasks

A general point-to-point reaching task consists in reaching a final state $(\boldsymbol{q}_T, \dot{\boldsymbol{q}}_T)$ from an initial state $(\boldsymbol{q}_0, \dot{\boldsymbol{q}}_0)$ in a given amount of time T:

$$\begin{aligned} \boldsymbol{q}(0) &= \boldsymbol{q}_0, \quad \dot{\boldsymbol{q}}(0) = \dot{\boldsymbol{q}}_0, \\ \boldsymbol{q}(T) &= \boldsymbol{q}_T, \quad \dot{\boldsymbol{q}}(T) = \dot{\boldsymbol{q}}_T. \end{aligned} \tag{C.3}$$

Controlling a system to perform such tasks amounts to finding the actuation $\boldsymbol{u}(t)$ that fulfills the point constraints[2] (C.3). Specifically, assuming that the synergies are known, the goal is to identify the appropriate synergy combinators $\boldsymbol{b}$. In this paper we consider only the subclass of reaching tasks that impose motionless initial and final postures, i.e. $\dot{\boldsymbol{q}}_T = \dot{\boldsymbol{q}}_0 = 0$.

The procedure consists of, first, solving the problem in kinematic space (i.e. finding the appropriate $\boldsymbol{q}(t)$), and then computing the corresponding actuations. From the kinematic point of view, the task can be seen as an interpolation problem; i.e. $\boldsymbol{q}(t)$ is a function that interpolates the data in (C.3). Therefore, a set of functions is used to build the interpolant trajectory that satisfies the constraints imposed by the task; these functions are herein the dynamic responses of the synergies:

$$\boldsymbol{q}(t) = \sum_{i=1}^{N_\theta} \boldsymbol{\theta}_i(t) a_i := \boldsymbol{\Theta}(t)\boldsymbol{a}, \tag{C.4}$$

[1] With respect to the model of time-varying synergies, in this paper we neglect the synergy onset times.
[2] In this paper we assume that the initial conditions of the systems are equal to $(\boldsymbol{q}_0, \dot{\boldsymbol{q}}_0)$

where the vector of combinators $\boldsymbol{a}$ is chosen such that the task is solved. As mentioned earlier, if time is discretized, $\boldsymbol{\Theta}(t)$ becomes a $N \dim(\boldsymbol{q})$-by-N_θ matrix, where N_θ is the number of dynamic responses. The quality of the DR as interpolants is evaluated in sections C.3.

Once a kinematic solution has been found (as linear combination of DRs), the corresponding actuation can be obtained by applying the differential operator; i.e. $\mathcal{D}(\boldsymbol{\Theta}(t)\boldsymbol{a}) = \tilde{\boldsymbol{u}}(t)$. Finally, the vector $\boldsymbol{b}$ can be computed by projecting $\tilde{\boldsymbol{u}}(t)$ onto the synergy set $\boldsymbol{\Phi}$. If $\tilde{\boldsymbol{u}}(t)$ does not belong to the linear span of $\boldsymbol{\Phi}$, the solution can only be approximated in terms of a defined norm (e.g. Euclidean):

$$\boldsymbol{b} = \arg\min_{\boldsymbol{b}} ||\tilde{\boldsymbol{u}}(t) - \boldsymbol{\Phi}(t)\boldsymbol{b}||. \tag{C.5}$$

When the time is discretized, all functions of time becomes vectors and this equation can be solved explicitly using the pseudoinverse of the matrix $\boldsymbol{\Phi}$,

$$\boldsymbol{\Phi}^+ \tilde{\boldsymbol{u}} = \boldsymbol{\Phi}^+ \mathcal{D}(\boldsymbol{\Theta}\boldsymbol{a}) = \boldsymbol{b}. \tag{C.6}$$

This equation highlights the operator $\boldsymbol{\Phi}^+ \circ \mathcal{D} \circ \boldsymbol{\Theta}$ ($\circ$ denotes operator composition) as the mapping between the kinematic combinators $\boldsymbol{a}$ (kinematic solution) and the synergy combinators $\boldsymbol{b}$ (dynamic solution). Generically, this operator represents a nonlinear mapping $\mathcal{M} : \mathbb{R}^{N_\theta} \to \mathbb{R}^{N_\phi}$, and it will be discussed in Section C.4.

To assess the quality of the solution we define the following measures:

Interpolation error: Measures the quality of the interpolant $\boldsymbol{\Theta}(t)\boldsymbol{a}$ with respect to the task. Strictly speaking, only the case of negligible errors corresponds to interpolation. A non-zero error indicates that the trajectory $\boldsymbol{\Theta}(t)\boldsymbol{a}$ only approximates the task

$$\mathrm{err}_I = \sqrt{||\boldsymbol{q}_T - \boldsymbol{\Theta}(T)\boldsymbol{a}||^2 + ||\dot{\boldsymbol{\Theta}}(T)\boldsymbol{a}||^2}, \tag{C.7}$$

where $||\cdot||$ denotes the Euclidean norm, and the difference between angles are mapped to the interval $(-\pi, \pi]$.

Projection error: Measures the distance between the actuation that solves the task $\tilde{\boldsymbol{u}}(t)$, and the linear span of the synergy set $\boldsymbol{\Phi}$

$$\mathrm{err}_P = \sqrt{\int_0^T ||\tilde{\boldsymbol{u}}(t) - \boldsymbol{\Phi}(t)\boldsymbol{b}||^2 \mathrm{d}t}. \tag{C.8}$$

Forward dynamics error: Measures the error of a trajectory $\tilde{\boldsymbol{q}}(t, \boldsymbol{\lambda})$ generated by an actuation $\boldsymbol{\Phi}(t)\boldsymbol{\lambda}$, in relation to the task.

$$\mathrm{err}_F = \sqrt{||\tilde{\boldsymbol{q}}(T, \boldsymbol{\lambda}) - \boldsymbol{q}_T||^2 + ||\dot{\tilde{\boldsymbol{q}}}(T, \boldsymbol{\lambda}) - \dot{\boldsymbol{q}}_T||^2}. \tag{C.9}$$

Replacing $\tilde{\boldsymbol{q}}(t, \boldsymbol{\lambda})$, $\boldsymbol{q}_T$ and $\dot{\boldsymbol{q}}_T$ with their corresponding end-effector values provides the *forward dynamics error of the end-effector*.

C.2.2 Synthesis and Development of Synergies

The synthesis of synergies is carried on in two phases: exploration and reduction. The exploration phase consists in actuating the system with an extensive set of motor signals $\boldsymbol{\Phi}_0$ in order to obtain the corresponding DRs $\boldsymbol{\Theta}_0$. The reduction phase consists in solving a small number of point-to-point reaching tasks in kinematic space (that we call *proto-tasks*) by creating the interpolants using the elements of set $\boldsymbol{\Theta}_0$, as described in Eq. (C.4). These solutions are then taken as the elements of the reduced set $\boldsymbol{\Theta}$. Finally, the synergy set $\boldsymbol{\Phi}$ is computed using relation (C.2), i.e. inverse dynamics. As a result, there will be as many synergies as the number of the proto-tasks

(i.e. $N_\phi = N_\theta$). The intuition behind this reduction is that the synergies that solve the proto-tasks may capture essential features both of the task and of the dynamics of the system. Despite the non-linearities of $\mathcal{D}$, linear combination of these synergies might be useful to solve point-to-point reaching tasks that are similar (in terms of Eq. (C.3)) to the proto-tasks (see Sec. C.3).

The number of proto-tasks as well as their specific instances determine the quality of the synergy-based controller. To obtain good performance in a wide variety of point-to-point reaching tasks, the proto-tasks should cover relevant regions of the state space (see Sec. C.3). Clearly, the higher the number of different proto-tasks, the more regions that can be reached with good performance. However, a large number of proto-tasks (and the corresponding synergies) increases the dimensionality of the controller. In order to tackle this trade-off, we propose a procedure that parsimoniously adds a new proto-task only when and where it is needed: if the performance in a new reaching task is not satisfactory, we add a new proto-task in one of the regions with highest projection error or we modify existing ones.

C.3 Results

We apply the methodology described in Sec. C.2 to a simulated planar kinematic chain (see [Hollerbach and Flash, 1982] for model details) modeling a human arm[Muceli et al., 2010]. In the exploration phase, we employ an extensive set of motor signals $\mathbf{\Phi}_0$ to actuate the arm model and generate the corresponding dynamic responses $\mathbf{\Theta}_0$. The panels in the first row of Fig. C.1 show the end-effector trajectories resulting from the exploration phase. We test two different classes of motor signals: actuations that generate minimum jerk end-effector trajectories (100 signals), and low-passed uniformly random signals (90 signals). In order to evaluate the validity of the general method described in Sec. C.2.1, we use the sets $\mathbf{\Phi}_0$ and $\mathbf{\Theta}_0$ to solve 13 different reaching tasks without performing the reduction phase. The second row of Fig. C.1 depicts the trajectories drawn by the end-effector when the computed mixture of synergies are applied as actuations (i.e. forward dynamics of the solution). It has to be noted how the nature of the solutions (as well as that of the responses), depends on the class of actuations used. The maximum errors are reported in Table C.1. The results are highly satisfactory for both the classes of actuations, and show the validity of the method proposed. Since the reduction phase has not been performed, the dimension of the combinator vectors $\boldsymbol{a}$ and $\boldsymbol{b}$ equals the number of actuations used in the exploration.

	Min. Jerk	Random
err_I	10^{-15}	10^{-15}
err_P	10^{-5}	10^{-3}
err_F	10^{-4}	10^{-3}

Table C.1: Order of the maximum errors obtained by using $\mathbf{\Phi}_0$ and $\mathbf{\Theta}_0$ (no reduction phase).

The objective of the reduction phase is to generate a small set of synergies and DRs that can solve desired reaching tasks effectively. As described in Sec. C.2.2, this is done by solving a handful of proto-tasks. The number (and the instances) of these proto-tasks determines the quality of the controller. Figure C.2 shows the projection error as a function of the number of proto-tasks. The reduction is applied to the low-passed random signal set. Initially, two targets are chosen randomly (top left panel); subsequent targets are then added on the regions characterized by higher projection error. As it can be seen, the introduction of new proto-tasks leads to better performance on wider regions of the end-effector space, and eventually the whole space can be reached with

reasonable errors. In fact, the figure shows that this procedure decreases the average projection error to 10^{-3} (comparable to the performance of the whole set $\mathbf{\Phi}_0$, see Tab. C.1) and reduces the dimension of the combinator vector to 6, a fifteen-fold reduction. This result shows that a set of "good" synergies can drastically reduce the dimensionality of the controller, while maintaining similar performance. The bottom right panel of the figure shows the forward dynamics error of the end-effector obtained with the 6 proto-tasks. Comparing this panel with the bottom left one, it can be seen that the forward dynamics error of the end-effector reproduces the distribution of the projection error, rendering the latter a good estimate for task performance.

To further demonstrate that the reduction phase we propose is not trivial, we compare the errors resulting from the set of 6 synthesized synergies, with the errors corresponding to 100 random subsets of size 6 drawn from the set of low-passed random motor signals. Figure C.3 shows this comparison. The task consists in reaching the 13 targets in Fig. C.1. The boxplots correspond to the errors of the random subsets, and the filled circles to the errors of the synergies resulting from the reduction phase. Observe that, the order of the error of the reduced set is, in the worst case, equal to error of the best random subset. However, the mean error of the reduced set is about 2 orders of magnitude lower. Therefore, the reduction by proto-tasks can produce a parsimonious set of synergies out of a extensive set of actuations. Evaluating the performance with different classes of proto-tasks (e.g. catching, hitting, via-points) is postponed to future works.

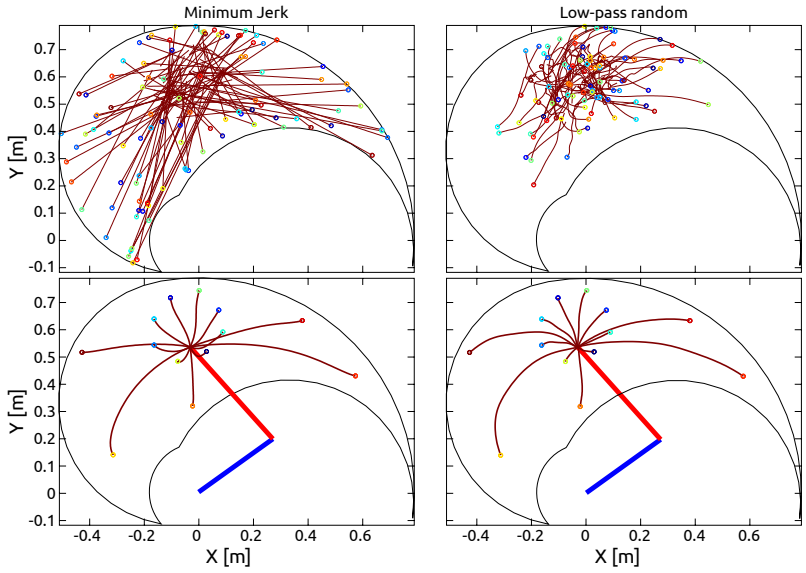

Figure C.1: Comparison of explorations with two different classes of actuation: minimum jerk and low-passed random signal. Each panel shows the kinematic chain in it initial posture (straight segments). The limits of the end-effector are shown as the boundary in solid line.

C.4 Discussion

The results shown in the previous section justify the interpretation of the methodology as a developmental framework. Initially, the agent explores its sensory-motor system employing a variety

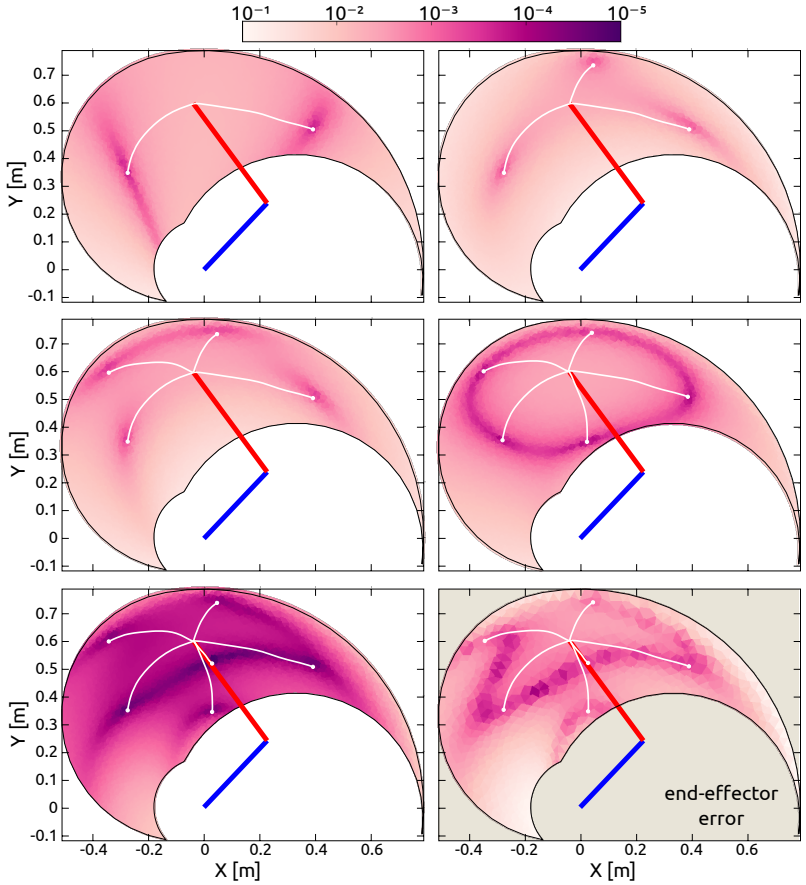

Figure C.2: Selection of targets based on projection error. Each panel shows the kinematic chain in its initial posture (straight segments). The limits of the end-effector are the boundary of the colored regions. The color of each point indicates the projection error produced to reach a target in that position. The bottom right diagram shows the forward dynamics error of the end-effector using 6 proto-tasks (6 synergies).

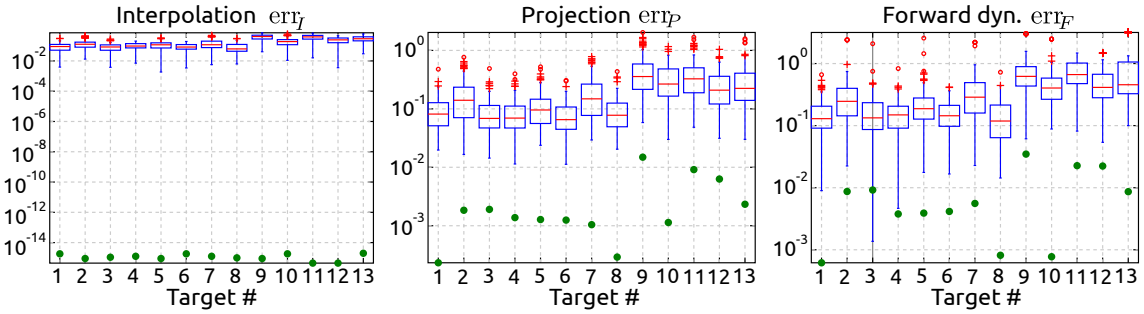

Figure C.3: Evaluation of the reduction phase. Errors produced by subsets randomly selected from the exploration-actuations (boxplots) are compared with the errors obtained after the reduction phase (filled circles).

of actuations. Later, it attempts to solve the first reaching tasks (proto-tasks), perhaps obtaining weak performance as the exploration phase may not have produced enough responses yet (see the box-plots in Fig. C.3). If the agent finds an acceptable solution to a proto-task, it is used to generate a new synergy (populating the set $\mathbf{\Phi}$), otherwise it continues with the exploration. The failure to solve tasks of importance for its survival, could motivate the agent to include additional proto-tasks; Figure C.2 illustrates this mechanism. As it can be seen, the development of the synergy set incrementally improves the ability of the agent to perform point-to-point reaching. Alternatively, existing proto-tasks could be modified by means of a gradient descent or other learning algorithms. In a nutshell, the methodology we propose endows the agent with the ability to autonomously generate and update a set of synergies (and dynamic responses) that solve reaching tasks effectively.

Despite the difficulty of the mathematical problem (i.e nonlinear differential operator), our method seems to generate a small set of synergies that span the space of actuations required to solve reaching tasks. This is not a trivial result, since these synergies over-perform many other set of synergies randomly taken from the set $\mathbf{\Phi}_0$ (see Fig. C.3). It appears as if the reduction phase builds features upon the exploration phase, that are necessary to solve new reaching tasks. To verify whether solving proto-tasks plays a fundamental role, our synergies could be compared with the principal components extracted from the exploration set. This verification goes beyond the scope of this paper.

An important aspect of our method is the relation between $\mathbf{\Theta}$ and $\mathbf{\Phi}$ (see Eq. (C.2)). This mapping makes explicit use of the body parameters (embedded in the differential operator $\mathcal{D}$), hence the synergies obtained can always be realized as actuations. The same cannot be said, in general, for synergies identified from numerical analyses of biomechanical data. Though some studies have verified the feasibility of extracted synergies as actuations [Neptune et al., 2009], biomechanical constraints are not explicitly included in the extraction algorithms. Additionally, Eq. (C.2) provides an automatic way to cope with smooth variations of the morphology of the agent. That is, both the synergies and their dynamic responses evolve together with the body. In line with Alessandro et al. [2012]; Nori [2005], these observations highlight the importance of the body in the hypothetical modularization of the CNS.

Once the task is solved in kinematic space, the corresponding actuation can be computed using the explicit inverse dynamical model of the system (i.e. the differential operator $\mathcal{D}$). It might appear that there is no particular advantage in projecting this solution onto the synergy set. However, the differential operator might be unknown. In this case, a synergy-based controller would allow to compute the appropriate actuation by evaluating the mapping $\mathcal{M}$ on the vector $\boldsymbol{a}$, hence obtaining the synergy combinators $\boldsymbol{b}$. Since $\mathcal{M}$ is a mapping between two finite low-dimensional vector spaces, estimating this map may turn to be easier than estimating the differential operator $\mathcal{D}$. Furthermore, we believe that the explicit use of $\mathcal{D}$ may harm the biological plausibility of our method. In order to estimate the map $\mathcal{M}$, the input-output data generated during the exploration phase (i.e. $\mathbf{\Phi}_0$ and $\mathbf{\Theta}_0$) could be used as learning data-set. Further work is required to test these ideas. Additionally, preliminary theoretical considerations (not reported here) indicate that the synthesis of synergies without the explicit knowledge of $\mathcal{D}$ is also feasible.

Finally, the current formulation of the method does not includes joint limits explicitly. The interpolated trajectories are valid, i.e. they do not go beyond the limits, due to the lack of intricacy of the boundaries. In higher dimensions, especially when configuration space and end-effector are not mapped one-to-one, this may not be the case anymore. Nevertheless, joint limits can be included by reformulating the interpolation as a constrained minimization problem. Another solution might be the creation of proto-tasks with a tree-topology, relating our method to tree based path planning algorithms [Shkolnik and Tedrake, 2011].

C.5 Conclusion and Future Work

The current work introduces a simple framework for the generation of open loop controllers based on synergies. The framework is applied to a planar kinematic chain to solve point-to-point reaching tasks. Synergies synthesized during the reduction phase over-perform hundreds of arbitrary choices of basic controllers taken from the exploration motor signals. Furthermore, our results confirm that the introduction of new synergies increases the performance of reaching tasks. Overall, this shows that our method is able to generate effective synergies, greatly reducing the dimensionality of the problem, while keeping a good performance level. Additionally, the methodology offers a developmental interpretation of the emergence of task-related synergies that could be validated experimentally.

Due to the nonlinear nature of the operator $\mathcal{D}$, the theoretical grounding of the method poses a difficult challenge, and it is the focus of our current research. Another interesting line of investigation is the validation of our method against biological data, paving the way towards a predictive model for the hypothesis of muscle synergies. Similarly, the development of an automatic estimation process for the mapping $\mathcal{M}$ would further increase the biological plausibility of the model.

The inclusion of joint limits into the current formulation must be prioritized. Solving this problem will allow to test the method on higher dimensional redundant systems. Tree-based path planning algorithms may offer a computationally effective way to approach the issue.

Funds: The research leading to these results has received funding from the European Community's Seventh Framework Programme FP7/2007-2013-Challenge 2 - Cognitive Systems, Interaction, Robotics- under grant agreement No 248311-AMARSi, and from the EU project RobotDoC under 235065 from the 7th Framework Programme (Marie Curie Action ITN).

Authors Contribution: **CA** and **JPC** worked on the implementation of the algorithm and the generation of the results reported here. The method was born during **JPC**'s visit to **AD**'s laboratory. **AD** provided material support for this development and uncountable conceptual inputs. All three authors have contributed to the creation of the manuscript. The authors list follows an alphabetical order.

Bibliography

Alessandro, C., Carbajal, J. P., and d'Avella, A. (2012). Synthesis and Adaptation of Effective Motor Synergies for the Solution of Reaching Tasks. In Ziemke, T., Balkenius, C., and Hallam, J., editors, *Lecture Notes in Artificial Intelligence (LNAI)*, pages 33–43, Berlin. Springer-Verlag.

Cappellini, G., Ivanenko, Y. P., Poppele, R. E., and Lacquaniti, F. (2006). Motor patterns in human walking and running. *Journal of Neurophysiology*, 95(6):3426–3437.

d'Avella, A., Fernandez, L., Portone, A., and Lacquaniti, F. (2008). Modulation of phasic and tonic muscle synergies with reaching direction and speed. *Journal of Neurophysiology*, 100(3):1433–54.

d'Avella, A., Saltiel, P., and Bizzi, E. (2003). Combinations of muscle synergies in the construction of a natural motor behavior. *Nature Neuroscience*, 6:300–308.

Dominici, N., Ivanenko, Y. P., Cappellini, G., D'Avella, A., Mondì, V., Cicchese, M., Fabiano, A., Silei, T., Di Paolo, A., Giannini, C., Poppele, R. E., and Lacquaniti, F. (2011). Locomotor primitives in newborn babies and their development. *Science*, 334(6058):997–9.

Hollerbach, J. M. and Flash, T. (1982). Dynamic interactions between limb segments during planar arm movement. *Biological Cybernetics*, 44(1):67–77.

Ivanenko, Y. P., Cappellini, G., Dominici, N., Poppele, R. E., and Lacquaniti, F. (2005). Coordination of locomotion with voluntary movements in humans. *The Journal of Neuroscience*, 25(31):7238–7253.

Muceli, S., Boye, A. T. l., D'Avella, A., and Farina, D. (2010). Identifying representative synergy matrices for describing muscular activation patterns during multidirectional reaching in the horizontal plane. *Journal of Neurophysiology*, 103(3):1532–1542.

Neptune, R. R., Clark, D. J., and Kautz, S. A. (2009). Modular control of human walking: a simulation study. *Journal of Biomechanics*, 42(9):1282–1287.

Nori, F. (2005). *Symbolic Control with Biologically Inspired Motion Primitives*. PhD thesis, Università degli Studi di Padova.

Schaal, S., Peters, J., Nakanishi, J., and Ijspeert, A. (2005). Learning movement primitives. In Dario, P. and Chatila, R., editors, *Robotics Research*, volume 15 of *Tracts in Adv. Rob.*, pages 561–572. Springer.

Shkolnik, A. and Tedrake, R. (2011). Sample-based planning with volumes in configuration space. *arXiv:1109.3145v1*.

Todorov, E. and Ghahramani, Z. (2003). Unsupervised learning of sensory-motor primitives. In *Proceedings of the 25th International Conference of the IEEE Engineering in Medicine and Biology Society*, pages 1750–1753. IEEE.

Appendix D

A computational analysis of motor synergies by dynamic response decomposition

Submitted article:

Alessandro, C., Carbajal, J. P., and d'Avella, A. (2013). A computational analysis of motor synergies by dynamic response decomposition.

Abstract

Analyses of experimental data acquired from humans and other vertebrates have suggested that motor commands may emerge from the combination of a limited set of modules. In this paper we analyze this idea from a computational standpoint, testing whether a planar kinematic chain can be controlled by restricting the admissible actuations to the linear combinations of a small set of torque profiles (i.e. motor synergies). This scheme is equivalent to the time-varying synergy model, and it is formalized by means of the dynamics response decomposition (DRD). DRD is a general method to generate open-loop controllers for a dynamical system to solve desired tasks, and it can also be used to synthesize effective motor synergies. We show that a control architecture based on synergies can greatly reduce the dimensionality of the control problem, while keeping a good performance level. The number and the shapes of the synergies are strictly tailored to the system as well as to the tasks to be solved; in particular DRD suggests that synergies might be solutions to proto-typical task instances. Inspired by the observation that movements can be composed by sequences of kinematic primitives, we test the concatenation of point-to-point actuations to solve via-point tasks. Compared to building solutions for the entire tasks without segmentation, this strategy is affected by more sources of error. However, it provides a viable approach to keep the number of synergies low. These results provide a proof of concept for the muscle synergy hypothesis, and highlight important aspects of the synthesis and the concatenation of synergies that could be verified experimentally.

D.1 Introduction

Richness, flexibility, and adaptability characterize the generation of movements in many animal species. During the last century these features have fascinated many scientists, who started to investigate the possible mechanisms underlying the observed motor performance. Although many questions remain open, today there is a large consensus that motor skills may arise from a modular and hierarchical organization of the movement system [Bizzi et al., 2008; d'Avella and Pai, 2010; Giszter et al., 2010; Ting and McKay, 2007]. This idea was initially introduced by Bernstein [1967] in the context of motor redundancy, and it has then evolved into different, yet related, concepts [Flash and Hochner, 2005]. The common denominator of these ideas is that motor actions emerge from the combination of a limited set of modules. This strategy would reduce the number of variables to be controlled, and therefore it might simplify motor control and learning.

One of the proposed forms of modularity are the so-called muscle synergies, coordinated activations of groups of muscles [d'Avella et al., 2003; Saltiel et al., 2001; Tresch et al., 1999]. Hypothetically, the central nervous system (CNS) encodes a parsimonious set of synergies and combines them in a task-dependent fashion to generate appropriate motor commands. This hypothesis is typically evaluated by analyzing the spatio-temporal regularities of electromyographic signals (EMG) recorded from a group of subjects. Decomposition-based techniques, such as principal component analysis (PCA) or non-negative matrix factorization (NMF), are used to extract the components that best reconstruct the recorded dataset. In many cases these components (i.e. synergies) appear very similar across different experimental conditions, and therefore they are regarded as an indirect evidence of the hypothesized neural modularity. This methodology has been successful in explaining muscle contractions across a wide range of complex tasks (e.g. running, walking, keeping balance, reaching and other combined movements) in humans [Cappellini et al., 2006; d'Avella et al., 2008, 2006, 2011; Ivanenko et al., 2005; Torres-Oviedo and Ting, 2007, 2010], in frogs [Giszter et al., 1993; Kargo and Giszter, 2000, 2008; Mussa-Ivaldi and Bizzi, 2000; Mussa-Ivaldi et al., 1994], cats [Ting and Macpherson, 2005; Torres-Oviedo et al., 2006], monkeys [Overduin et al., 2012, 2008], and other species [Dominici et al., 2011]. However the results are often descriptive in nature and they do not offer a principled investigation of the hypothesized synergy-based control strategy [Alessandro et al., 2013].

In this paper we analyze the muscle synergy hypothesis from a computational point of view, and in particular from the perspective of controlling an idealized arm. We formulate the control signals for a planar kinematic chain as linear combinations of a small set of predefined actuations (i.e. synergies) in accordance with the model of time-varying synergies [d'Avella et al., 2003]. For this purpose we propose the dynamic response decomposition (DRD), a general tool to find the open-loop controllers that allow a dynamical system to solve desired tasks [Alessandro et al., 2012; Carbajal, 2012]. Our method initially solves the task in state variables by interpolation; then, it identifies the combination of synergies (i.e. actuation) that leads to the closest kinematic trajectory to the computed interpolant. Additionally we propose a procedure to synthesize a limited set of effective synergies. In this manuscript we apply the DRD to point-to-point reaching tasks, and to via-point movements. Within the latter class of tasks we analyze two specific scenarios: (1) moving to a desired target and coming back to the initial posture (i.e. reversal task), and (2) reaching a desired location, passing though a given via-point (i.e. via-point reaching).

Reversal and via-point reaching movements can be subdivided in two distinct kinematic phases: from the initial to the intermediate point, and from the intermediate to the final point. A possible strategy to solve these tasks is therefore to concatenate the actuations associated to the two phases; each actuation is in turn realized as a combination of synergies. This idea is related to another form of modularity, the composition of movements into sequences of kinematic primitives, or strokes [Flash et al., 1992; Novak et al., 2003]. While this segmentation explains a vast

amount of experimental data, there is no consensus on whether such strokes effectively reflect a segmented control strategy [Fishbach et al., 2005, 2007]. Alternatively they could just emerge as a result of a possible trajectory optimization [Dagmar and Schaal, 1999], or even be artifacts of the data analysis. In these latter cases the actuation could be computed in its entirety without concatenation. In this manuscript we analyze both strategies: the concatenation of simple synergy-based control signals, and the computation of a synergy-based actuation for the whole task. This investigation provides some computational insights on the advantages and the disadvantages of these two approaches, and it offers a proof of concept on how muscle synergies and kinematic modularity might be integrated into a unified framework.

This paper is organized as follows. In Sec. D.2 we introduce the mathematical formulation of DRD, the method that we employ throughout the paper to synthesize synergies and to compute task solutions. Section D.3 presents the results obtained for reversal and via-point reaching tasks. Such results are further discussed in Sec. D.4, where we additionally summarize and speculate on important aspects of the muscle synergy hypothesis that are highlighted by DRD; finally we provide some concluding remarks.

D.2 Methods

In this section we introduce the mathematical details of the dynamic response decomposition (DRD). After some definitions, we present the core element of the method: a general procedure to compute actuations that solve generic reaching tasks (see Sec. D.2.1). Subsequently, in Sec. D.2.2, we show how DRD can be used for the synthesis of a set of synergies.

Let us consider a differential equation modeling a physical system

$$\mathcal{D}\left(\boldsymbol{q}(t)\right) = \boldsymbol{u}(t),$$

where $\boldsymbol{q}(t)$ represents the time-evolution of its configuration variables (their derivatives with respect to time are $\dot{\boldsymbol{q}}(t)$), and $\boldsymbol{u}(t)$ is the actuation applied. Inspired by the hypothesis of muscle synergies, we formulate the actuation as a linear combination of predefined motor co-activation patterns:

$$\boldsymbol{u}(t) = \sum_{i=1}^{N_\phi} \boldsymbol{\phi}_i(t) b_i := \boldsymbol{\Phi}(t)\boldsymbol{b}, \tag{D.1}$$

where the functions $\boldsymbol{\phi}_i(t) \in \boldsymbol{\Phi}$ are called *motor synergies*. Equation (D.1) is essentially equivalent to the model of time-varying synergies [d'Avella et al., 2003], however in this paper we assume that synergies cannot be shifted in time. The notation $\boldsymbol{\Phi}(t)$ describes a formal matrix where each column is a different synergy. If we consider a time discretization, $\boldsymbol{\Phi}(t)$ becomes a $N \dim(\boldsymbol{q})$-by-N_ϕ matrix, where N is the number of time steps, $\dim(\boldsymbol{q})$ the dimension of the configuration space and N_ϕ the number of synergies.

We define *dynamic responses* (DR) of the set of synergies the responses $\boldsymbol{\theta}_i(\cdot) \in \boldsymbol{\Theta}$ of the system to each synergy (i.e. forward dynamics):

$$\mathcal{D}(\boldsymbol{\theta}_i(t)) = \boldsymbol{\phi}_i(t) \qquad i = 1...N_\phi. \tag{D.2}$$

with initial conditions chosen arbitrarily.

D.2.1 The dynamic responses decomposition

Here we extend the formalism recently introduced for solving point-to-point reaching tasks [Alessandro et al., 2012] to more general reaching movements that involve via-points. A generic

reaching task consists in reaching a final state $(\boldsymbol{q}_T, \dot{\boldsymbol{q}}_T)$ from an initial state $(\boldsymbol{q}_0, \dot{\boldsymbol{q}}_0)$ in a given amount of time T satisfying intermediate constraints called via-points. In the case of a single via-point defined at time t_v, the task can be formalized as follows:

$$\begin{aligned} \boldsymbol{q}(0) &\doteq \boldsymbol{q}_0, \quad & \dot{\boldsymbol{q}}(0) &\doteq \dot{\boldsymbol{q}}_0, \\ \boldsymbol{q}(t_v) &\doteq \boldsymbol{q}_v, \quad & \dot{\boldsymbol{q}}(t_v) &\doteq \dot{\boldsymbol{q}}_v, \\ \boldsymbol{q}(T) &\doteq \boldsymbol{q}_T, \quad & \dot{\boldsymbol{q}}(T) &\doteq \dot{\boldsymbol{q}}_T, \end{aligned} \tag{D.3}$$

where $\doteq$ indicates a prescribed value, i.e. a point constraint. Depending on the desired task, more or less requirements can be imposed. For example a simple point-to-point reaching task consists only of the constraints defined at $t = 0$ and $t = T$. Furthermore, one could formulate via-point tasks without prescribing any velocity. This would define a class of tasks where the system is free to traverse the desired positions with any velocity. In addition, it is also possible to constrain higher order time derivatives of the configuration vector, e.g acceleration, jerk, etc.

Controlling a system to perform a given task amounts to finding the actuation $\boldsymbol{u}(t)$ that allow the system-variables to fulfill the point constraints (D.3). Specifically, assuming that the synergies are known, the goal is to identify the appropriate synergy combination coefficients $\boldsymbol{b}$. The DRD procedure consists of, first, solving the problem in kinematic space (i.e. finding an appropriate $\boldsymbol{q}(t)$), and then computing the corresponding actuations. From the kinematic point of view, solving the task can be seen as an interpolation problem; i.e. a set of functions is used to generate a trajectory $\boldsymbol{q}(t)$ that interpolates the constraints defined in (D.3). To build this interpolant one could employ orthonormal polynomials, trigonometric or Gaussian functions, to mention just a few possibilities. One of the most salient properties of DRD is that it employs the dynamic responses of the synergies (given by Eq. (D.2)), that is:

$$\boldsymbol{q}(t) = \sum_{i=1}^{N_\theta} \boldsymbol{\theta}_i(t) a_i := \boldsymbol{\Theta}(t)\boldsymbol{a}. \tag{D.4}$$

The quality of the DRs as building blocks for the interpolation was evaluated in our previous works on planar kinematic chains [Alessandro et al., 2012] and other dynamical systems [Carbajal, 2012]. As we mentioned before, if time is discretized, $\boldsymbol{\Theta}(t)$ becomes a $N \dim(\boldsymbol{q})$-by-N_θ matrix, where N_θ is the number of dynamic responses. The vector of combination coefficients $\boldsymbol{a}$ is chosen such that the task constraints are satisfied (i.e. the task is solved). Specifically, this vector is computed by solving the following linear system of equations:

$$\begin{pmatrix} \boldsymbol{\theta}_1(0) & \dots & \boldsymbol{\theta}_{N_\theta}(0) \\ \boldsymbol{\theta}_1(t_v) & \dots & \boldsymbol{\theta}_{N_\theta}(t_v) \\ \boldsymbol{\theta}_1(T) & \dots & \boldsymbol{\theta}_{N_\theta}(T) \\ \dot{\boldsymbol{\theta}}_1(0) & \dots & \dot{\boldsymbol{\theta}}_{N_\theta}(0) \\ \dot{\boldsymbol{\theta}}_1(t_v) & \dots & \dot{\boldsymbol{\theta}}_{N_\theta}(t_v) \\ \dot{\boldsymbol{\theta}}_1(T) & \dots & \dot{\boldsymbol{\theta}}_{N_\theta}(T) \end{pmatrix} \boldsymbol{a} = M\boldsymbol{a} = \begin{pmatrix} \boldsymbol{q}_0 \\ \boldsymbol{q}_v \\ \boldsymbol{q}_T \\ \dot{\boldsymbol{q}}_0 \\ \dot{\boldsymbol{q}}_v \\ \dot{\boldsymbol{q}}_T \end{pmatrix}. \tag{D.5}$$

The matrix M in the left-hand side is called *alternant matrix*; the solvability of the problem depends on its rank. If the matrix has full row rank, any point constraint can be solved. Otherwise, the possibility to find an exact solution (as opposed to an approximation) becomes strictly dependent on the specific task. According to the Rouché–Capelli theorem, if the rank of the alternant matrix (not necessarily equal to number of rows) is equal to the rank of the augmented matrix $[M|P]$, where P is the vector of point constraints, the specific problem can be solved exactly. Section D.3 presents some examples. These observations, and their implications for the hypothesis of muscle synergies, are further discussed in Sec. D.4.

Once a kinematic solution has been found (as a linear combination of DRs), the corresponding actuation can be obtained by applying the differential operator (i.e. inverse dynamics);

$$\mathcal{D}\left(\boldsymbol{\Theta}(t)\boldsymbol{a}\right) = \tilde{\boldsymbol{u}}(t).$$

Finally, the vector $\boldsymbol{b}$ can be computed by projecting $\tilde{\boldsymbol{u}}(t)$ onto the linear span of the synergy set $\boldsymbol{\Phi}$. If $\tilde{\boldsymbol{u}}(t)$ does not belong to the linear span of $\boldsymbol{\Phi}$, the solution can only be approximated in terms of a defined norm (e.g. Euclidean):

$$\boldsymbol{b} = \arg\min_{\boldsymbol{b}} ||\tilde{\boldsymbol{u}}(t) - \boldsymbol{\Phi}(t)\boldsymbol{b}||. \tag{D.6}$$

When time is discretized, all functions of time become vectors and this problem can be solved explicitly using the pseudo-inverse of the matrix $\boldsymbol{\Phi}(t)$,

$$\boldsymbol{\Phi}^{+}\tilde{\boldsymbol{u}} = \boldsymbol{\Phi}^{+}\mathcal{D}\left(\boldsymbol{\Theta}\boldsymbol{a}\right) = \boldsymbol{b}. \tag{D.7}$$

This equation highlights the mapping between the kinematic combination coefficients $\boldsymbol{a}$ (kinematic solution) and the synergy combination coefficients $\boldsymbol{b}$ (dynamic solution):

$$\mathcal{F} = \boldsymbol{\Phi}^{+} \circ \mathcal{D} \circ \boldsymbol{\Theta}, \tag{D.8}$$

where $\circ$ denotes composition. Generically, this operator represents a nonlinear mapping $\mathcal{F} : \mathbb{R}^{N_\theta} \to \mathbb{R}^{N_\phi}$, and it will be discussed in Sec. D.4.3.

To assess the quality of the solution we define the following measures:
Interpolation error: measures the quality of the interpolant $\boldsymbol{\Theta}(t)\boldsymbol{a}$ with respect to the task. Strictly speaking, only the case of negligible error corresponds to an interpolation; a non-zero error indicates that the trajectory $\boldsymbol{\Theta}(t)\boldsymbol{a}$ only approximates the task-constraints. The interpolation error is formulated as

$$\begin{aligned} \mathrm{err}_I &= \sqrt{\sum_{k\in K} e_{Ik}^2} \\ K &= \{0, v_1, \ldots, v_n, T\} \\ e_{Ik}^2 &= ||\boldsymbol{q}_k - \boldsymbol{\Theta}(t_k)\boldsymbol{a}||^2 + ||\dot{\boldsymbol{q}}_k - \dot{\boldsymbol{\Theta}}(t_k)\boldsymbol{a}||^2 \end{aligned} \tag{D.9}$$

where $||\cdot||$ denotes the Euclidean norm, and the difference between angles are mapped to the interval $(-\pi, \pi]$. The subindex k identifies the point constraint, i.e. $k = 0$ for the initial condition, $k = v_i$ for the i-th via-point, and $k = T$ for the final condition. In this work we consider tasks with a single or with no via-points (the latter case corresponding to simple point-to-point tasks).
Projection error: measures the distance between the actuation $\tilde{\boldsymbol{u}}(t)$, that solves the task, and the control signal obtained by the linear combination of the synergies $\boldsymbol{\Phi}$

$$\mathrm{err}_P = \sqrt{\int_0^T ||\tilde{\boldsymbol{u}}(t) - \boldsymbol{\Phi}(t)\boldsymbol{b}||^2 \mathrm{d}t}. \tag{D.10}$$

Forward dynamics error: measures the error of a trajectory $\tilde{\boldsymbol{q}}(t, \boldsymbol{\lambda})$, generated by the actuation $\boldsymbol{\Phi}(t)\boldsymbol{\lambda}$, in relation to the task

$$\begin{aligned} \mathrm{err}_F &= \sqrt{\sum_{k\in K} e_{Fk}^2} \\ K &= \{0, v_1, \ldots, v_n, T\} \\ e_{Fk}^2 &= ||\boldsymbol{q}_k - \tilde{\boldsymbol{q}}(t_k, \boldsymbol{\lambda})||^2 + ||\dot{\boldsymbol{q}}_k - \dot{\tilde{\boldsymbol{q}}}(t_k, \boldsymbol{\lambda})||^2 \end{aligned} \tag{D.11}$$

Replacing $\tilde{\boldsymbol{q}}(t_k, \boldsymbol{\lambda})$, $\boldsymbol{q}_k$ and $\dot{\boldsymbol{q}}_k$ with their corresponding end-effector values provides the *forward dynamics error of the end-effector*.

D.2.2 Synthesis and development of synergies

The synthesis of synergies is carried out in two phases: exploration and reduction. The exploration phase consists in actuating the system with an extensive set of motor signals $\mathbf{\Phi}_0$ to obtain the corresponding DRs $\mathbf{\Theta}_0$. The reduction phase consists in solving a small set of tasks (that we call proto-tasks) in kinematic space, and then computing the corresponding actuations. The elements of the set $\mathbf{\Theta}_0$ are used to interpolate the proto-tasks as described in Eq. (D.4) and (D.5); the obtained trajectories are taken as the elements of the reduced set $\mathbf{\Theta}$. Finally, the synergy set $\mathbf{\Phi}$ is computed using relation (D.2), i.e. inverse dynamics. As a result, there will be as many synergies as the number of proto-tasks (i.e. $N_\phi = N_\theta$).

In a nutshell, the synthesized synergies are the actuations solving the proto-tasks. A legitimate question is: "how do we choose the proto-tasks?". In principle, the DRD method does not impose any restriction. However, in order to obtain satisfactory performance, synergies should be able to approximate the desired actuations. Since the control signals corresponding to similar tasks are likely to be characterized by similar features, a reasonable choice is that the proto-tasks belong to class of the desired tasks (e.g. reversal, via-point reaching). In such a case, the synthesized synergies are samples of the desired set of actuations, and therefore they embed the characteristic features of such control signals. Thus, we expect that appropriate linear combinations of these synergies are able to approximate the other actuations belonging to the desired set. In general, the more similar the proto-tasks are to the tasks to be solved (in terms of Eq. (D.3)), the better the performance of the corresponding synergies. Section D.3.4 provides some examples and addresses these issues in detail.

Two other aspects that directly influence the quality of the synergy-based controller are the number of the proto-tasks and their particular instances. To obtain good performance in a wide variety of tasks, the constraints defining the proto-tasks should cover relevant regions of the state space. Clearly, an increasing number of (different) proto-tasks corresponds to a gradual improvement of the overall performance. However, it also systematically expands the synergy-set, thus affecting the dimensionality of the controller. In order to tackle this trade-off, we propose a procedure that parsimoniously adds a new proto-task only when and where it is needed: if the performance in a desired task is not satisfactory, we add a new proto-task in one of the regions of the state-space with the highest projection error. In other words, the new proto-task is the task with the worst approximated actuation. Note that the procedure to evaluate the projection error in the entire workspace does not involve any actual task execution nor forward dynamics integration, and therefore it is relatively light in calculation.

D.3 Results

We apply the methodology described in Sec. D.2 to a simulated planar kinematic chain modeling a human arm (see [Hollerbach and Flash, 1982] for model details). In the exploration phase, we employ an extensive set of motor signals $\mathbf{\Phi}_0$ to actuate the arm model and generate the corresponding dynamic responses $\mathbf{\Theta}_0$. The nature of these signals has a marginal role and it does not affect the quality of the obtained results [Alessandro et al., 2012; Carbajal, 2012]. Here we use a set of 90 low-pass filtered uniformly random signals (butterworth with cutoff frequency of 0.314 rad). We test the performance of the method on three classes of tasks: point-to-point (Sec. D.3.1), reversal (Sec. D.3.2) and via-point-reaching (Sec. D.3.3).

D.3.1 Point-to-point tasks

A point-to-point reaching task consists in reaching a final state from an initial state in a given amount of time. Thus, a task instance is specified by four two-dimensional point constraints: initial and final joint angles and velocities. In this section we restrict our analysis to the subclass of tasks that are characterized by the initial position $\boldsymbol{q}_c$ (red cross in Fig. D.1), and that impose initial and final velocities equal to zero, i.e. $\dot{\boldsymbol{q}}_T = \dot{\boldsymbol{q}}_0 = 0$. The only unspecified constraints are the joint-coordinates of the target; i.e. since the kinematic chain has two degrees of freedom (DoF) there are 2 free task-parameters. Essentially the arm is required to start from the configuration $\boldsymbol{q}_c$ and reach a desired target with zero velocity. Note that the velocity constraints are added just to restrict the class of desired tasks, and therefore to simplify the explanations throughout the paper. The method is mathematically general, and therefore can also be used to solve tasks in which these constraints are not imposed.

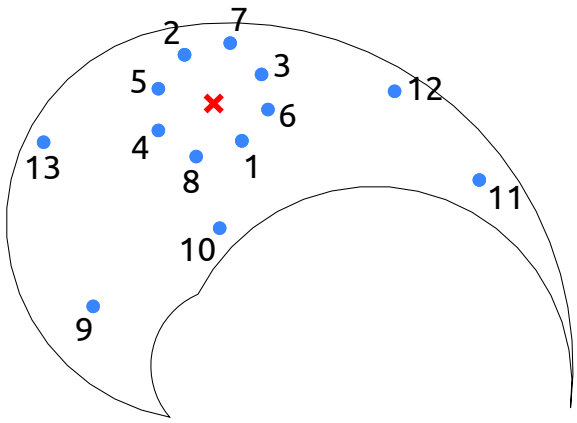

Figure D.1: Salient points of the testing-tasks in end-effector space. The solid line delimits the workspace of the kinematic chain. For point-to-point testing tasks, the red cross represents the initial position of the arm, and the blue dots indicate the final targets. For reversal tasks, the red cross represents the initial and final position of the arm, and the blue dots illustrate the intermediate targets. Finally, for the via-point reaching tasks the red cross indicates the location of the via-point, and the blue dots represent the initial and the final positions of the arm. In the text, the joint configuration vector corresponding to the red cross is referred as $\boldsymbol{q}_c$.

Since the proto-tasks that we employ adhere to the same restrictions, after the reduction phase the linear system in Eq. (D.5) becomes:

$$\begin{pmatrix} \boldsymbol{q}_c & \dots & \boldsymbol{q}_c \\ \boldsymbol{\theta}_1(T) & \dots & \boldsymbol{\theta}_{N_\theta}(T) \\ 0 & \dots & 0 \\ 0 & \dots & 0 \end{pmatrix} \boldsymbol{a} = \begin{pmatrix} \boldsymbol{q}_c \\ \boldsymbol{q}_T \\ 0 \\ 0 \end{pmatrix}, \tag{D.12}$$

where $\boldsymbol{\theta}$ are the reduced DRs, and $\boldsymbol{q}_T$ is the target posture (that uniquely defines a desired task instance as $\boldsymbol{q}_c$ is a fixed value).

From the kinematic point of view and as we discussed in Sec. D.2.1, this formulation shows that any problem of this class can be solved if the rank of the alternant matrix is equal to the rank of the extended matrix. In this case, since each element is a two-dimensional column vector, the extended matrix consists of 4 non-zero rows; the first two rows consist of repetitions of the same numerical values (the components of $\boldsymbol{q}_c$). As a result, an exact kinematic solution is guaranteed if the rank of the alternant matrix is equal to 3; i.e. there should be at least 3 linearly independent

columns. This poses a lower bound on the minimum required number of DRs and therefore of synergies. However, a higher number of synergies might be necessary to achieve satisfactory approximations of the desired actuations, and ultimately to fulfill the task requirements.

Notice that in order to obtain the alternant matrix described in Eq. (D.13), the proto-tasks should belong to the same class of the desired tasks (i.e. point-to-point, starting at $\boldsymbol{q}_c$). Additionally, the exploration DRs $\boldsymbol{\Theta}_0$ should be able to generate kinematic solutions that fulfills all the constraints of the proto-tasks (i.e. zero interpolation error). As it was shown by Carbajal [2012], for systems with non-linear dynamics this is likely to happen as the 8-by-90 alternant matrix, built from the exploration DRs, most probably contains more than 8 linearly independent columns. Thus any point-to-point task could be solved.

Figure D.2 shows the distribution of the projection error for an increasing number of synergies, and exemplifies the proposed procedure to incrementally add new proto-tasks. Initially, two targets are chosen randomly (top left panel); subsequent targets are added in the regions characterized by higher projection error. As it can be seen, the introduction of new proto-tasks leads to better performance on wider regions of the space, and eventually the actuations needed to solve any point-to-point task can be reasonably approximated ($< 10^{-2}$ with 7 synergies). The bottom right panel shows the distribution of the forward dynamics error of the end-effector obtained with 7 proto-tasks. Comparing this panel with the bottom center one (projection error with 7 proto-tasks), it can be seen that the forward dynamics error reproduces the distribution of the projection error, rendering the latter a good estimate of the relative forward performance across tasks. However, it is important to stress that, due to the non-linearity of the dynamical system, the projection error serves only as an heuristic estimate of the actual error made when executing the task.

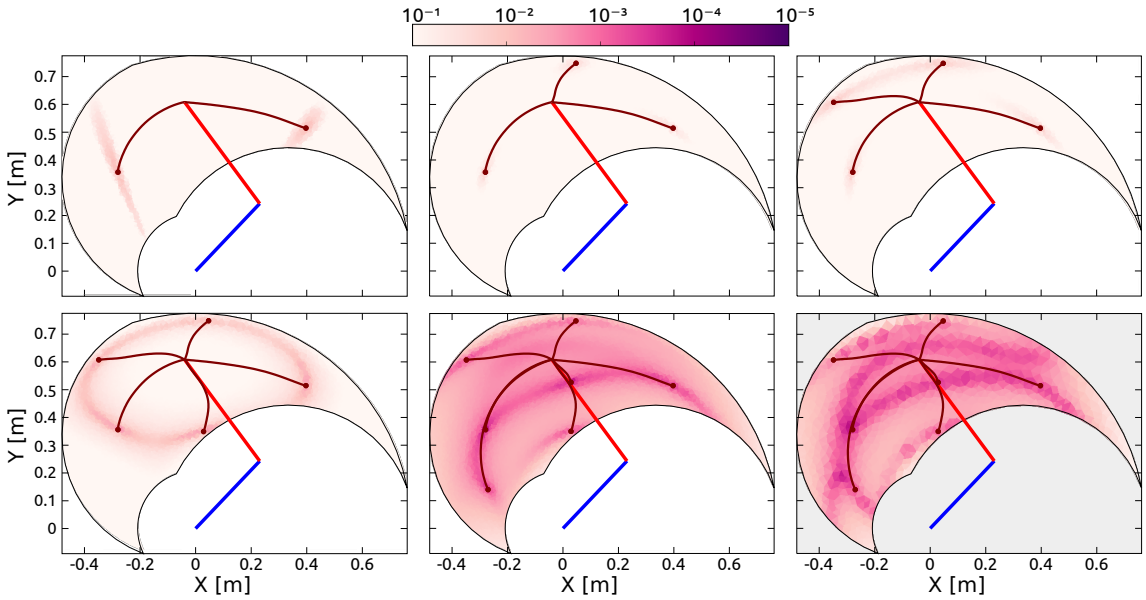

Figure D.2: Selection of proto-tasks based on projection error for point-to-point tasks. Each panel shows the kinematic chain in its initial posture (straight segments), and the distribution of the projection error over the end-effector space (colored region). The color of each point indicates the projection error produced to reach a target in that position. The bottom right panel shows the distribution of the forward dynamics error of the end-effector using 7 proto-tasks (7 synergies).

Figure D.3 shows the trend of the average projection error (across the targets distributed in

the workspace) as a function of the number of proto-tasks. Depending on the precision required, more or less proto-tasks can be used. Here we employ 7 proto-tasks to obtain an average projection error $< 10^{-2}$. This means that the actuations to solve any point-to-point task (starting at $\boldsymbol{q}_c$) can be approximated by combining only 7 synergies. The average forward dynamics error using 7 synergies amounts to $\approx 10^{-2}$. These results show that a set of "good" synergies can drastically reduce the dimensionality of the controller, while maintaining satisfactory performance. Note that the controller has to "choose" the values of two joint-torques at each time-step, thus its dimensionality is much higher than the number of DoF of the system (in fact it is infinite dimensional if we consider actuations as continuous vector-valued functions of time). Hence, 7 synergies contribute a dimensionality reduction even if the system has 2 DoF [Alessandro et al., 2013]. It is important to stress that, due to the nonlinearities of the dynamical system, the projection error serves only as an heuristic estimate of the actual error made when the task is executed; the latter is directly quantified by the forward dynamics error.

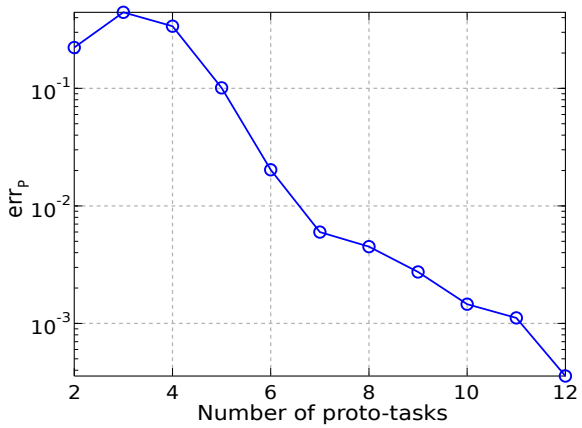

Figure D.3: Average projection error (across targets distributed in the workspace) as a function of the number of synergies for point-to-point tasks.

To further demonstrate that the reduction phase is not trivial, we compare the errors resulting from the set of 7 synthesized synergies, with the errors corresponding to 100 random subsets of size 7 drawn from the exploration signals. The testing point-to-point tasks are identified by the 13 targets depicted in Fig. D.1. Figure D.4 shows that the errors of the random subsets (box-plots) are always orders of magnitude higher than the errors of the synergies resulting from the reduction phase (filled circles). The 7 reduced DRs lead to an alternant matrix with rank equal to 3, therefore any point-to-point constrain-vector of this class can be interpolated exactly. As a result, in contrast to the case of random DRs, the obtained interpolation error is negligible for all the testing tasks ($err_I \simeq 10^{-15} \sim 0$). In terms of projection and forward dynamics error, the reduced synergies perform about 2–3 orders of magnitude better than any random subset. Additionally, they lead to high task performance (forward dynamics errors in the range $[10^{-3}, 10^{-2}]$), yet greatly reducing the dimensionality of the controller.

D.3.2 Reversal tasks

A reversal task consists in reaching a desired target and coming back to the initial state. The tasks considered in this subsection are characterized by zero velocity in all the point constraint, i.e. $\dot{\boldsymbol{q}}(0) = \dot{\boldsymbol{q}}(t_v) = \dot{\boldsymbol{q}}(T) = 0$, and by the initial (and final) posture placed in the center of the op-

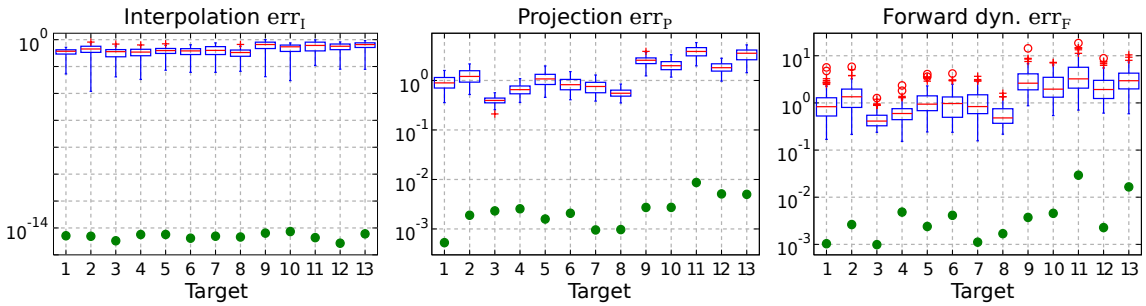

Figure D.4: Evaluation of the reduction phase for the testing point-to-point tasks. Comparison between the synthesized synergies (filled circles) and subsets randomly selected from the exploration-actuations (box-plots).

erational space, i.e. $\boldsymbol{q}(0) = \boldsymbol{q}(T) = \boldsymbol{q}_c$ (red cross in Fig. D.1). Thus, the only free task-parameters are the joint-coordinates of the intermediate target (2 parameters). In other words, the agent is required to reach a certain location with zero velocity (i.e. the via-point), and return to its initial posture. These reversal tasks have relevance as they resemble the motion performed for carrying objects to and from the agent, e.g. reaching for food and bringing it to the mouth, or picking up a salient object and moving it closer for examination.

After the reduction phase, the linear system of equations (D.5) becomes:

$$\begin{pmatrix} \boldsymbol{q}_c & \dots & \boldsymbol{q}_c \\ \boldsymbol{\theta}_1(t_v) & \dots & \boldsymbol{\theta}_{N_\theta}(t_v) \\ \boldsymbol{q}_c & \dots & \boldsymbol{q}_c \\ 0 & \dots & 0 \\ 0 & \dots & 0 \\ 0 & \dots & 0 \end{pmatrix} \boldsymbol{a} = \begin{pmatrix} \boldsymbol{q}_c \\ \boldsymbol{q}_v \\ \boldsymbol{q}_c \\ 0 \\ 0 \\ 0 \end{pmatrix}. \tag{D.13}$$

where $\boldsymbol{\theta}$ are the reduced DRs, and $\boldsymbol{q}_v$ is the intermediate desired position (that uniquely defines the specific task instance). For the same rationale discussed in Sec. D.3.1, to guarantee the existence of an exact kinematic solution for any reversal task belonging to this class, the rank of the alternant matrix, and therefore the minimal number of DRs, should be equal to 3. However, the number of synergies required to obtain satisfactory values of projection and forward dynamics errors might be higher.

Like in the case of point-to-point movements, proto-tasks belong to same class of the desired tasks (i.e. reversal, $\boldsymbol{q}_0 = \boldsymbol{q}_T = \boldsymbol{q}_c$), and they are added incrementally. Since the position of the desired intermediate target is the only unknown, the newly added proto-task is identified by placing the via-point in the region of the operational space with the highest projection error. As shown in Fig. D.5, this strategy aims at decreasing the projection error over the entire configuration space, such that eventually the actuations necessary to solve any reversal task can be approximated satisfactorily. In particular, 8 synergies are enough to obtain an average projection error $< 10^{-2}$ (see Fig. D.6, blue line), and an average forward dynamics error of $\approx 10^{-2}$.

The reduced synergies are compared to 100 subsets of 8 actuations, randomly chosen from the exploration motor signals. The testing reversal tasks are identified by the 13 intermediate targets depicted in Fig. D.1. The results shown in Fig. D.7 provide additional evidence that the reduction phase identify effective synergies: the mean errors of the random subsets (boxplot) are orders of magnitude higher than those corresponding to the reduced synergies (filled circles), and the forward dynamics errors lie in the range $[10^{-3}, 10^{-2}]$, meaning that the 13 approximated actuations lead to good task performance.

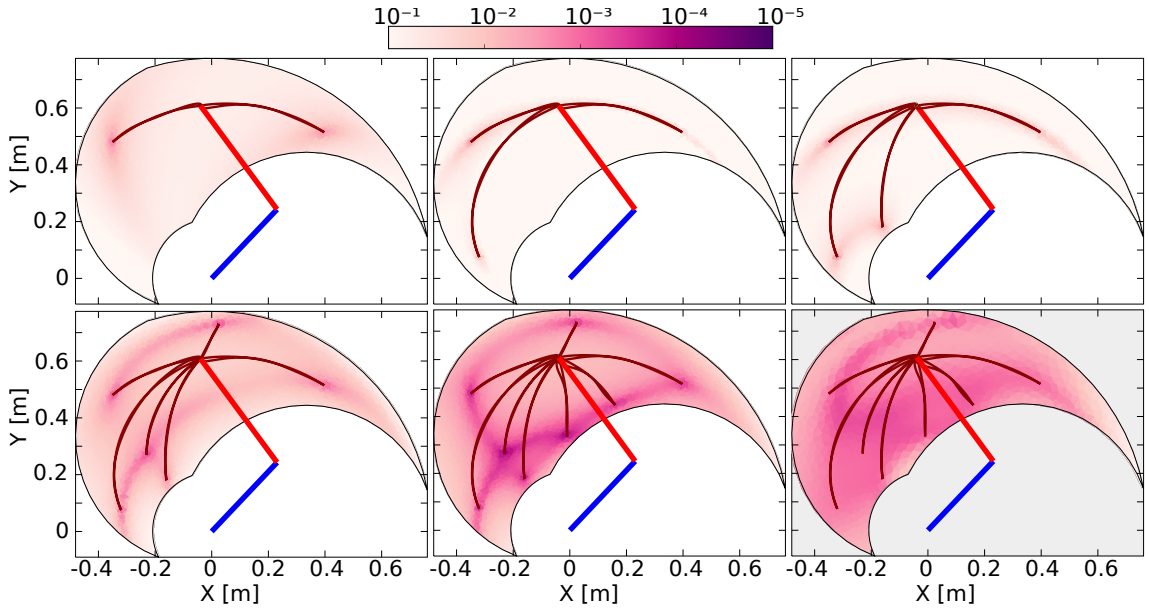

Figure D.5: Selection of proto-tasks based on projection error for reversal tasks. Each panel shows the kinematic chain in its initial posture (straight segments), and the distribution of the projection error over the end-effector space (colored region). The color of each point indicates the projection error produced to reach that position and to go back to the initial posture. The bottom right panel shows the distribution of the forward dynamics error of the end-effector using 8 proto-tasks (8 synergies).

Concatenation of point-to-point actuations

Reversal tasks are composed by two kinematically different phases: from the initial point to the target (center-out), and from the target back to the initial position (out-center). Therefore, it should be possible to generate suitable control signals by concatenating the actuations associated to the individual point-to-point tasks. Each of these subtasks are solved by means of DRD. In the following we explore this possibility, and we compare the obtained solutions to the results of applying DRD to the entire reversal tasks.

In order to produce a meaningful solution from the concatenation, at the beginning of the out-center movement all the system variables (positions, velocities and accelerations) should match the values obtained at the end of the center-out phase. This condition can be enforced by imposing additional constraints on the acceleration of the joints. Here we prescribe zero velocity and acceleration at the end of the center-out tasks, at the beginning of the out-center, as well as at the target-point of the reversal tasks. Clearly, any other value would represent an equally suitable choice. Additionally, we assign zero velocity at the beginning and at the end of the reversal movements. Formally, the tasks are defined as follows:

Center-out

$$\begin{aligned} \boldsymbol{q}(0) &= \boldsymbol{q}_c, \quad & \dot{\boldsymbol{q}}(0) &= 0, \\ \boldsymbol{q}(t_v) &= \boldsymbol{q}_v, \quad & \dot{\boldsymbol{q}}(t_v) &= 0, \quad \ddot{\boldsymbol{q}}(t_v) = 0 \end{aligned} \tag{D.14}$$

Out-center

$$\begin{aligned} \boldsymbol{q}(t_v) &= \boldsymbol{q}_v, \quad & \dot{\boldsymbol{q}}(t_v) &= 0, \quad \ddot{\boldsymbol{q}}(t_v) = 0, \\ \boldsymbol{q}(T) &= \boldsymbol{q}_c, \quad & \dot{\boldsymbol{q}}(T) &= 0 \end{aligned} \tag{D.15}$$

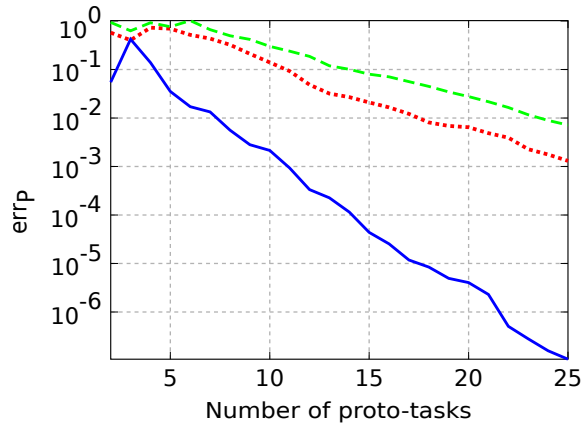

Figure D.6: Averaged projection error as a function of the number of proto-tasks for increasingly general classes of via-point tasks. The least general tasks are reversal motions (blue continuous line), characterized by two free task-parameters (i.e. configuration of the intermediate target). An increase in generality consists in fixing only the initial posture, while intermediate target and final position represents free task-parameters (red dotted line). Finally the most general class (green dashed line) does not fix any posture (6 free task-parameters). The number of synergies required to achieve the same error increases with the generality of the class of tasks.

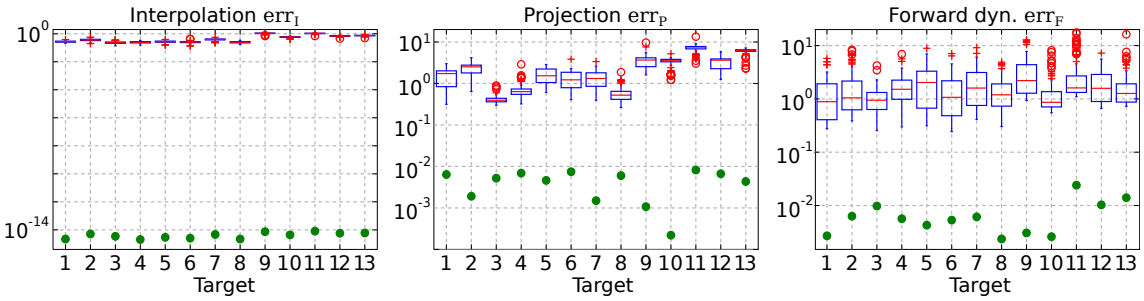

Figure D.7: Evaluation of the reduction phase for the testing reversal tasks. Comparison between the synthesized synergies (filled circles) and subsets randomly selected from the exploration-actuations (boxplots).

Reversal

$$\begin{aligned} \boldsymbol{q}(0) &= \boldsymbol{q}_c, \quad & \dot{\boldsymbol{q}}(0) &= 0, \\ \boldsymbol{q}(t_v) &= \boldsymbol{q}_v, \quad & \dot{\boldsymbol{q}}(t_v) &= 0, \quad & \ddot{\boldsymbol{q}}(t_v) &= 0, \\ \boldsymbol{q}(T) &= \boldsymbol{q}_c, \quad & \dot{\boldsymbol{q}}(T) &= 0. \end{aligned} \tag{D.16}$$

The synthesis of the synergies for each class of tasks follows the same procedure described in Sec. D.2.2 and exemplified in Fig. D.5. We choose the number of synergies for the point-to-point (6 synergies) and for the reversal tasks (7 synergies) in order to achieve comparable average projection errors across the 13 testing targets (0.011 for center-out, 0.014 for out-center, 0.016 for reversal tasks as computed by DRD, and 0.013 for the concatenation of DRD point-to-point solutions). The individual projection errors are depicted in Fig. D.8A. For the targets 1-8,10 and 13, the actuations provided by the concatenation of point-to-point DRD solutions are better suited than those computed by applying DRD to the entire tasks. However, the forward dynamics errors do not always follow the same relation (Fig. D.8B). As an example, for the targets 2-7, the entire DRD solution performs better than the concatenation of the point-to-point actuations. The relation is however kept for targets 1, 8, 10, 11 and 12. Although these results might seem counter intuitive, they can

be explained by analyzing the forward dynamics errors of the single center-out and the out-center tasks. It can be noticed that when the error of the entire DRD reversal solution is lower than any of the point-to-point errors, the former solution is preferable to the concatenation-based trajectory (targets 2-7, 9, 11-13). On the other hand, when the forward errors of both point-to-point tasks are lower than the error of the entire reversal solution, concatenation seems to be a better strategy (targets 1, 8, 10). In most of the cases, the forward error of the concatenation err_{Fcoc} is almost close to the "sum" of the single point-to-point errors, err_{Fco} and err_{Foc}. In order to conform the definition of the error (see Eq. (D.11)), this sum is computed as $err_{Fcoc} = \sqrt{err_{Fco}^2 + err_{Foc}^2}$.

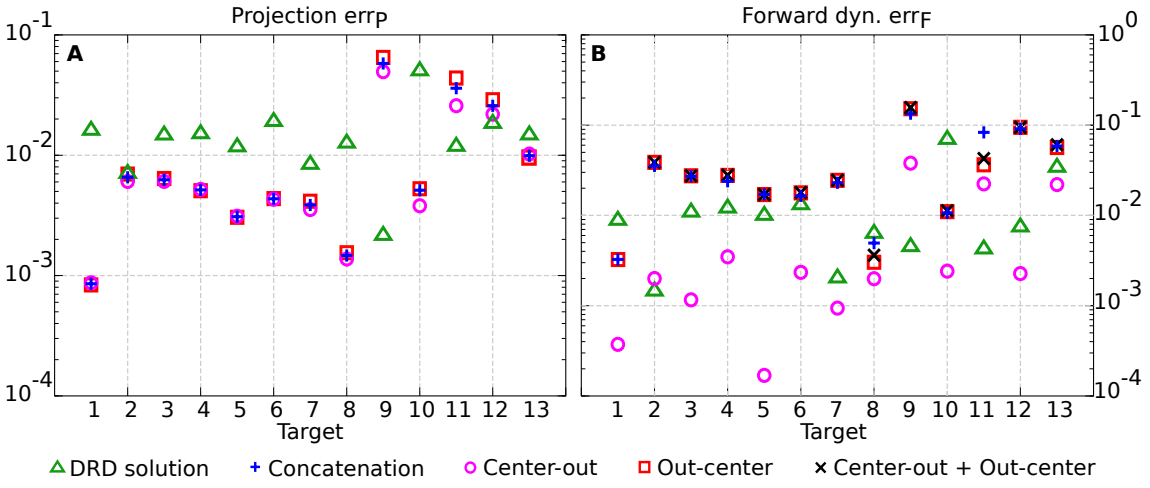

Figure D.8: Comparison between the DRD solutions to the entire testing reversal tasks (green triangles) and the concatenation of DRD point-to-point solutions (blue crosses) in terms of projection (**A**) and forward dynamics errors (**B**). The plot also indicates the performance of the individual center-out (magenta circles) and out-center tasks (red squares), and the sum of their corresponding errors (black xs).

The relation between the forward error of the concatenation and the forward errors of the individual point-to-point DRD solutions is, in reality, far from trivial. The scenario is depicted schematically in Fig. D.9, where the red line represents a possible solution to a reversal task. Trivially, in the first part of the movement the trajectory obtained from the concatenation strategy (dashed line) corresponds to the DRD solution to the center-out task (dashed green). The actuation corresponding to the out-center task is then applied. Since the first submotion is affected by errors (i.e. forward error of the center-out task, $e_{co}(t_{vp})$), the system does not lie in the initial conditions associated to the out-center task (orange line). This initial error propagates over the course of the movement according to the dynamical properties of the system (dashed blue line), and affects the state at the end of the motion. The resultant final error $e_{coc}(T)$ is in general different from the forward error of the DRD out-center solution $e_{oc}(T)$. As a result, the overall forward error of the concatenation can be higher (e.g. target 11) or lower (e.g. target 9) than the "sum" of the point-to-point errors. In theory, due to this effect, applying DRD to the entire task could lead to better performance than concatenating DRD point-to-point actuations even if the error of the entire solution is higher than both the errors of center-out and out-center tasks. Such a scenario is however not very likely if the error associated to center-out task is very low (as in our examples).

In general terms, none of the two methods seems to be better than the other, however the following conclusions can be drawn. The concatenation-based solution accumulates the errors of the single movement phases. Furthermore, this strategy requires additional conditions on the

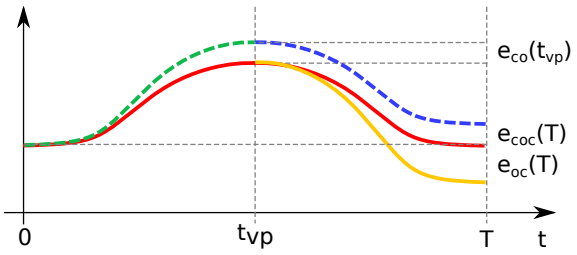

Figure D.9: Schematic representation of the concatenation of DRD point-to-point solutions. The red line represents a possible exact solution to a reversal task. The first part of the concatenation-based trajectory (until the time of the via-point t_{vp}) corresponds to the individual center-out solution (dashed green line), which is affected by the forward dynamics error $e_{co}(t_{vp})$. This error propagates over the course of the second submovement (dashed blue line), leading to the final error $e_{coc}(T)$. The latter is in general different from the final forward dynamics error $e_{oc}(T)$ of the individual out-center movement (orange continuous line).

	Reversal		Via-point reaching	
	Error ($\times 10^{-2}$)	N_ϕ	Error ($\times 10^{-2}$)	N_ϕ
1st phase	1.1	6	1.2	6
2nd phase	1.4	6	1.4	6
Concatenation	1.3	12	1.5	12
DRD	1.6	7	1.3	17

Table D.1: Mean projection errors obtained for the testing instances of reversal and via-point reaching tasks using N_ϕ synergies. See text for more details.

kinematic variables to allow the compatibility between the two point-to-point trajectories. On the other hand, the application of DRD to the entire reversal task requires the definition of adequate proto-tasks. If these details are not available (the class of desired tasks is too general, see Sec. D.3.4), the concatenation method might be a viable alternative. Table D.1, summarizes the results from this section and the next one.

D.3.3 Via-point reaching

In this section we show the performance of DRD to solve via-point reaching tasks. These motions require the agent to reach a desired final position, passing through a given via-point. Specifically, in this section we set the via-point to be the center of the operational space $\boldsymbol{q}_c$ (red cross in Fig. D.1, see SM), and the initial, intermediate, and final velocities to be equal to zero. The joint-coordinates of initial and final postures, $\boldsymbol{q}_0$ and $\boldsymbol{q}_T$, represent the free task-parameters as they can be chosen arbitrarily to instantiate specific tasks (4 parameters). Finally, we prescribe acceleration equal to zero at the via-point. As described in the previous section, this allows to generate meaningful task solutions by concatenating the actuations corresponding to the two phases of the movement. Formally, the desired class of tasks can be described as follows:

$$\begin{aligned} &\boldsymbol{q}(0) = \boldsymbol{q}_0, && \dot{\boldsymbol{q}}(0) = 0, && \\ &\boldsymbol{q}(t_v) = \boldsymbol{q}_c, && \dot{\boldsymbol{q}}(t_v) = 0, && \ddot{\boldsymbol{q}}(t_v) = 0 \\ &\boldsymbol{q}(T) = \boldsymbol{q}_T, && \dot{\boldsymbol{q}}(T) = 0. && \end{aligned} \tag{D.17}$$

The synergies are synthesized as described in Sec. D.2.2. Since the parameters $\boldsymbol{q}_0$ and $\boldsymbol{q}_T$ can be chosen arbitrarily, the parameter space is four-dimensional. This condition does not affect the general procedure; i.e. proto-tasks are sequentially added in the point of the space characterized

by the highest projection error. Figure D.10 depicts the averaged projection error (across the targets distributed in the parameter space) as a function of the number of synergies.

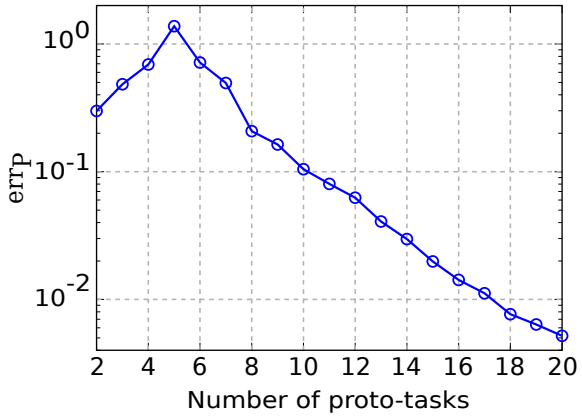

Figure D.10: Average projection error (across initial and final positions distributed in the workspace) as a function of the number of synergies for via-point reaching tasks.

The synthesized synergies are tested on 18 tasks, the initial and final positions of which are drawn from the targets in Fig. D.1. Figure D.11 reports the errors obtained by using 17 reduced synergies (upward green triangles), and the performance of 100 sets of size 17 drawn from the exploration signals (box-plots). The interpolation errors corresponding to the synthesized synergies are lower than, but comparable to, the mean errors of the random sets ($\approx 10^{-15}$). This is not surprising since 17 random signals are likely to produce an alternant matrix with full row-rank, that can therefore interpolate any constraint. However, it is interesting to notice that the information added by the reduction phase leads to lower interpolation errors. In relation to projection and forward dynamics errors, the synthesized synergies perform about 2 orders of magnitude better than the random signals, providing further evidence that the reduction phase is a valuable procedure.

Finally, we compare the use of DRD for solving the entire tasks, to the concatenation of individual DRD point-to-point solutions. In the same vein of the reversal tasks, the considered via-point reaching movements can be composed of an initial out-center motion (from $\boldsymbol{q}_0$ to $\boldsymbol{q}_c$), followed by a center-out movement (from $\boldsymbol{q}_c$ to $\boldsymbol{q}_T$). The number of synergies is chosen to obtain a comparable mean projection error across the 18 testing tasks. We used 6 synergies for both out-center and center-out tasks, and 17 synergies for via-point reaching, leading to the following average errors: 0.012 for center-out, 0.014 for out-center, 0.013 for via-point reaching as solved by DRD, and 0.015 for the concatenation. Table D.1 summarizes these results.

The yellow downward triangles in Fig. D.11 indicate the performance of the concatenation strategy. In line with the rationale in Sec. D.3.2, this method accumulates the errors of the sequential point-to-point solutions, resulting in higher values of forward dynamics and interpolation error. From the point of view of dimensionality reduction, the concatenation strategy might be convenient as the the number of synergies is reduced from 17 to 6 for each movement phase (12 in total) with a small loss of performance (see Table D.1).

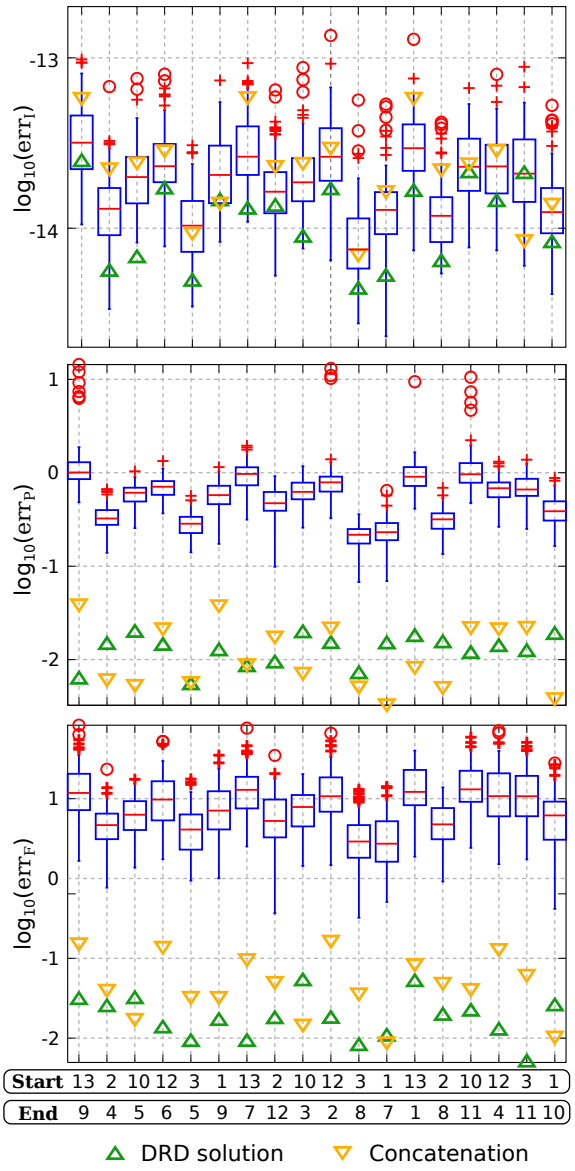

Figure D.11: Evaluation of the reduction phase for 18 testing via-point reaching tasks; "Start" and "End" indicate the indexes of the initial and final points respectively (see Fig. D.1). The plots also present the errors obtained by concatenating individual out-center and center-out DRD solutions (orange downward triangles).

D.3.4 Task generality and number of synergies

The obtained results show that via-point reaching tasks require a higher number of synergies than reversal tasks. To achieve a mean projection $< 10^{-2}$, via-point reaching needs at least 17 synergies, and the reversal tasks at least 7. In this section, we provide a plausible interpretation of this difference, accompanied by additional results to support our rationale.

For the sake of clarity let us first define the *generality* of a class of tasks as the number of its free task-parameters. As discussed above, the desired class of tasks can be defined by imposing certain values to the state variables and their derivatives. For example, the reversal tasks presented in Sec. D.3.2 impose zero velocities, and additionally fix initial and final postures to a specific point of the configuration space, $\boldsymbol{q}_c$. Although they are essentially via-point tasks, each instance is defined only by the position of the desired intermediate target. Thus the generality of this class of task is 2 as the target is specified by two values (i.e. its joint-coordinates). Via-point reaching tasks, as defined in Sec. D.3.3, fix the position of the via-point to $\boldsymbol{q}_c$, and impose initial, intermediate and final velocities equal to zero; each task instance is therefore defined by the desired initial and final postures, thus the generality of this class of tasks is 4.

The lower the generality of the desired class of tasks, the lower the variability of the control signals. If the task is very generic, the set of required actuations may result diverse. This observation is exemplified in Fig. D.12, which shows the actuations associated to the reversal (panel **A**) and the via-point reaching testing tasks (panel **B**). As expected, the actuations in panel **A** are more regular than those in panel **B**. Quantitatively, the mean correlations between the (absolute values of the) control signals of the shoulder are 0.97 and 0.67 for reversal and via-point reaching respectively, and the correlations between the actuations of the elbow are 0.70 and 0.53. The regularities that can be observed in the first phase of the via-point reaching movements are simply due to the fact that groups of testing tasks are characterized by the same initial position (see the abscissas label of Fig. D.11). If this was not the case, the corresponding mean correlation values would be even lower.

The number of required synergies is strictly related to the previous observations. Since the proto-tasks belong to the desired class of tasks (see Sec. D.2.2), the reduced synergies are samples of the desired actuations. If these control signals are characterized by a low degree of variability (e.g. reversal case), their essential features can be captured by a handful of samples. Otherwise, a higher number of synergies is required.

To further test the validity of our rationale, we consider three increasingly more general classes of tasks. The first class (a) consists of the reversal tasks described in Sec. D.3.2, in which the only free task-parameters are the joint-coordinates of the via-point. The second one (b) fixes only the initial position, while via-point and final posture can be chosen arbitrarily. Finally, the third class of tasks (c) does not impose any fixed posture. Figure D.6 shows the trends of the average projection errors as a function of the number of synergies for the three cases (blue continuous, red dotted and green dashed lines respectively). As expected, the number of synergies that are needed to obtain a certain degree of performance increases with the generality of the class of tasks. The projection error is meaningful only if the kinematic solution fulfills the task constraints, thus the trends in Fig. D.6 should be considered starting from the minimum number of proto-tasks that guarantees this condition (i.e. 3, 5 and 6 synergies). The oscillations that can be observed for a smaller number of synergies can therefore be ignored as they are not representative of task performance in any way.

The effectiveness of the reduction phase is strictly related to the generality of the desired class of tasks. If this class is maximally generic (i.e. no task constraints impose invariant values across the tasks), the control signals will not be characterized by any particular feature related to the tasks. Thus, the reduction phase becomes less useful, and the synthesized synergies will embed regularities that are solely due to the dynamics of the system. Additionally, in order to obtain good performance in all the desired tasks, a large number of synergies will be required. As a

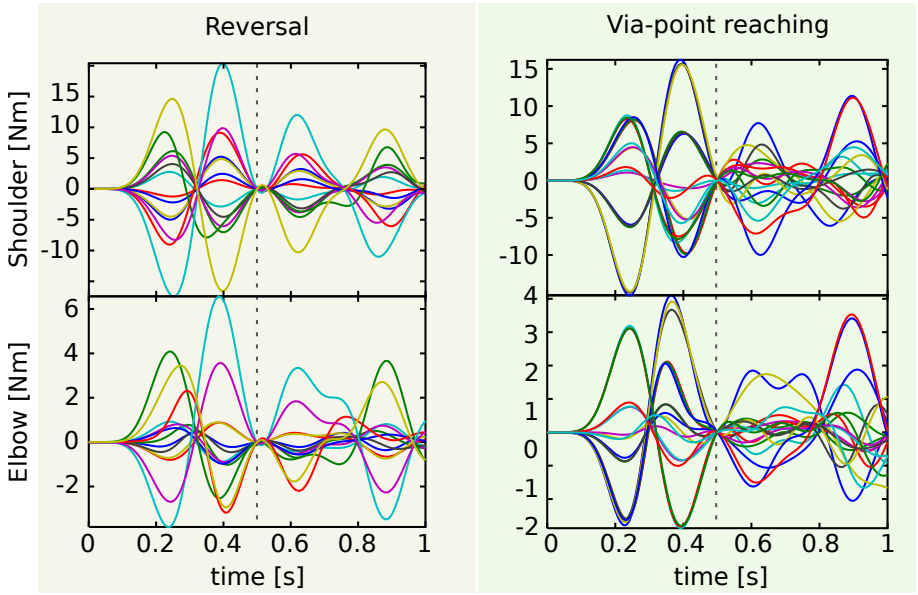

Figure D.12: Actuations corresponding to the testing reversal and via-point reaching tasks. Since the latter class of tasks is more general, the corresponding control signals are less correlated than the reversal ones. This is particularly visible in the second phase of the movement (after the dashed vertical line that mark the time of the via-point). See text for more details and for the values of the correlation.

direct consequence, the performance of the synthesized synergies will approach the performance of generic actuations. To illustrate this concept we compare the synergies synthesized for each of the previous classes of tasks with random sets of exploration actuations. The latter control signals are not generated through the process of reduction, and therefore they are not expected to embed any information about the tasks to be solved. We choose the minimum number of synergies that guarantees a mean projection error $< 10^{-2}$, i.e. 8, 18, 24 for classes (a), (b) and (c) respectively (see Fig. D.6). Then we use these groups of synergies to solve the 13 reversal testing tasks. Figure D.13 depicts the difference between the mean projection errors obtained by using the random sets e_{ri}, and the projection errors corresponding to the three sets of synergies e_{si} (i.e. $I_i = e_{ri} - e_{si}$ for each class i). As expected, this difference reduces for increasingly more general tasks.

D.4 Discussion

We performed an analysis of the muscle synergy hypothesis from a computational perspective; i.e. the control of a planar kinematic chain through linear combinations of a limited set of torque profiles (motor synergies). We propose the DRD [Alessandro et al., 2012; Carbajal, 2012] to solve point-to-point as well as via-point tasks, and to synthesize the corresponding synergies. DRD generates a kinematic solution to a task by combining the dynamic responses of the synergies, and it employs the inverse dynamics to compute the corresponding actuation. This control signal is finally approximated by a linear combination of synergies. The problem of finding a kinematic solution is therefore reduced to a simple interpolation, and the quality of the approximation (and ultimately the task performance) depends on the set of synergies. The synergies synthesized by means of the reduction phase over-perform hundreds of arbitrary choices of basic controllers taken from the exploration motor signals. This result, that is consistent across all the error mea-

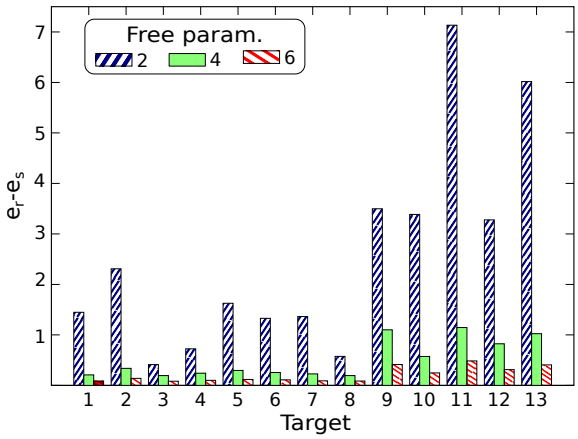

Figure D.13: Difference between the mean projection errors obtained by using the random sets, e_{ri}, and the projection errors corresponding to three sets of synergies, e_{si} (i.e. $I_i = e_{ri} - e_{si}$ for each set i) for solving the reversal testing tasks. The sets of synergies correspond to increasingly more general classes of tasks; i.e two, four and six free task-parameters (right diagonal blue, green and left diagonal red bars respectively). This difference reduces for increasingly more general tasks, showing that the effectiveness of the reduction phase decreases as the actuations become less regular.

sures, suggests that synergies might represent solutions to prototypical task instances. The number of required synergies to achieve a given performance depends on the generality of the desired class of tasks (i.e. number of free task-parameters); general tasks (e.g. via-point reaching) require more synergies than highly specific ones (e.g. reversal). Thus, synergies are strictly tailored to the tasks to be solved. Since via-point tasks are constituted by two distinguished kinematic phases, they could be solved by concatenating the actuations associated to the different submovements; such actuations are in turn generated by linearly combining appropriate point-to-point synergies. This strategy is related to the notion of kinematic primitives [Flash et al., 1992], and it represents a control scheme that, for the first time, integrates this form of modularity together with muscle synergies. The obtained results show that the concatenation method accumulates the errors of the individual submotions, and it requires additional conditions to smoothly join the kinematic trajectories. On the other hand, the application of DRD to the entire via-point task requires the definition of well specified proto-tasks. If the class of task is too general, and therefore it requires a high number of synergies, concatenation could be a viable strategy (see Table D.1).

The goal of this work was not to provide a model of the formation and the development of muscle synergies, nor at the current stage we claim that the reduced synergies fit human data. Rather our goal was to analyze the muscle synergy hypothesis from a computational point of view. Although our approach involves many assumptions and simplifications, we believe that it conceptually highlights important aspects of this form of modularity, aspects that are not always taken into account in experimental studies. Certainly, our work serves as a proof of concept for the idea of generating useful motor signals from the linear combination of a limited set of control primitives.

A simplification that is worth discussing is the usage of a kinematic chain rather than a muscle-driven skeletal model. This implies the definition of control signals (and therefore synergies) in the space of joint torques, and not in muscle activation space. In a musculoskeletal system, the non-linear relation between torques and kinematic variables is complemented by the additional non-linear dynamics that translates muscle activations into joint torques. The total mapping between muscle activations and kinematic variables is non-trivial. The chain of the two non-linear relations might either compensate each other, resulting in overall milder non-linearities, or form

an even stronger one. In any case, from the conceptual point of view, the essence of the problem does not change, i.e. the possibility of controlling the output variables of a non-linear dynamical system (i.e. kinematic chain or musculoskeletal model) by means of a linear input strategy (i.e. linear combination of torque or muscle synergies). We intend to evaluate DRD in more biologically plausible systems in future developments of our work.

D.4.1 Computational insights on the muscle synergy hypothesis

Due to the nonlinearity of the body dynamics, small actuation errors might lead to unsatisfactory task performance. This justifies the need to distinguish between projection and forward dynamics error; while the former can be considered only as an heuristic measure, the latter explicitly quantifies the quality of the synergy-based controller. Many studies in experimental neuroscience analyze the validity of the muscle synergy hypothesis solely in terms of a measure that is equivalent to our projection error, i.e. the accuracy in approximating recorded EMG signals [Cheung et al., 2009; d'Avella and Bizzi, 2005; d'Avella et al., 2003; Torres-Oviedo and Ting, 2007, 2010]. We believe that the introduction of complementary task-based measures could shed new lights on the hypothetical modularity of the CNS [Alessandro et al., 2013; Delis et al., 2013].

In this vein, some researchers introduced the concept of functional synergies, i.e. the components of an extended dataset that includes muscle activations as well as measurements of task variables (e.g. joint angles, end-limb force) [Chvatal et al., 2011; Torres-Oviedo et al., 2006]. As a result, each component consists of two elements: a pattern of muscle contractions, and the corresponding evolution of the task variables. Such an approach is not too different from the idea behind DRD: synergies are associated to their DRs (i.e. biomechanical functionalities), which are linearly combined to obtain the kinematic solution of the task. However, the identification of functional synergies by means of non-negative matrix factorization (NMF), implies that muscle synergies and their biomechanical functionalities are scaled by the same coefficients. This contrasts with our theoretical results, which show a nonlinear relationship (the mapping $\mathcal{F}$, see Eq.(D.8)) between the mixing weights of the synergies and those of the DRs. Ideally, one should go beyond the use of NMF, and develop novel techniques that do not impose a linear mapping between the two sets of coefficients.

The mathematical formulation of DRD, and in particular the system of linear equations (D.5), allows the following observations. First, it shows a clear relation between the minimum number of synergies and the difficulty of the task. To guarantee the existence of a kinematic solution, the alternant matrix should be full-row rank. In other words, the minimum number of proto-tasks, and therefore of synergies, should correspond to the dimensionality of the task-constraint vector. For a two-DoF kinematic chain, general via-point tasks consist of three position and three velocity constraints (each of them is two-dimensional); thus, at least twelve DRs are required to be able to solve any task in kinematic space. Second, a highly specified class of tasks reduces the minimum number of required synergies. For example, point-to-point and reversal tasks, that are characterized by two free task-parameters (i.e. location of the target), require at least 3 synergies (instead of 8 and 12); for via-point reaching this number increases to 5 (see Sec. D.3). It is important to stress that these considerations represent the necessary conditions to guarantee the existence of a kinematic solution for any task that belongs to the desired class. If only specific instances of such tasks are relevant (e.g. reaching some given points of the phase space), the minimum number of synergies can be reduced even further. Having this in mind, it is not surprising that a dataset of recorded biomechanical signals can be approximated by a number of synergies that is lower than what is suggested by our framework. Such datasets are indeed recorded during specific and constrained task instances. Finally, in our method, the minimum number of synergies is computed solely based on kinematic considerations; since the dynamical system is non-linear, this number does not guarantee low values of projection and forward dynamics error. In fact, as shown in

Sec. D.3, the number of synergies that is required to obtain satisfactory performance is certainly higher than the theoretical kinematic-based estimation. This number still follows the principle that more general tasks require a higher number of synergies (see Fig. D.6 and Sec. D.3.4).

An important aspect of our method is that the synergies $\mathbf{\Phi}$ are related to the DRs $\mathbf{\Theta}$ through the dynamics of the system. As a result, since the DRs are feasible kinematic solutions to the proto-tasks, the obtained synergies can always be realized as actuations. The same cannot be said, in general, for synergies identified from numerical analyses of biomechanical data. Though some studies have verified the feasibility of the extracted synergies as actuations [Allen and Neptune, 2012; McGowan et al., 2010; Neptune et al., 2009], biomechanical constraints are not explicitly included in the extraction algorithms. Additionally, Eq. (D.2) provides an automatic way to cope with smooth variations of the agent morphology. That is, both the synergies and their dynamic responses evolve together with the body. In line with Nori [2005] and Alessandro and Nori [2012], these observations highlight the importance of the body in the hypothetical modularization of the CNS.

The concatenation of point-to-point control signals to solve via-point tasks is based on the observation that movements can be composed by sequences of kinematic strokes, or submovements. There is still no agreement on whether these motion chunks reflect a segmented form of control, however it has been hypothesized that they could serve as the building blocks to internally represent and plan complex motions (e.g. handwriting and drawing trajectories [Morasso and Mussa-Ivaldi, 1982]). The relation between this form of planning modularity and muscle synergies is still under debate. Possibly, as implemented in our formulation, each kinematic stroke translates into a combination of time-varying synergies, and therefore the final movement plan corresponds to a sequence of mixing patterns. This strategy would be in line with the hypothesis of an intermittent controller that sequentially initiates discrete movement primitives [Fishbach et al., 2005; Karniel, 2013; Loram et al., 2010; Squeri et al., 2010]. Submovements might be combined in time succession [Meyer et al., 1988; Soechting and Terzuolo, 1987], or based on the vectorial summation of overlapping preplanned trajectories [Flash and Henis, 1991; Henis and Flash, 1995; Novak et al., 2003; Pasalar et al., 2005; Roitman et al., 2004]. In this manuscript we exemplify the case in which the kinematic submovements are sequenced in time. Interestingly enough, d'Avella et al. [2011] showed that the synergies underlying point-to-point kinematic trajectories could also account for more complex trajectories involved in reaching a jumping target, by modulation and delayed superposition. The analysis of this approach within our framework is non-trivial, and it is therefore left for future work. This development will probably involve trajectory-modification tasks rather than via-point constraints. Finally, it is important to notice that the kinematic solution to a via-point task appears to be composed of different movement-chunks even when it is obtained from a single composition of highly specified synergies. This observation supports the idea that strokes could just emerge as a result of the trajectory optimization [Dagmar and Schaal, 1999] or even be data analysis artifacts.

Lastly, we would like to speculate on a possible developmental interpretation of the method we propose to synthesize synergies. Initially, the agent explores its sensory-motor system employing a variety of actuations. Later, it attempts to solve the first tasks (proto-tasks), perhaps obtaining weak performance as the exploration phase may not have produced enough responses yet (see the box-plots in Fig. D.4, D.7 and D.11). If the agent finds an acceptable solution to a proto-task, such a solution is used to generate a new synergy (populating the set $\mathbf{\Phi}$), otherwise it continues with the exploration. The failure to solve important tasks for its survival, could motivate the agent to include additional proto-tasks; Fig. D.5 illustrates this mechanism. The development of the synergy-set incrementally improves the overall abilities of the agent. Alternatively, existing proto-tasks could be modified. It has to be clear that we are not arguing in any way that this procedure resembles the mechanisms involved in the motor development of biological organisms. It is however interesting that our procedure allows the autonomous generation of new

synergies, and the possible adaptation of the existing ones to cope with the changes in the body dynamics (see Eq. (D.2)). These features are in line with the recent findings by Dominici et al. [2011]. An alternative strategy for synergy development (not implemented in this paper) might be the concatenation of movement chunks. If the agent has already developed the synergies to solve point-to-point tasks, via-point proto-tasks could be solved by the concatenation of point-to-point actuations. As shown in Fig. D.7 and D.11 the results might not be as good as if the solution were computed ad-hoc (i.e. for the entire via-point proto-tasks). However, inspired by Sosnik et al. [2004] and Rohrer et al. [2004], one could imagine that such solutions might improve with practice, eventually leading to appropriate via-point modules.

D.4.2 Comparison with other computational studies

While many studies try to validate or falsify the hypothesis of muscle synergies, only a few researchers have focused on developing and testing control architectures based on this concept. Some of these works aim at proposing novel techniques for robot control, other intend to analyze the hypothesized modularity from a computational point of view. Our work falls into the second category; in this section we briefly compare it to similar contributions, in particular to those studies that provide a possible interpretation of muscle synergies. The reader is referred to [Alessandro et al., 2013] for a more comprehensive review.

Inspired by the original work by Mussa-Ivaldi [1997], Nori and Frezza [2005] developed a control architecture for non-linear systems based on the idea of spinal force fields [Giszter et al., 1993; Mussa-Ivaldi and Bizzi, 2000; Mussa-Ivaldi et al., 1994; Nori, 2005]. Relying on the technique of feedback linearization, the method yields a set of synergies that is able to generate a complete repertoire of movements (i.e. the system can reach any arbitrary state in an arbitrary amount of time). Thus, the authors interpreted muscle synergies as a basis of the entire control action space. Berniker et al. [2009] defines synergies as the smallest set of input vectors that influences the output of a reduced-order model of the agent, and that minimally restrict the commands useful to solve the desired tasks. Practically, this set is found by optimizing the synergies against a representative dataset of desired sensory-motor signals. Similarly, Todorov and Ghahramani [2003] employ an unsupervised learning procedure to identify muscle synergies from a collection of sensory-motor data, which is obtained by actuating the robot with random signals. Their work proposes that synergies are a constituent part of an inverse model of the sensory-motor system. Another interpretation is given by Marques et al. [2012], who suggest that synergies solely reflect the biomechanical constraints of the agent.

As discussed in Sec. D.3.4, our work suggests that synergies are solutions to well-defined control problems. Similar ideas have already been proposed [Alessandro and Nori, 2012; Chhabra and Jacobs, 2008; Thomas and Barto, 2012; Todorov, 2009]. However, these studies do not investigate which class of problems is best suited for this purpose. In this manuscript we show that these problems (i.e. proto-tasks) may belong to the same class of the desired tasks; this would lead to a compact set of effective synergies. Additionally we show a clear relation between the number of synergies and two characteristics of the task: generality (i.e. number of free task parameters), and difficulty (i.e. number of constraints). Further, we propose a possible integration scheme between kinematic stroke and muscle synergies; to the best of our knowledge no other synthetic study has tested this idea.

D.4.3 The DRD method and its relevance to robotics

In the DRD method, once the task is solved in kinematic space, the corresponding actuation can be computed using the explicit inverse dynamical model of the system (i.e. the differential operator $\mathcal{D}$). It might appear that there is no particular advantage in projecting this solution onto the linear

span of the synergy set. However, the differential operator might be unknown or affected by errors; this is very often the case in robotics, where learning inverse models is still a hot topic of research [Nguyen-Tuong and Peters, 2011]. A synergy-based controller would allow to compute the appropriate actuation by evaluating the mapping $\mathcal{F}$ on the vector $\boldsymbol{a}$, hence obtaining the synergy combinators $\boldsymbol{b}$. Since $\mathcal{F}$ is a mapping between two finite low-dimensional vector spaces, estimating this map may turn out to be easier than estimating the differential operator $\mathcal{D}$. In order to estimate the map $\mathcal{F}$, the input-output data generated during the exploration phase (i.e. $\boldsymbol{\Phi}_0$ and $\boldsymbol{\Theta}_0$) could be used as learning data-set. The obtained relation could be instrumental to estimate a first guess of the synergy set; $\mathcal{F}$ and $\boldsymbol{\Theta}$ could then be iteratively modified until convergence. Further work is required to test these ideas.

The current formulation of the method does not include joint limits explicitly. The interpolated trajectories are valid, i.e. they do not go beyond the limits, due to the lack of intricacy of the boundaries. In higher dimensions, especially when configuration space and end-effector are not mapped one-to-one, this may not be the case anymore. Nevertheless, joint limits can be included by reformulating the interpolation as a constrained minimization problem. Another solution might be the creation of proto-tasks with a tree-topology, relating our method to tree-based path planning algorithms [Shkolnik and Tedrake, 2011] and the concatenation of solutions.

Despite the difficulty of the mathematical problem (i.e nonlinear differential operator), our method seems to generate a small set of synergies that span the set of required actuations. Similar results have been reported using other nonlinear differential operators besides kinematic chains [Carbajal, 2012]. These are not trivial results since the reduced synergies over-perform the subsets randomly taken from the exploration set $\boldsymbol{\Phi}_0$ (see Fig. D.4, D.7 and D.11). By gradually increasing the generality of the desired class of task, the performance difference between the synergies and the random signals reduces systematically, and the number of synergies required to reach a certain error threshold increases. It appears as if the reduction phase captures important features of the desired actuation space. A theoretical formulation of these empirical observations is currently under development.

D.4.4 Conclusions

The current work analyzes the hypothesis of muscle synergies from a computational perspective; i.e. the control of a planar kinematic chain through linear combinations of a limited set of torque profiles (motor synergies). The proposed Dynamic Response Decomposition is able to generate effective synergies, greatly reducing the dimensionality of the problem, while keeping a good performance level. Its formulation offers a lower bound on the minimum number of required synergies. Additionally, it shows a clear relation between synergies and desired tasks. In particular, it suggests that synergies might be solutions to proto-typical task instances, and that the number of required synergies depends on the generality of the desired class of tasks. Simple point-to-point synergies can be used to generate solutions to via-point tasks by concatenating the actuations associated to the individual movement phases. However, the usage of specific via-point synergies reduces the sources of possible errors, and in many cases it leads to better task performance. Overall our work serves as a proof of concept for the notion of muscle synergies. It highlights the advantages and the limitations for this approach, and it draws attention to important aspects that are not easily accessible in experimental studies.

The future developments of this research point towards different directions. The relations between muscle synergies and kinematic submovements will be further investigated. In particular, we will analyze the idea of overlapping point-to-point strokes [Flash et al., 1992]. Another interesting line of investigation is the validation of our method against biological data, paving the way towards a predictive model of the muscle synergy hypothesis. To this end, a first step will be the evaluation of DRD on realistic musculoskeletal models. From the theoretical point of view, we

are currently studying the mathematical properties of the synergies synthesized by means of the reduction procedure. Finally, we plan to include joint limits in the formulation of DRD, and to tackle the challenge of learning the mapping between kinematic and synergy coefficients.

The software used to produce all the results reported in this paper is available as a GNU Octave package under free and open source license[1]. The reader is encouraged to download, test, report bugs and submit improvements to the algorithm.

Acknowledgement

Funding The research leading to these results has received funding from the European Community's Seventh Framework Programme FP7/2007-2013-Challenge 2 - Cognitive Systems, Interaction, Robotics- under grant agreement No 248311-AMARSi, and from the EU project RobotDoC under 235065 from the 7th Framework Programme (Marie Curie Action ITN).

Author Contributions **CA** performed all numerical simulations and data analyses. **CA** and **JPC** worked on the implementation of the algorithm. The DRD method was born during **JPC**'s visit to **AD**'s laboratory. **AD** provided material support for this development and uncountable conceptual inputs. All three authors have contributed to the creation of the manuscript.

Bibliography

Alessandro, C., Carbajal, J. P., and d'Avella, A. (2012). Synthesis and Adaptation of Effective Motor Synergies for the Solution of Reaching Tasks. In Ziemke, T., Balkenius, C., and Hallam, J., editors, *Lecture Notes in Artificial Intelligence (LNAI)*, pages 33–43, Berlin. Springer-Verlag.

Alessandro, C., Delis, I., Nori, F., Panzeri, S., and Berret, B. (2013). Muscle synergies in neuroscience and robotics: from input-space to task-space perspectives. *Frontiers in Computational Neuroscience*, 7(43).

Alessandro, C. and Nori, F. (2012). Identification of Synergies by Optimization of Trajectory Tracking Tasks. In *IEEE RAS/EMBS International Conference on Biomedical Robotics and Biomechatronics*, pages 924–930, Rome. IEEE.

Allen, J. L. and Neptune, R. R. (2012). Three-dimensional modular control of human walking. *Journal of Biomechanics*, 45(12):2157–2163.

Berniker, M., Jarc, A., Bizzi, E., and Tresch, M. C. (2009). Simplified and effective motor control based on muscle synergies to exploit musculoskeletal dynamics. *Proceedings of the National Academy of Sciences of the United States of America*, 106(18):7601–7606.

Bernstein, N. A. (1967). *The Co-ordination and Regulation of Movements*. Pergamon.

Bizzi, E., Cheung, V. C. K., d'Avella, A., and Saltiel, P. F. (2008). Combining modules for movement. *Brain Research Reviews*, 57:125–133.

Cappellini, G., Ivanenko, Y. P., Poppele, R. E., and Lacquaniti, F. (2006). Motor patterns in human walking and running. *Journal of Neurophysiology*, 95(6):3426–3437.

Carbajal, J. P. (2012). *Harnessing Nonlinearities: Generating Behavior from Natural Dynamics*. Phd, University of Zürich.

[1] http://users.elis.ugent.be/~jcarbaja/DRD/drd.html

Cheung, V. C. K., d'Avella, A., and Bizzi, E. (2009). Adjustments of motor pattern for load compensation via modulated activations of muscle synergies during natural behaviors. *Journal of Neurophysiology*, 101(3):1235–1257.

Chhabra, M. and Jacobs, R. A. (2008). Learning to Combine Motor Primitives Via Greedy Additive Regression. *The Journal of Machine Learning Research*, 9(6):1535–1558.

Chvatal, S. A., Torres-Oviedo, G., Safavynia, S. A., and Ting, L. H. (2011). Common muscle synergies for control of center of mass and force in nonstepping and stepping postural behaviors. *Journal of Neurophysiology*, 106(2):999–1015.

Dagmar, S. and Schaal, S. (1999). Segmentation of endpoint trajectories does not imply segmented control. *Experimental Brain Research*, 124:118–136.

d'Avella, A. and Bizzi, E. (2005). Shared and specific muscle synergies in natural motor behaviors. *Proceedings of the National Academy of Sciences*, 102(8):3076–3081.

d'Avella, A., Fernandez, L., Portone, A., and Lacquaniti, F. (2008). Modulation of phasic and tonic muscle synergies with reaching direction and speed. *Journal of Neurophysiology*, 100(3):1433–54.

d'Avella, A. and Pai, D. K. (2010). Modularity for sensorimotor control: evidence and a new prediction. *Journal of Motor Behavior*, 42(6):361–369.

d'Avella, A., Portone, A., Fernandez, L., and Lacquaniti, F. (2006). Control of fast-reaching movements by muscle synergy combinations. *The Journal of Neuroscience*, 26(30):7791–7810.

d'Avella, A., Portone, A., and Lacquaniti, F. (2011). Superposition and modulation of muscle synergies for reaching in response to a change in target location. *Journal of Neurophysiology*, 106(6):2796–2812.

d'Avella, A., Saltiel, P., and Bizzi, E. (2003). Combinations of muscle synergies in the construction of a natural motor behavior. *Nature Neuroscience*, 6:300–308.

Delis, I., Berret, B., Pozzo, T., and Panzeri, S. (2013). Quantitative evaluation of muscle synergy models: a single-trial task decoding approach. *Frontiers in Computational Neuroscience*, 7:8.

Dominici, N., Ivanenko, Y. P., Cappellini, G., D'Avella, A., Mondì, V., Cicchese, M., Fabiano, A., Silei, T., Di Paolo, A., Giannini, C., Poppele, R. E., and Lacquaniti, F. (2011). Locomotor primitives in newborn babies and their development. *Science*, 334(6058):997–9.

Fishbach, A., Roy, S. A., Bastianen, C., Miller, L. E., and Houk, J. C. (2005). Kinematic properties of on-line error corrections in the monkey. *Experimental Brain Research*, 164(4):42–457.

Fishbach, A., Roy, S. A., Bastianen, C., Miller, L. E., and Houk, J. C. (2007). Deciding when and how to correct a movement: discrete submovements as a decision making process. *Experimental Brain Research*, 177(1):45–63.

Flash, T. and Henis, E. (1991). Arm trajectory modifications during reaching towards visual targets. *Journal of Cognitive Neuroscience*, 3(3):220–230.

Flash, T., Henis, E., Inzelbergb, R., and Korczynb, A. (1992). Timing and sequencing of human arm trajectories: normal and abnormal motor behaviour. *Human Movement Science*, 11(1-2):83–100.

Flash, T. and Hochner, B. (2005). Motor primitives in vertebrates and invertebrates. *Current Opinion in Neurobiology*, 15(6):660–666.

Giszter, S. F., Hart, C. B., and Silfies, S. P. (2010). Spinal cord modularity: evolution, development, and optimization and the possible relevance to low back pain in man. *Experimental Brain Research*, 200(3-4):283–306.

Giszter, S. F., Mussa-Ivaldi, F. A., and Bizzi, E. (1993). Convergent force fields organized in the frog's spinal cord. *Journal of Neuroscience*, 13(2):467–491.

Henis, E. A. and Flash, T. (1995). Mechanisms underlying the generation of averaged modified trajectories. *Biological Cybernetics*, 72(5):407–419.

Hollerbach, J. M. and Flash, T. (1982). Dynamic interactions between limb segments during planar arm movement. *Biological Cybernetics*, 44(1):67–77.

Ivanenko, Y. P., Cappellini, G., Dominici, N., Poppele, R. E., and Lacquaniti, F. (2005). Coordination of locomotion with voluntary movements in humans. *The Journal of Neuroscience*, 25(31):7238–7253.

Kargo, W. J. and Giszter, S. F. (2000). Rapid correction of aimed movements by summation of force-field primitives. *The Journal of Neuroscience*, 20(1):409–426.

Kargo, W. J. and Giszter, S. F. (2008). Individual premotor drive pulses, not time-varying synergies, are the units of adjustment for limb trajectories constructed in spinal cord. *The Journal of N euroscience*, 28(10):2409–2425.

Karniel, A. (2013). The minimum transition hypothesis for intermittent hierarchical motor control. *Frontiers in Computational Neuroscience*, 7(12).

Loram, I. D., Gollee, H., Lakie, M., and Gawthrop, P. J. (2010). Human control of an inverted pendulum: Is continuous control necessary? is intermittent control effective? is intermittent control physiological? *The Journal of Physiology*, 589:307–324.

Marques, H., Schaffner, P., and Kuppuswamy, N. (2012). Unsupervised Learning of a Reduced Dimensional Controller for a Tendon Driven Robot Platform. In Ziemke, T., Balkenius, C., and Hallam, J., editors, *Lecture Notes in Artificial Intelligence (LNAI)*, pages 351–360, Berlin. Springer-Verlag.

McGowan, C. P., Neptune, R. R., Clark, D. J., and Kautz, S. A. (2010). Modular control of human walking: Adaptations to altered mechanical demands. *Journal of Biomechanics*, 43(3):412–419.

Meyer, D. E., Abrams, R. A., Kornblum, S., Wright, C. E., and Smith, J. E. K. (1988). Optimality in human motor performance: ideal control of rapid aimed movements. *Psychological Review*, 95:340–370.

Morasso, P. and Mussa-Ivaldi, F. A. (1982). Trajectory formation and handwriting: a computational model. *Biological Cybernetics*, 45(2):131–142.

Mussa-Ivaldi, F. A. (1997). Nonlinear force fields: a distributed system of control primitives for representing and learning movements. In *IEEE International Symposium on Computational Intelligence in Robotics and Automation*, pages 84–90, Albuquerque, New Mexico, USA. IEEE.

Mussa-Ivaldi, F. A. and Bizzi, E. (2000). Motor learning through the combination of primitives. *Philosophical Transactions of the Royal Society of London - Series B: Biological Sciences*, 355(1404):1755–1769.

Mussa-Ivaldi, F. A., Giszter, S. F., and Bizzi, E. (1994). Linear combinations of primitives in vertebrate motor control. *Proceedings of the National Academy of Sciences of the United States of America (PNAS)*, 19(16):7534–7538.

Neptune, R. R., Clark, D. J., and Kautz, S. A. (2009). Modular control of human walking: a simulation study. *Journal of Biomechanics*, 42(9):1282–1287.

Nguyen-Tuong, D. and Peters, J. (2011). Model learning for robot control: a survey. *Cognitive Processing*, 12(4):319–340.

Nori, F. (2005). *Symbolic Control with Biologically Inspired Motion Primitives*. PhD thesis, Università degli Studi di Padova.

Nori, F. and Frezza, R. (2005). A control theory approach to the analysis and synthesis of the experimentally observed motion primitives. *Biological Cybernetics*, 93(5):323–342.

Novak, K., Miller, L., and Houk, J. (2003). Features of motor performance that drive adaptation in rapid hand movements. *Experimental Brain Research*, 148(3):388–400.

Overduin, S. A., d'Avella, A., Carmena, J. M., and Bizzi, E. (2012). Microstimulation activates a handful of muscle synergies. *Neuron*, 76:1071–1077.

Overduin, S. A., d'Avella, A., Roh, J., and Bizzi, E. (2008). Modulation of muscle synergy recruitment in primate grasping. *The Journal of Neuroscience*, 28(4):880 – 892.

Pasalar, S., Roitman, A. V., and Ebner, T. J. (2005). Effects of speeds and force fields on submovements during circular manual tracking in humans. *Experimental Brain Research*, 163(2):214–225.

Rohrer, B., Fasoli, S., Krebs, H. I., Volpe, B., Frontera, W. R., Stein, J., and Hogan, N. (2004). Submovements grow larger, fewer, and more blended during stroke recovery. *Motor Control*, 8(4):472–483.

Roitman, A. V., Massaquoi, S. G., Takahashi, K., and Ebner, T. J. (2004). Kinematic analysis of manual tracking in monkeys: characterization of movement intermittencies during a circular tracking task. *Journal of Neurophysiology*, 91(2):901–911.

Saltiel, P., Wyler-Duda, K., D'Avella, A., Tresch, M. C., and Bizzi, E. (2001). Muscle synergies encoded within the spinal cord: evidence from focal intraspinal NMDA iontophoresis in the frog. *Journal of Neurophysiology*, 85(2):605–619.

Shkolnik, A. and Tedrake, R. (2011). Sample-based planning with volumes in configuration space. *arXiv:1109.3145v1*.

Soechting, J. and Terzuolo, C. (1987). Organization of arm movements in three-dimensional space. wrist motion is piecewise planar. *Neuroscience*, 23:53–61.

Sosnik, R., Hauptmann, B., Karni, A., and Flash, T. (2004). When practice leads to co-articulation: the evolution of geometrically defined movement primitives. *Experimental Brain Research*, 154(4):422–438.

Squeri, V., Masia, L., Casadio, M., Morasso, P., and Vergaro, E. (2010). Force-field compensation in a manual tracking task. *PLoS ONE*, 5(6):e11189.

Thomas, P. and Barto, A. (2012). Motor primitive discovery. In *International Conference on Development and Learning - EpiRob (ICDL)*, San Diego, California, USA.

Ting, L. H. and Macpherson, J. M. (2005). A limited set of muscle synergies for force control during a postural task. *Journal of Neurophysiology*, 93(1):609–613.

Ting, L. H. and McKay, J. L. (2007). Neuromechanics of muscle synergies for posture and movement. *Current Opinion in Neurobiology*, 17(6):622–8.

Todorov, E. (2009). Compositionality of optimal control laws. In Koller, D., Bengio, Y., Bottou, L., and Culotta, A., editors, *Advances in Neural Information Processing Systems, 2009a*, volume 3, pages 1856–1864. Nips Foundation (http://books.nips.cc).

Todorov, E. and Ghahramani, Z. (2003). Unsupervised learning of sensory-motor primitives. In *Proceedings of the 25th International Conference of the IEEE Engineering in Medicine and Biology Society*, pages 1750–1753. IEEE.

Torres-Oviedo, G., Macpherson, J. M., and Ting, L. H. (2006). Muscle synergy organization is robust across a variety of postural perturbations. *Journal of Neurophysiology*, 96(3):1530–1546.

Torres-Oviedo, G. and Ting, L. H. (2007). Muscle synergies characterizing human postural responses. *Journal of Neurophysiology*, 98(4):2144–2156.

Torres-Oviedo, G. and Ting, L. H. (2010). Subject-specific muscle synergies in human balance control are consistent across different biomechanical contexts. *Journal of Neurophysiology*, 103(6):3084–3098.

Tresch, M. C., Saltiel, P., and Bizzi, E. (1999). The construction of movement by the spinal cord. *Nature Neuroscience*, 2(2):162–167.

Appendix E

Computational complexity of DRD

E.1 Introduction

In this appendix we derive the time computational complexity of DRD (see chapter 5, and appendices C and D). Such property depends on the specific algorithms used (e.g. to solve linear systems of equations, SVD, matrix multiplications). In what follows, we consider the algorithms provided by GNU Octave/Matlab®(tools used to perform all the experiments in this thesis); their detailed descriptions as well as their time complexities can be found in [Golub and van Van Loan, 1996]. Furthermore, we restrict our analysis to the control of a kinematic chain; this simplifies the analysis of the computational complexity of the function to compute the inverse dynamics.

To simplify the exposition, DRD is presented in Matlab-like pseudo-code in algorithms 2 and 3; table E.1 summarizes the notation used. Section E.2 presents the time complexity of the procedure to compute the solution to a task, and Sec. E.3 discusses the complexity of the method for the synthesis of synergies.

Symbol	Meaning
N_c	Number of task-constraints defining a task
N_p	Number of proto-tasks
N_θ	Number of Dynamic Responses (DRs)
N_ϕ	Number of synergies
N_{θ_0}	Number of exploration signals
N_d	Number of degrees of freedom of the kinematic chain
n_t	Number of time samples
$\boldsymbol{M}$	N_c-by-N_θ alternant matrix
$\boldsymbol{M}_0$	N_c-by-N_{θ_0} alternant matrix of the exploration phase
$\boldsymbol{\Theta}(t)$	$3n_t$-by-N_θ matrix containing the DRs and their derivatives
$\boldsymbol{\Phi}(t)$	$n_t N_d$-by-N_ϕ matrix containing the synergies
$\boldsymbol{\Theta}_0(t)$	$3n_t$-by-N_{θ_0} matrix containing the DRs of the exploration signals and their derivatives
$\boldsymbol{c}$	N_cx1 vector of task-constraints defining a task
$\boldsymbol{t_c}$	vector containing the time-samples of the task-constraints
$\boldsymbol{B}$	N_dxN_d inertia matrix of the kinematic chain
$\boldsymbol{C}$	N_dxN_d Coriolis matrix of the kinematic chain
$\boldsymbol{g}$	N_dx1 gravity vector of the kinematic chain
$\backslash$	Operator to solve linear systems of equations (e.g. $\boldsymbol{x} = \boldsymbol{A}\backslash\boldsymbol{b}$ is the least-square solution of $\boldsymbol{A}\boldsymbol{x} = \boldsymbol{b}$

Table E.1: Notation used in algorithms 2 and 3.

E.2 Solution to task-constraints

The DRD method to compute a synergy-based controller that solves some given task-constraints is summarized in algorithm 2. This algorithm consists of generating the alternant matrix (line 1), finding a kinematic solution to the task (lines 2–3), computing the inverse dynamics (line 4), and projecting the obtained actuation onto the synergy-span (lines 5–6). The computational complexities of the functions CREATEALTERNANT and INVERSEDYNAMICS are $\mathcal{O}(N_c^2 N_\theta + N_c N_\theta^2 + N_\theta^3)$ and $\mathcal{O}(n_t N_d^2)$ respectively (see Sec. E.2.1 and E.2.2).

The linear systems of equations at lines 2 and 5 are solved by means of the operator $\backslash$, which in the worst case scenario (i.e. if the coefficient matrix does not have any particular structure)

employs the QR decomposition. The computational complexity of this procedure is described in Sec. E.2.3, and depends on whether the number of rows of the coefficient matrix is higher or lower than the number of columns. For the operation at line 2 if $N_c \geq N_\theta$ (i.e. number of rows of $\boldsymbol{M}$ is greater or equal than the number of columns), the complexity results $\mathcal{O}(N_c^2 N_\theta)$; otherwise it is $\mathcal{O}(N_c N_\theta^2)$. Similarly at line 5, if $n_t N_d \geq N_\phi$, the complexity is $\mathcal{O}(n_t^2 N_d^2 N_\phi)$; otherwise it is $\mathcal{O}(n_t N_d N_\phi^2)$. Note that very likely the number of time-samples n_t is much greater than the number of synergies N_ϕ, thus we will assume the complexity of line 5 to be $\mathcal{O}(n_t^2 N_d^2 N_\phi)$.

Finally, we need to analyze lines 3 and 6. These operations only involve matrix-vector multiplications, which take $(2n-1)m$ flops (where m is the number of columns and n the number of rows of the matrix [Golub and van Van Loan, 1996]). Therefore, the multiplications at line 3 and 6 have complexities $\mathcal{O}(n_t N_\theta)$ and $\mathcal{O}(n_t N_d N_\phi)$ respectively.

All these results are summarized in table E.2. As it can be seen, the complexity of line 2 already appears in the complexity of line 1 independently on whether $N_c \geq N_\theta$ or $N_c < N_\theta$. Furthermore, $n_t N_d N_\phi$ (line 6) $< n_t^2 N_d^2 N_\phi$ (line 5), and $n_t N_d^2$ (line 4) $< n_t^2 N_d^2 N_\phi$ (line 5). As a result, the overall time complexity of this algorithm is $\mathcal{O}(N_c^2 N_\theta + N_c N_\theta^2 + N_\theta^3 + n_t N_\theta + n_t^2 N_d^2 N_\phi)$.

Line	$N_c \geq N_\theta$	$N_c < N_\theta$
1	$\mathcal{O}(N_c^2 N_\theta + N_c N_\theta^2 + N_\theta^3)$	$\mathcal{O}(N_c^2 N_\theta + N_c N_\theta^2 + N_\theta^3)$
2	$\mathcal{O}(N_c^2 N_\theta)$	$\mathcal{O}(N_c N_\theta^2)$
3	$\mathcal{O}(n_t N_\theta)$	$\mathcal{O}(n_t N_\theta)$
4	$\mathcal{O}(n_t N_d^2)$	$\mathcal{O}(n_t N_d^2)$
5	$\mathcal{O}(n_t^2 N_d^2 N_\phi)$	$\mathcal{O}(n_t^2 N_d^2 N_\phi)$
6	$\mathcal{O}(n_t N_d N_\phi)$	$\mathcal{O}(n_t N_d N_\phi)$

Table E.2: Complexity breakdown of algorithm 2.

E.2.1 Function CreateAlternant

The function CreateAlternant computes the alternant matrix $\boldsymbol{M}$ and modifies the vector of task-constraints $\boldsymbol{c}$ based on the Dynamic Responses (DRs) $\boldsymbol{\Theta}(t)$. Essentially, the alternant matrix contains the values of the DRs and their derivatives evaluated at the time-instant $\boldsymbol{t}_c$ in which the constraints are defined (see Appendix D, equation D.5). This evaluation is performed in line 8. The number of flops required to compute each element of the matrix depends on the function to be evaluated, and it is therefore difficult estimate. However, each element is the value of a real-valued function of time evaluated at a specific point, thus its computational-time does not depend on the size of the problem. As a result, we can safely say that the complexity to compute each element of the matrix is $\mathcal{O}(1)$, and therefore that to compute the whole matrix is $\mathcal{O}(N_c N_\theta)$, ($N_c$ and N_θ are the numbers of rows and columns respectively, see table E.1).

The remaining lines of code (9–18) reduce the size of the alternant matrix (if possible). The rank is calculated by Singular Value Decomposition (SVD), which is in turn computed through the Golub-Reinsch algorithm. Such algorithm takes $4m^2 n + 8mn^2 + 9n^3$ flops, where m and n are the numbers of rows and columns of the matrix [Golub and van Van Loan, 1996]. The complexity of line 9 is therefore $\mathcal{O}(N_c^2 N_\theta + N_c N_\theta^2 + N_\theta^3)$. The computation of the length of c is trivially $\mathcal{O}(N_c)$.

If the condition at line 11 holds true (worst case scenario), we need to compute the complexity of the block at lines 12–17. As we discussed above, line 12 results in $\mathcal{O}(N_c^2 N_\theta + N_c N_\theta^2 + N_\theta^3)$. $\boldsymbol{S}$ is a diagonal matrix, therefore line 13 involves the evaluation of r numbers only, resulting in $\mathcal{O}(r)$. Following similar rationales, lines 14 and 15 have complexity $\mathcal{O}(rN_c)$ and $\mathcal{O}(rN_\theta)$. The matrix-vector multiplication at line 15 takes $(2N_c - 1)r$ flops, which is $\mathcal{O}(rN_c)$. Since $\boldsymbol{S}$ is diagonal, line

Algorithm 2 Dynamic Response Decomposition

Require: Dynamic Response Matrix $\boldsymbol{\Theta}(t)$
Synergy matrix $\boldsymbol{\Phi}(t)$
Point-constraints vector $\boldsymbol{c}$
Time of constraints $\boldsymbol{t}_c$
Rigid kinematic chain dynamics $\boldsymbol{B}, \boldsymbol{C}, \boldsymbol{g}$

Ensure: Torques projected onto the synergy-span $\boldsymbol{u}(t)$
Synergy mixing coefficients $\boldsymbol{b}$

$[\boldsymbol{M}, \boldsymbol{c}] \leftarrow$ CREATEALTERNANT($\boldsymbol{\Theta}(t), \boldsymbol{t}_c, \boldsymbol{c}$)

$\boldsymbol{a} \leftarrow \boldsymbol{M} \setminus \boldsymbol{c}$
$[\boldsymbol{q}(t), \dot{\boldsymbol{q}}(t), \ddot{\boldsymbol{q}}(t)] \leftarrow \boldsymbol{\Theta}(t)\boldsymbol{a}$

$\tilde{\boldsymbol{u}}(t) \leftarrow$ INVERSEDYNAMICS($[\boldsymbol{q}(t), \dot{\boldsymbol{q}}(t), \ddot{\boldsymbol{q}}(t)], \boldsymbol{B}, \boldsymbol{C}, \boldsymbol{g}$)

$\boldsymbol{b} \leftarrow \boldsymbol{\Phi}(t) \setminus \tilde{\boldsymbol{u}}$
$\boldsymbol{u}(t) \leftarrow \boldsymbol{\Phi}(t)\boldsymbol{b}$

function CREATEALTERNANT($\boldsymbol{\Theta}(t), \boldsymbol{t}_c, \boldsymbol{c}$)
    $\boldsymbol{M} \leftarrow$ EVALUATEDR($\boldsymbol{\Theta}(t), \boldsymbol{t}_c$)
    $r \leftarrow$ RANK($\boldsymbol{M}$)
    $N_c \leftarrow$ LENGTH($\boldsymbol{c}$)
    if $r < N_c$ **then**
        $[\boldsymbol{U}, \boldsymbol{S}, \boldsymbol{V}] \leftarrow$ SVD($\boldsymbol{M}$)
        $\boldsymbol{S} \leftarrow \boldsymbol{S}(1:r, 1:r)$
        $\boldsymbol{U} \leftarrow \boldsymbol{U}(:, 1:r)$
        $\boldsymbol{V} \leftarrow \boldsymbol{V}(:, 1:r)$
        $\boldsymbol{c} \leftarrow \boldsymbol{U}^T\boldsymbol{c}$
        $\boldsymbol{M} \leftarrow \boldsymbol{S}\boldsymbol{V}^T$
    end if
    return $\boldsymbol{M}, \boldsymbol{c}$
end function

function INVERSEDYNAMICS($[\boldsymbol{q}(t), \dot{\boldsymbol{q}}(t), \ddot{\boldsymbol{q}}(t)], \boldsymbol{B}, \boldsymbol{C}, \boldsymbol{g}$)
    $n_t \leftarrow$ LENGTH($\boldsymbol{q}(t)$)
    for $t_i = 1 \rightarrow n_t$ **do**
        $\boldsymbol{\tau}(t_i) = \boldsymbol{B}(\boldsymbol{q}(t_i))\ddot{\boldsymbol{q}}(t_i) + \boldsymbol{C}(\boldsymbol{q}(t_i), \dot{\boldsymbol{q}}(t_i))\dot{\boldsymbol{q}}(t_i) + \boldsymbol{g}(\boldsymbol{q}(t_i))$
    end for
    return $\boldsymbol{\tau}$
end function

16 results in $\mathcal{O}(rN_\theta)$. The computational cost of the "if" block is therefore determined by the computation of the SVD at line 12, which is more costly than line 8 and equal to line 9. As a result, the time complexity of the function CREATEALTERNANT is $\mathcal{O}(N_c^2 N_\theta + N_c N_\theta^2 + N_\theta^3)$.

E.2.2 Function INVERSEDYNAMICS

The function INVERSEDYNAMICS involves the evaluation of the matrices $\boldsymbol{B}$, $\boldsymbol{C}$ and $\boldsymbol{g}$, the computation of their products by $\ddot{\boldsymbol{q}}$ and $\dot{\boldsymbol{q}}$, and the sum of the resulting vectors. These operations are repeated for each time-sample (i.e. n_t times). As we said above, the complexity of evaluating a matrix is linear to the number of its elements, resulting in $\mathcal{O}(N_d^2)$, $\mathcal{O}(N_d^2)$ and $\mathcal{O}(N_d)$ for $\boldsymbol{B}$, $\boldsymbol{C}$ and $\boldsymbol{g}$ respectively. Each matrix-vector multiplication is $\mathcal{O}(N_d^2)$, and the sum of the vectors is $\mathcal{O}(N_d)$ (where N_d is the size of the vector). The complexity of the function INVERSEDYNAMICS is therefore $\mathcal{O}(n_t N_d^2)$.

E.2.3 Solution of linear systems of equations

Let us assume a matrix $\boldsymbol{A} \in \mathbb{R}^{m \times n}$ and a linear system of equation $\boldsymbol{Ax} = \boldsymbol{b}$. The method employed by the Matlab®/GNU Octave operator \ to compute $\boldsymbol{x} = \boldsymbol{A} \backslash \boldsymbol{b}$ depends on the structure of the matrix $\boldsymbol{A}$ (e.g. sparse, diagonal, etc.); if this matrix does not have any particular structure, the system is solved by means of the QR decomposition of $\boldsymbol{A}$. Using the Householder transformation, such a decomposition takes $4(m^2 n - mn^2 + n^3)$ flops. Since the condition $m \geq n$ is required, the computational complexity is $\mathcal{O}(m^2 n)$. If $m < n$, the system of equations can be solved by computing the QR decomposition of the matrix $\boldsymbol{A}^T$; the complexity of this operation is therefore $\mathcal{O}(mn^2)$. In what follows we derive the overall computational complexity of $\boldsymbol{x} = \boldsymbol{A} \backslash \boldsymbol{b}$ for both cases.

Case $m \geq n$

Initially the QR decomposition is applied to the matrix $\boldsymbol{A} = \boldsymbol{QR}$, where $\boldsymbol{Q}$ is a $m \times m$ orthogonal matrix, and $\boldsymbol{R} = \left[\begin{array}{c|c} \boldsymbol{R}_1^T & \boldsymbol{0} \end{array} \right]^T$ with $\boldsymbol{R}_1$ being a $n \times n$ upper triangular matrix. The least-square solution of the (overdetermined) system is therefore $\boldsymbol{x} = \left[\begin{array}{c|c} \boldsymbol{R}_1^{-1} & \boldsymbol{0} \end{array} \right] \boldsymbol{Q}^T \boldsymbol{b}$. The matrix-vector multiplication $\tilde{\boldsymbol{b}} = \boldsymbol{Q}^T \boldsymbol{b}$ has complexity $\mathcal{O}(m^2)$; since $\boldsymbol{R}_1$ is upper triangular, the operation $\left[\begin{array}{c|c} \boldsymbol{R}_1^{-1} & \boldsymbol{0} \end{array} \right] \tilde{\boldsymbol{b}}$ can be computed by forward-substitution, which has complexity $\mathcal{O}(n^2)$ [Golub and van Van Loan, 1996]. Both these terms are lower than the complexity of the QR decomposition. Thus the overall complexity to solve the system $\boldsymbol{Ax} = \boldsymbol{b}$ is $\mathcal{O}(m^2 n)$.

Case $m < n$

In this case the QR decomposition is applied to the matrix $\boldsymbol{A}^T = \boldsymbol{QR}$, where $\boldsymbol{Q}$ is a $n \times n$ orthogonal matrix, and $\boldsymbol{R} = \left[\begin{array}{c|c} \boldsymbol{R}_1^T & \boldsymbol{0} \end{array} \right]^T$ with $\boldsymbol{R}_1$ being a $m \times m$ upper triangular matrix. The least-square solution of the (underdetermined) system is $\boldsymbol{x} = \boldsymbol{A}^T (\boldsymbol{A}\boldsymbol{A}^T)^{-1} \boldsymbol{b} = \boldsymbol{Q} \left[\begin{array}{c|c} \boldsymbol{R}_1^{-1} & \boldsymbol{0} \end{array} \right]^T \boldsymbol{b}$. The operation $\tilde{\boldsymbol{b}} = \boldsymbol{R}_1^{-T} \boldsymbol{b}$ can be solved by forward substitution, with complexity $\mathcal{O}(m^2)$; the matrix multiplication $\boldsymbol{Q} \left[\begin{array}{c|c} \tilde{\boldsymbol{b}}^T & \boldsymbol{0} \end{array} \right]^T$ costs $\mathcal{O}(n^2)$. Both these terms are lower than the complexity of the QR decomposition. Thus the overall complexity to solve the system $\boldsymbol{Ax} = \boldsymbol{b}$ is $\mathcal{O}(mn^2)$.

E.3 Synthesis of synergies

The pseudo-code for the synthesis of synergies is presented in algorithm 3. It consists of creating the alternant matrix for the i-th proto-task (line 2), solving such a task in kinematic variables (lines 3–4), and computing the corresponding synergy by applying inverse dynamics (line 6); this procedure is repeated for all proto-tasks (N_p times). The complexities of these operations have been discussed in the previous sections, and are summarized in table E.3.

Line	$N_c \geq N_{\theta_0}$	$N_c < N_{\theta_0}$
2	$\mathcal{O}(N_c^2 N_{\theta_0} + N_c N_{\theta_0}^2 + N_{\theta_0}^3)$	$\mathcal{O}(N_c^2 N_{\theta_0} + N_c N_{\theta_0}^2 + N_{\theta_0}^3)$
3	$\mathcal{O}(N_c^2 N_{\theta_0})$	$\mathcal{O}(N_c N_{\theta_0}^2)$
4	$\mathcal{O}(n_t N_{\theta_0})$	$\mathcal{O}(n_t N_{\theta_0})$
5	$\mathcal{O}(n_t N_d)$	$\mathcal{O}(n_t N_d)$
6	$\mathcal{O}(n_t N_d^2)$	$\mathcal{O}(n_t N_d^2)$

Table E.3: Complexity breakdown of algorithm 3 (lines 2–6).

As it can be seen, the complexity of line 3 already appears in the complexity of line 2 independently on whether $N_c \geq N_{\theta_0}$ or $N_c < N_{\theta_0}$. Furthermore, $n_t N_d$ (line 5) $< n_t N_d^2$ (line 6). Since the instructions in lines 2–6 are repeated for each proto-tasks, the final complexity results $\mathcal{O}(N_p(N_c^2 N_{\theta_0} + N_c N_{\theta_0}^2 + N_{\theta_0}^3 + n_t N_{\theta_0} + n_t N_d^2))$.

Algorithm 3 Synthesis of synergies (DRD)

Require: Exploration DR Matrix $\boldsymbol{\Theta}_0(t)$
Proto-tasks constraint vectors $\{\boldsymbol{c}_i\}_{i=1\ldots N_p}$
Time of constraints $\boldsymbol{t}_c$
Rigid kinematic chain dynamics $\boldsymbol{B}, \boldsymbol{C}, \boldsymbol{g}$

Ensure: Synergies $\boldsymbol{\Phi}(t)$
Dynamic Responses $\boldsymbol{\Theta}(t)$

1: **for** $j = 1 \rightarrow N_p$ **do**
2: $[\boldsymbol{M}_0, \boldsymbol{c}_j] \leftarrow$ CREATEALTERNANT($\boldsymbol{\Theta}_0(t), \boldsymbol{t}_c, \boldsymbol{c}_j$)
3: $\boldsymbol{a} \leftarrow \boldsymbol{M}_0 \setminus \boldsymbol{c}_j$
4: $[\boldsymbol{q}_j(t), \dot{\boldsymbol{q}}_j(t), \ddot{\boldsymbol{q}}_j(t)] \leftarrow \boldsymbol{\Theta}_0(t)\boldsymbol{a}$
5: $\boldsymbol{\Theta}_j(t) \leftarrow [\boldsymbol{q}_j(t), \dot{\boldsymbol{q}}_j(t), \ddot{\boldsymbol{q}}_j(t)]$
6: $\boldsymbol{\Phi}_j(t) \leftarrow$ INVERSEDYNAMICS($\boldsymbol{\Theta}_j(t), \boldsymbol{B}, \boldsymbol{C}, \boldsymbol{g}$)
7: **end for**

Bibliography

Golub, G. H. and van Van Loan, C. F. (1996). *Matrix Computations*. Johns Hopkins University Press; 3rd edition.

Appendix F

Curriculum Vitae

CURRICULUM VITAE of CRISTIANO ALESSANDRO

I authorize the treatment of the personal information provided according to the European Community Law 95/46/CE regarding the protection of privacy (in Italy the Law 196/03)

PERSONAL INFORMATION

Name:	Cristiano Alessandro
Address:	Sandacker, 15 – 8052 Zurich, Switzerland
E-mail:	alessandro@ifi.uzh.ch
Mobile:	+41767308814
	+393403470894
Birth:	Catania, 22/01/1984
Civil Status:	Single

EDUCATION

February 2009/Today	**University of Zurich. Institut für Informatik, AI Lab** **PhD Candidate** - Research interests: Motor control, Robotics, Bio-Inspired Control, Reduced dimensional control, Neuroscience. - Supervisor: Prof. Rolf Pfeifer
October 2005/April 2008	**Politecnico di Milano** **Master of Science in Engineering Computer Systems** - Degree mark: 110/110 cum laude - Main subjects: Artificial Intelligence, Robotics, Control Systems - Thesis: "A tool for evaluating architectures for autonomous robots" - Supervisor: Prof. Andrea Bonarini
September 2006/January 2007	**Chalmers Institute of Technology, Gothenburg, Sweden** - Erasmus exchange student
October 2002/July 2005	**Università degli Studi di Catania** **Bachelor in Computer Science Engineering (3 years)** - Degree mark: 110/110 cum laude - Thesis: "Navigation Control Algorithms based on spiking networks" (refer to publications paragraph) - Supervisors: Dr. Mattia Frasca, Dr. Luca Patanè, Prof. Paolo Arena
September 1997/June 2002	**Liceo Scientifico S.Giovanni Bosco, Catania** **Scientific Diploma** - Diploma mark: 100/100

WORK EXPERIENCES AND APPRENTICESHIPS

- **October 2009/Today:** RobotDoC project (Marie Curie Fellowship, ITN)

The RobotDoC (Robotics for Development of Cognition) Collegium is a multi-national doctoral training network for the interdisciplinary training on developmental cognitive robotics. The RobotDoc Fellows are trained to develop advanced expertise of domain-specific robotics research skills and of complementary transferrable skills for careers in academia and industry.
Website: http://robotdoc.org/

- **November 2012/Today:** AMARSi project (EU FP7)

AMARSi (Adaptive Modular Architectures for Rich Motor Skills) aims at a qualitative jump in robotic motor skills towards biological richness. The project consists in a close coordination between research in neuroscience and robotics, and it investigates the development of bio-inspired adaptive modular architectures for robot control.
Website: http://www.amarsi-project.eu/

- **February 2009/December 2011:** ECCEROBOT project (EU FP7)

The ECCEROBOT (Embodied Cognition in a Compliant Engineered Robot) project aimed at designing a series of anthropomimetic robots, i.e. humanoid robots that mimic the inner structures and mechanisms of the human body (bones, joints, muscles and tendons), and at investigating novel methods to control such structures.
Website: http://eccerobot.org/

- **September 2012:** Financial chair of the "Post-graduate conference on Robotics and Development of Cognition". Lausanne (Switzerland), 10-12 September 2012.

- **March/July 2012**: Visiting student at the Italian Institute of Technology (IIT) "Robotics, Brain and Cognitive Science" department (RBCS).

- **February/June 2011:** Teaching assistant. "Designing and Programming Embedded System for Robots". University of Zurich.

- **February/June 2010:** Teaching assistant. "Artificial Life". University of Zurich.

- **September 2009/January 2010:** Teaching assistant. "Introduction to AI". University of Zurich.

- **February/June 2009:** Teaching assistant. "Neural Networks". University of Zurich.

- **September/December 2008**:
  - Research collaborator at the Department of Electronics and Computer Science (DEI) of the Politecnico di Milano. Topic: Statistical analysis of biosignals for affective interaction.
  - Teaching assistant. "Information Systems". Politecnico di Milano.
  - Teaching assistant. "Computer Science A". Politecnico di Milano.

- **April/June 2008:** Teaching assistant. "Software Engineering". Politecnico di Milano.

- **October 2007/January 2008:** Teaching assistant. "Computer Science A". Politecnico di Milano.

- **2005:**
  - Implementation of biological inspired control algorithms for navigation and control of mobile robots (C++.NET). Università degli studi di Catania. 300 hours.
  - COASCO: Web-site implementation. Technologies: ASP.NET and Access database.

- **2004:** Tutoring service towards students of first year of engineering university.

MEMBERSHIPS

- International Electrical and Electronics Engineers (IEEE)
- Italian Association for Artificial Intelligence (AI*IA)

PUBLICATIONS

Journals

- Alessandro C., Ioannis D., Nori F., Panzeri S., Berret B. **Muscle synergies in neuroscience and robotics: from input to task-space perspectives.** *Frontiers in Computational Neuroscience* (2013). 7:43.

- Wittmeier S., Alessandro C., Bascarevic N., Dalamagkidis K., Diamond A., Jäntsch M., Jovanovic K., Knight R., Gravato Marques H., Milosavljevic P., Svetozarevic P., Potkonjak V., Pfeifer R., Knoll A., and Holland O. **Towards anthropomimetic robotics**. *Artificial Life* (2012). 19(1):171-193.

- Alessandro C., Carbajal J.P., d'Avella A. **Computational analyses of the muscle synergy hypothesis via the Dynamic Response Decomposition** (submitted).

Peer-reviewed conference

- Alessandro C., Carbajal J.P., d'Avella A. **Synthesis and Adaptation of Effective Motor Synergies for the Solution of Reaching Tasks**. *Lecture Notes in Artificial Intelligence (LNAI)* (2012). Eds. T. Ziemke, C. Balkenius, and J. Hallam (Berlin Springer-Verlag), pag. 33-43.

- Alessandro C. and Nori F. **Identification of Synergies by Optimization of Trajectory Tracking Tasks.** *The Fourth IEEE RAS/EMBS International Conference on Biomedical Robotics and Biomechatronics*. Roma, Italy. June 24-27, 2012. pag. 924-930.

- Mutti F., Alessandro C., Angioletti M., Bianchi A., Gini G. **Learning and evaluation of a vergence control system inspired by Hering's law.** *The Fourth IEEE RAS/EMBS International Conference on Biomedical Robotics and Biomechatronics*. Roma, Italy. June 24-27, 2012. pag. 931-936.

- Kuppuswamy N., Alessandro C. **Impact of Body Parameters on Dynamic Movement Primitives for Robot Control.** *The European Future Technologies Conference and Exhibition*, FET 2011. Budapest, Hungary.

- Marques G. H., Jäntsch M., Wittmeier S., Alessandro C., Lungarella M., Knight R., Holland O. **ECCE1: the first of a series of anthropomimetic musculoskeletal upper torsos**. IEEE *International Conference on Humanoid Robotics, Humanoid 2010*. Nashville, USA.

- Alessandro Cristiano. **Movement Control of Biologically Inspired Humanoid Robots.** Marie Curie Workshop, European Science Forum, ESOF 2010. Turin, Italy. (talk)

- Tognetti S., Alessandro C., Bonarini A., Matteucci M., **Fundamental issues on the recognition of autonomic patterns produced by visual stimuli**. *Affective Computing and Intelligent Interaction*, ACII 2009 – 10/09/2009 Amsterdam, Netherlands.

- Arena P., Fortuna L., Frasca M., Patanè L., Alessandro C., Barbagallo D., **Learning high sensors from reflexes via spiking networks in roving robots**. 8th international *IFAC symposium on robot control*, IFAC Syrco 2006 - 06/08/2006 Bologna, Italy.

AWARDS

- Alessandro C., Carbajal J.P., d'Avella A., Nori F. **Computational Implications of the hypothesis of muscle synergies**. 9th Computational Motor Control Workshop, Ben-Gurion University of Negev, Beer-Sheva, Israel. 9th May 2013. **Best poster award** (2nd prize)

SEMINARS

- **2011:** "Machine Learning Summer School" – Biopolis, Singapore. 45 hours.
- **2011:** "Summer school on impedance" – Frauenchiemsee (Germany). 40 hours.
- **2010:** "Veni, Vidi, Vici 2010, the iCub Summer School" – Fondazione Mediterraneo, Sestri Levante (Italy). 64 hours.
- **2009:** "Robot Learning Summer School" – Instituto Superior Tecnico, ISR. Lisbon (Portugal). 35 hours.
- **2009:** "Multimodal and Cognitive System Summer School" – University of Zurich. Zurich (Switzerland). 40 hours.
- **2007:** "From Kalman to Particle Filters" - Ecole Nazionale Superieure des Telecommunications. Paris (France). ATHENS program. 40 hours.
- **2003:** Linux Web Developer. ARCES association. 40 hours.

LANGUAGE SKILLS

- **English**: advanced oral and written.
  - **2005:** Preliminary English Test. University of Cambridge, ESOL Examinations.
  - **2000:** Trinity. The international examination board. Grade 3, "Spoken English for Speakers of Other Languages", passed with Distinction (90/100).

- **German:** basic level.
  - **2010:** Course for beginners (Level A1). Klubschule Migros. Zurich, Switzerland.

- **Swedish**: basic level.
  - **2006:** Swedish for beginners. Certificate achieved at Folkuniversitet. Gothenburg, Sweden.

TECHNICAL SKILLS

- **Operating Systems:** Windows OS, Linux OS.
- **Programming Languages:** C/C++, Java (SE, ME, EE), SQL, Python (basic level).
- **Software:** Matlab, Octave, SVN, Inkscape, SolidWorks (basic level), Labview (basic level).
- **Hardware:** Sensor testing, embedded programming, analog circuit design (basic level), Data Acquisition (comedi library).